JOURNAL OF BIOLOGICAL REGULATORS & HOMEOSTATIC AGENTS
Volume 31, No. 4 (Supplement 1), September - December 2017
Italian Orthopaedic Research Society 2017
Guest Editors: Paolo Domenico Parchi, Nicola Piolanti and Lorenzo Andreani

CONTENTS

THE EFFECT OF ANTI-IGE THERAPY IN KNEE OSTEOARTHRITIS: A PILOT OBSERVATIONAL STUDY

A. AQUILI[1], L. FARINELLI[1], C. BOTTEGONI[1], L. ANTONICELLI[2] and A. GIGANTE[1]

[1]Clinical Orthopaedics, Università Politecnica delle Marche, Ancona, Italy; [2]Allergy Unit, Department of Internal Medicine, Ospedali Riuniti, Ancona, Italy

Osteoarthritis is a whole-joint disease and its pathogenesis remains poorly understood. Recent evidence proposed the importance of the innate immune system as trigger of synovium inflammation following the degeneration of cartilage. Moreover, synovial mast cells (MCs) might be correlated with pain and disability reported by patients. Anti IgE therapy represents a new class of MCs stabilizing agent, licensed for people with asthma and chronic urticaria. Therefore, we studied if the stabilizing effect of anti IgE would improve the pain and disability in patients affected by knee osteoarthritis and atopic disease. This pilot study provides the first evidence that anti IgE treatment induces a short-term clinical improvement supporting the role of MCs in osteoarthritis.

Osteoarthritis (OA) is the most widespread form of arthritis, typically seen in elderly patients affecting all joints (1). Originally seen as a cartilage only disease, OA should be considered an inflammatory illness involving cartilage, bone and synovium (2).

It has been established that synovial inflammation plays a key role in symptoms and pathophysiology of OA (3). An interesting field of research questioned the triggering of synovium activation and the pathways that characterize the inflammatory response. Recent data suggest that the damage of cellular and cartilage extracellular matrix, produced from trauma, instability, deformity, microtrauma, meniscopathies or normal aging in OA, generates damage-associated molecular patterns (DAMPs) that might activate the innate immune system by Toll-like receptors (TLRs) (4).

TLR activation is an important stimulus for NFkB activation and subsequent production of chemokines and cytokines, which recruit macrophages, granulocytes and lymphocytes in synovium (5). TLRs are constitutively expressed by a variety of innate immune cells including macrophages and mast cells (MCs). It has been established that pain in OA is correlated to the inflammation grade of synovium (6) and several researches pointed out the relationship between clinical symptoms of OA and the abundance of MCs in inflammatory infiltrate of synovial specimens. For these reasons, several researches began to investigate the possible role of MCs in OA, in order to assess future therapeutic challenges (7).

MCs can be considered "sentinels" of the innate

Key words: osteoarthritis, synovial mast cells, Omalizumab

Mailing address:
Antonio Gigante,
Clinical Orthopaedics,
Università Politecnica delle Marche,
Via Tronto 10/A, 60020 Ancona, Italy
Tel.: +39.0712206066
e-mail: a.gigante@univpm.it

0393-974X (2017)

immune system, ready to take action in response to antigens, infection and other stimuli (8). These stimuli are either Ig-E and non Ig-E mediated (9). Anti IgE therapy represents a new class of MCs stabilizing agents that attenuates the degree of responsiveness of MCs to stimulators. Omalizumab (Xolair, Novartis, Camberley, United Kingdom) is a recombinant humanised IgG1 monoclonal antibody that targets circulating IgE. It represents a safe biological therapy for treating patients with asthma or chronic urticaria who are not being adequately treated with standard therapy (10, 11).

The aim of this study was to assess any changes of knee pain and disability in patients affected by knee OA in therapy with Omalizumab in order to look for more evidence supporting the role of MCs in OA.

MATERIAL AND METHODS

This prospective, single-center, pilot study was conducted with the highest respect for individual participants. All patients included in our study, in treatment with Omalizumab, were prospectively evaluated at 0, 3 and 6 months from the beginning of anti IgE therapy.

Inclusion criteria were: Asthma allergic or chronic urticaria not responsive to standard therapy and symptomatic knee osteoarthritis with radiographic imaging findings of degenerative joint changes (Kellgren-Lowrence grade I-IV). Exclusion criteria were: use of intraarticular corticosteroids or viscosupplementation from 3 months before the start of anti-IgE therapy to the entire follow-up period, use of NSAIDs or nutraceutical supplements in the 3 weeks before treatment and during follow-up period, rheumatic diseases, osteonecrosis.

All patients were treated in the Azienda Ospedaliera-Universitaria Ospedali Riuniti of Ancona (Italy), in particular, regarding OA, each patient was referred to the Clinical Orthopaedics, meanwhile regarding atopic disease, they were referred to the Allergy unit. During each visit, each patient was assessed by measurement of the subjective knee pain, rated on a visual-analogue scale of 100 mm (EQ VAS) and by measurement of joint disability scored by KOOS (Knee injury and Osteoarthritis Outcome Score) latest version available 2012.

All patients received a series of instructions after every injection. In case of knee pain during the treatment and follow-up period, patients were recommended to not use any analgesic medications but only cold therapy and limiting the use of the knee for at least 24 h. Obviously, if patients could not handle the pain, the use of any medication to relieve it made them unsuitable for the study. Mild activities were indicated and sport or recreational activities was allowed as tolerated. The Student *t*-test was performed for the KOOS score and the EQ VAS to compare pre- and postoperative values. Data are expressed as means with standard deviations (SD). For all tests, $p<0.05$ was considered significant for a one-tailed tests.

RESULT

From September 2016 to February 2017, 42 patients followed by Allergy unit of Ospedali Riuniti, Ancona, under anti-IgE treatment, were assessed for eligibility. The study sample consisted of 10 patients, 9 women and 1 man, mean age 60.2±11.77. Seven patients were affected by allergic asthma, while three patients had chronic urticaria. All of them had symptomatic knee OA. Each patient included in the current study received six subcutaneous injections of Xolair at a 4-week intervals and no further injection during the follow-up period. Regarding patients affected by allergic asthma, three patients received 600 mg of Xolair in each injection, two patients 300 mg, one 150 mg and one 450 mg.

On the other hand, patients with chronic urticaria, received 300 mg of Xolair in each injection. All patients completed the follow-up at 6 months. The radiological classification, according to the Kellgren and Lawrence criteria (KL) by two experimenters, allowed to stratify the sample of the study: 2 patients (20% of the sample) had I degree, 5 patients (50% of the sample) II degree and 3 patients (30%) III degree.

In regards to the overall clinical effect of the Omalizumab in knee OA, there were statistically significant differences in pre- and post-treatment values of EQ VAS and KOOS ($p<0.05$) (Fig. 1). The values of mean±SD of EQ VAS at baseline were 64.34±9.64, at 3 months follow-up 40.94±6.38, at 6 months follow- up 37.5±7.07. The values of mean±SD of KOOS at baseline were 43.3±5.3, at 3 months follow-up were 73.4±6.2 at 6 months follow-up were 75.8±5.8.

DISCUSSION

Omalizumab has multiple pharmacologic and immunoregolatory effects (12). It has been reported that the administration of anti IgE reduces IgE concentrations in the blood and tissue. Moreover, anti IgE treatment gradually decreases the density of IgE-FcεRI on MCs by 95% within a few months (13). Considering the ability of anti IgE treatment to reduce the release of mediators following MCs activation and the promising role of MCs in OA, we wondered if the stabilizing effect of Omalizumab on MCs would change the pain and disability in knee osteoarthritis. Our data showed that patients in therapy with Omalizumab, affected by knee OA, had a statistically significant improvement in reducing pain and recovering articular function from basal evaluation to 3- and 6-month follow-up visits.

To date, a growing evidence suggests the potential role of MCs in inflammatory arthritis (14), but at the same time, recent investigations questioned if MCs might be implicated in OA clinic and pathogenesis (7). Following their activation, a wide range of mediators, both preformed and newly produced, are released. Some of these mediators, such as histamine, cytokines and neurotrophins (e.g. NGF) might contribute to the synovium inflammation and pain

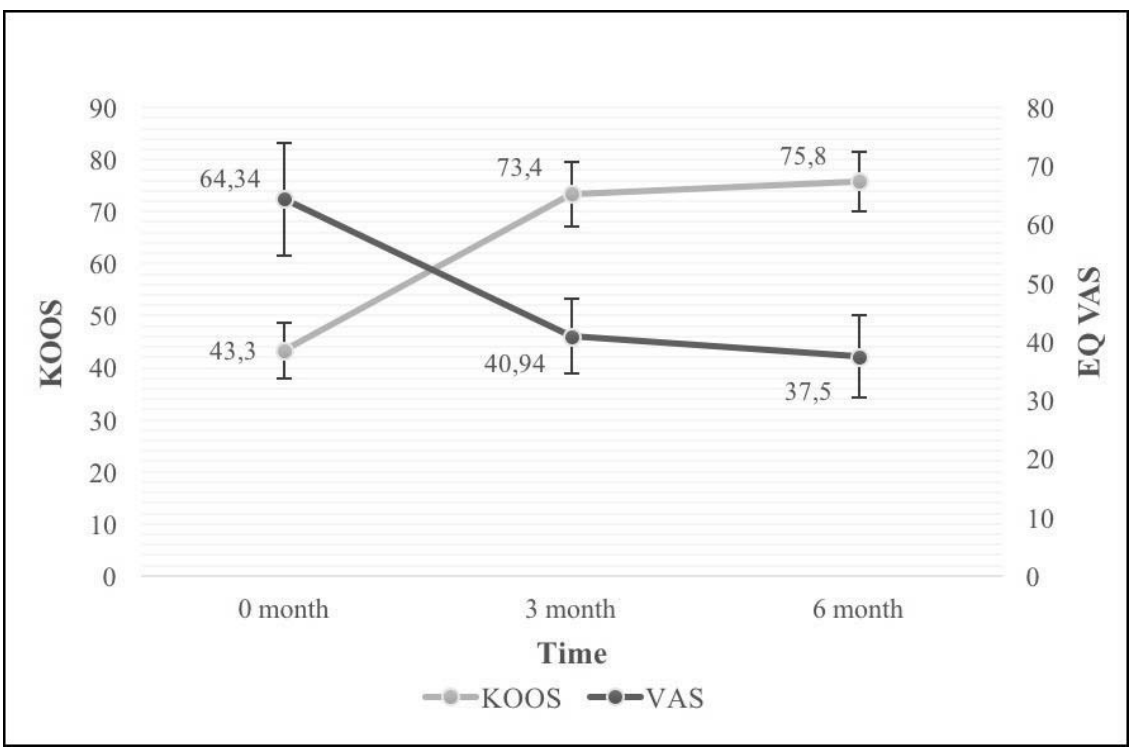

Fig. 1. *Pre- and post-treatment values of EQ VAS and KOOS.*

reported by patient. Although the most conceivable and latest theories of OA pathogenesis implicate that the activation of the innate immune system as MCs is mediated by TLRs (15), we can hypothesize that in these atopic patients, the improvement of clinical data were due to the partial blockage of MCs activation, via IgE related. This is not surprising, considering that the mechanisms involved in MCs activation or recruitment in OA could be very different.

However, these results have limitations. First, only a small cohort of patients was included, because the majority of patients in treatment with Omalizumab were too young to be affected by OA.

It would be interesting to understand if Xolair might be effective to decrease the prevalence of OA in atopic patients, supporting the role of MCs in the pathogenesis of the disease. Moreover, these data were obtained in a hypothesis generating setting and require replication. Secondly, we did not analyze the serum of these patients and we did not know if the improvement was correlated to the amount of IgE in serum.

To the best of our knowledge, no research has been conducted to underline the differences of OA in atopic and non-atopic patients, regarding synovium inflammation and characterization of inflammatory infiltrate. Therefore, the role of MCs in the different subtypes of OA is still unclear. Even considering these limitations, the results of our study are quite intriguing.

We presented evidence suggesting that the activation of MCs might be correlated to the pain and disability reported by patients. Hence, it could be hypothesized that future biological therapies involving IgE activation pathways might be useful tools to lead symptomatic improvement through inhibition of MCs degranulation and reduction of synovium inflammation (16).

Thus, additional research is required to understand the interplay between MCs, synovitis and activation of innate immune system in OA.

REFERENCES

1. Cross M, Smith E, Hoy D, et al. The global burden of hip and knee osteoarthritis: estimates from the global burden of disease 2010 study. Ann Rheum Dis 2014; 73(7):1323-30.
2. Samuels J, Krasnokutsky S, Abramson SB. Osteoarthritis: a tale of three tissues. Bull NYU Hosp Jt Dis 2008; 66(3):244-50.
3. de Lange-Brokaar BJ, Ioan-Facsinay A, Yusuf E, et al. Association of pain in knee osteoarthritis with distinct patterns of synovitis. Arthritis Rheumatol 2015; 67(3):733-40.
4. Orlowsky EW, Kraus VB. The role of innate immunity in osteoarthritis: when our first line of defense goes on the offensive. J Rheumatol 2015; 42(3):363-71.
5. Akira S, Takeda K. Toll-like receptor signalling. Nat Rev Immunol 2004; 4(7):499-511.
6. Sellam J, Berenbaum F. The role of synovitis in pathophysiology and clinical symptoms of osteoarthritis. Nat Rev Rheumatol 2010; 6(11):625-35.
7. de Lange-Brokaar BJ, Kloppenburg M, Andersen SN, et al. Characterization of synovial mast cells in knee osteoarthritis: association with clinical parameters. Osteoarthritis Cartilage 2016; 24(4):664-71.
8. Galli SJ, Maurer M and Lantz CS. Mast cells as sentinels of innate immunity. Curr Opin Immunol 1999; 11:53-9.
9. Suurmond J, Rivellese F, Dorjee AL, et al. Toll-like receptor triggering augments activation of human mast cells by anti- citrullinated protein antibodies. Ann Rheum Dis 2015; 74:1915-23.
10. Giménez-Arnau AM. Omalizumab for treating chronic spontaneous urticaria: an expert review on efficacy and safety. Expert Opin Biol Ther 2017; 17(3):375-385.
11. Normansell R, Walker S, Milan SJ, Walters EH, Nair P. Omalizumab for asthma in adults and children. Cochrane Database of Systematic Reviews 2014, Issue 1. Art. No.: CD003559.
12. Chang TW. The pharmacological basis of anti-IgE therapy. Nat Biotechnol 2000; 18:157-62.
13. Chang TW, Shiung YY. Anti-IgE as a mast cell-stabilizing therapeutic agent. J Allergy Clin Immunol 2006; 117(6):1203-12.

14. Rivellese F, Nerviani A, Rossi FW, Marone G, Matucci-Cerinic M, de Paulis A, Pitzalis C. Mast cells in rheumatoid arthritis: friends or foes? Autoimmun Rev 2017; 16(6):557-63.
15. Liu-Bryan R. Synovium and the innate inflammatory network in osteoarthritis progression. Curr Rheumatol Rep 2013; 15(5):323.
16. Nigrovic PA, Lee DM. Synovial mast cells: role in acute and chronic arthritis. Immunol Rev 2007; 217:19-37.

CLINICAL AND RADIOGRAPHIC SHORT MID-TERM OUTCOMES OF PRIMARY TOTAL STABILIZER KNEE ARTHROPLASTY

E. BONICOLI, N. PIOLANTI, M. GIUNTOLI, S. POLLONI, G. CIAPINI, P.D. PARCHI and M. SCAGLIONE

First Orthopaedic Division, University of Pisa, Pisa, Italy

A successful Total Knee Arthroplasty (TKA) requires stability, but rarely in primary TKA, a prosthesis with more constraint than a posterior-stabilizer (PS) is necessary. In patients with severe varus/valgus deformities with incompetent collateral ligaments or in knees that cannot be adequately balanced after ligaments release, a total-stabilizer (TS) prosthesis may be required. The purpose of our retrospective study is to evaluate clinical and radiographic outcomes at short mid-term follow-up in patients treated with a TS TKA. Between January 2013 and August 2016, 36 patients (38 knees) were treated with Stryker Triathlon TS cemented implants. Clinical and radiographic evaluation were performed preoperatively and postoperatively at 1 month, 3 months, 6 months, 1 year and at 1-year intervals thereafter. At final follow-up, 33 patients (35 knees) remained and were included in this study and followed with a mean follow-up of 26.6 months. Clinical evaluation was performed using the Western Ontario and McMaster Universities Arthritis Index (WOMAC score) and the Knee Society rating system that is subdivided into a knee score (KS) that rates only the knee joint itself and a functional score (FS). Knee Score (KS) and Functional Score (FS) increased significantly from a mean pre-operative value of 48 and 45, respectively, to a post-operative value at last follow-up of 86 and 82, respectively. Also WOMAC score improved significantly: the mean pre-operative WOMAC score was 45, while the mean post-operative WOMAC score, at last follow-up, was 19. The difference between pre- and post- operative results was significant at statistical analysis. In our opinion, when the adequately prosthesis balancing isn't possible, because of primary or secondary severe varus/valgus deformity or severe soft tissues retraction, an available option is to perform a total knee arthroplasty with a total stabilizer polyethylene insert. TS prosthesis gives more stability during the most of ROM and, in addition, Triathlon system provides surgeons the possibility to choose a more constrained implant, than a standard PS one, during surgical procedure saving the bone stock. Our experience with this kind of prosthesis has provided good clinical and radiographic outcomes at a short mid-term follow-up with a low-rate of complications.

A successful Total Knee Arthroplasty (TKA) requires stability; in fact, instability is a well-known cause of prosthesis failure (1-4). Using a prosthesis with increased component constraint may reduce instability, but Constrained Condylar Knee (CCK) has several theoretical disadvantages due to increased forces transmission to implant interfaces and to the presence of polyethylene particle shedding, that may lead to premature aseptic loosening (5). Rarely the use of a prosthesis with more constraint than a

Key words: primary total knee arthroplasty, TKA, total stabilizer, semi constrained condylar knee, CCK

Mailing address:
Dr. Giuntoli Michele,
1st Orthopaedic Division,
University of Pisa,
Via Paradisa 2, 56100 Pisa, PI, Italy
Tel.: +39 050996527
e-mail: michelegiuntoli87@gmail.com

0393-974X (2017)

posterior stabilizer is necessary in primary TKA (6-8). However, constrained condylar knees (CCKs) may be required in patients with severe varus/valgus deformities and incompetent collateral ligaments, or in those knees that cannot be adequately balanced (like severe fixed varus/valgus deformity or fixed flexion contracture) after ligaments release (6). Although relative few studies describing the use of CCKs prostheses for primary TKA were published (4), the use of this kind of system does not seem to reduce the range-of-motion (ROM) or functional outcomes compared to PS TKA (9).

The purpose of our retrospective study is to evaluate clinical and radiographic outcomes at a short mid-term follow-up (FU) in patients with severe varus/valgus deformities or knee instability treated with a Total Stabilizer (TS) prosthesis.

MATERIALS AND METHODS

This single-centre retrospective study was approved by our local ethical committee, and has therefore been performed in accordance with the ethical standards laid down in the 1964 Declaration of Helsinki and its later amendments. All patients gave written consent.

A review of our database was carried out between January 2013 and August 2016 for primary TKA. In this period, we performed 607 TKA; we selected patients who underwent a primary TKA with Stryker Triathlon Total Stabilizer cemented implants only, therefore 36 patients (38 knees) were enrolled. Information about ages, sex, clinical history, drugs treatments, and preoperative and postoperative X-rays studies were collected and recorded. Stryker Triathlon prosthesis design provides the possibility to shift from PS polyethylene insert to a TS one intra-operatively; if the stability is not satisfactory, the surgeon can choose to provide more stability by changing the polyethylene insert (Fig. 1).

Our indications for Total Stabilizer TKA were tibial-femoral arthritis (Ahlbäck Grades 4 or 5, Kallgren-Lawrence's stages III or IV) with severe varus/valgus deformities, varus/valgus laxity over 3 mm during the whole range of movement, elderly patients with knee instability or body mass index (BMI) over 35. Standard antibiotic prophylaxis was performed according to international guidelines (10). All patients performed anti-thromboembolic prophylaxis with low molecular weight heparin.

All procedures were always performed by the same experienced orthopedic surgeons (ML, EB) using the same design of TKA prostheses (Triathlon Total Knee Replacement System with Total Stabilizer polyethylene insert, Stryker®, Kalamazoo, MI, USA) with cemented 50 mm tibial-stem extension. An inflated pneumatic tourniquet (350 mmHg) was set around the upper thigh of the lower limb before starting the cementation stage and deflated after the closure of the wound and the bandage of the leg.

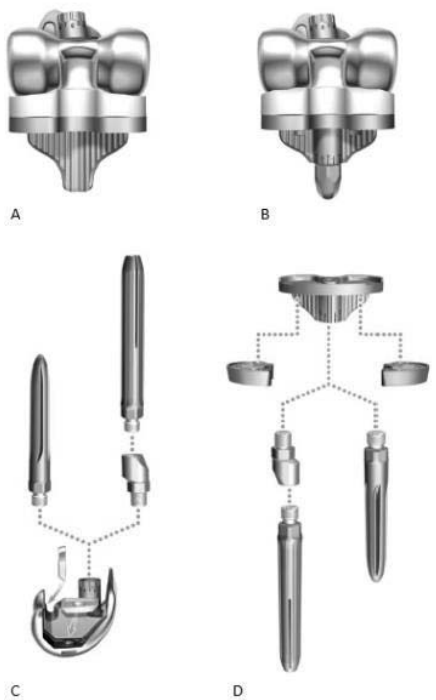

Fig 1. ***A****: Stryker Triathlon System with TS femoral component, PS insert and standard tibial tray.* ***B****: Stryker Triathlon System with TS femoral component, TS insert and universal tibial tray. (TS insert can be applied only with universal tibial tray, while PS insert can be applied with both tibial tray: standard and universal).* ***C****: Modularity of TS femoral component provides the possibility to employ different length stems; in our series for primary TKA we didn't employed stems for femoral component.* ***D****: Modularity of universal tibial tray provides the possibility to employ augments and different length stems; in our series for primary TKA we employed 50 mm-length stems for tibial component.*

All procedures were performed through a standard mid-vastus approach. The distal femur cut (8/10 mm) was made using an intramedullary guide, setting the degrees of valgus to perform femoral cut perpendicular to femoral mechanical axis according to pre-operative planning based on the angle between anatomical and mechanical axes of the femur. Subsequently, the proximal tibial cut was performed perpendicular to tibial mechanical axis with zero degrees of posterior slope, using an extra-medullary guide. The extension gap was then checked with a specific spacer block and soft tissues release was accurately performed. Subsequently, flexion gap was compared to extension gap and distal femur cut was completed after the evaluation of varus/valgus laxity using Mc. Bride instrumentation. The trial components were placed and range of motion, stability, geometry of the implant and patellar tracking were evaluated. Varus/valgus laxity was evaluated at 0, 40, 60 and 90 degrees of ROM with trial components correctly positioned: if the residual gap in lateral or medial knee compartment was wider than 3 mm, a TS polyethylene insert was chosen, as previously indicated. If necessary patellar resurfacing was made with a freehand cut. Trial components were removed and final components were positioned. An intra-articular drainage was applied until the second day after surgery.

Patients were allowed to bear weight the day after surgery and to get up and down the stairs the second day after surgery with the aid of a physiotherapist.

Patients had clinical and radiographic evaluations preoperatively and postoperatively at 1 month, 3 months, 6 months, 1 year, and at 1-year intervals thereafter. The clinical evaluation was performed using the Western Ontario and McMaster Universities Arthritis Index (WOMAC score) that is subdivided in three parts and measures pain (score range 0-20), stiffness (score range 0-8), and functional limitation (score range 0-68) (11-14), and the Knee Society rating system that is subdivided into a knee score (KS) that rates only the knee joint itself and a functional score (FS) that rates the patient's ability to walk and climb stairs (15-17). WOMAC score ranges from a minimum of 0 (excellent) to a maximum of 96 (poor). The KS and FS range from 0 (poor) to 100 (excellent). Radiographic evaluation consisted of AP view (weightbearing) and a lateral view. Radiolucent lines were measured in millimeters for the femoral and tibial prostheses in the coronal and sagittal planes according to the method recommended by the Knee Society roentgenographic score. Preoperative planning and post-operative radiographic evaluation (lower limb alignment, polyethylene wear and osteolysis) was performed using Synapse®PACS, Fujifilm Tokyo Japan. Statistical analysis was performed calculating the mean value of each score and compared the pre- and post-operative results using a *t*-student test with Microsoft Excel 2013 data analysis program.

RESULTS

At time of surgery the mean age was 70-years-old (range 60-82) and gender distribution was 26 females and 10 males. The mean BMI was 27.2 (range 20.1-43.8). Two patients (two knees) were excluded because they were lost to follow-up and 1 other patient was deceased (1 knee). At final follow-up, 33 patients (35 knees) remained and were included in this study, with a mean follow-up of 26.6 months (range 13-55) (Table I). In 32 knees, the diagnosis was primary arthritis, while in 3 knees the diagnosis was post-traumatic arthritis. Two patients underwent arthroscopic procedures beforehand (one for anterior cruciate ligament (ACL) reconstruction and the other one for meniscal regularization).

Knee Score (KS) and Functional Score (FS) increased significantly from a mean pre-operative value of 48 and 45, respectively, to a post-operative value at last follow-up of 86 and 82, respectively. Also WOMAC score improved significantly. The mean pre-operative WOMAC score was 45, while the mean post-operative WOMAC score was 19 at last follow-up. The difference between pre- and post- operative results was significant at statistical analysis (Table II). Almost all patients achieved pain-relief, gained a better functional autonomy (such as climbing stairs, walking for long distances, tying shoes), better articular mobility and alignment.

Only two patients resulted in a post-operative score worse than the pre-operative one. One of these, a 77-year-old woman, suffered from wound

Table I. *Main patients' characteristics.*

Demographics features	Number or mean	Range
Mean age, years	70	60-82
Patients/knees at final FU	33/35	
Follow-Up mean months	26.6	13-55
BMI mean	27.2	20.1-43.8

Table II. *Clinical results and statistical analysis.*

Clinical test	mean pre-operative	mean post-operative	P-value (T≤t)
KSS KS	48	86	< 0.00000001
KSS FS	45	82	< 0.000001
WOMAC score	45	19	< 0.00001

KS: *Knee Score;* ***FS:*** *Functional Score.*

Table III. *Radiographic results.*

Deformity	N°	mean pre-op degrees	mean post-op degrees
Pre-op. varus deformity <15°	22	5.3° (range 4°-7°)	
Pre-op. valgus deformity ≥7°	13	17.7° (range 2°-26°)	
Mean aFTA			3.5° of valgus

aFTA: *anatomical femoro-tibial angle.*

dehiscence and patellar tendon rupture a few days after discharge, which resulted in a pre-operative KS of 50, a pre-operative FS of 55 and a WOMAC pre-operative score of 45. Post-operative scores were 38 at KS, 35 at FS and a 65 at WOMAC score, respectively. The other patient, a 65-year-old male, resulted in a WOMAC pre-operative score of 35 in contrast to the WOMAC post-operative score of 42. He suffered for a symptomatic spinal disc disease. Clinical outcomes of the operated knee had clearly improved, but the patient was not able to reach a greater global autonomy due to the worsening of spinal symptoms.

The anatomical Femoral-Tibial Angle (aFTA), was used to evaluate pre- and post- operative alignment of knees on X-rays. We assumed an angle of 7° of valgus as normal. At pre-operative radiographic analysis, 22 knees had varus deformity less than 15°; none of them had varus deformity more than 15° and 13 knees had excessive valgus deformity (≥7°). Considering the aFTA, the mean preoperative varus deformity was 5.3° (range 4°-7°) and the mean preoperative valgus deformity was 17.7° (range 2°-26°). The mean postoperative aFTA was 3.5° of valgus (Table III). Two knees presented radiolucent lines (RLLs) around the stem of tibial component on AP X-rays, while another knee showed RLLs around femoral component on the lateral X-rays.

One of these patients presented radiolucent lines around the tip of tibial stem over 2 mm in thickness with pain during loading in the proximal tibia, probably a sign of initial mobilization. RLLs detected in the others cases were <2 mm in thickness and non-progressive at last follow-up. Unclear polyethylene wear or osteolysis was detected at last follow-up. Remaining knees did not show RLLs on postoperative X-rays (Fig. 2).

At post-operative X-rays, in two cases, tibial stem pointed towards lateral bone cortical of the proximal tibia, even if mechanical axis was restored. In these two cases, pre-operative X-rays had shown severe varus deformity, but patients didn't have pain at last follow-up and their clinical outcomes had improved.

We reported wound dehiscence and patellar tendon rupture in one patient that was treated with wound debridement, antibiotics therapy and patellar tendon repair. Any infections, peri-prosthetic fractures or aseptic loosening was kept under observation during the follow-up. Only one patient presented signs of initial aseptic mobilization.

DISCUSSION

Most preoperative deformities of osteoarthritic knees can be successfully treated with a standard PS prosthesis by carefully balancing the soft tissues. Often in varus knee deformities an accurate release of the medial structures associated with an accurate tensioning of lateral compartment can reduce instability. However there are varus/valgus deformities associated with severe medial or lateral instability that cannot be carefully treated with a PS TKA but require the use of more constrained system to provide stability throughout the whole range of movement (ROM) (18). Instability in TKA is an important cause of early revision surgery (1-4, 19). Therefore, in selected cases, a CCK prosthesis may be required, but there is a moderate distrust in its use due to increased stress at implant surfaces and to the risk of aseptic loosening. In any case, the use of stems seems to decrease stress at bone-implant interface (20-23), although good results were also reported with the use of non-stemmed constrained condylar knee (24-27).

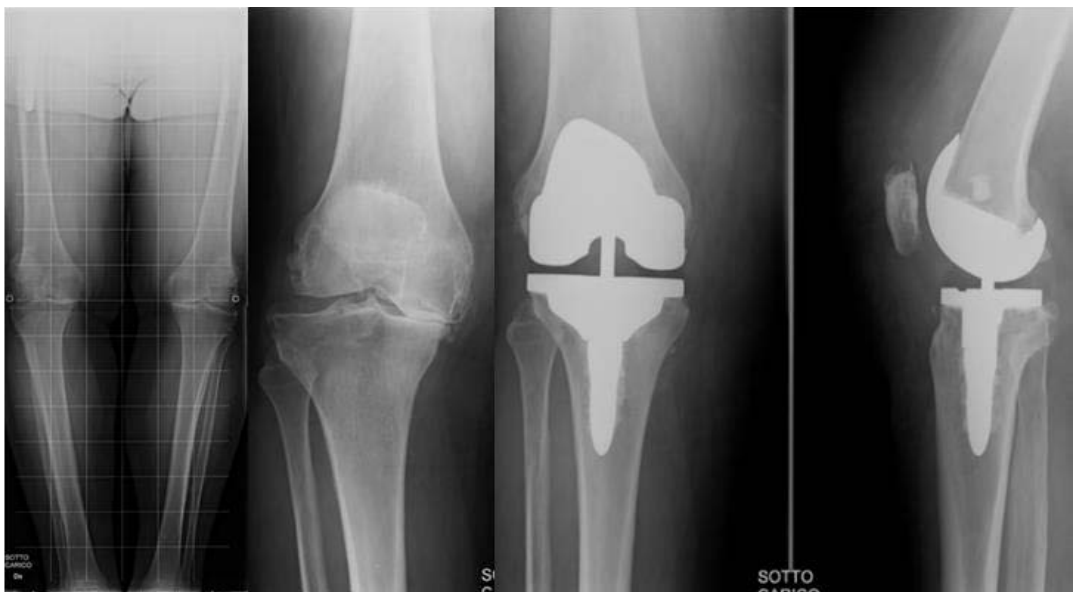

Fig. 2: *Female patient with BMI of 40 affected by severe pre-operative varus deformity (aFTA: 176°) treated with Stryker Triathlon TS TKA. Preoperative KS was 57/100 , preoperative FS was 50/100 and preoperative WOMAC score was 53/96 while postoperative outcomes were 87/100, 90/100 and 14/96 for KS,FC and WOMAC scores respectively.*

As reported, non-stemmed constrained condylar knee require less surgical time, reduce risk of infection and allow greater saving of bone stock, making revision surgery easier (28). Nevertheless, use of increased constraint polyethylene without a stem may cause component loosening due to increased stress forces at implant bone interfaces (29-30). In our series, the use of 50 mm cemented tibial-stem gave more stability and decreased stress forces, reducing risk of aseptic loosening. No cases of component mobilization were recorded at last follow-up, only one knee presented non-progressive radiolucent lines around tibial component. However, the patient was satisfied and no pain increase or functional decrease were recorded.

In a retrospective study, Maynard et al. (4) analyse clinical and radiographic outcomes of 127 NexGen Legacy Constrained Condylar Knees LCCK (Zimmer, Warsaw, IN), as primary TKA in 119 patients at a minimum follow-up of 7 years. Their inclusion criteria were varus/valgus deformities associated with a persistent laxity (medial or lateral) greater than 5mm after ligamentous balance. They had 19.6% of complications (25 knees): in particular they did not have any case of aseptic loosening, 2 cases (1.6%) of infection, 6 cases of Patellar clunk syndrome (4.8%) and 4 cases of peri-prosthetic fractures (3.2%). The revision rate was 10.2% (10 knees) and radiolucent lines were found in 9.4% cases. Lachiewicz et al. in a prospective study (31) reported clinical and radiographic results of 27 consecutive knees treated with a LCCK prosthesis with a mean follow-up of 5.4 years. In their study, there were no revisions for loosening or tibial post fractures. Cholewinski et al. (32) studied 43 knees after LCCK prosthesis with a 12.7 years long-term follow-up. They reported 16% of complications including 3 patients that required revision surgery (2 of them for septic loosening), while they had no cases of osteolysis or aseptic loosening and clinical outcomes increased significantly at final follow-up.

They concluded that functional gains after CCK TKA are similar to those reported after standard PS TKA, but complication rates are higher. In our series, there were 2 patients that did not have clinical improvement. In the first case on a female patient, the negative results were due to the partial rupture of the patellar tendon after surgery (which required a reinsertion of the tendon itself) and to the comorbidity of the patient, (she presented severe valgus deformity of the other knee, severe contralateral hip arthritis and a BMI of 43.3 at the last FU). The second patient was suffering for symptomatic spinal disc disease, which limited the overall performance.

We report only few cases of complications and in only one case, surgical revision was necessary for patellar tendon breakage, with no infection, fracture or aseptic loosening. The main limitation of this study is the type of study (retrospective with relative complication), the small number of patient samples and short follow-up. The small number of patients included is due to the closed inclusion criteria. It is important to emphasize that clinical and radiographic results overlap the classical PS TKA, despite severe deformity and instability of the knees before surgery. In our series, two patients presented tibial stem pointing towards lateral bone cortical of the proximal tibia. These two patients presented a severe preoperative varus deformity, but lower limb mechanical axis was restored and the patients did not have clinical disadvantages at last follow-up. This limitation is due to implant design that does not provide the possibility to implant offset stems. We suggest performing a detailed preoperative planning to avoid this "complication". Furthermore, modularity of Triathlon prosthesis provides us with the possibility to shift from a PS design to a TS one intra-operatively simply changing the polyethylene insert giving more stability without cutting more bone tissue.

Cam-post engagement in Triathlon TS TKA system takes place at 40-45 flexion degrees, just like in a normal knee. This feature, coupled with an increased width and height of the post, provides more stability than a standard PS prosthesis during the most of ROM. The cam slides along the post during knee flexion reducing stress forces on polyethylene insert fixation system and reducing dislocation probability, while increasing the height of dislocation (33, 34). The possibility to shift from a PS insert to a TS one intra-operatively, allows the surgeon to choose the right knee constraint, especially in severe varus/valgus knee where collateral ligaments (medial or lateral respectively in varus or valgus osteoarthritic knee) are very retract, making a

correct balancing of soft tissue difficult. In these knees, a semi-constrained prosthesis, like TS, gives more stability providing a good articular ROM.

In our opinion elderly patients (over 75-years-old) have advantages from this kind of prosthesis, in fact their knees often present advanced osteoarthritis with severe deformities and more instability than younger patients due to less activity, reduced tissue quality and reduced muscular tropism. Obese patients with BMI over 35 can also take great advantage from TS prosthesis; in these patients, mechanical stress on prosthesis are greater than in a normal population and the risk of aseptic loosening or mechanical failure is higher. Several authors (35, 36) report good results using a primary CCK prosthesis in elderly patients with severe varus/valgus knee also, supporting our hypothesis.

In conclusion, even if in the last years improvements have been achieved in TKA, stability remains the most important factor that influence the success of a total knee arthroplasty (37). This result is due to a careful balancing of soft tissues. If it is not possible because of primary or secondary severe varus/valgus deformity or severe soft tissues retraction, a possibility is to implant a total knee arthroplasty with a total stabilizer polyethylene insert. TS prosthesis gives more stability during the most of ROM and in addition, Triathlon system give surgeons the chance to choose a more constrained implant compared to a standard PS one during the surgical procedure, saving the bone stock. These features make it indicated, in our opinion, in severe varus/valgus knees and in elderly patients (over 75). Our experience with this kind of prosthesis has provided good clinical and radiographic outcomes at a short mid-term follow-up with a low-rate of complications. However, further studies are needed to confirm these results at long-term follow-up.

REFERENCES

1. Fehring TK, Odum S, Griffin WL, Mason JB, Nadaud M. Early failures in total knee arthroplasty. Clin Orthop Relat Res 2001; 392:315-8.
2. Clarke HD, Scuderi GR. Flexion instability in primary total knee replacement. J Knee Surg 2003; 16:123-8.
3. Besson A, Brazier J, Chantelot C, Migaud H, Gougeon F, Duquennoy A. Laxityand functional results of Miller-Galante total knee prosthesis with posterior cruciate ligament sparing after a 6-year follow-up. Rev Chir Orthop 1999; 85: 797-802.
4. Maynard LM, Sauber TJ, Kostopoulos VK, Lavigne GS, Sewecke JJ, Sotereanos NG. Survival of primary condylar-constrained total knee arthroplasty at a minimum of 7 years. J Arthroplasty 2014; 29:1197-201.
5. Morgan H, Battista V, Leopold SS. Constraint in primary total knee arthroplasty. J Am Acad Orthop Surg 2005; 13:515
6. Paul F. Lachiewicz, MD, and Elizabeth S. Soileau, BSN, RN. Ten-year survival and clinical results of constrained components in primary total knee arthroplasty. J Arthroplasty 2006; 21(6):803-8.
7. Naudie DDR, Rorabeck CH. Managing instability in total knee arthroplasty with constrained and linked implants. AAOS Inst Course Lect 2004; 53:207.
8. Insall J, Lachiewicz PF, Burstein AH. The posterior stabilized condylar prosthesis: a modification of the total condylar design: two to four year clinical experience. J Bone Joint Surg 1982; 64A:1317.
9. King BR, Gladnick BP, Lee YY, Lyman S, Della Valle AG. Range of motion and function are not affected by increased post constraint in patients undergoing posterior stabilized total knee arthroplasty. Knee 2014; 21:194-8.
10. Lisanti M, Piolanti N, Tagliaferri E, Andreani L, Parchi P, Menichetti F. The fight against the slime: can we ever win? Springer International Publishing, Switzerland. Perioperative medical management for total joint arthroplasty. 253-67.
11. Bellamy N, Buchanan WW, Goldsmith CH, Campbell J, Stitt LW. Validation study of WOMAC: a health status instrument for measuring clinically important patient relevant outcomes to antirheumatic drug therapy in patients with osteoarthritis of the hip or knee. J Rheumatol 1988; 15(12):1833-40.
12. Davies GM, Watson DJ, Bellamy N. Comparison of the responsiveness and relative effect size of the western Ontario and McMaster Universities Osteoarthritis Index and the short-form Medical Outcomes Study Survey in a randomized, clinical trial of osteoarthritis patients. Arthritis Care Res 1999; 12(3):172-9.
13. Bellamy N. The WOMAC Knee and Hip

Osteoarthritis Indices: development, validation, globalization and influence on the development of the AUSCAN Hand Osteoarthritis Indices. Clin Exp Rheumatol 2005; 23(5S39):S148-53.
14. Western Ontario and McMaster Universities Osteoarthritis Index (WOMAC) - http://www.rheumatology.org/I-Am-A/Rheumatologist/Research/Clinician-Researchers/Western-Ontario-McMaster-Universities-Osteoarthritis-Index-WOMAC.
15. Insall JN, Dorr LD, Scott RD, Scott WN. Rationale of the Knee Society clinical rating system. Clin Orthop Relat Res 1989; 248:13-4.
16. Ewald FC. The Knee Society total knee arthroplasty roentgenographic evaluation and scoring system. Clin Orthop Relat Res 1989; (248:9-12.
17. Giles R. Scuderi, Robert B. Bourne, Philip C. Noble, James B. Benjamin, Jess H. Lonner, W. N. Scott. The New Knee Society Knee Scoring System. Clin Orthop Relat Res 2012; 470(1):3-19.
18. Callaghan JJ, O'Rourke MR, Liu SS. The role of implant constraint in revision total knee arthroplasty: not too little, not too much. J Arthroplasty 2005; 20(4S2):41-3.
19. Sharkey PF, Hozack WJ, Rothman RH, et al. Why are total knee arthroplasties failing today? Clin Orthop Relat Res 2002; 404:7-13.
20. Bertin KC. Tibial component fixation in total knee arthroplasty: a comparison of pegged and stemmed designs. J Arthroplasty 2007; 22(5):670-8.
21. Rawlinson JJ, Peters LE, Campbell DA, et al. Cancellous bone strains indicate efficacy of stem augmentation in constrained condylar knees. Clin Orthop 2005; 440:107.
22. Conlisk N, Gray H, Pankaj P, et al. The influence of stem length and fixation on initial femoral component stability in revision total knee replacement. Bone Joint Res 2012; 1(11):281.
23. Pérez-Blanca A, Prado M, Ezquerro F, et al. Addition of a short central extension to surface cemented tibial trays in primary TKA: an in vitro study of the effect on initial fixation stability and its relationship to supporting bone density. Clin Biomech 2008; 23(4):483.
24. Anderson JA, Baldini A, MacDonald JH, et al. Primary constrained condylar knee arthroplasty without stem extensions for the valgus knee. Clin Orthop 2004; 443:199.
25. Anderson JA, Baldini A, MacDonald JH, et al. Constrained condylar knee without stem extensions for difficult primary total knee arthroplasty. J Knee Surg 2007; 20:195.
26. Nam D, Umunna BP, Cross MB, et al. Clinical results and failure mechanisms of a nonmodular constrained knee without stem extensions. HSS J 2012; 8:96.
27. Padgett DE, Cottrell J, Kelly N, et al. Retrieval analysis of nonmodular constrained tibial inserts after primary total knee replacement. Orthop Clin North Am 2012; 43:e39.
28. Moussa ME, Lee YY, Patel AR, Westrich GH et al. Clinical Outcomes Following the Use of Constrained Condylar Knees in Primary Total Knee Arthroplasty. J Arthroplasty. 2017; S0883-5403(17)30002-5.
29. Stern SH, Wills RD, Gilbert JL. The effect of tibial stem design on component micromotion in knee arthroplasty. Clin Orthop Relat Res 1997; (345):44.
30. Yoshii I, Whiteside LA, Milliano MT, et al. The effect of central stem and stem length on micromovement of the tibial tray. J Arthroplasty 1992; 7(S):433-8.
31. Lachiewicz PF, Soileau ES. Results of a second generation constrained condylar prosthesis in primary total knee arthroplasty. J Arthroplasty 2011; 26:1228.
32. Cholewinski P, Putman S, Vasseur L, Migaud H, Duhamel A, Behal H, Pasquier G. Long-term outcomes of primary constrained condylar knee arthroplasty. Orthop Traumatol Surg Res 2015; 101(4):449-54.
33. Fu, Freddie, et al. Biomechanics of Knee Ligaments: Basic concepts and Clinical Application JBJS Noc 1993; 75:1716-27.
34. Puloski, S.K.T.,McCalden, R.W. et al. Tibial Post wear in Posterior Stabilized Total Knee Arthroplasty JBJS 2001; 83.
35. Sabatini L, Risitano S, Rissolio L, Bonani A, Atzori F, Massè A. Condylar constrained system in primary total knee replacement: our experience and literature review. Ann Transl Med 2017; 5(6):135.
36. Easley ME, Insall JN, Scuderi GR, Bullek DD. Primary Constrained Condylar Knee Arthroplasty for the Arthritic Valgus Knee. Clinical orthopaedics and related research number 2000; 380:58-64.
37. Bonicoli E, Andreani L, Parchi P, et al. Custom-fit total knee arthroplasty: our initial experience with 30 Knees. Eur J Orthop Surg Traumatol 2014; 24:1249-54.

RECONSTRUCTIVE TECHNIQUES FOR REVISION AND LIMB SALVAGE SURGERY IN PERSONS WITH HAEMOPHILIA

C. CARULLI, M. ZAGO, A.R. RIZZO and M. INNOCENTI

Orthopaedic Clinic, Department of Surgery and Translational Medicine University of Florence, Italy

Haemophilia is an inherited haemorrhagic disease characterized by the lack of coagulative factors associated nowadays mostly to musculoskeletal complications, particularly severe secondary arthritis in specific joints. Recurrent traumatic or spontaneous joint bleeding, induce severe arthropathy at a young age that can be treated only by joint replacement. Total knee or hip arthroplasty in young subjects may fail earlier due to wear or infections and in the haemophilic population, this means bone loss, pseudo tumours and the need of revision or even limb salvage surgery. Modern modular implants and the use of bone graft enriched by tissue engineering techniques such as a concentration of autologous mesenchymal cells or PRP may be helpful to compensate all bone loss and anatomic alterations due to failures of orthopaedic implants. The authors present their experience with this type of surgery and their biological approach to these challenging cases.

Haemophilia is an inherited haemorrhagic disease affecting mostly male subjects and characterized by the lack of coagulative factor VIII or IX. Once associated to high rates of mortality, nowadays its main complications are found in musculoskeletal disorders (1). Subjects with Haemophilia (PWH) usually present symptoms and functional impairments in their joints as early as childhood: the so-called "target joints" are affected by recurrent bleeding and the induction of a specific condition over time called "haemophilic arthropathy" (1, 2). The early stages of disease can be treated by conservative or minimally invasive approaches (3, 4).

Moderate to late stages of arthropathy have to be managed through joint replacement even in the younger patients (5-9). An orthopaedic implant can fail for several reasons: the most frequent are aseptic loosening, infection, and instability (10, 11). In PWH, a joint replacement is generally performed at a very young age and can be at risk of early failure compared to osteoarthritic and older patients for two main reasons: aseptic loosening and infection (16-18). Aseptic loosening often related to bleeding after surgery (6, 9, 11-13) represents a common cause of failure in PWH. On the other hand, many generations of PWH suffer from infections with a dramatic rate of incidence, following joint replacements (12-14). Several factors are likely involved, such as recurrence of bleeding before and after surgery, the presence of inhibitors (antibodies against clotting factors) and the history of co-infections in haemophilic patients (HIV and Hepatitis) (14, 15).

Whatever the cause, loosening of orthopaedic implants in PWH are dramatic and usually are associated with bone loss, gross migration of components and in the more severe cases, to the

Key words: Haemophilia, revision arthroplasty, limb salvage surgery, issue engineering, mesenchymal cells, platelet rich plasma, bone graft

Mailing address:
Christian Carulli, MD,
Orthopaedic Clinic,
University of Florence,
Largo P. Palagi 1,
50139 Florence, FI, Italy
e-mail: christian.carulli@unifi.it

0393-974X (2017)

formation of pseudotumors (masses characterized by areas of destructured bone and fibrous tissue in bone segments close to the prosthetic components) (14). Specific patterns are infective failures associated with wide sinus tract infections and severe compromission of soft tissues, up to skin necrosis.

When an orthopaedic implant in these patients fails, various conditions may be found and most of them need a complex revision, sometimes configuring a limb salvage surgery. Such procedures may be rather difficult to be planned, usually have to be performed with intraoperative choice of strategy, and need reconstructive surgery techniques and modular prosthetic designs to be adapted to a very altered anatomy (14, 16, 17).

The aim of this paper is the evaluation of the results of complex revisions performed in a series of PWH affected by failures of orthopaedic implants.

MATERIALS AND METHODS

In the period 1999-2015, more than 1500 PWH have been visited and treated at the Multidisciplinary Outpatient office and Unit of Orthopaedics and Traumatology of the authors' Institution. Specifically, more than 200 PWH have been operated for several traumatic or degenerative alterations due to Haemophilia or its complications. Sixteen PWH have been treated for reconstructive surgery following failure of a previous joint replacement. The mean age of these male subjects was 43.6 (range: 37-55). Twelve presented a failure of a Total Knee Arthroplasty (TKA), while 4 a failure of Total Hip Arthroplasty (THA).

Diagnosis of implant failure was performed as for other orthopaedic patients. Clinical signs, blood examinations, synovial fluid analysis, imaging, and exclusion of other causes have been performed to confirm the suspect. Radiolucent lines and areas of osteolysis around acetabular cups, femoral stems, or femoral and tibial components were detected by standard radiographic studies. In the presence of pseudotumours, a MRI with contrast or a bone scan by marked leucocytes were prescribed to exclude any actual malignant lesion. Finally, in case of sinus tract or soft tissue mortifications, suspension of any antibiotic therapy before surgery was observed.

Once obtained the consent by patients, a revision was scheduled and planned with the other specialists of the institutional Haemophilia team.

Dedicated haematologists provided a tailored haematological prophylaxis by preoperative boli of the deficient coagulative factor and tranexamic acid, followed by administration of other boli at discrete postoperative intervals for at least two weeks. Antibiotic prophylaxis and general anaesthesia were performed. Direct lateral access for revision THA (rTHA) and longitudinal standard anterior access for rTKA were performed, following the previous scars. Coltural samples were taken and infected or loose components were removed. Depending on the integrity of bone, capsular and ligamentous structures, standard revision or modular megaprosthetic components were chosen for reconstruction.

Based on the evaluation of bone loss, tissue-engineering techniques were applied. In case of severe bone loss, following the classification of Paproswky in the hip (18) and of Anderson Orthopaedic Research Institute in the knee (19), harvest of bone marrow from the ipsilateral anterior and mid iliac crest combined with peripheral blood harvest were performed in order to obtain concentrated mesenchymal cells and PRP respectively. These were mixed with bone chips deriving either from the same iliac crest or from the local tissue bank (fresh frozen), obtaining a "biological composite" to fill any defect.

Nonetheless, in cases of severe joint destruction or pseudotumors (needing "*salvage surgery*"), it is necessary to adapt the implant to an altered anatomy of a joint with a previously failed prosthesis. The availability of wedges, stems, cones, offsets in the knee or wedges, insert, necks and heads in the hip is mandatory during surgery.

The choice of constraint in the knee and the diameter of the head and cup in the hip were chosen based on intraoperative X-rays and the experience of the two senior surgeons. In case of infected TKA or THA, the two-stage revision was performed. Nonetheless, in case of large sinus tract or wide skin defects, a staged or simultaneous surgical step with skin coverage by a local or free flap was performed. Timing for the first of two stages and for the second stage was generally equivalent to non-haemophilic subjects.

After surgery, patients were helped in a slow and careful early mobilization in their bed, generally for the first two days. Depending on their clinical conditions, they were then conducted to weight bearing exercises. No bracing was provided except for cases of postoperative instability.

All intraoperative parameters and complications were recorded. Postoperative rehabilitation was prolonged up to a sufficient weight bearing autonomy with crutches.

Follow-up visits were then performed at 1, 3 and 6 months and yearly after surgery. Evaluation were made by the Haemophilia Joint Health Score (HJHS)(20) and Numeric Rating Score (NRS), and radiograms were acquired for the analysis of implant positioning and integration.

RESULTS

No patient was lost at follow-up. The mean follow-up was 4.7 years (range: 2-11). In 7 cases, a limb salvage surgery was made, while in the remainders a revision was performed. Three out of 12 rTKAs and 2 out of 4 rTHAs were related to deep infection. The others were related to aseptic loosening, mostly due to recurrent bleedings and pseudotumors. In all cases of infected TKA, a two-stage revision was conducted. Among these cases, three patients underwent a procedure of plastic surgery with a local rotation of ipsilateral gemellus medialis graft to cover a sinus tract of the anterior aspect of the knee prior the two stages. One of the two infective THA failures were treated by a single-stage procedure, using antibiotic-loaded heterologous bone chips and implant revision, while the other case by a two-stage surgery. The other two cases were aseptic mechanical failures.

Cones, wedges, offests and cementless stems were used for rTKA following a previously released flowchart of intraoperative procedures (21). Cages and dual mobility cups were used for the revision of THA failures (22). In all cases, biological composites were used. Megaprostheses were used for more difficult cases.

No intraoperative complication was recorded. Postoperative complications were: a non fatal pulmonary embolism (rTHA), managed by intensive care unit monitoring; a delayed healing of the surgical scar (rTKA), managed by advanced medications; a postoperative haematoma in a rTKA, managed by local compression.

NRS scores, starting from a mean preoperative of 5.7 points (range: 4-8), improved to 1.2 (range: 0-2). HJHS was 112.2 (range: 98-122); postoperatively at the last follow-up, the mean value was 28.4 (range: 18–35) at the latest follow-up.

A single patient with Haemophilia A and inhibitors had another mechanical loosening due to recurrence

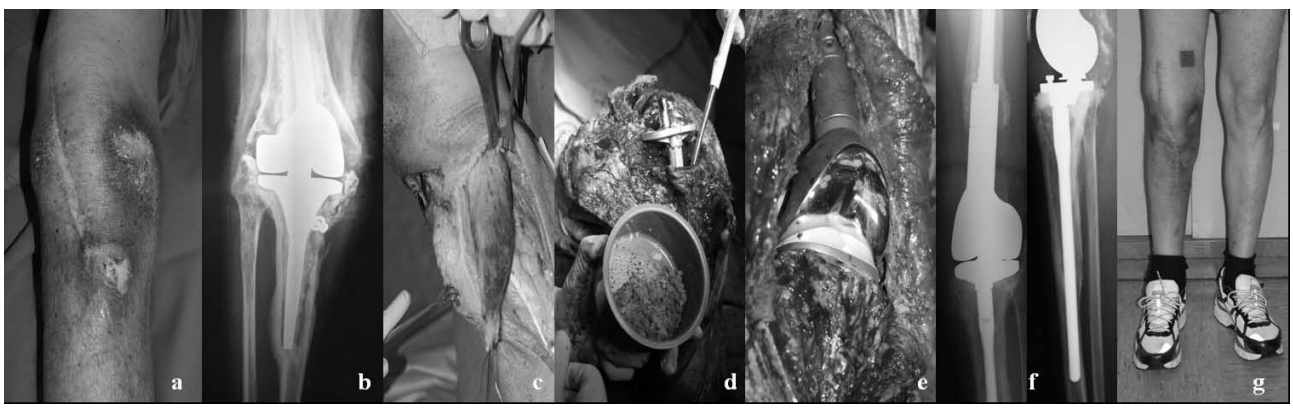

Fig. 1. *Case of surgery on a 57-year-old haemophilic with inhibitors and an infected failure of a cemented TKA implanted in another hospital 6 years prior. Wide sinus tract and soft tissue mortification (**a**) and severe septic loosening at X-rays (**b**). First procedure: plastic surgery for sinus tract removal and gemellus medialis coverage (**c**). After 2 months, two-stage procedure for revision and implant of a megaprosthesis with bone loss filling by a biological composite (**e**). Postoperative X-rays (**f**) and clinical aspect (**g**) 3 years after surgery.*

of bleedings 4 years after revision surgery. He was reoperated by a new revision and after 3.5 years, no recurrence was recorded.

At the radiographic study, progressive and <2mm radiolucent lines (but no osteolysis) were found over the years in the medial tibial plateau and in the anterior cortex of the femur in 4 rTKSs; radiolucency was also found in 2 of the 4 rTHAs around the femoral stem, but non progressive and not indicating further revision.

DISCUSSION

Haemophilic patients with joint replacements are at high risk of failure, mainly due to complications of the disease (bleedings and infections), and to their generally very young age. Revision rates are thus significant, as literature witnesses, particularly for PWH and inhibitors (6, 7, 12, 13, 23). Moreover, revisions in such patients are highly demanding and associated to further risks of complications. This is one of the reasons why few multidisciplinary equipes are dedicated to such surgery.

Once the implant failure is ascertained at time of revision, cement removal and management of bone defects and ligaments incompetency represent the most challenging steps, particularly in young subjects. The typical settings are pseudotumors, sinus tract infections, and severe bone loss: modern modular revision implants, bone substitutes, Tissue engineering techniques, and high-technology materials are mandatory to ensure good results. Autologous mesenchymal cell concentrations, PRP combined with bone grafts or synthetic bioceramics to enhance the local metabolism of the host bone (creating the so-called "biological composite") seems to be very useful in reconstructive surgery, particularly in failed THA or TKA implants (14). Often, megaprostheses have to be used instead of standard revision implants, as microsurgery techniques (rotational or propeller flaps) are usually applied to cover soft tissues defects related to infection. In the authors' institution, both choices are routinely adopted, while in other very few experiences are occasional (14, 24, 25).

Finally, the management of failed THAs or TKAs in PWH does not only mean great expertise during orthopaedic surgery, but a dedicated knowledge on behalf of the haematologists, anaesthesiologists, physical therapists, nurses and all the characters interacting with such patients (1, 14).

The management of a failed orthopaedic implants in haemophilic subjects may nowadays find in the application of Tissue engineering techniques a new useful tool to be associated to a rigorous surgical reconstruction and the use of modular prostheses, in order to ensure acceptable outcomes and low rates of complications, generally expected in such patients.

REFERENCES

1. White B, Lee CA. The diagnosis and management of inherited bleeding disorders. Chapter 1 in: Rodriguez-Merchan EC, Goddard NJ, Lee CA, editors. Musculoskeletal aspects of Haemophilia. Blackwell Science Ltd 2000.
2. Castaman G, Linari S. Haematological care of the haemophilic patient. Chapter 3 in: Christian Carulli editor, Frontiers in Arthritis, volume 2: The management of Haemophilic arthropathy. Bentham Science 2017; 25-40.
3. Carulli C, Civinini R, Martini C, et al. Viscosupplementation in haemophilic arthropathy: a long-term follow-up study. Haemophilia 2012; 18:e210.
4. Carulli C, Matassi F, Civinini R, et al. Intra-articular injections of hyaluronic acid induce positive clinical effects in knees of patients affected by haemophilic arthropathy. Knee 2013; 20:36.
5. Innocenti M, Civinini R, Carulli C, Villano M, Linari S, Morfini M. A modular total knee arthroplasty in haemophilic arthropathy. Knee 2007; 14(4):264–8.
6. Rodriguez-Merchan EC. Total knee replacement in haemophilic arthropathy. J Bone Joint Surg Br 2007; 89(2):186-8.
7. Kelley SS, Lachiewicz PF, Gilbert MS, Bolander ME, Jankiewicz JJ. Hip arthroplasty in hemophilic arthropathy. J Bone Joint Surg Am 1995; 77(6): 828-34.
8. Carulli C, Rizzo AR, Innocenti M. Hip Arthropathy in Haemophilia. J Clin Med 2017; 8:6(4).
9. Carulli C, Felici I, Martini C, Linari S, Castaman G, Civinini R, Innocenti M. Total Hip

Arthroplasty in Haemophilic Patients with Modern Cementless Implants. J Arthroplasty 2015; S0883-5403(15)00325-3.
10. Sharkey PF, Hozack WJ, Rothman RH, Shastri S, Jacoby SM. Insall Award paper. Why are total knee arthroplasties failing today? Clin Orthop Relat Res 2002; (404):7-13.
11. Carulli C, Villano M, Bucciarelli G, Martini C, Innocenti M. Painful knee arthroplasty: definition and overview. Clin Cases Miner Bone Metab 2011; 8(2):23-5.
12. Solimeno LP, Mancuso ME, Pasta G, Santagostino E, Perfetto S, Mannucci PM. Factors influencing the long-term outcome of primary total knee replacement in haemophiliacs: a review of 116 procedures at a single institution. Br J Haematol 2009; 145(2):227-34.
13. Sikkema T, Boerboom AL, Meijer K. A comparison between the complications and long-term outcome of hip and knee replacement therapy in patients with and without haemophilia; a controlled retrospective cohort study. Haemophilia 2011; 17(2):300-3.
14. Innocenti M, Carulli C, Civinini R. Revision surgery in the lower limbs of haemophilic patients. Chapter 15 in: Christian Carulli editor, Frontiers in Arthritis, volume 2: The management of Haemophilic arthropathy. Bentham Science 2017; 196-2012.
15. Rodriguez-Merchan EC. HIV and HCV coinfected haemophilia patients: what are the best options of orthopaedic treatment? Haemophilia 2006; 12(S3):90-101.
16. Carulli C, Matassi F, Civinini R, Innocenti M. Tissue engineering applications in the management of bone loss. Clin Cases Miner Bone Metab 2013; 10(1): 22-5.
17. Matassi F, Botti A, Sirleo L, Carulli C, Innocenti M. Porous metal for orthopedics implants. Clin Cases Miner Bone Metab 2013; 10(2): 111-5.
18. Paprosky WG, Perona PG, Lawrence JM. Acetabular defect classification and surgical reconstruction in revision arthroplasty: a 6-year follow-up evaluation. J Arthroplasty 1994; 9:33-44.
19. Engh GA, Ammeen DJ. Classification and preoperative radiographic evaluation: knee. Orthop Clin N Am 1998; 29:205-17.
20. 20Hiliard P, Funk S, Zourikian N, et al. Haemophilia joint health score reliability study. Haemophilia 2006; 12:518.
21. Innocenti M, Matassi F, Carulli C, Soderi S, Villano M, Civinini R. Joint line position in revision total knee arthroplasty: the role of posterior femoral off-set stems. Knee 2013; 20(6):447-50.
22. Civinini R, Carulli C, Matassi F, Nistri L, Innocenti M. A dual mobility cup is effective for reducing dislocations in isolated acetabular revisions. Clin Orthop Relat Res 2012; 470:3542-8.
23. Rodriguez-Merchan EC, De La Corte H. Orthopaedic surgery in haemophilic patients with inhibitors: a review of the literature In: Rodriguez-Merchan EC, Goddard NJ, Lee CA, Eds. Musculoskeletal aspect of Haemophilia. Blackwell Science Ltd 2000.
24. Sunnassee Y, Wan R, Shen Y, Xu J, Southern EP, Zhang W. Preliminary results for the use of knee mega-endoprosthesis in the treatment of musculoskeletal complications of haemophilia. Haemophilia 2015; 21(2): 258-65.
25. Menichini G, Melita D, Cipriani F, Amenta A, Innocenti M. Microsurgery and plastic surgery in Haemophilia. in: Christian Carulli editor, Frontiers in Arthritis, volume 2: The management of Haemophilic arthropathy. Bentham Science 2017; 18:240-264.

IRISIN LEVELS CORRELATE WITH BONE MINERAL DENSITY IN SOCCER PLAYERS

G. COLAIANNI[1]*, A. NOTARNICOLA[1]*, L. SANESI[2], G. BRUNETTI[1], L. LIPPO[2], M. CELI[3], L. MORETTI[1], V. PESCE[1], G. VICENTI[1], B. MORETTI[1], S. COLUCCI[1]* and M. GRANO[2]*

[1]Department of Basic Medical Sciences, Neuroscience and Sense Organs, Section of Human Anatomy and Histology, School of Medicine-University of Bari, Italy; [2]Department of Emergency and Organ Transplantation, School of Medicine-University of Bari, Italy; [3]Department of Orthopedics and Traumatology, Tor Vergata University of Rome, Rome, Italy

*these authors contributed equally to this work.

Irisin, a novel myokine produced in response to physical exercise by skeletal muscle, displays anabolic effect on bone and can improve the bone-loss-induced osteoporosis in hind limb suspended mice. It is well known that muscles positively impact the skeleton and in different sports, including soccer, total body bone mineral density (TB-BMD) is elevated. Therefore, we have investigated the correlation between irisin serum levels and total and bone sub-regional BMD in soccer players never studied before. In this study, Caucasian football players of Bari team have been enrolled. Their sera were collected to measure by ELISA kit irisin levels and by dual-energy X-ray absorptiometry (DEXA) analysis measurements of BMD (g • cm^{-2}) in the whole body and different bone sub-regions (head, arms, legs, ribs, dorsal vertebrae, lumbar vertebrae, pelvis) were performed. The BMC (g) was measured in the whole body. By means of Pearson's (R) and Cohen's (d) coefficient we investigated the linear association between the irisin serum levels and BMD. In soccer players, we have found a positive correlation between irisin and TB-BMD as demonstrated by the values of Pearson and Cohen's (d) coefficient. Furthermore, linear association was detected between irisin and BMD of different bone-site such as right arm, lumbar vertebrae and head. A positive trend was also observed analyzing circulating levels of irisin and bone mineral content as well as total Z-score. In conclusion, we have demonstrated the correlation between irisin and total or bone sub-regional BMD in soccer players for the first time, an additional systemic effect of the "sport-hormone" defined myokine.

Irisin is a recently identified molecule produced by skeletal muscle during physical activity. This myokine is released as a cleavage product of the transmembrane protein fibronectin type III domain–containing 5 (FNDC5) highly expressed under the control of peroxisome proliferator-activated receptor gamma coactivator 1-alpha (PGC1α) after exercise in the skeletal muscle of mice and humans.

In 2012, irisin was defined as a hormone-like molecule that determines the "browning response" consisting in the trans-differentiation of white adipose tissue into brown (1). It was only two years ago that we published that irisin displays anabolic effect on bone at concentrations much lower than those inducing browning response, indicating that the skeleton could be the first target of the myokine. In the same paper, we demonstrated that irisin prevalently acts on bone forming cells, the osteoblasts, through

Key words: irisin, bone, bone mineral density, soccer

Mailing address:
Maria Grano, PhD,
Full Professor at Department of Emergency and Organ Transplantation, University of Bari,
Piazza Giulio Cesare 11, 70124 Bari, Italy
Tel.: +39 080 5478361
e-mail: maria.grano@uniba.it

0393-974X (2017)

the stimulation of their differentiation and activity, thereby improving bone quality (2).

Even more recently, by using hind-limb suspended mice, a well established model of disuse-induced osteoporosis in which bone formation is reduced and bone resorption exceeds, we have shown that irisin treatment importantly ameliorates the loss of bone mass induced by unloading condition. Moreover, in the same animal model, in which muscle wasting concurrently occurs by the absence of load, we have proved that irisin is able to prevent disuse-induced muscle atrophy (3). Therefore, irisin, due to its ability to improve bone and muscle quality in osteoporosis and sarcopenia in one shot, results a novel key molecule involved in the skeletal-muscle crosstalk.

Unlike the knowledge of the past, in which the coupling between bone and muscle was only anatomical and dependent upon mechanical interaction, nowadays, it has been extensively recognized that molecular signals from both bone and muscle can mutually affect both tissues with positive or negative effects in both physiological and pathological conditions. It has been shown that an increase in muscle mass is correlated to an increase in BMD and reduced risk of fractures in women after menopause (4). It has been also proposed that bone strength is homeostatically adapted to habitual skeletal loading.

Physical activity is one of the major determinant of BMD, indeed, in men engaged in different sporting activities total BMD and regional BMD, measured by dual-energy X-ray absorptiometry, were significantly increased (5). Moreover, by using peripheral quantitative computed tomography (pQCT), it has been proved that muscle size is strongly linked to the size and the strength of bone as well as a positive correlation between muscle size with cortical and trabecular BMD has been also proved (6). In 2014, Singhal studied the levels of irisin in a cohort of athletic adolescent girls and showed that adolescent amenorrhoeic athletes display lower irisin levels with respect to both eumenorrheic and non-athletes and irisin positively correlates with total BMD Z-score (7).

In 2015, Spiegelman demonstrated that circulating irisin levels increase in patients undergoing aerobic interval training compared to sedentary subjects (8). Therefore, since in different sports, including soccer, the players have a high total or sub-regional BMD and irisin is known as a "sport hormone", we investigated the correlation between irisin serum levels and total or bone sub-regional BMD never studied before in soccer players.

MATERIALS AND METHODS

Subjects

Eighteen Caucasian professional players of Bari football team (second division of Italian football league) have been enrolled in the present study. All the athletes maintained a constant workout during the year, and are characterized by the following features: the average age is 24.7±1.21, the mean weight is 76.12±1.6 and the average of the BMI is 22.66±0.29. All the samples were kept at the end of the 2015 season. All the participants provided written consent.

ELISA assay

Irisin serum concentrations were measured by a competitive ELISA kit (Cat. No. AG-45A-0046YEK-KI01, AdipoGen,Liestal, Switzerland). This ELISA kit has intra-assay coefficient of variation (CV) 6.9%, inter-assay CV 9.07%, detection limit 0.001 μg/mL. For the protocol, we followed the manufacturer's instruction. In this assay, the native Irisin and recombinant Irisin are recognized by a polyclonal antibody under competition in the Irisin-coated plate. The dosage of Adipogen ELISA KIT was chosen because, compared to others commercially available, it has the largest range of measurement (0001-5 μg/mL) and was the most sensitive (0.001 μg/mL). The colorimetric reaction was subsequently measured in a spectrophotometer (Eon, BioTek, Winooski, Vermont, USA). All serum samples were obtained after centrifugation (1500 rpm at 4°C for 10 min) in our laboratory and stored at -80°C.

Bone mass measurements

The bone mass, fat mass and lean mass were calculated by means of dual-energy X-ray absorptiometry (DEXA) analysis (Hologic Inc EXPLORER QDR series-Mo 010-157, 35 Crosby Drive Bedford, MA, 01730 USA). DXA equipment was calibrated using a lumbar spine phantom

and following the Hologic guidelines. Scans were performed in early afternoon. Measurement sessions were taken in early July (at the beginning of the conditioning period). All scanning and analyses were performed by the same operator (FR) to ensure consistency. In our laboratory, the precision error (per cent coefficient of variation with repositioning) of whole-body DXA measurements is 1.1, 0.9, 2.3, 0.5 and 2.8% for BMC, BMD, FM, FFSTM, and per cent FM, respectively. Participants were scanned in supine position, with their body and limbs fully extended and inside the limits set by the scan lines.

The BMC (g) was measured in the whole body. The lean mass was expressed in grams and the fat mass in percentage and grams. The BMD ($g \bullet cm^{-2}$) was measured in the whole body and in the following sub-regions: head, arms, legs, ribs, dorsal vertebrae, lumbar vertebrae and pelvis. For hip and lumbar vertebrae, the BMD was used to calculate T-score and/or Z-score. Both T-scores and Z-scores are derived by comparison to a reference population on a standard deviation scale. T-score is bone density compared with what is normally expected in a healthy young adult of the same sex (normal is between +1 and -1; Osteopenia is between -1 and -2.5; Osteoporosis is <-2.5). The z-score is the number of standard deviations away from the average value of the reference group, consisting of people of the same age and gender. When the value is equal to or less than -2, the definition is lower than the reference values.

Statistical analysis

The statistical analysis was performed by IBM SPSS statistics version 22. We provided comparisons between serum concentration of Irisin and bone parameters. All variables were checked for normality (Shapiro-Wilk normality test) to see the population distribution. Then we provided Pearson or Spearman correlation. We adopted Pearson correlation when both variables passed normality test; in the other cases, we used Spearman correlation. We considered a significant relationship for pairs of variables with P values below 0.05.

To report the strength of the phenomenon we reported the effect size. We converted R Peason in Choens's d; for interpreting the magnitude of effect sizes we utilized the table as suggested by Cohen (1988). Multiple regression analyses were performed to identify the relative strength of each bone parameter in predicting irisin. We put the limit of statistical significance at 0.05.

RESULTS

Anthropometric parameters of a selected group of homogenous professional soccer players enrolling in the current work are shown in Table I. All the players were in good health, not one of them was taking any form of doping or supplements during the study (Table I).

Therefore, based on the knowing that physical activity enhances BMD in soccer players (5), by means of Pearson's correlation coefficient (R) we have here investigated the linear association between the irisin serum levels and BMD in soccer players of Bari team. In the present study, we have included 18 Caucasian players whereas 3 African professional players and 1 Brazilian Hispanic have been excluded.

BMD (g/cm2) was measured in the total body (TB BMD) and in different bone sub-regions (head, arms, legs, ribs, thoracic and lumbar vertebrae, pelvis); circulating irisin levels were determined by ELISA assay (mean value of the myokine: 3.5 μg/ml±0.2 SE) in serum samples of the players. Interestingly, in the Caucasian soccer players we have found a significantly positive correlation between irisin and TB-BMD, as demonstrated by the values of R=0.476 and p=0.046 (Fig. 1). We have further observed that the values of R and p increased when the Pearson correlation between the two parameters was measured in different bone-sites. In detail, just higher values were found between irisin and BMD of the right arm (R=0.485 and p=0.042) and they were even more elevated at level of lumbar vertebrae (R=0.526 and p=0.025) as well as for the head (R=0.6 and p=0.008) (Fig. 2. A-C, respectively).

All these findings were further supported by the values of Cohen's d (d), which is a coefficient that represents the degree of accuracy and consistency in a statistical analysis useful to measure an appropriate effect size for the comparison between irisin and BMD. No linear association was found when irisin levels were correlated to BMD of: left arm, right and left legs, ribs, thoracic vertebrae and pelvis (Fig. 3. A-F). In addition, we observed a positive trend in the linear association between irisin levels and bone mineral content likewise in the correlation between the myokine and total Z-score, in fact, positive

Table I. *Somatic and skeletal characteristics of Caucasian football players (n=18).*

	Mean ± SD	Max	Min
Age (years)	24.7 ± 5.1	34	18
Height (m)	1.81 ± 0.06	1.94	1.7
Weight (kg)	76.2 ± 6.8	88	67
BMI (kg/m^2)*	22.7 ± 1.24	25	20
FM (g)*	9243.4 ± 2335.7	15039.6	6664.3
LBM (g)*	63504.4 ± 5374.1	72750.8	55892.5
TBM (g)*	76247.8 ± 7029.7	88612.5	67384.7
FM %*	12.05 ± 2.3	17.6	8.2
BMD left arm (HA g/cm2)*	0.82 ± 0.06	0.93	0.73
BMD right arm (HA g/cm2)*	0.83 ± 0.05	0.928	0.76
BMD ribs (HA g/cm2)*	0.70 ± 0.06	0.85	0.62
BMD trabecular vetebrae (HA g/cm2)*	0.98 ± 0.13	1.35	0.80
BMD lumbar vetebrae(HA g/cm2)*	1.47 ± 0.25	2.11	1.12
BMD pelvis (HA g/cm2)*	1.54 ± 0.13	1.87	1.35
BMD left leg (HA g/cm2)*	1.47 ± 0.11	1.74	1.26
BMD right leg (HA g/cm2)*	1.42 ± 0.11	1.66	1.156
BMD head (HA g/cm2)*	2.94 ± 0.28	3.58	2.56
TB BMD (HA g/cm2)*	1.38 ± 0.08	1.59	1.28
Z score*	2.44 ± 0.97	4.8	1
BMC (g/cm^2)*	3499.41 ± 420.65	4580.78	2863.79
Femur T score*	2.02 ± 0.96	3.7	0.01
Femur Z score*	2.07 ± 0.99	3.7	0.01
Spine T score*	1.91 ± 1.14	4.5	-0.1
Spine Z score*	2.07 ± 1.16	4.5	-0.1

BMI: *body mass index;* ***FM:*** *fat mass;* ***LBM:*** *lean body mass;* ***TBM:*** *total body mass;* ***FM:*** *% fat mass as a percentage of body weight;* ***BMD:*** *bone mineral density;* ***TB BMD:*** *total body bone mineral density;* ***BMC:*** *bone mineral content. *:Data obtained from DXA.*

values of Person correlation (R=0.457 and p=0.057; R=0.464 and p=0.053) were found (Fig. 4. A, B respectively). Finally, Z-score and T-score of spine and femurs do not correlate with irisin (Fig. 5).

DISCUSSION

This study highlights the correlation between irisin serum levels and total or sub-regional BMD in soccer players for the first time.

Irisin is a small molecule produced by skeletal muscle following physical exercise. In 2012 this myokine has become known for its involvement in the "browning response", and shortly after it has been positively associated with body mass index (9) and energy expenditure (10). Recently, it has been

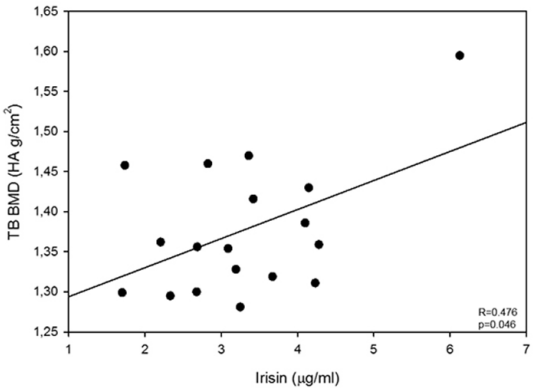

Fig. 1. *Correlation between TB-BMD and Irisin. Values of Pearson's correlation coefficient (**R**) and statistical significance (**p**) are reported in the graph; the value of Cohen's d coefficient (d) is d=1.082.*

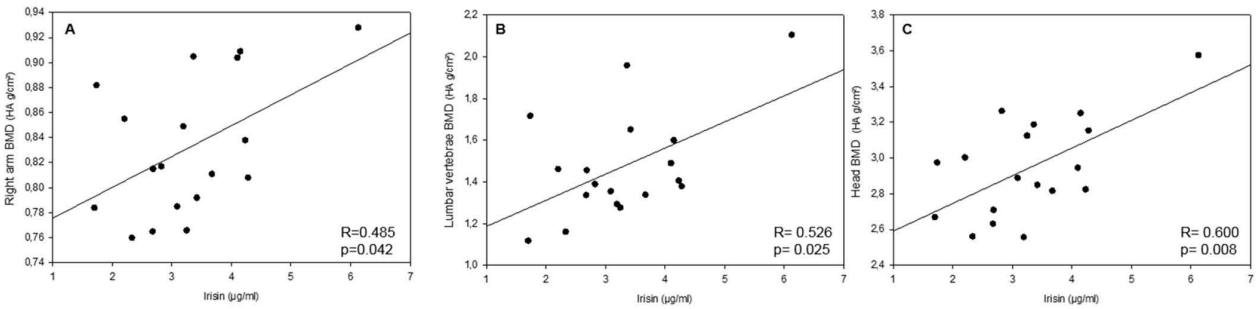

Fig. 2. *Correlation between Irisin serum levels and BMD of different bone sub-regions such as **A**: right arm BMD (R=0.485; p=0.042; d=1.1092); **B**: lumbar vertebrae (R=0.526; p= 0.025; d=1.2369); **C**: head (R= 0.600; p= 0.008; d=1.5).*

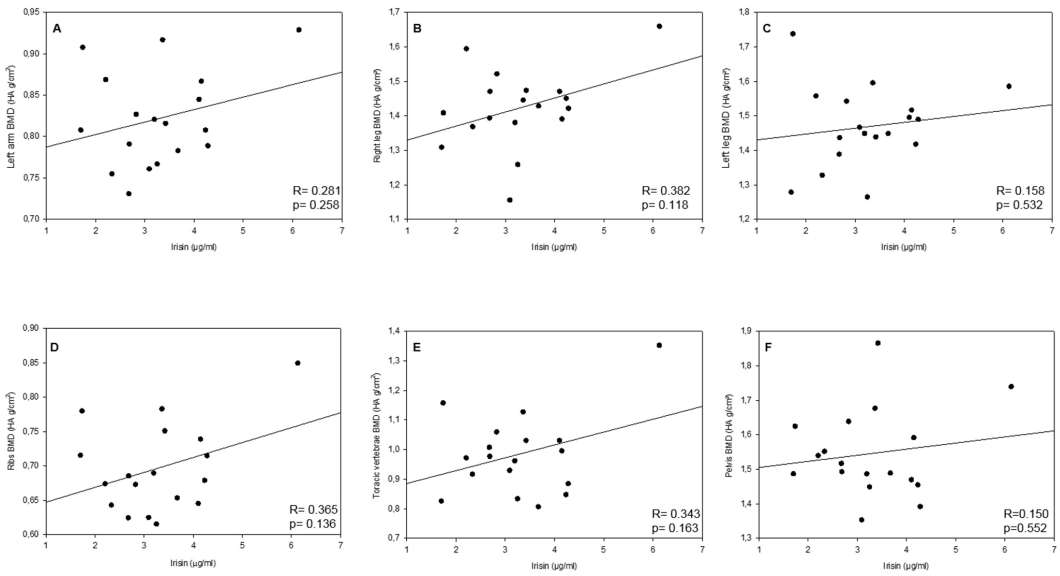

Fig. 3. *No linear association between Irisin and BMD of same bone sub-regions as **A**: left arm R=0.281, p=0.258, d=0.586; **B**: right leg, R=0.382 p=0.118, d=0.827; **C**: left leg, R=0.158, p=0.532 d=0.32; **D**: ribs, R=0.365, p=0.136,*

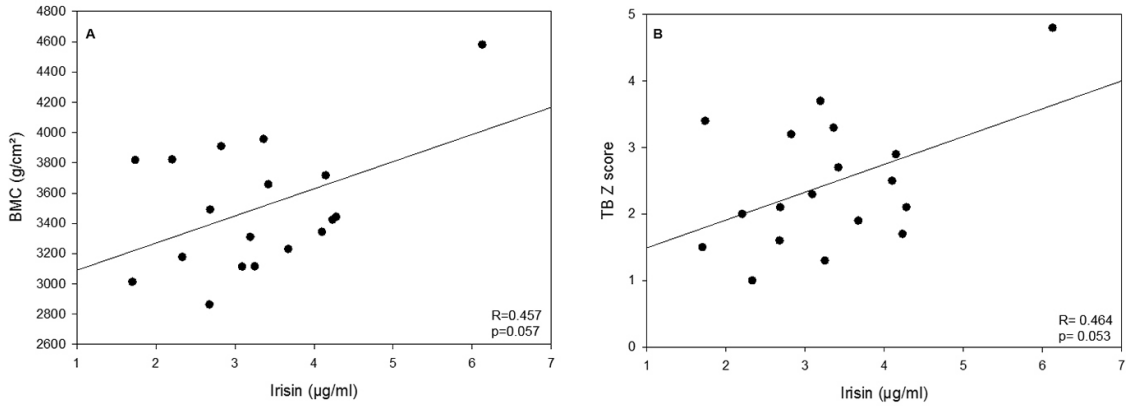

Fig. 4. *Two bone parameters show the tendency to correlate with Irisin.* ***A:*** *irisin and BMC, R=0.457 p=0.057, d=1.0276;* ***B:*** *irisin and TB Z score, R=0.464, p=0.053 d=1.0476.*

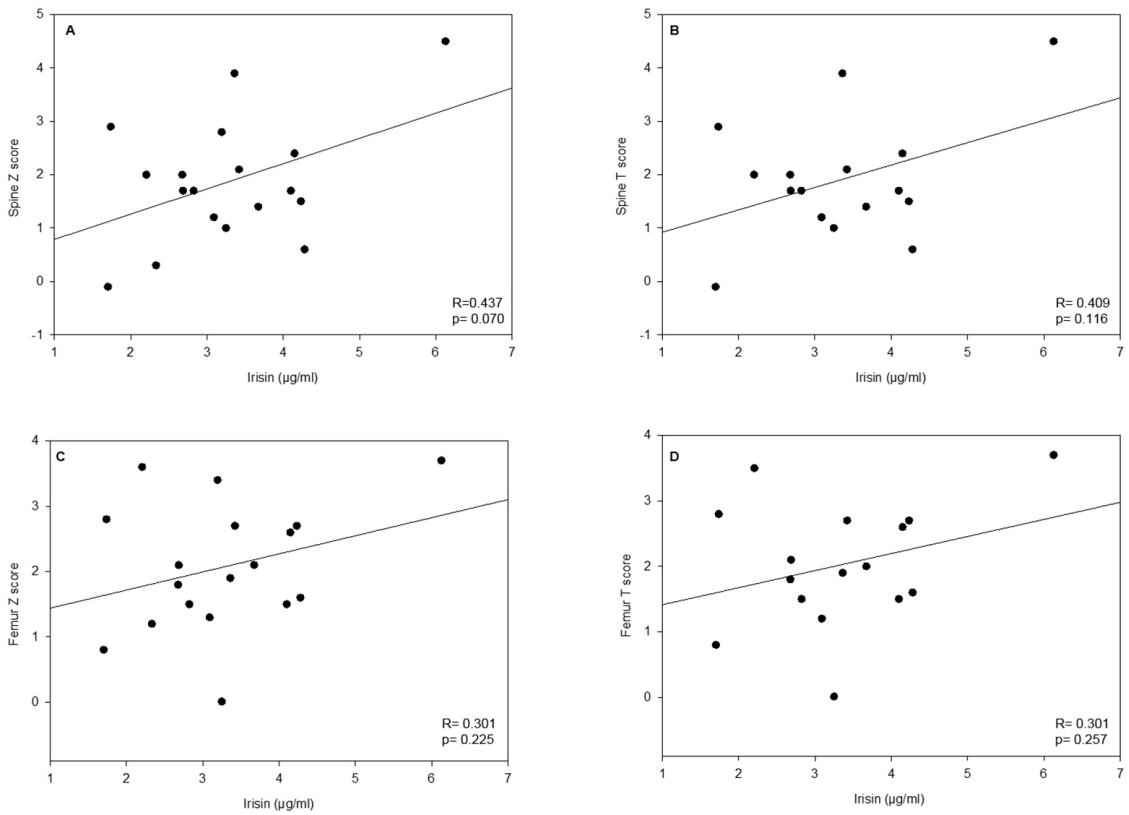

Fig. 5. *Irisin does not correlate with:* ***A****. spine Z score, R=0.437, p=0.070, d=0.971;* ***B****. spine T score, R=0.409, p=0.116, d 0.896;* ***C****. femur Z score, R=0.301, p=0.225, d=0.631;* ***D****. femur T score, R=0.301, p=0.257, d=0.631.*

also shown that irisin stimulated insulin synthesis and glucose-stimulated insulin secretion (GSIS) and prevented saturated fatty acid-induced apoptosis in human and rat pancreatic beta-cells, as well as in human and murine pancreatic islets (11). Furthermore, overexpression of irisin enhances insulin sensitivity, while reducing hyperglycemia and hyperlipidemia in mice (12), therefore suggesting irisin as potential use to fight obesity and diabetes.

The close linkage between irisin with bone tissue has emerged in 2015, when we demonstrated that the myokine stimulates bone formation and more recently, in 2017, we showed that irisin protects from bone and muscle loss (2-3).

It is widely recognized that to preserve bone quality, physical activity is critically important and it has been shown that BMD increases in several sportsmen, including soccer players. However, no data are at present known about irisin and BMD in soccer players. Therefore, we studied here this issue enrolling Caucasian soccer players of Bari team. Due to racial differences in bone density, we excluded three African and one Brazilian Hispanic players belonging to the team since it has been widely accepted that bone density is higher in black compared to white people (13).

We found that the mean value of TB-BMD in players of Bari football team was similar to that found by other authors in soccer players (5) and interestingly, as shown in fig. 1, we demonstrated that irisin serum levels positively correlate with TB-BMD. We also showed the linear association between the myokine and some bone sub-regional BMD such as right arm, lumbar vertebrae and head and no correlation with other bone sites. These finding are not surprising if we consider that the effect of circulating irisin is systemic. Therefore, we could expect a more evident correlation between irisin and BMD in upper limbs, even if these bone segments receive a lower impact by mechanical load, than lower limbs, whose bone accrual is mainly regulated by the mechano-sensor cells, the osteocytes. Moreover, this is also in accordance with our previous studies in which we showed that the main target of Irisin are the bone forming cells, the osteoblasts (2-3).

Taken together, our results suggest that, independently from loading, the positive correlation between irisin and total body or subregional BMD can be explained by the systemic effect irisin, following the contractile event of skeletal muscle that increases its synthesis and release into the bloodstream.

ACKNOWLEDGEMENTS

This work was supported in part by MIUR grant ex60% (to M.G.), by SIOMMMS grant (to G.C.) and by ERISTO (ESA) grant (to M.G.).

REFERENCES

1. Boström P, Wu J, Jedrychowski MP, et al. A PGC1-α-dependent myokine that drives brown-fat-like development of white fat and thermogenesis. Nature 2012; 481(7382):463-8.
2. Colaianni G, Cuscito C, Mongelli T, et al. The myokine irisin increases cortical bone mass. Proc Natl Acad Sci USA 2015; 112(39):12157-62.
3. Colaianni G, Mongelli T, Cuscito C, et al. Irisin prevents and restores bone loss and muscle atrophy in hind-limb suspended mice. Sci Rep 2017; 7:2811.
4. Clarke BL, Khosla S. Physiology of bone loss. Radiol Clin North Am 2010; 48(3):483-95.
5. Morel J, Combe B, Francisco J, Bernard J. Bone mineral density of 704 amateur sportsmen involved in different physical activities. Osteoporos Int 2001; 12(2):152-7.
6. Edwards MH, Gregson CL, Patel HP, Jameson KA, Harvey NC, Sayer AA, Dennison EM, Cooper C. Muscle size, strength, and physical performance and their associations with bone structure in the Hertfordshire Cohort Study. Bone Miner Res 2013; 28(11):2295-304.
7. Singhal V, Lawson EA, Ackerman KE, et al. Irisin levels are lower in young amenorrheic athletes compared with eumenorrheic athletes and non-athletes and are associated with bone density and strength estimates. PLoS One 2014; 9(6):e100218.
8. Jedrychowski MP, Wrann CD, Paulo JA, et al. Detection and Quantitation of Circulating Human Irisin by Tandem Mass Spectrometry. Cell Metab 2015; 22(4):734-40.
9. Crujeiras AB, Pardo M, Arturo RR, Navas-

Carretero S, Zulet MA, Martínez JA, Casanueva FF. Longitudinal variation of circulating irisin after an energy restriction-induced weight loss and following weight regain in obese men and women. Am J Hum Biol 2014 Mar-Apr; 26(2):198-207.

10. Perakakis N, Triantafyllou GA, Fernández-Real JM, Huh JY, Park KH, Seufert J, Mantzoros CS. Physiology and role of irisin in glucose homeostasis. Nat Rev Endocrinol 2017; 13(6):324-337.
11. Natalicchio A, Marrano N, Biondi G, et al. The myokine irisin is released in response to saturated fatty acids and promotes pancreatic beta-cell survival and insulin secretion. Diabetes 2017; pii:db170002.
12. Xiong XQ, Chen D, Sun HJ, et al. FNDC5 overexpression and irisin ameliorate glucose/lipid metabolic derangements and enhance lipolysis in obesity. Biochim Biophys Acta 2015; 1852:1867-75.
13. Ettinger B, Sidney S, Cummings SR, Libanati C, Bikle DD, Tekawa IS, Tolan K, Steiger P. Racial differences in bone density between young adult black and white subjects persist after adjustment for anthropometric, lifestyle, and biochemical differences. J Clin Endocrinol Metab 1997; 82(2):429-34.

C3F IS A POTENTIAL TOOL FOR THE STAGING OF OSTEOARTHRITIS

A. CORIGLIANO[1*], M. PREIANÒ[2*], R. TERRACCIANO[2], R. SAVINO[2], M. DE GORI[1], O. GALASSO[1] and G. GASPARINI[1]

[1]Division of Orthopaedic and Trauma Surgery, Department of Medical and Surgical Sciences, "Magna Graecia" University and "Mater Domini" University Hospital, Catanzaro, Italy; [2]Laboratory of Mass Spectrometry and Proteomics, Department of Health Sciences, Magna Graecia University, Catanzaro, Italy

*These 2 authors contributed equally to this work.

An attractive method for osteoarthritis (OA) staging is the measurement of biochemical markers in biological fluids, which could reflect dynamic and quantitative changes in joint remodeling and therefore disease progression. Proteome analysis has been recognized as one of the most effective tools to explore biomarkers as it can furnish a wealth of information in both diagnosis and prognosis of diseases. We have recently described an innovative tool for peptidome and lipidome profiling of fluids based on mesoporous aluminosilicate (MPAS) and Matrix-Assisted Laser Desorption/Ionization time-of-flight Mass Spectrometry (MALDI-TOF MS). The aim of this study was to analyze peptide profiles of human synovial fluid in patients with different grade of OA using MALDI-TOF-MS technique in order to identify potential markers of disease progression. Twenty-five patients older than 50 years and affected by primary knee OA diagnosed according to clinical and radiological criteria were enrolled. For each patient a synovial fluid sample was aspirated from the affected knee and analyzed using MALDI-TOF-MS technique. A statistically significant difference in the normalized area of two peaks (*m/z*=1865 and *m/z*=2021) was detected among different stages of OA. The 2 peaks were identified as Complement C3 peptide fragments: C3f and C3f Des-Arg. The expression levels of these two peptides (m/z=1865 and 2021) decreased with the progression of OA degrees severity (ρ_s=-0.434, p=0.03, and ρ_s=-0.532, p=0.006, respectively). This marker may be a useful tool for assessing the severity of knee OA and it may be a novel target for drug discovery, specifically for the development of disease modifying OA drugs. However further studies are required to clarify the role of C3f in OA pathogenesis.

Osteoarthritis (OA) is the most common form of arthritis and a major cause of pain and disability in older adults. The pathologic changes seen in OA joints include degradation of the articular cartilage, thickening of the subchondral bone, osteophyte formation, synovial inflammation, degeneration of ligaments and hypertrophy of the joint capsule (1). Both intrinsic and extrinsic risk factors promote its development but the true pathogenesis of the disease remains unclear (2).

Therapeutic spectrum ranges from physiotherapy to orthopedic aids and orthoses, pharmacotherapy, rehabilitation and surgery. Treatment options vary according to the stage of OA, therefore an accurate diagnosis enables proper treatments.

To date, imaging methods represent the gold standard for staging and X-ray examination is commonly used to grade joint damage. However,

Key words: osteoarthritis, knee, proteomics, C3, complement system

Mailing address:
Olimpio Galasso, MD,
Associate Professor of Orthopedics and Trauma Surgery,
Division of Orthopaedic and Trauma Surgery,
Department of Medical and Surgical Sciences,
"Magna Graecia" University and "Mater Domini" University Hospital, Catanzaro, Italy

0393-974X (2017)

radiographic markers of OA (i.e. the presence of osteophytes or joint space narrowing) have a low sensitivity and are late stage indicators of disease (3). In addition, the demonstration of typical signs of osteoarthritis of the knee is not correlated with symptoms (4). A more accurate evaluation is possible with magnetic resonance imaging (MRI) to asses changes in cartilage volume or thickness (5). However, the routinely use of MRI to grade the disease is limited by cost, by availability and by the absence of a validated international score (6). An attractive method to stage the disease is the measurement of biochemical markers in blood, urine or synovial fluid (SF) samples, which could reflect dynamic and quantitative changes in joint remodeling and therefore disease progression. SF bathes all the intrinsic structures of diarthrodial joints, therefore an analysis of its constituents offers a unique opportunity to study the osteoarthritic joint. SF is a dialysate of plasma to which components produced locally by joint tissues, including hyaluronan and lubricin are added (7).

Only a limited number of studies investigated the relationship between radiographic grading and the synovial fluid biochemical markers of OA (6, 7). Proteome analysis has been recognized as one of the most effective tools to explore biomarkers as it can assist in diagnosis and prognosis of diseases (8). Proteomic analysis can provide information regarding changes in protein levels throughout disease and has contributed substantially to clinical disease research. Several proteomics studies have been carried out in the last decade for increasing knowledge on the pathogenesis of OA and the search of novel protein biomarkers (8). As a core technology of proteome analysis, Matrix-Assisted Laser Desorption/Ionization time-of-flight Mass Spectrometry (MALDI-TOF-MS) has been widely used to analyze proteomic characteristics due to its sensitivity and efficacy (9, 10).

To the best of our knowledge, few studies used this platform for SF analyses (11, 12) and an innovative tool for profiling the peptidome and lipidome of SF based on mesoporous aluminosilicate (MPAS) and MALDI-TOF MS has been recently described (13). In the present study, we analyzed peptide profiles of human synovial fluid in patients with different grade of OA using the MPAS MALDI-TOF-MS technique we recently developed (13) in order to identify potential markers of disease progression.

MATERIALS AND METHODS

Patients

This study was approved by the Researchers Ethics Committee (number 2010.29) and was conducted in accordance with the Declaration of Helsinki and the Guideline for Good Clinical Practice. All of the participants signed written informed consent prior to enrollment. We enrolled twenty-five patients older than 50 years and affected by primary knee OA diagnosed according to the clinical and radiological criteria of the American Rheumatism Association (14). Both the inclusion and exclusion criteria of the study subjects were as described in our previous study (15).

Exclusion criteria were a diagnosis of rheumatic diseases based on the physical examination and laboratory data, alcohol consumption (consuming >3 alcoholic beverages daily), substance abuse, anticoagulant treatment and inability to give informed consent. Patients were also excluded if they were currently, or within the 3 months prior to inclusion, being treated with corticosteroids or indomethacin. Patients who received intra-articular treatment with corticosteroids or hyaluronic acid within 6 months preceding the study or systemic nonsteroidal anti-inflammatory drugs (NSAIDs) within 15 days before the study were also excluded. Finally, patients with other diseases (i.e cancers, liver or kidney failure) that could possibly confound the proteomic profile were also excluded.

OA grading

Antero-posterior and lateral weight-bearing radiographs of both knees were taken. The grading of radiographs was scored by 2 observers, and evaluations were repeated twice on 2 separate days; a consensus decision was reached in a final common readout, and correlation coefficients were determined: correlation coefficients for interobserver and intraobserver reliability of measures were >0.8 in both cases. The severity of OA was evaluated according to the Ahlbäck classification (16). Therefore, the knee joint osteoarthritis was classified as:

grade I, joint space narrowing (joint space <3 mm); grade II, joint space obliteration; grade III, minor bone attrition (0-5 mm); grade IV, moderate bone attrition (5–10 mm); grade V, severe bone attrition (>10 mm).

Sample collection and preparation

For each enrolled patient a SF sample (1-2 ml) was aspirated from the affected knee with a sterile puncture needle. Each SF sample was immediately centrifuged at 1000×*g* for 10 min at 4°C, the supernatant was then treated, with a protease inhibitor cocktail containing 4-(2-aminoethyl) benzenesulfonyl fluoride 104 mM, pepstatinA 1.5 mM, E-64 1.4 mM, bestatin 4 M, leupeptin 2 mM, and aprotinin 80 M (P8340; Sigma-Aldrich, St Louis, MO, USA), according to the manufacturer instruction, aliquoted and immediately stored at -80°C, until used.

PT extraction

The protocol proposed is divided into four steps: adsorption, separation, washing, and elution. In the first step, a small amount of particles was suspended in SF. During this step, molecules with sizes smaller than or comparable to the pore size diffused into the mesopores, where a selective binding of a subclass of molecules occurred on the basis of electrostatic interactions with silica surface, silanols, and aluminols. In particular, the MPAS particles were preconditioned in ammonium bicarbonate buffer at pH 7.8 and incubated with the biological matrix (SF) previously diluted in the same buffer. After the incubation (1 h at room temperature), the separation of the particles from the supernatant occurred by gentle centrifugation to avoid diffusion and dispersion of adsorbed molecules. With a rapid washing step, salts, and other contaminants, which can interfere with MALDI-TOF MS analysis, were eliminated with aqueous solution. Finally, the analytes adsorbed onto MPAS were eluted and immediately used for MALDI-TOF MS analysis.

MPAS saturation experiments

Based on our previous work (13), in this study we fixed the amount of MPAS at 2 mg, using increasing SF (10.0-20.0-25.0-45.0 µL) volumes in order to evaluate saturation parameters. The bicinchoninic acid assay (BCA) was used to determine total protein content of plasma and SF loaded on the MPAS, and then the fraction recovered from the eluate.

MPAS-SF processing

MPAS of 2 mg was mixed with 120 µL of either diluted SF sample (20 µL in 100 L of 50 mM ammonium bicarbonate pH 7.8) and shaken at room temperature for 1 h. The suspension was centrifuged at 600×*g* for 2 min, and then MPAS was separated from the supernatant and rapidly washed twice with 0.1% TFA (20 µL). After the last wash, species retained on MPAS surface were extracted in 30 µL of eluting solution (75:25 ACN/0.1% TFA). The eluate was immediately prepared for MALDI-TOF MS analysis. For MALDI-TOF MS analysis of PT, 1 µL of the eluate of either SF sample or plasma sample was mixed with 4 µL of 4 mg/mL CHCA solution (50:50 ACN/0.1% TFA), then 1 µL of the resulting solution was deposited on the MALDI target plate and allowed to dry at room temperature. The spotting was repeated on other two consecutive wells of the MALDI target plate.

MALDI-TOF MS analysis

MALDI MS analysis was performed on a MALDI-TOF MS (Voyager DE-STR, Applied Biosystems, Foster City, CA, USA) equipped with a 337-nm nitrogen laser. External mass calibration was performed before MALDI measurements using peptide standards for MS, prepared from the Sequazime peptide mass standard kit (Applied Biosystems). MALDI measurements were performed both in linear and in reflectron positive ion mode and delayed extraction was applied. In linear mode, the acceleration voltage was 20 kV, the guide wire was 0.05% of the accelerating voltage, the grid voltage was 91.5%, and the delay time was 220 ns. In reflectron mode, the acceleration voltage was 20 kV, the grid voltage was 68.5%, the mirror voltage ratio 1.12, the extraction delay time was 300 ns, and the low mass gate was fixed at 700 Da. Five 100-laser shots were averaged for each mass spectrum.

All spectra were processed using Data Explorer Software (Applied Biosystems). Accelerating voltage was set to 20 kV, with grid voltage of 66% and extraction delay time fixed at 220 ns. Each mass spectrum was generated by accumulating three spectra of 165 laser shots for a total of 495 laser shots. Laser intensity was optimized in order to ensure the best S/N. Negative ion mass spectra were acquired in reflector mode in a mass range from 450 to 1100 and with a low mass gate of 400 Da. Accelerating voltage was set to 20 kV, with grid voltage of 66% and extraction delay time fixed at 220 ns. Each mass spectrum

was generated by accumulating four spectra of 165 laser shots for a total of 660 laser shots. Preliminary MALDI-TOF MS measurements were performed in order to exclude any interference of components from protease inhibitor cocktail with MALDI-TOF analysis.

MALDI-TOF/TOF MS analysis

For peptide sequence analysis, the spectra were acquired in reflector mode within a mass range of 750-3500 Da, on a AB SCIEX MALDI-TOF/TOF 5800 System (ABSciex, Framingham, MA, USA) equipped with a diode-pumped, Nd:YLF laser with λ=345 nm wavelength. Fragmentation of native peptides was carried out in the CID mode (collision energy: 1 keV). RawMS/MS spectra were processed on Data Explorer Software by baseline correction and noise removal. Peptide identification was performed using Mascot (version 2.1.0; Matrix Science), where monoisotopic masses were searched against the Swiss-Prot human database.

Statistical analysis

Models of Spearman's rank correlation were created to test whether the severity of OA could affect the expression levels of the studied peptides. The IBM SPSS Statistics 21.0.0.1 software (IBM Corp., Armonk, NY, USA) was used for the database construction and the statistical analysis. A 2-tailed $p<0.05$ was considered significant.

RESULTS

In this study, we compared the proteome profiles of SF samples obtained from 25 patients with different grades of OA, as determined by Ahlbäck classification (Table I). In particular, we took advantage of the MPAS MALDI-TOF-MS technique we recently developed to produce spectra from the SF samples of the patients described in Table I. As example, 5 representative spectra (one for each OA grade) are shown in Fig. 1 in the range between *m/z*=1800 and *m/z*=2100.

The normalized areas of each peak were compared between the five groups of patients and a statistically significant difference was observed for two peaks (*m/z*=1865 and 2021) identified with asterisks in Fig. 1. In particular, the area of these two peaks decreased with the progression of OA degrees severity (ρ_s=-0.434, p=0.03, and ρ_s=-0.532, p=0.006, respectively). This association was independent of age and BMI. As example, the areas of peak *m/z*=2021 are shown in Fig. 2.

These two peaks were selected for MALDI-TOF/TOF sequencing as described in Materials and Methods. Peak *m/z*=1865 was assigned as fragment SSKITHRIHWESASLL, while peak *m/z*=2021 was assigned as fragment SSKITHRIHWESASLLR,

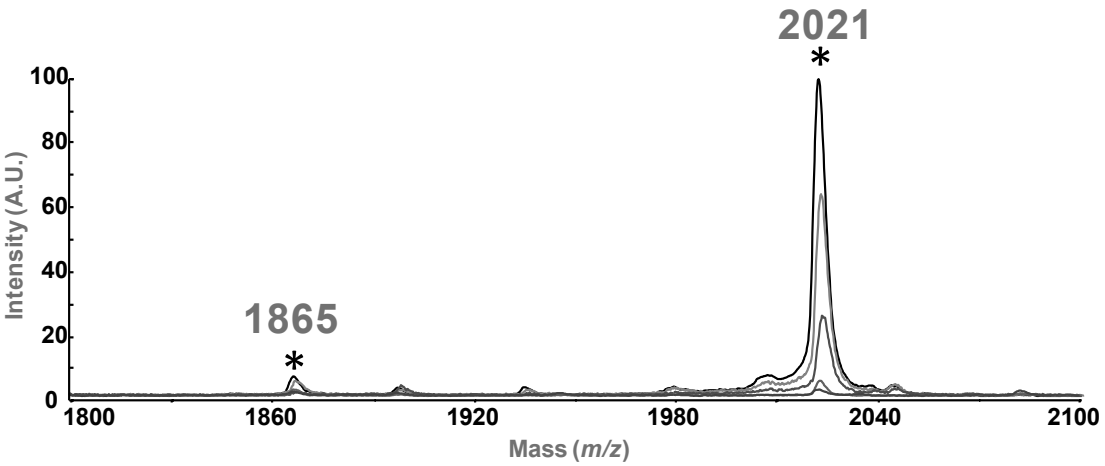

Fig. 1. *MALDI-TOF mass spectra of peptides extracted by MPAS from SF of 5 patients with different grades of OA. Overlaid traces are shown of grade 1 OA (**black**), grade 2 OA (**light blue**), grade 3 OA (**red**), grade 4 OA (**green**) and grade 5 OA (**blue**). Asterisks indicate peaks that showed a statistically significant reduction of the normalized peak area with the progression of OA degrees severity.*

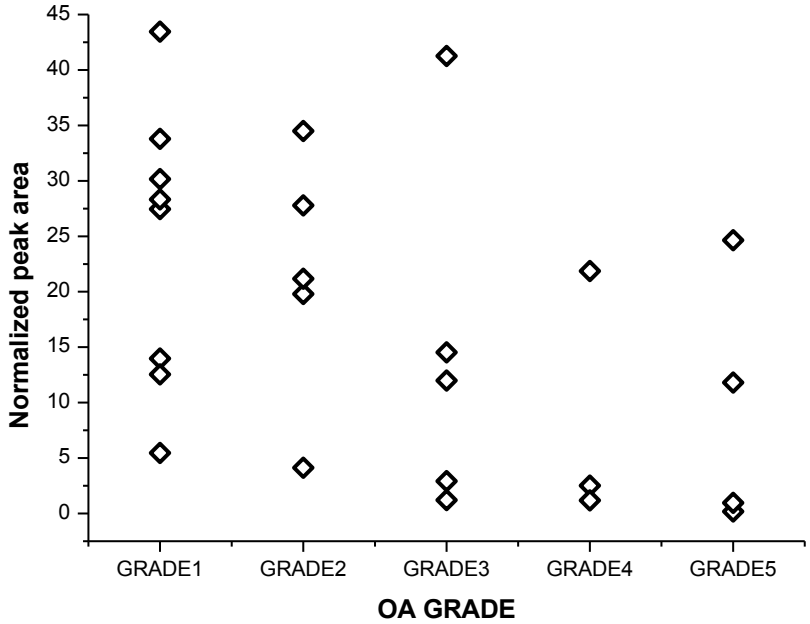

Fig. 2. *Representative expression profile of discriminating peak with m/z 2021. Individual peak areas (**diamonds**) among groups with different grade of OA severity are shown.*

Table I. *Demographic and radiographic data of patients.*

Patient	Sex	Age	BMI	Side	Ahlbäck grade
AA	F	66	27,3	R	1
CV	M	70	33,1	R	1
TG	M	68	33,1	R	1
AM	F	72	30	R	1
FA	F	79	30,1	L	1
RR	F	53	23,4	R	1
LE	F	58	33,2	R	1
NR	F	67	25,6	R	1
DG	F	52	39,1	R	2
DCL	F	60	32,7	L	2
PM	M	63	33,7	R	2
UL	F	69	29,4	L	2
AV	F	63	26	L	2
AV	F	79	33,3	L	3
CG	M	63	36,5	L	3
ML	F	58	45,2	L	3
TV	M	70	28,7	L	3
LF	F	78	29,4	L	3
CA	F	76	25,6	R	4
SC	F	82	24	L	4
FC	F	60	28,8	R	4
VI	F	65	31,2	R	5
LG	M	73	23	L	5
TA	M	72	38,6	L	5
GM	F	76	25,8	L	5

both recorded in Mascot database as Complement C3 fragments: C3f (*m/z*=2021) and C3f Des-Arg (*m/z*=1865).

DISCUSSION

The present study demonstrates an inverse correlation between the C3f and C3f des-Arg SF concentration and the radiographic OA severity.

C3f peptide was first isolated in SF by de Seny et al (17). It is a complement factor released during the catabolic degradation of C3b by Factor H after C3 activation. C3f is degraded to form C3f-des-Arg by carboxypeptidase N (18). OA has traditionally been classified as a non-inflammatory artropathy, however the latest theories of OA pathogenesis implicate the interplay between mechanical damage and low-grade of articular inflammation; it should be taken into account that activation of the innate immune system is intricately involved in initiation and perpetuation of this low-grade inflammation (19). Complement is a key part of innate immunity and comprises a cluster of activation pathways that are triggered in various ways and progress through several amplifying enzymes to converge on a final common cell-killing pathway. Moreover several studies support the observation of inflammation in the earliest phases of OA (20). Previous studies examining the association between biochemical markers of inflammation and OA have provided conflicting results; showing either increased or decreased markers in subjects with OA (6, 21, 22).

Benito and colleagues compared early and late OA and demonstrated increased mononuclear cell infiltration and over-expression of inflammatory mediators in early compared with late disease [21]. Similarly, Scanzello and colleagues found increased levels of SF interleukin-15 (IL-15) cytokine in the early knee OA patients when compared to end-stage OA (23). Conversely, the patients with higher disease severity had higher levels of IL-18 and adipokines in SF than patients with early OA (6, 22).

This report is the first demonstration of the correlation of SF C3f concentration with OA disease severity. This result is consistent with the result of Wang et al., who showed that complement activation occurs in synovial joints early in the course of OA and persists, albeit at a lower level, during the late phases of osteoarthritis (24). However, the authors failed to report significant higher levels of C3a Des-Arg in early-stage OA compared to end-stage OA with ELISA quantification. Significant pathophysiological roles could be played by C3f in cartilage and other joint tissues. De Seny and colleagues suggested that C3f activation is consequence of extracellular matrix degradation and further release of small leucine-rich repeat proteins in SF. Some of these proteins, such as fibromodulin and osteoadherin, interact with C1q to activate the classical and alternative pathways of complement factors (17). Previous studies showed that C3f is a potential biomarker in degenerative liver disease (25). In conclusion, C3f concentrations were shown to be closely related to the radiographic severity of OA and showed a marked decrease in advanced stage compared to early stage. This marker may be a useful tool for assessing the severity of knee OA and it may be a novel target for drug discovery, specifically the development of disease modifying OA drugs. However further studies are required to clarify the role of C3f in OA pathogenesis.

REFERENCES

1. Loeser RF, Goldring SR , Scanzello CR, Goldring MB. Osteoarthritis: a disease of the joint as an organ. Arthritis Rheum 2012; 64:1697-707.
2. Felson DT, Couropmitree NN, Chaisson CE, et al. Evidence for a Mendelian gene in a segregation analysis of generalized radiographic osteoarthritis: the Framingham Study. Arthritis Rheum 1998; 41:1064-71.
3. Bruyere O, Collette J, Kothari M, et al. Osteoarthritis, magnetic resonance imaging, and biochemical markers: a one year prospective study. Ann Rheum Dis 2006; 65:1050-4.
4. Michael JW, Schlüter-Brust KU, Eysel P. The epidemiology, etiology, diagnosis and treatment of osteoarthritis of the knee. Dtsch Arztebl Int 2010; 107:152-62.
5. Pelletier JP, Cooper C, Peterfy C, et al. What is the predictive value of MRI for the occurrence of knee replacement surgery in knee osteoarthritis? Ann

Rheum Dis 2013; 72:1594–604.
6. Lotz M, Martel-Pelletier J, Christiansen C, et al. Value of biomarkers in osteoarthritis: current status and perspectives. Ann Rheum Dis 2013; 72:1756-63
7. Mobasheri A, Bay-Jensen AC, Van Spil WE, Larkin J, Levesque MC. Osteoarthritis Year in Review 2016: biomarkers (biochemical markers). Osteoarthritis Cartilage 2017; 25:199-208.
8. Hsueh MF, Önnerfjord P, Kraus VB. Biomarkers and proteomic analysis of osteoarthritis. Matrix Biol 2014; 39:56-66.
9. Amadei GA, Cho CF, Lewis JD, Luyt LG. A fast, reproducible and low-cost method for sequence deconvolution of 'on-bead' peptides via 'on-target' maldi-TOF/TOF mass spectrometry. J Mass Spectrom 2010; 45:241-51.
10. Dong M, Wu M, Wang F, Qin H, Han G, Dong J. Coupling strong anion-exchange monolithic capillary with MALDI-TOF MS for sensitive detection of phosphopeptides in protein digest. Anal Chem 2010; 82:2907-15.
11. Pan X, Huang L, Chen J, Dai Y, Chen X. Analysis of synovial fluid in knee joint of osteoarthritis: 5 proteome patterns of joint inflammation based on matrix-assisted laser desorption/ionization time-of-flight mass spectrometry. Int Orthop 2012; 36:57-64.
12. Mateos J, Lourido L, Fernández-Puente P, Calamia V, Fernández-López C, Oreiro N, Ruiz-Romero C, Blanco FJ. Differential protein profiling of synovial fluid from rheumatoid arthritis and osteoarthritis patients using LC-MALDI TOF/TOF. J Proteomics 2012; 75:2869-78.
13. Preianò M, Pasqua L, Gallelli L, Galasso O, Gasparini G, Savino R, Terracciano R. Simultaneous extraction and rapid visualization of peptidomic and lipidomic body fluids finger prints using mesoporous aluminosilicate and MALDI TOF MS. Proteomics 2012; 12:3286-94.
14. Altman R, Asch E, Bloch D, Bole G, Borenstein D, Brandt K. Development of criteria for the classification and reporting of OA. Classification of osteoarthritis of the knee. Diagnostic and therapeutic criteria committee of the American Rheumatism Association. Arthritis Rheum 1986; 29:1039e49.
15. Gallelli L, Galasso O, Falcone D, et al. The effects of nonsteroidal anti-inflammatory drugs on clinical outcomes, synovial fluid cytokine concentration and signal transduction pathways in knee osteoarthritis. A randomized open label trial. Osteoarthritis Cartilage 2013; 21:1400-8.
16. Ahlbäck S. Osteoarthrosis of the knee: a radiographic investigation. Acta Radiol Diagn 1968; S277:7-72.
17. de Seny D, Sharif M, Fillet M, et al. Discovery and biochemical characterisation of four novel biomarkers for osteoarthritis. Ann Rheum Dis 2011; 70:1144-52.
18. Ganu VS, Müller-Eberhard HJ, Hugli TE. Factor C3f is a spasmogenic fragment released from C3b by factors I and H: the heptadeca-peptide C3f was synthesized and characterized. Mol Immunol 1989; 26:939-48.
19. Scanzello CR, Goldring SR. The role of synovitis in osteoarthritis pathogenesis. Bone 2012; 51:249-57.
20. Sokolove J, Lepus CM. Role of inflammation in the pathogenesis of osteoarthritis: latest findings and interpretations. Ther Adv Musculoskelet Dis 2013; 5:77-94.
21. Benito M, Veale D, FitzGerald O, van den Berg W, Bresnihan B. Synovial tissue inflammation in early and late osteoarthritis. Ann Rheum Dis 2005; 64:1263-7.
22. Mabey T, Honsawek S. Cytokines as biochemical markers for knee osteoarthritis. World J Orthop 2015; 6:95-105.
23. Scanzello CR, Umoh E, Pessler F, et al. Local cytokine profiles in knee osteoarthritis: elevated synovial fluid interleukin-15 differentiates early from end-stage disease. Osteoarthritis Cartilage 2009; 17:1040-8.
24. Wang Q, Rozelle AL, Lepus CM, et al. Identification of a central role for complement in osteoarthritis. Nat Med 2011; 17:1674-9.
25. Xin Y-N , Geng N, Lin Z-H, Cui Y-Z , Duan H-P, Zhang M, Xuan S-Y , Yu M-L. Serum complement C3F and fibrinopeptide A are potential novel diagnostic biomarkers for non-alcoholic fatty liver disease: a study in Qingdao twins. PLoS One 2014; 9:e108132.

SOFT TISSUE ADHESION PATTERNS OVER TREVIRA TUBE ON MODULAR ENDOPROSTHESIS FOR MALIGNANT BONE TUMOURS: AN IN VITRO STUDY

S. D'ADAMIO[1], G. CAZZATO[1], A. ZIRANU[1] A.SGAMBATO[2], M.A. ROSA[3] and G. MACCAURO[1]

[1]Department of Orthopaedics and Traumatology, Università Cattolica del Sacro Cuore, Rome, Italy; [2]Institute of General Pathology, Università Cattolica del Sacro Cuore, Rome, Italy; [3]Department of Orthopaedics and Traumatology, Department of Biomedical Sciences and Morphological and Functional Images, Università di Messina, Messina, Italy

A reliable and effective technique in case of limb salvage surgery after resection of extensive bone tumors is represented by the implant of modular or custom-made megaprosthesis. Fixation of the residual surrounding soft tissue on the implant represent a challenge for the surgeon and the use of a polyethylene terephthalate (PET) tube over it, also known as Trevira, is currently a common choice for reattachment with good clinical outcomes. We compared fibroblastic cell culture potential over simple titanium coating *vs* titanium surrounded by Trevira and evaluated cell viability and replication at 24, 48 and 72 h using MTT cell growth assay and scanning electron microscopy to determine if there was any difference in the potential of cell growth associated to the material used. No significant difference was found at different timings in terms of total cell count for cultures over the two materials, but the absolute cell count was slightly higher in the Trevira group in the early time points, reversing the trend at 72 h of incubation. Ninety-four % of the cells analyzed were vital, regardless of the materials involved in the experiment, confirming the biocompatibility of titanium and PET. According to the results shown, we are able to confirm the *in vitro* safety and efficacy, in terms of newly formed cells extension and adhesion pattern, of using an attachment tube made from Trevira fibers surrounding an oncological megaprosthesis in order to achieve the most anatomical reinsertion of remaining soft tissue following resection.

Currently there are two main approaches to choose from in the field of limb salvage surgery after resection of extensive bone tumors: the "biological" reconstruction procedures and the prosthetic reconstruction procedures (1).

The first type of technique relies on the use of bone graft such as fresh frozen cadaveric allografts as well as vascularized autograft (i.e. fibular autograft) or even combination of both, depending on the skeletal section to replace the resected segment, in order to regain the bone stock, which had to be removed with the tumor (2, 3). Soft tissues are then usually anchored onto the tendon footprints commonly featured by the graft utilized, or transosseus sutures are needed to obtain a solid attachment. Nevertheless, this demanding approach cannot be considered the gold standard because it often does not provide adequate mechanical strength of the construct, postoperative immobilization is very long, indications are very limited and the risk of infective disease transmission from grafts are relatively high (4). For these reason, this kind of surgery is mainly adopted for the treatment of skeletally immature children in which prosthetic implants are challenging to manage over long periods during skeletal growth. (5)

On the other hand, reconstruction with modular or custom-made megaprosthesis results in stronger construct with reliable stability, thanks to the strong materials involved (titanium and cobalt-chrome) and the improvements in technology and techniques

key words: tumour, endoprostesis, cell adhesion, soft tissue

Mailing address:
Prof. Giulio Maccauro,
Department of Orthopaedics and Traumatology,
Università Cattolica del Sacro Cuore,
00168 Rome, Italy
e-mail: giuliomac@tiscali.it

0393-974X (2017)

achieved over the last few years (6, 7). This step eventually has a direct impact on the functional outcome of the procedure. If the muscle anchorage is inadequate, the prosthesis implant becomes just a bone spacer, losing most of the potential benefits of limb salvage (8). To overcome this complication, different solutions were developed; some implants feature attachment holes on their surface to suture tendons through, even though integration of tissues on the surface depends on many variables (materials involved, tension of the construct etc.). For this reason, alternative fixation of the soft tissues can be accomplished by suturing them onto the tumor prosthesis by means of attachment tubes, usually made from polyethylene terephthalate (PET), known by its commercial name, Trevira (Fig. 1) (9). Attachment tubes enable a stable muscle connection on the whole tumor prosthesis by primary suture as well as secondary scar tissue ingrowth (10).

The good clinical outcomes achieved through the use of this device in skeletal reconstruction has been already investigated in published literature, but still there is a need for a better understanding of how this device allows and stimulates the ingrowth of soft tissue (9).

Therefore, the goal of this investigation is to microscopically analyze and evaluate the stages, the quality and the extension of tissue anchorage on Trevira tube when compared to traditional suturing technique in an experimental in vitro model.

MATERIALS AND METHODS

Fifty-four circular disks were manufacture from titanium (diameter: 2cm; height: 2mm) equivalent to those currently used for production of megaprosthesis. Then they were divided and allocated into 2 study groups: 1cm^2 of Trevira tissue was apposed on 27 disks, while the others were made of sole titanium and were used as control group (Fig. 2). RAT1 murine embryonal fibroblasts cells were used for this experiment given the most relevant role of this kind of cells in regeneration and repair of tendons and ligaments (11). Cells were cultured on RPMI medium (Gibco®) supplemented with fetal bovine serum at a

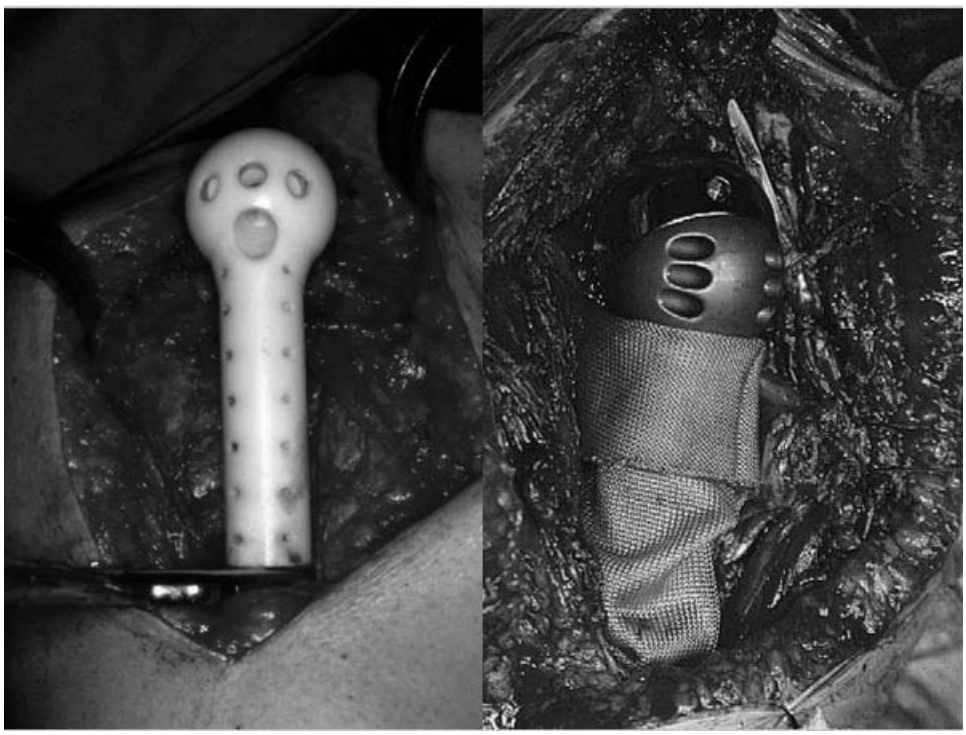

Fig. 1. *The two available options for soft tissue reattachment: direct fixation on the prosthetic dedicated holes (left) or indirect fixation using a tube made from different biocompatible materials such as Trevira (right).*

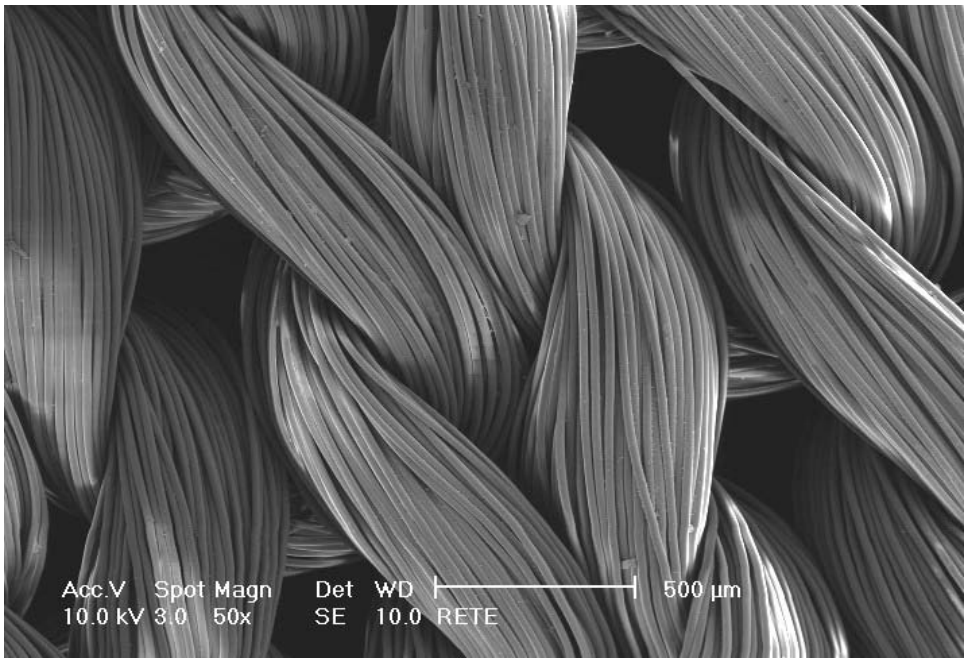

Fig. 2. *Trevira fibers appearance on high magnification. This particular texture offers a very high resistance to tensile forces such as those involved in soft tissue reconstruction and eventual function.*

concentration of 10%.

Different cellular tests and analysis were performed in order to evaluate viability and evolution of cell cultures using additional MTT (3-(4,5-dimethylthiazol-2-y1)-2,5-diphenyltetrazolium bromide; Sigma-Aldrich), whose colorimetric assay can be used for either proliferation or complement-mediated cytotoxicity evaluation (12). We also performed ultrastructural analysis of the specimens using scanning electron microscopy (SEM) to examine the morphology of the newly formed tissues.

MTT cell growth assay

RAT1 cells were seeded at a concentration of $2,5x10^4$ on a flat-bottomed tissue culture plate and sat 36 h for incubation on simple medium. We then proceeded to put the cells in contact with experimental disks of titanium and Trevira: this incubation lasted an additional 72 h and we then replaced the medium with 1 mG/Ml of MTT, proceeding with 2 more h of incubation at a fixed temperature of 37°C for cleavage of MTT to occur. We therefore added 0.1 mL isopropanol with 0.04 N HCl to each well: this step is crucial because the HCl converts the phenol red in tissue culture medium to a yellow color that does not interfere with MTT formazan measurement. The isopropanol dissolves the formazan to give a homogeneous blue solution suitable for absorbance measurement. In fact, we measured absorbance on an ELISA plate reader with a test wavelength of 540 nm after gently mixing the tray for about 20 min (13).

Adhesive proliferation assay

Procedures were performed at different time points (0 h, 24 h, 48 h and 72 h) after seeding of RAT1 cells on the disks from the two experimental groups. At any time point cells cultured from both groups were harvested and counted for three times using a semi-automated system, then the mean value between measurements was calculated.

Statistical analysis

A p value <0.05 was considered to be statistically significant. Statistical analysis was carried out by using the Statistical Package for the Social Sciences (SPSS) software version 20.0 (SPSS Inc., Chicago, USA).

Scanning electron microscopy (SEM)

The experimental disks at different timepoints of the previously described cell cultures were fixed in Karnovsky's solution followed by a second fixing in

osmium tetroxide, which increases the bulk conductivity of the sample. Samples were completely dried and finally, fixed samples are sputter coated with colloidal gold to further enhance their conductivity and their ultrastructure was analyzed using SEM.

RESULTS

Twenty-four hours after seeding the mean cell count was 4±3 x 10^4 on sole titanium disks and 4.5±1 x 10^4 on titanium disks + Trevira. Mean cell count after 48 h of incubation was 19±7 x 10^4 on sole titanium and 22±2 x 10^4 on titanium + Trevira. At 72 h time point, the mean cell count was 92±3 x 10^4 on sole titanium while 87±8 x 10^4 on titanium + Trevira (Table I). Differences in values between the experimental group and control group were not statistically significant at any given timepoint ($p>0.05$). MTT colorimetric assay showed that an average 94% of the incubated cells on any given disk, regardless of disk composition, were biologically vital.

Scanning electron microscopic analysis showed how colonization and progressive covering by RAT 1 cells occurred over both surfaces experimented; the microscopic analysis of cells after 72 h of incubation showed this was the first time point where the seeded cells on any given disk replicated and spread over the surface enough to merge together creating tissue continuity.

DISCUSSION

Techniques of muscolo-skeletal reconstruction following resections for bone neoplasms really improved over the last decades, and are now the most frequently adopted option for the surgical treatment of these pathologies since limb amputation are now taken into consideration only in case of rare aggressive tumors or failure of previous limb-salvage procedures (14). One reliable surgical option for skeletal reconstruction after extensive bone resections due to malignant neoplasms of long bones is represented by the implant of modular or custom-made megaprosthesis. This system provides high mechanical resistance properties while manufactured mainly from titanium, known for its optimal biocompatibility.

In order to achieve safe excision of tumor mass in long bones the surrounding pathological soft tissue must be resected with adequate margins to ensure the lowest rate of recurrence, as demonstrated by Enneking and many others over last decades (15, 16). The extent of bone, as well as of muscle, resection is key not only for the choice of the technique of reconstruction to use, but it especially influences the expected postoperative limb function which will dramatically affect the independence and, in fact, the quality of patient's life following such procedures (17).

Some sites of resection are usually affected by inadequate functional outcomes, especially sections distal to the deltoid muscle insertion on the humerus as regards for the upper limb and distal to the insertion of gluteus maximus muscle on the femur as for the lower limb. (8, 18, 19). In these cases, choosing the right reconstruction procedure is key to meet surgeon and patient's best expectations.

Therefore, the two most relevant points in obtaining an acceptable and functional reconstruction of segment resected are represented by the need to provide adequate mechanical resistance and stability

Table 1: *Mean cell number count at different timepoint for experimental groups.*

	24h	48h	72h	P value
Titanium	4.0±3 x 10^4	19±7 x 10^4	92±3 x 10^4	p>0.05
Titanium + Trevira	4.5±1 x 10^4	22±2 x 10^4	87±8 x 10^4	p>0.05

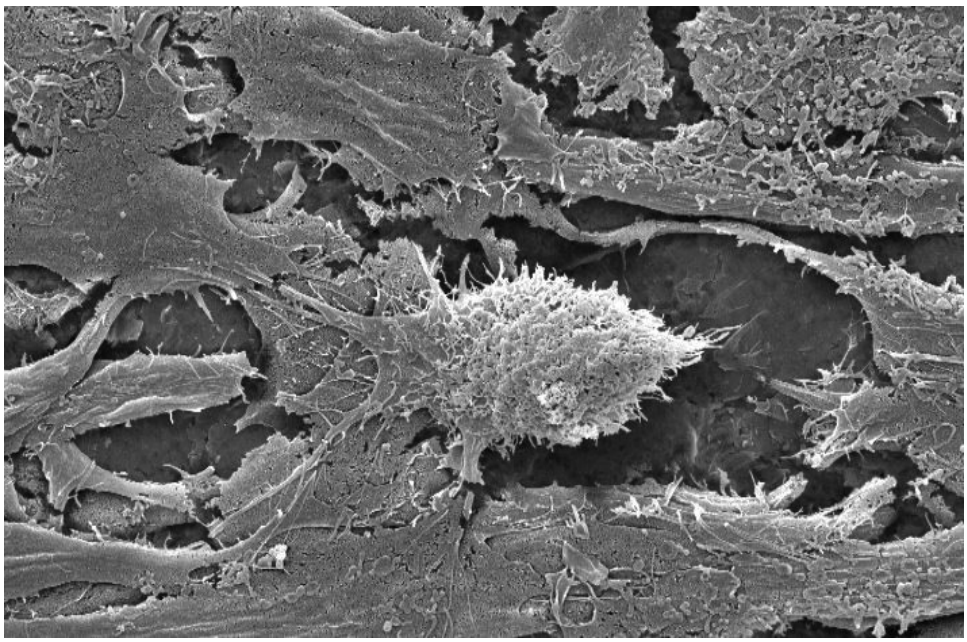

Fig. 3. *Very high magnification (2000x) of a cell in the experimental group showing evident signs of adhesion and featuring the cytoskeleton modifications typical of "cell spreading" indicating ongoing active replication.*

to the skeletal "substitute" while providing anatomical and firm fixation of the marginal soft tissues (joint capsules, muscles, tendons, ligaments etc.) at the surgical site.

Published literature as well as our clinical experience support the clinical evidence that soft tissues suturing over a Trevira tube surrounding megaprosthesis represent a valid anchoring system of these structures after resection for bone malignant neoplasm and provide an acceptable functional outcome in most cases.

This *in vitro* analysis aimed to confirm if an experimental culture of fibroblast-like cells are able to replicate and bind to Trevira as it will be expected during postoperative recovery from oncologic bone resection and prosthetic implant. The second goal was to microscopically analyze the viability and microscopic appearance of the eventually ingrown tissue. The results collected showed how the simulated cell replication over Trevira is equivalent to pure titanium, and even if the difference is not statically significant, the absolute cell count in the first 48 h after their seeding is relatively higher for the Trevira experimental group if compared to controls. This trend seems to reverse at 72 h incubation when the cell count from the sole titanium group exceeded that from the Trevira group, even though the differences are still not significant. The morphological evaluation of cells over the Trevira tube confirmed a satisfactory intracellular appearance and a healthy metabolic state as proven by sign of swelling of the cytoskeleton, a sign of active cellular replication (Fig. 3).

The same indications were given by the MTT cell growth and viability assay, which could not not show any significant difference at any time point between the cells grown over the two different materials with an equivalent very high rate of viable cells at ELISA immunoassay.

According to the results shown, we are able to confirm the *in vitro* safety and efficacy, in terms of newly formed cells extension and adhesion pattern, of using an attachment tube made from Trevira fibers surrounding an oncological megaprosthesis in order to achieve the most anatomical reinsertion of remaining soft tissue following resection. From a clinical point of view, the data presented may suggest that the use of a Trevira coated modular or custom-made megaprosthesis could be indicated for early functional

rehabilitation, given the relatively quicker and larger adhesion of soft tissues over the device, making it particularly useful in young and active patients willing to regain the best musculoskeletal function after such devastating and invasive procedure as soon as possible. However, this evidence must be confirmed in an *in vivo* environment and good designed clinical studies are expected to test and eventually confirm our conclusion in order to prove this device have relevant benefits on postoperative clinical and functional outcomes of these surgical procedures

REFERENCES

1. Manfrini M, Tiwari A, Ham J, Colangeli M, Mercuri M. Evolution of surgical treatment for sarcomas of proximal humerus in children: retrospective review at a single institute over 30 years. J Pediatr Orthop 2011; 31(1):56-64.
2. Emori M, Kaya M, Irifune H, Takahashi N, Shimizu J, Mizushima E, Murahashi Y, Yamashita T. Vascularised fibular grafts for reconstruction of extremity bone defects after resection of bone and soft-tissue tumours: a single institutional study of 49 patients. Bone Joint J 2017; 99(9):1237-43.
3. Kamal AF, Putra A, Widodo W. Vascularized fibular graft as asurgical option for osteosarcoma of distal humerus: A Case Report. Int J Surg Case Rep 2017; 39:280-4.
4. Abed Y, et al. Biological reconstruction after resection of bone tumours around the knee. J Bone Joint Surg Br 2009; 91(10):1366-72.
5. Puri A. Limb salvage in musculoskeletal oncology: Recent advances. Indian J Plast Surg 2014; 47(2):175-84
6. Pala E, Trovarelli G, Calabrò T, Angelini A, Abati CN, Ruggieri P. Survival of modern knee tumor megaprostheses: failures, functional results, and a comparative statistical analysis. Clin Orthop Relat Res 2015; 473(3):891-9.
7. Donati F, Di Giacomo G, D'Adamio S, Ziranu A, Careri S, Rosa M, Maccauro G. Silver-Coated Hip Megaprosthesis in Oncological Limb Savage Surgery. BioMed res int 2016; 2016: 9079041.
8. Schleifenbaum S, Schmidt M, Möbius R, Wolfskämpf T, Schröder C, Grunert R, Hammer N, Prietzel T. Load and failure behavior of human muscle samples in the context of proximal femur replacement. BMC musculoskelet dis 2016; 17(1):149.
9. Gosheger G1, Hillmann A, Lindner N, Rödl R, Hoffmann C, Bürger H, Winkelmann W. Soft tissue reconstruction of megaprostheses using a trevira tube. Clin Orthop Relat Res 200; (393):264-71.
10. Winkelmann, W. Proximaler Femurersatz mit dem MUTARS®-System. Der Orthopäde, 2010; 39(10):942-8.
11. Yang G, Rothrauff BB, Tuan RS. Tendon and ligament regeneration and repair: clinical relevance and developmental paradigm. Birth Defects Research Part C: Embryo Today: Reviews 2013; 99(3):203-22.
12. Rosa MA, Maccauro G, Sgambato A, Ardito R, Falcone G, De Santis V, Muratori F. Acrylic cement added with antiblastics in the treatment of bone metastases. J Bone Joint Surg Br 2003; 85(5):712-6.
13. Riss TL, Moravec RA, Niles AL, Duellman S, Benink HA, Worzella TJ, Minor L. Cell viability assays. Advancing Translational Sciences; 2004-2013 May 1 [updated 2016 Jul 1].
14. Palumbo BT1, Henderson ER, Groundland JS, Cheong D, Pala E, Letson GD, Ruggieri P. Advances in segmental endoprosthetic reconstruction for extremity tumors: a review of contemporary designs and techniques. Cancer Control 2011; 18(3):160-70.
15. Enneking WF, Dunham W. Resection and reconstruction for primary neoplasms involving the innominate bone. JBJS 1978; 60(6):731-46.
16. Kawaguchi N, Ahmed AR, Matsumoto S, Manabe J, Matsushita Y. The concept of curative margin in surgery for bone and soft tissue sarcoma. Clin Orthop Relat Res 2004; (419):165-72.
17. Xu S, Yu X, Xu M, Fu Z, Chen Y, Sun Y, Su Q. Limb function and quality of life after various reconstruction methods according to tumor location following resection of osteosarcoma in distal femur. BMC musculoskelet dis 2014; 15(1):453.
18. Cladière-Nassif V, Bourdet C, Audard V, Babinet A, Anract P, Biau D. Is it safe to preserve the deltoid when resecting the proximal humerus for a primary malignant bone tumour?: A comparative study. Bone Joint J 2017; 99(9):1244-9.
19. Bernthal NM, Greenberg M, Heberer K, Eckardt JJ, Fowler EG. What are the functional outcomes of endoprosthestic reconstructions after tumor resection? Clin Orthop Relat Res 2015; 473(3):812-9.

COMPLICATIONS AND SURVIVAL OF MEGAPROSTHESES AFTER RESECTION OF BONE METASTASES

M. DE GORI[1*], A. D'ARIENZO[2*], L. ANDREANI[2], G. BELTRAMI[3], D.A. CAMPANACCI[3], P. DE BIASE[4], F. FRENOS[3], S. GIANNOTTI[5], F. SACCHETTI[2], F. TOTTI[3], P. PARCHI[2] and R. CAPANNA[2]

[1]Department of Orthopedic and Trauma Surgery, AO "SS. Antonio e Biagio e Cesare Arrigo" Alessandria, Italy; [2]Department of Orthopedic and Trauma Surgery, University of Pisa, Italy; [3]Department of Orthopedic Oncology, AOUC Firenze; [4]Department of Orthopedic and Trauma Surgery, AOUC Firenze; [5]Department of Orthopedic and Trauma Surgery, University of Siena

[*]M. De Gori and A. D'Arienzo contributed equally to this work.

Treatment of bone metastases is often palliative, aiming at pain control and stabilization or prevention of pathological fractures. However, a complete resection with healing purposes can be performed in selected cases. The aim of our work was to evaluate the survival of megaprostheses used for reconstruction after bone metastases. Between January 2001 and March 2015, we implanted 169 Megasystem-C® (Waldemar LINK® GmbH & Co. KG, Hamburg, Germany) after bone metastasis resection. Patients, 95 females and 74 males, were operated at an average age of 61 (12-87) years for proximal femoral resection in 135 (79.9%) cases, distal femur in 24 (14.2%), proximal tibia in 6 (3.6%), total femur in 3 (1.8%) and intercalary femur in 1 (0.6%). Mostly, breast cancer metastases (30.8%), kidney (17.8%) and lung (14.2%) were treated. At an average follow-up of 21 (1-150) months, we found a 99.4% overall limb salvage and a 96.1% overall survival rate at 1 year, 92.8% at 2 years, and 86.8% at 5 and 10 years. We found 9 (5.3%) mobilization cases of the proximal femoral implant, 3 needed surgical reduction; 2 (1.2%) cases of aseptic loosening of the prosthetic stem; 2 (1.2%) periprotetic infection cases, one requiring a 2-stage revision. Few literature studies have evaluated the survival of megaprosthetic implant in the treatment of bone metastases. Our data show how in this specific context the rate of complications is significantly lower than expected in general orthopedic orthopedic surgery. The use of modular prostheses is a valid reconstructive strategy after bone metastasis resection in selected patients. The rate of short-term complications is exceptionally low; further studies will have to confirm this in the longer term.

During recent decades, advances in chemotherapy, radiotherapy, immunotherapy, and hormonal treatment have led to a prolonged life expectancy of oncologic patients. Consequently, this improvement results in an increased risk of developing bone metastases. The skeleton is the third most frequent site of metastastic spread after the lung and the liver. Despite the treatment of a bone metastasis is usually palliative (with the goal to achieve adequate control of pain and/or to stabilize or prevent pathological fractures), in selected cases a complete resection may be attempted to improve the survival of the patient (1).

Capanna and Campanacci (2) previously described a protocol for the treatment of bone

Key words: megaprostheses, bone metastases, survival rate, complications

Mailing address:
Marco De Gori, MD,
Specialist in Orthopaedic and Trauma Surgery,
Department of Orthopaedic and Trauma Surgery,
AO "SS.Antonio e Biagio e Cesare Arrigo", Via Venezia 16,
15121, Alessandria, Italy
e-mail: madegori@hotmail.it

0393-974X (2017)

metastases of the appendicular skeleton, addressing indications for surgery, the type of operation to be undertaken, and the methods of reconstruction. It is well known that patients suffering from a solitary metastasic lesion with good prognosis and those with either a pathological or an impending fracture may benefit from a surgical treatment. The use of megaprostheses is currently gaining momentum as a viable reconstructive technique after resection of metaepiphyseal bone metastases of major weight-bearing bones (3, 4).

In these cases the life expectancy of the megaprosthetic implant should exceed that of the patient (5, 6). In this light, we sought to investigate what is the overall survival of megaprostheses used for reconstruction after resection of bone metastases originating from different primary tumors.

MATERIALS AND METHODS

Study population

The study was approved by the local Ethical Committee, and the research was performed in compliance with the Helsinki Declaration. We reviewed data from consecutive patients who have undergone a modular megaprosthetic replacement from January 2001 to March 2015 at the Department of Orthopaedic Oncology and Reconstructive Surgery, University of Florence, Italy. In this study period, 517 modular endoprostheses of the lower limb were implanted in 517 patients. We included in this retrospective study 169 patients who received a megaprosthetic implant for treatment of a bone metastasis, as previously described (2). There were 95 (56.2%) females and 74 (43.8%) males, with an average age of 61 (12-87) years. As shown in Table I, metastases from primary tumors of the breast (30.8%), kidney (17.8%), and lung (14.2%) accounted for the majority of cases. At the date of the current study, 87 (51%) patients are still under observation 22 months (1-150) after the index procedure, 69 (41%) were died 22 months (1-88) after surgery, and 13 (8%) were lost at follow-up 6 months (5-7) after surgery.

Surgical technique

All surgical procedures were performed under general anesthesia, and with the use of the same megaprosthetic modular system (Megasystem-C® (Waldemar LINK® GmbH & Co. KG, Hamburg, FRG) (Fig.1a-1b, Fig. 2). In details, 135 (79.9%) proximal femoral endoprostheses, 24 (14.2%) distal femoral endoprostheses, 6 (3.6%) proximal tibial endoprostheses, 3 (1.8%) total femoral endoprostheses, and 1 (0.6%) intercalary femoral endoprosthesis were implanted.

In procedures around the knee, in the cases of an isolated distal femoral resection the patellar tendon was not detached from the anterior tibial tuberosity; in the cases of a proximal tibial resection, reconstruction of the extensor mechanism was accomplished by suturing the patellar tendon on the tibial component, which provides a fixation cage on its proximal part. A rotating hinge mechanism was used in all cases, and resurfacing of the patella was not performed. In proximal and total femoral procedures, reconstruction of the abductor mechanism was accomplished by suturing the vastus lateralis and gluteus medius on the prosthesis, which provides holes on its proximal part. The hip articulation reconstruction consisted in a bipolar hip unless acetabular involvement required a total hip arthroplasty [4 out of 138 procedures (3%)].

The implant system may have either cemented or cementless stems. In our clinical practice, resection of

Table I. *Incidence of different primary tumors in our series and type of implant used.*

Primary tumor	Number	Percentage	PF	DF	TF IF	PT		
Breast	52	30.8%	46	3	1	2		
Kidney	30	17.8%	21	9				
Lung	24	14.2%	21	3				
Thyroid	6	3.6%	5	1				
Unknown primary origin	6	3.6%	3	1		2		
Prostate	5	3%	5					
Bladder	4	2.4%	3	1				
Other primary tumors	42	24.9%	31	6	2 1	2		

PF: *proximal femur;* ***DF:*** *distal femur;* ***TF:*** *total femur;* ***IF:*** *intercalary femur;* ***PT:*** *proximal tibia.*

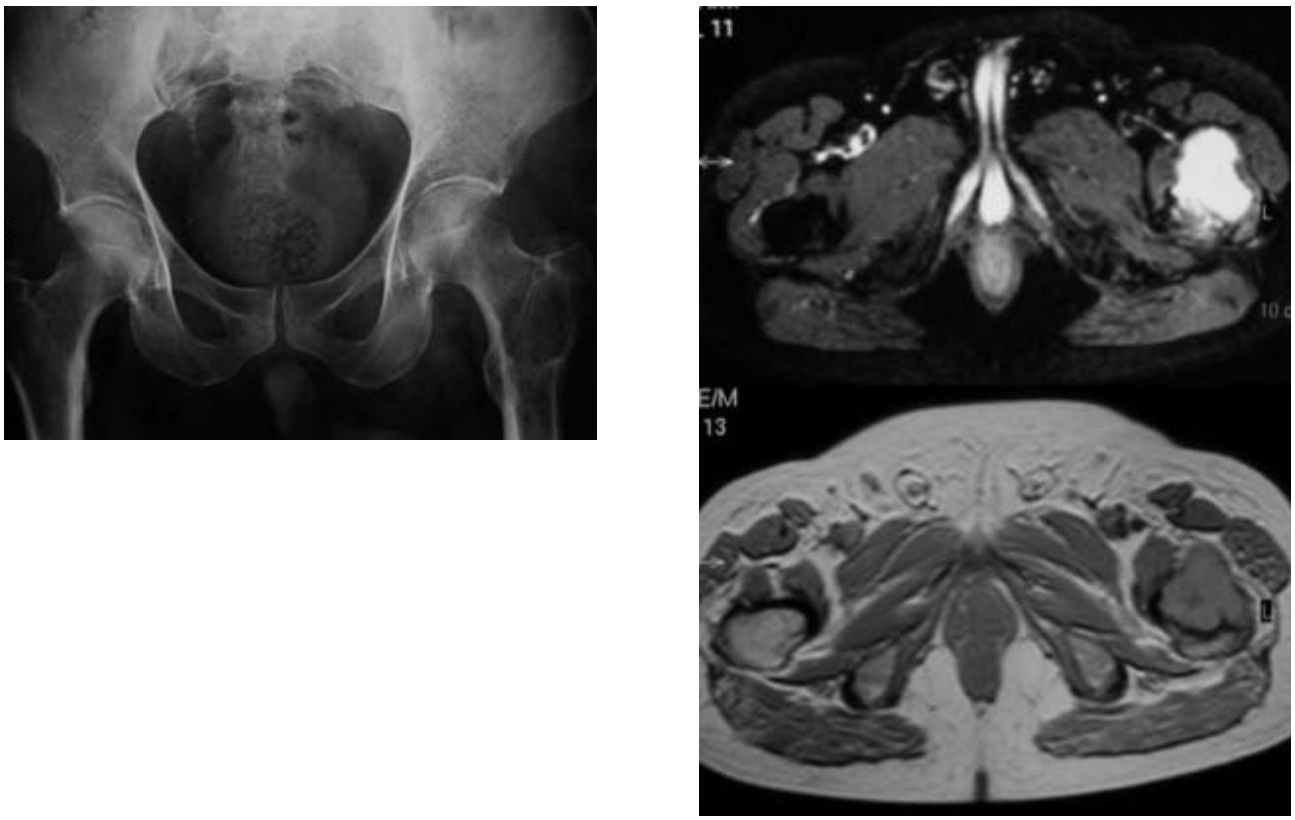

Fig. 1a, b. *X-rays and MRI shows proximal femur metastases from renal cell carcinoma.*

bone metastases is usually reconstructed with cemented implants. Accordingly, cemented fixation was used in the current series in 158 out of 167 (94.6%) femoral stems and in 31 out of 33 (93.9%) tibial stems. In details, cemented stems were preferred in irradiated bone, in old patients with osteoporotic bone, when postoperative radiotherapy was required, and when the shape of the medullary canal did not allow an adequate press-fit fixation. Cementless stems were used in young and active patients, when postoperative radiotherapy was not expected, and when an adequate press-fit was achievable (7, 8).

Postoperative protocol

All patients received a minimum 6-week pharmacological subcutaneous thromboembolism prevention therapy with low-molecular-weight heparin, until restoration of adequate walking ability. An aggressive antibiotic preventive therapy regimen consisting of a one-week pharmacological venous administration of vancomycin and tobramycin followed by a one-week oral administration of β-lactams was used routinely; the regimen was modified in only specific cases as renal insufficiency, or allergy.

The postoperative rehabilitation regimen varied according to the surgical site, reconstruction of the extensor mechanism in procedures involving the proximal tibia, and fixation of the stems. In proximal femoral reconstructions, a hip brace was used for 2 months after surgery allowing hip range of motion from 0° to 60° for the first month and from 0° to 90° for the second month. Full weight bearing was immediately allowed in cemented implants, whereas progressive weight bearing was adopted in cementless implants with partial to full weight-bearing progressing within 1 month. In procedures involving reconstruction of the knee extensor mechanism, weight bearing was delayed, and the knee was immediately immobilized in extension for 1 month.

Patient evaluation

A complete clinical history was obtained from all

patients. Initial and follow-up data were extracted from our medical records relating to follow-up evaluations. Patients with insufficient data in our database were recalled and evaluated. Specifically, patients were reviewed for both complications and failures of their megaprosthetic implant that were classified according to the system by Henderson et al. (9). In details, this system categorizes complications as mechanical and nonmechanical. Mechanical complications includes those related to loss of normal function of the endoprosthesis and/or relationships between the endoprosthetic components and adjacent bone and soft tissue attachment. They are furtherly divided into three types: soft tissue complications, including instability, tendon rupture, or aseptic wound dehiscence (type 1), aseptic loosening with both clinical and radiographic evidence (type 2), and structural failures, including periprosthetic or prosthetic fracture or deficient osseous supporting structure (type 3). Nonmechanical complications include those not compromising the function of the endoprosthesis and its surrounding connective tissue. They are furtherly divided into two types: perimegaprosthetic infection (type 4), and tumor progression or recurrence (type 5). Failures are defined as those complications having required complete revision of the mega implant, unplanned revision of a failed portion of the endoprosthesis, fixation of a periprosthetic fracture, soft-tissue reconstruction to restore joint stability, endoprosthetic removal without revision, and amputation (9).

Statistical analysis

The mean and range were reported for the continuous variables, whereas count and percent described the categorical variables. Survival curves were established with the Kaplan-Meier method (10), and the difference in cumulative survival between groups of patients was assessed with the Mantel-Cox log-rank test. The IBM SPSS Statistics 21.0.0.1 software (IBM Corp, Armonk, NY, USA) software was used for the database construction and the statistical analysis. A 2-tailed $p<0.05$ was considered significant.

RESULTS

Type 1: soft-tissue complications

Nine (5.3%) cases of dislocation were recorded among the proximal femoral endoprostheses, occurring 9 (1-36) months after the index procedure. A closed reduction was effectively performed in 6 patients, one further patient was treated with an open reduction without component revision, whereas 2 patients underwent an isolated acetabular component revision.

Two (1.2%) patients treated with a proximal femoral megaimplants experienced an aseptic wound dehiscence 2 and 4 months postoperatively. Both cases were effectively treated with a debridement of the surgical wound.

With failures related to soft-tissue complications considered as endpoint, the prosthetic survival was 98.6% at 1 and 2 years, and 95.7% at 5 and 10 years.

Type 2: aseptic loosening

Overall, aseptic loosening occurred in 2 (1.2%) cases 13 and 37 postoperatively. Both patients complained mobilization of the cemented femoral stem of a distal femoral prosthesis, and were treated with megaprosthetic revision. In one case, revision required a total femoral endoprosthesis.

With failures related to aseptic loosening considered as endpoint, endoprostheses survival was 100% at 1 year, 98.6% at 2 years, and 95.5% at 5 and 10 years.

Type 3: structural complications

Three (1.8%) mechanical failures occurred at 28 months (12-56) postoperatively due to a rupture of a Morse taper between two modular components and a revision was then performed. These complications were observed in the initial experience with prostheses, and were related to a flaw design. After the correction, no further structural complications were observed in the last 10 years.

With failures related to structural complications considered as endpoint, endoprostheses survival was 98.6% at 1 year, 97.1% at 2 years, and 90.2% at 5 and 10 years.

Type 4: perimegaprosthetic infections

Overall, infection occurred in 2 (1.2%) patients. In details, one patient experiencing infection 9 months after the implant of a distal femoral endoprosthesis

underwent a one-stage revision; one further patient experiencing infection 22 months after the implant of a proximal femoral endoprosthesis underwent a two-stage revision with a silver-coated megaprosthesis being implanted. Both healed with no evidence of new infection.

With failures related to perimegaprosthetic infections considered as endpoint, endoprostheses survival was 98.8% at 1 year, 97% at 2, 5, and 10 years.

Type 5: tumor progression

Five (3%) cases of tumor progression occurred 19 (2-74) months after the index procedure. Three patients received combined chemotherapy and radiation therapy. One patient suffering from thyroid cancer showed a pelvic tumor progression 74 months after the implant of a proximal femoral endoprosthesis; a pelvic resection with massive allograft reconstruction was performed. One further patient suffering from colon cancer showed tumor progression 16 months after the implant of a proximal femoral endoprosthesis; as the new metastasis occurred in the proximal thigh, the patient finally underwent a hindquarter amputation.

With failures related to tumor progressions considered as endpoint, endoprostheses survival was 100% at 1 year, 98.5% at 2 and 5 years, and 87.5% at 10 years.

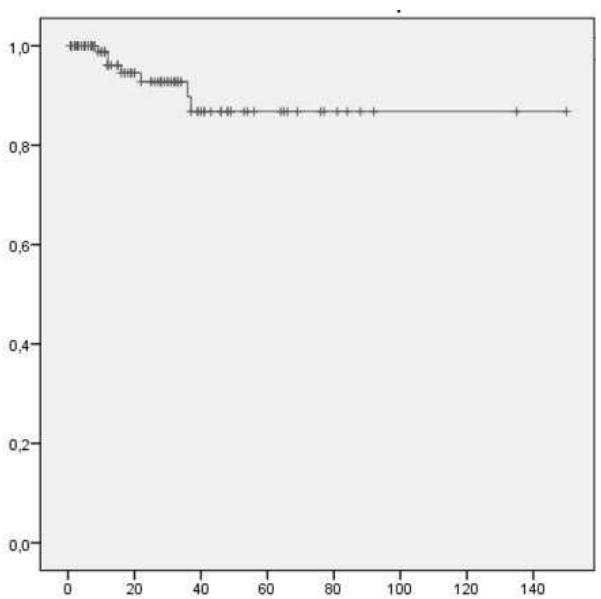

Graph 1. *Overall survival, excluding type 5 failures.*

Overall survival analysis

Overall limb salvage was 99.4% with only one amputation resulting from tumor recurrence. As done previously (7), overall survival was calculated excluding type 5 failures, as they are not related to the implant, but rather to the resection or aggressiveness of the tumor. Overall survival, excluding type 5 failures, was 96.1% at 1 year, 92.8% at 2 years, and 86.8% at 5 and 10 years (Fig. 1). Megaprostheses used for reconstruction after resection of a metastasis from kidney tumor showed a lower survival rate in comparison with the other types of tumors (odds ratio=6.244, p=0.012, Fig. 2). Despite there was no significant difference in survivorship among the different locations, distal femoral reconstructions showed a trend towards a lower survival rate (p=0.073). Including also type 5 failures, overall survival was 96.1% at 1 year, 91.2% at 2 years, 85.3% at 5 years, and 74.7% at 10 years.

Assuming that a good megaprosthetic reconstruction implies an implant survival exceeding that of the patient (5-6), we next sought to determine the theoretical overall complication rate among the sole patients that developed complications or were still under observation at the end of the study; that is, we excluded those patients who died or were lost at follow-up without developing complications. Excluding type 5 failures, overall survival was 93.2% at 1 year, 87.4% at 2 years, and 79.1% at 5 and 10 years.

DISCUSSION

To the best of our knowledge, this is the largest series even published addressing the survival of megaprostheses in the treatment of bone metastases, and Table I, very few similar studies (3, 6, 11, 12) have been previously published.

Implant survival is still the main concern that limits the routine use of megaprostheses to manage bone metastases in conventional orthopaedic centres, therefore more routine treatment (as ORIF with or without cement) are chosen. However, both the implant survival and fast recovery of function have been recognized as key outcome-indicators of a

Fig. 2. *The resected metastases with the megaprosthesis and the post-operative X-ray.*

successful surgical management of bone metastases (6). We found an overall failure-free survival of 96.1% at 1 year, 92.8% at 2 years and 86.8% at 5 and 10 years. Proper comparison of our results with previous published data (3, 6, 12) is difficult as methodological discrepancies may occur. Indeed, our survival analysis was carried out considering failures according to Henderson et al. (9) rather than overall reoperations as endpoints; moreover, tumor progressions was separately analyzed. Using a similar statistical analysis, we previously found that the use of megaprostheses had lower failure-free survivals of 75.9% at 5 years and 66.2% at 10 years after overall tumor resection (7), and of 91.5% at 1 year, 80% at 2 years, 71.6% at 5 years, and 69.1% at 5 and 10 years in the management of non-neoplastic diseases (8).

We observed a lower implant survival after kidney tumor resection in comparison with the other types. It has been previously observed that at least one third of patients suffering from a kidney tumor develops a chronic kidney disease; we can hypothesize that the occurrence of a concomitant disease-related osteomalacia may affect the bone quality and therefore the implant survival (13). Moreover, antiangiogenic factors used in therapy may jeopardize bone quality. Finally, the site of kidney metastases is more often around the knee compared to other tumor sites and this reflects the poor behavior of knee implants compared to others.

Overall, our data show that an encouraging low failure rate is expected with a megaprosthetic reconstruction after bone metastasis resection. This is correlated to the relatively low rate of occurring complications. Periprosthetic joint infection remains one of the most challenging complications following a megaprosthetic reconstruction and a leading cause of early implant failure. According to a previously published systematic review (14), a mean infection rate of 10% should be expected following tumor resection, and even higher rates of up to 43% may follow revision surgery (15). Interestingly, we detected an infection rate of 1.2% following bone metastasis resection and megaprosthetic reconstruction. This rate is exceptionally lower than those of previous series ranging from 5.3% to 8.6% (3, 6, 11, 12). Notably, we usually perform both a gastrocnemius flap to manage difficult soft tissue coverages of the proximal tibia (16) and a long-term (i.e., more than 24 h) perioperative antibiotic prophylaxis (14).

These strategies have demonstrated to minimize infection risk after megaprosthetic reconstruction (17). Moreover, it should be considered that the majority of bone metastases included in this study were located in the proximal extremity of the femur, that are less exposed to develop perimegaprosthetic infections than tumors arising around the knee (17).

We detected a 5.3% rate of dislocation among the proximal femoral endoprostheses, lower than those reported by previous published series ranging from 8.6% to 12.8% (3, 6, 11), being solely in agreement with Chandrasekar et al. (12), reporting a rate of 3% at a mean follow-up of 15.9 months. We may assume that our routine use of bipolar hip endoprostheses (3) unless rare acetabular involvements may justify such result: indeed, several oncologic series have previously demonstrated improved stability and lower dislocation rates with bipolar hemiarthroplasty versus total hip reconstruction with acetabular resurfacing (5, 18, 19).

As a main limitation of this study, we acknowledge that length of follow-up (i.e., 21 months) is still inadequate to draw definite conclusions on the implant longevity and survivorship, posing a certain risk to underestimate the actual failure rate. It should also be noted that, except in some cases, the survival of these patients is limited and our data, which show megaimplants reconstruction is tailored to their needs not only for short-term survival (2 years) but also for medium to long term survival (5-10 years), contrary to the results observed in reinforced osteosynthesis and cemented reconstruction with fracture risk related over time (9).

Notably, the characteristics of the included patients and their expected survival impede to design long-term follow-up studies (3, 6, 11, 12). However, it should be considered that more than 80% of our complications occurred within 2 years after surgery, so that no substantial detrimental rates overtime should be expected. Limits and potential biases arising from the retrospective design should be also considered.

CONCLUSIONS

Our results support the use of modular endoprostheses as a solution for reconstruction after resection of bone metastases in selected patients. An overall survival rate of 86.8% at 10 years, with a low overall complication rate, represents a promising result is such a complex surgical procedure. Notably, despite perimegaprosthetic infection is commonly reported as a worrisome complication in orthopaedic oncology, our 1.2% infection rate is encouraging being comparable to those of primary procedures. Physicians should consider these results when discussing the outcomes of this complex reconstructive surgery with patients. Long-term studies should be performed to confirm that these successful results are maintained overtime.

ACKNOWLEDGEMENTS

Marco De Gori was supported by a scholarship from the Italian Society of Orthopaedics and Traumatology (SIOT).

REFERENCES

1. Hage WD, Aboulafia AJ, Aboulafia DM. Incidence, location and diagnostic evaluation of metastastic bone disease. Orthop Clin North Am 2000; 31:515-28.
2. Capanna R, Campanacci DA. The treatment of metastases in the appendicular skeleton. J Bone Joint Surg Br 2001; 83:471-81.
3. Chan D, Carter SR, Grimer RJ, Sneath RS. Endoprosthetic replacement for bony metastases. Ann R Coll Surg Engl 1992; 74:13-18.
4. Harvey N, Ahlmann ER, Allison DC, Wang L, Menendez LR. Endoprostheses last longer than intramedullary devices in proximal femur metastases. Clin Orthop Relat Res 2012; 470:684-91.
5. Potter BK, Chow VE, Adams SC, Letson GD, Temple HT. Endoprosthetic proximal femur replacement: metastatic versus primary tumors. Surg Oncol 2009; 18:343-9.
6. Henrichs MP, Krebs J, Gosheger G, et al. Modular tumor endoprostheses in surgical palliation of long-bone metastases: a reduction in tumor burden and a durable reconstruction. World J Surg Oncol 2014; 12:330.
7. Capanna R, Scoccianti G, Frenos F, Vilardi A, Beltrami G, Campanacci DA. What was the survival

of megaprostheses in lower limb reconstructions after tumor resections? Clin Orthop Relat Res 2015; 473:820-30.
8. De Gori M, Scoccianti G, Frenos F, et al. Modular endoprostheses for nonneoplastic conditions: midterm complications and survival. Biomed Res Int 2016; 2016:2606521.
9. Henderson ER, Groundland JS, Pala E, et al. Failure mode classification for tumor endoprostheses: retrospective review of five institutions and a literature review. J Bone Joint Surg Am 2011; 93:418-29.
10. Kaplan EL, Meier P. Nonparametric estimation from incomplete observations. J Am Stat Assoc 1958; 53:457-81.
11. Park DH, Jaiswal PK, Al-Hakim W, Aston WJS, Pollock RC, Skinner JA, Cannon SR, Briggs TWR. The use of massive endoprostheses for the treatment of bone metastases. Sarcoma 2007; 2007:62151.
12. Chandrasekar CR, Grimer RJ, Carter SR, Tillman RM, Abudu AT. Modular endoprosthetic replacement for metastatic tumours of the proximal femur. J Orthop Surg Res 2008; 3:50.
13. Chang A, Finelli A, Berns JS, Rosner M. Chronic kidney disease in patients with renal cell carcinoma. Adv Chronic Kidney Dis 2014; 21:91-5.
14. Racano A, Pazionis T, Farrokhyar F, Deheshi B, Ghert M. High infection rate outcomes in long-bone tumor surgery with endoprosthetic reconstruction in adults: a systematic review. Clin Orthop Relat Res 2013; 471:2017-27.
15. Capanna R, Morris HG, Campanacci D, Del Ben M, Campanacci M. Modular 237 uncemented prosthetic reconstruction after resection of tumours of the distal femur. J Bone Joint Surg Br 1994; 76:178-186.
16. Myers GJ, Abudu AT, Carter SR, Tillman RM, Grimer RJ. The long-term results of endoprosthetic replacement of the proximal tibia for bone tumours. J Bone Joint Surg Br 2007; 89:1632-7.
17. De Gori M, Gasparini G, Capanna R. Risk factors for perimegaprosthetic infections after tumor resection. Orthopedics 2016; 40(1):e11-e16.
18. Morris HG, Capanna R, Del Ben M, Campanacci DA. Prosthetic reconstruction of the proximal femur after resection of bone tumors. J Arthroplasty 1995; 10:293-9.
19. Torbert JT, Fox EJ, Hosalkar HS, Ogilvie CM, Lackman RD. Endoprosthetic reconstructions: long-term followup of 139 patients. Clin Orthop Relat Res 2005; 438:51-9.

EDITORIAL

EVALUATION OF ACCURACY OF BONE CUTS AND IMPLANT POSITIONING IN TOTAL KNEE ARTHROPLASTY USING PATIENT SPECIFIC INSTRUMENTATION

V. DE SANTIS[1], A. BURROFATO[1], R. D'APOLITO[1], C. DE IESO[1], N. MAGARELLI[2], G. MACCAURO[1] and A. ZIRANU[1]

[1]Orthopaedics and Traumatology Institute, Catholic University of Sacred Heart. Rome, Italy;
[2]Department of Radiological Sciences, Catholic University of Sacred Heart, Rome, Italy

In the last years new surgical techniques are developing to improve prosthesis positioning, increasing clinical and functional results and reducing invasiveness. In this scenario patient-specific instrumentations have been introduced in order to enhance surgical accuracy and ease of implantation. The purpose of this study was to assess the compliance of the pre-operative planning data with bone resections measured intraoperatively and to evaluate prosthesis positioning in patients undergoing total knee arthroplasty (TKA) using an MRI-based pin-guides instrumentation. Thirty consecutive patients (20 women and 10 men) undergoing 30 total knee replacements (20 right- and 10 left-sided knees) were included in this study. The same cemented cruciate ligament sacrificing prosthesis (NexGen LPS, Zimmer, Warsaw, Indiana, USA) was implanted in all patients by a single surgeon using Patient-Specific Instruments (PSI, Zimmer, Warsaw, Indiana, USA). Femoral and tibial bone resections were measured using a manual caliper intra-operatively and compared with the corresponding pre-operative values. Each patient underwent A CT examination following surgery in order to investigate individual component positioning. None of the cases was converted from PSI technique to conventional TKA and adequate femoral and tibial bone cuts were performed without the need for intraoperative adjustments. Two outliers were detected among the intra-operative bone cuts measurements. In all patients the size of femoral and tibial prosthetic components, hypothesized at preoperative planning, was confirmed intra-operatively. Two outliers were detected among post-operative CT measurements as for components positioning. PSI system can assist in obtaining good component positioning with reduction of outliers. Despite the small number of patients, our data demonstrate the validity of this patient-specific pin-guides system in TKA and may support repeatable improvements in surgical accuracy. Level of evidence: IV.

Total knee arthroplasty (TKA) is one of the most clinically successful and cost-effective interventions in orthopedics (1). The success of primary TKA in most patients is strongly supported by more than 20 years of follow-up data. Literature showed a rapid and substantial improvement in patient's pain, functional status, and overall health-related quality of life in about 90% of patients, 85% of them being satisfied with the results of surgery (2).

The aging population has resulted in an increased request in the number of implants over the next years, which justifies the need for further improvement of surgical techniques in order to obtain better implant positioning with highest short- and long-term clinical and functional results. The correct alignment of the components has been cited as one of the most important aspects for a successful TKA (3-5), whereas malalignment can lead to early loosening,

Key words: patient specific guides, alignment, knee replacement, CT

Mailing address:
De Ieso Carmine, MD,
Orthopaedics and Traumatology Institute,
Catholic University of Sacred Heart,
Largo Francesco Vito 1, 00168 Roma, ITALY
Tel.: +390630156638 - Fax: +390630157229
e-mail: carmine.deieso@gmail.com

0393-974X (2017)

increase in polyethylene wear and worsen function (6-9). Manual instrumentation, using intra and extra-medullary alignment rods, results in overall coronal malalignment in approximately 28% of patients (10). Computer-assisted navigation (CAN) reduces the number of outliers, although the difficulty with intra-operative landmarks registration, lengthening of operative time, pin loosening, pin-site fractures, learning curve, increased costs associated with both longer time and equipment investment represent potential drawbacks of this technique (10-12).

With the goal of improving post-operative alignment and positioning, the first patient-specific instrumentation was introduced at the beginning of the 21th century (OtisMed system). Since then, other patient-specific systems have been introduced. These devices, based on pre-operative planning through magnetic resonance imaging (MRI) or computed tomography (CT), allow creating cutting blocks or pin-guides conforming to the anatomy of patient's knee. On the one hand, these surgical devices offer potential advantages such as reduction in overall surgical time, less invasiveness, decrease in peri-operative blood loss, short lasting hospitalization, better component alignment and successful clinical results. On the other hand the raise in price to produce single-use boxes and to perform pre-operative imaging (13), lengthening in the waiting time for surgery, use of ionizing radiations in CT-based methods, possible errors in the choice of components size and their positioning, as well as learning curve are potential disadvantages. There are controversial data in literature regarding alignment and spatial positioning of components obtained using these new procedures (6, 10, 14-21).

The purpose of this investigation was to evaluate the compliance of the pre-operative planning with prosthesis positioning, assessed with post-operative CT, in patients undergoing TKA using an MRI-based pin-guides instrumentation. Furthermore, the bone cuts estimated pre-operatively were compared with those measured intra-operatively

.

MATERIALS AND METHODS

Thirty consecutive patients (20 women and 10 men) undergoing 30 total knee replacements (20 right- and 10 left-sided knees) using a patient specific instrumentation technique between June 2014 and November 2014 were included in this study. Patient inclusion criteria were primary knee osteoarthritis, failure of conservative treatments, no medical contraindications to surgery, acceptance of a relatively new method and willingness to wait the additional 7-8 weeks required for instrumentation to be prepared. Patient exclusion criteria consisted in previous surgery of the knee or hip of the examined limb leading to artifacts at MRI, history of trauma, coronal deformity (>10° varus/valgus) and general contraindications to perform an MRI examination (patients with pacemaker, claustrophobia or metalwork). The same cemented posterior stabilized prosthesis (NexGen LPS, Zimmer, Warsaw, Indiana, USA) was implanted in all patients by a single experienced surgeon (V.D.S.) using Patient-Specific Instruments (PSI, Zimmer, Warsaw, Indiana, USA). None of the patient had the patella resurfaced. Mean age of patients was 75.3±6.7 years, range 65-85 years. Mean BMI was 28.4±3.6 kg/m^2.

All patients underwent pre-operative radiographic assessment including full-length weight-bearing radiographs of both lower limbs and a lateral view of the knee to be implanted. MRI was performed about eight weeks before surgery with a 1.5 T unit (Achieva, Philips Healthcare, Best, the Netherlands) as per a standardized protocol validated by the manufacturer (Materialise, Leuven, Belgium), consisting of three consecutive sequences of the knee, hip and ankle, respectively (Table I). For the knee, fat saturation was adopted on high resolution T1-weighted images, to obtain an adequate visualization of residual articular cartilage. The most important factor influencing image quality was the complete immobility of patients during examinations. This goal was achieved through the supervision of a radiologist experienced in musculoskeletal imaging (N.M.), who checked in real time the correct positioning of patients, adherence to technical acquisition parameters and absence of artifacts. Patients were examined in the supine position, lying as comfortable as possible, with joints locked inside the coils by means of foam pads. All images were acquired along planes perpendicular or parallel to the table, avoiding oblique orientations. MRI data were sent to the manufacturer through an online management system (OMS) at least 28 days before the established date of surgery. Medical

images were anonymized upon receipt: a unique patient identifier was assigned to each case throughout its entire life cycle to protect the privacy of patients.

A quality check of images was performed again, to exclude artifacts due to patient motion, image wrap around, chemical shift, low signal to noise ratio or not adequate fat saturation, all implying the need to repeat MRI. Two-dimensional images were then segmented by a specific software (Materialise N.V., Leuven, Belgium), which created a 3D model of the patient's anatomy (Fig. 1).

Based on this model, engineers performed a planning of each TKA, which was then submitted to the surgeon's default alignment protocol. The default settings were neutral coronal alignment, 3° of femoral flexion and 7° of posterior tibial slope. Therefore, the surgeon, integrating this default alignment protocol with the data acquired from pre-operative clinical and radiological examinations, controlled and eventually adjusted the planning for each patient, by choosing the distal and posterior bone resections of femoral condyles, as well as the proximal bone resection of tibial plateau. Following planning approval, a computer-assisted manufacturing technology, using a selective laser sintering, created PSI jigs perfectly conforming to the patient's anatomy, including osteophytes.

All TKAs were implanted by the same experienced surgeon (V.D.S.), following a standardized femur-first technique through an antero-medial approach. PSI guides were carefully positioned over the previously cleaned and dried articular surfaces, ensuring an accurate fit between them, and then drill holes and pins were placed in the bone under the guidance of PSI jigs (Fig. 2).

The pins were left in the bone and used to place the standard cutting blocks. No osteophytes or cartilage were removed. The femoral distal and posterior bone resections, as well as the proximal tibial bone resections, were measured intra-operatively using manual caliper. These resections were compared with the corresponding values of pre-operative planning. Each patient underwent a post-operative CT examination, from 6 to 8 weeks after surgery, through a 64-slice scanner (Lightspeed VCT 64, GE Healthcare, Waukesha, Wisconsin, USA), following an acquisition protocol of the knee, hip and ankle similar to the preoperative MRI (Table I). CT data were transferred to a work station (Advantage Windows 4.4, GE Healthcare, Waukesha, Wisconsin, USA) for post-processing, including multi-planar reconstructions (MPR) and maximum intensity projections (MIP). The same experienced radiologist (N.M.) evaluated the positioning of both prosthetic components in the three planes of space by measuring on CT the same angles considered in the 3D MRI-based pre-operative planning.

For each lower limb, the presumed mechanical axis for the femur and tibia was drawn by connecting with a line the centre of femoral head with the middle point

Table I. *Acquisition protocol for the pre-operative MRI and post-opertive CT.*

Modality	Joint	Acquisition range	FOV (cm)	Matrix size	ST (mm)	NS	Mode	Orientation	Acquisition	TC (kVp)	Coil	TR/TE (ms)	FA (°)	Fat sat
MRI (1.5 T)	Hip	Acetabularroof-lessertrochanter	36	256x256	5.0	20	2D	Axial	FSE	NA	Body coil	500/20	90	Off
	Knee	Femoral condyles-tibial plates	20	512x512	1.0	120	3D	Sagittal	SPGR	NA	Knee coil (phased array)	20/minimum	25	On
	Ankle	Tibial malleoli-talar dome	26	256x256	5.0	20	2D	Axial	FSE	NA	Body coil	600/20	90	Off
CT (64 slices)	Hip	Acetabularroof-lessertrochanter	36	256x256	1.0	100	3D	Axial	Helical	120	NA	NA	NA	NA
	Knee	Femoral condyles-tibial plates	20	512x512	1.0	120	3D	Axial	Helical	120	NA	NA	NA	NA
	Ankle	Tibial malleoli-talar dome	36	256x256	1.0	100	3D	Axial	Helical	120	NA	NA	NA	NA

MRI: *magnetic resonance imaging;* ***CT:*** *computed tomography;* ***FOV:*** *field of view;* ***ST:*** *slice thickness;* ***NS:*** *number of slices;* ***2D:*** *two-dimensional;* ***3D:*** *three-dimensional;* ***FSE:*** *fast spin echo;* ***SPGR:*** *spoiled gradient echo;* ***TC:*** *tube current;* ***kVp:*** *kilo-Volt peak;* ***TR:*** *repetition time;* ***TE:*** *echo time;* ***FA:*** *flip angle;* ***Fat sat:*** *fat saturation;* ***NA:*** *not applicable.*

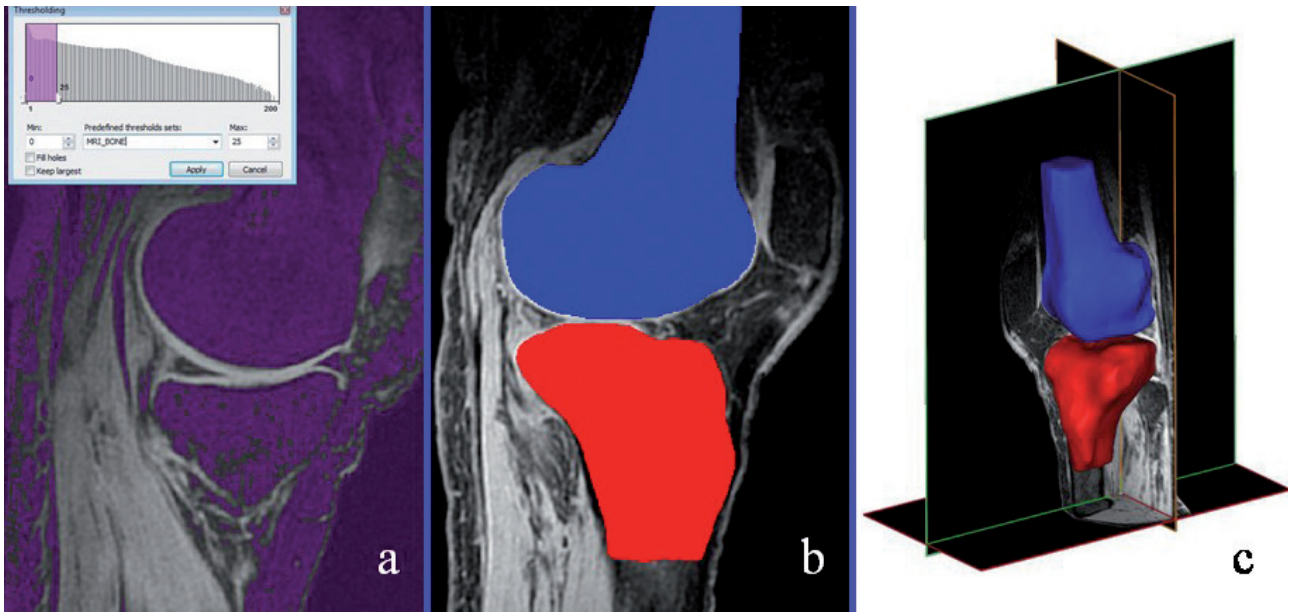

Fig. 1. *The MRI segmentation implied an automatic threshold-based marking of regions of interest on each sagittal T1-weighted high-resolution image of the knee (**a**), identifying two distinct areas for the femur and tibia (**b**). Repeating this process for all the 2D images and interpolating data, a 3D model was built (**c**).*

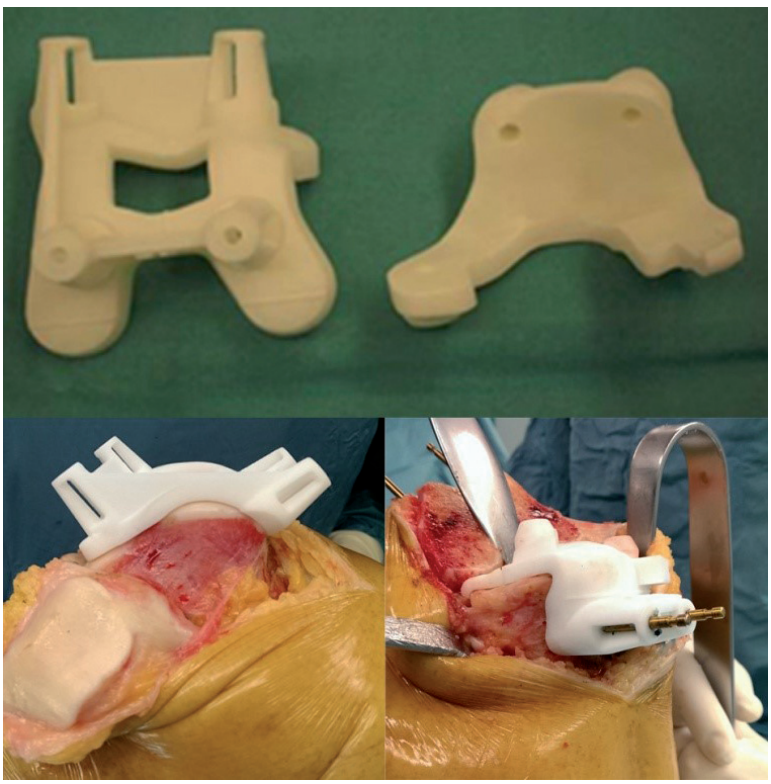

Fig. 2. *Femoral (on the left in **a**) and tibial (on the right in **a**) custom-made jigs, used as a guidance for placing cutting guides on the patient's knee (**b** and **c**).*

of intercondylar notch and the talar dome with the intercondylar eminence, respectively (Fig. 3a, b). Taking as a reference these two axes, the degree of varus-valgus deviation and of flexion-extension for both the femoral and tibial component was evaluated (Fig. 4c, d). Positive values of the measured angles were attributed to valgus deviation and flexion, whereas negatives to varus and extension, respectively. Finally, the trans-epicondylar axis (TEA) was set as a reference to assess the rotational alignment of femoral implant (Fig. 4e) and a line passing through the anterior tuberosity and the geometric centre of tibial tray (defined as the intersection between its maximum antero-posterior and medio-lateral diameters) was used for determining the axial rotation of tibial component (Fig. 4f). Positive values of measured angles indicated extra-rotation, negatives intra-rotation. These post-operative CT measurements were compared to pre-operative 3D MRI parameters concerning the spatial orientation of both prosthetic components.

Statistical analysis

Continuous data were presented as mean ± standard deviation. Bland-Altman plots were constructed to compare the pre-operative MRI parameters, concerning both the depth of surgical bone cuts and the spatial positioning of implants, with the corresponding intra-operative measurements and the post-operative CT values, respectively. Outliers were identified as measurements differing from the corresponding pre-operative values beyond the limits of agreement, i.e. ±1.96 times the standard deviation of differences between values. Pearson r correlation coefficients were used to assess the relationships of both the intra-operative measurements of bone cuts and the post-operative CT values on component orientation with the corresponding MRI pre-operative parameters. The MedCalc software version 12.5.0.0 (Mariakerke, Belgium) was used for inferential statistics. A p value less than 0.05 was considered significant.

RESULTS

Except for one case, in which the MRI had to be repeated due to the presence of motion artifacts, high-resolution images of the knee were correctly acquired and considered adherent to the standards required by the producer for pin-guides construction. The acquisition time of MRI examinations was 19.7±1.5 min. None of the cases were converted from PSI technique to conventional TKA. Adequate femoral and tibial bone cuts were performed without the need for intraoperative adjustments. For all patients the size of the femoral and tibial prosthetic components, hypothesized at pre-operative planning, was confirmed intra-operatively. The same applies to the predicted tibial polyethylene insert (10 mm). A good to excellent correlation was found between the data concerning the depth of the femoral and tibial bone cuts, hypothesized at pre-operative planning,

Table II. *Comparison between the pre-operative MRI data, concerning the depth of femoral and tibial bone cuts, and the corresponding intraoperative measurements.*

Component		Cut	Preoperative MRI data (mm)	Intraoperative measurements (mm)	Mean difference (mm)	Limits of agreement (±1.6 SD)	Number of outliers	Correlation coefficient	95 % CI	p value
Femoral condyles	Medial	Distal	9.3±0.5	8.2±1.3	1.1	-1.1 - 3.1	0	0.67	0.25 - 0.89	<0.01
		Posterior	11.7±1.3	10.2±1.7	1.5	-0.7- 3.7	1	0.82	0.56 - 0.93	<0.01
	Lateral	Distal	8.8±1.5	8.5±167	0.3	-2.1 - 2.5	1	0.73	0.39 - 0.92	<0.01
		Posterior	10.1±2.3	8.3±2.2	0.8	-1.6 - 2.8	0	0.89	0.71 - 0.95	<0.01
Tibial plates	Medial	Proximal	4.8±2.1	4.6±2.2	0.2	-1.1 - 1.5	0	0.94	0.89 - 0.98	<0.01
	Lateral	Proximal	9.5±0.6	8.5±1.4	1	-1.2 - 3.3	0	0.65	0.19 - 0.87	0.01

Unless otherwise indicated, data are expressed in mm and reported as mean±standard deviation. ***MRI:*** *magnetic resonance imaging;* ***SD:*** *standard deviation;* ***CI:*** *confidence interval.*

and the corresponding intra-operative measurements (Table II). Two outliers were detected among the values measured during the surgery, concerning the thickness of the distal resection of a lateral condyle (11 mm) and the posterior resection of a medial condyle (6 mm), respectively.

Additionally, a good matching was also found between the pre-operative MRI values concerning the positioning of femoral and tibial components and the corresponding post-operative CT measurements (Table III). Two outliers were detected among these measurements, notably the sagittal orientation of a femoral component (5.5° flexion) and the rotational femoral component alignment of another implant (2.8° external rotation), respectively. Furthermore, a favorable correlation was found between the values planned pre-operatively and those measured on post-operative CT with regard to the sagittal orientation of the femoral component (r=0.88, 95% confidence interval 0.67-0.96, p<0.01) and the tibial slope (r=0.72, 95% confidence interval 0.33-0.90, p<0.01).

DISCUSSION

The success of TKA depends on multiple factors, including patient's characteristics, implant selection, operative technique, accurate positioning and alignment of prosthetic components (22). In recent years the use of 3D models for templating and custom block manufacturing increased exponentially (21). Measurements obtained from conventional radiographs (2D images of 3D anatomical structures)

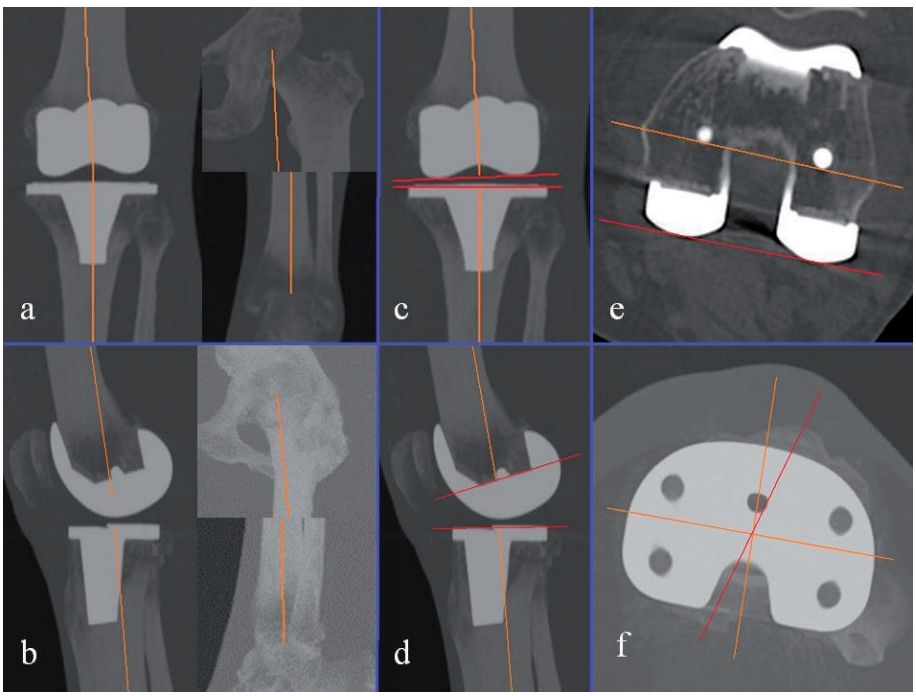

Fig. 3. *Coronal (**a**) and sagittal (**b**) MIP images of the implanted knee, hip and ankle showing the CT-derived mechanical axis for the femur and tibia, respectively. The varus-valgus deviation of the femoral and tibial components was assessed on coronal MIP images, by measuring the angle formed between each mechanical axis and a line tangent to the prosthetic femoral condyles and the tibial tray, respectively (**c**). The sagittal orientation of the femoral and tibial components was similarly evaluated on MIP images by calculating the angle formed between each mechanical axis and a line tangent to the distal femoral bone cut and the prosthetic tibial tray, respectively (**d**). The rotational alignment of the femoral component was assessed on axial images by measuring the angle formed between a line tangent to the posterior prosthetic condyles and the TEA (**e**). Otherwise, the axial rotation of the tibial component was evaluated on MIP images by calculating the angle formed between a line perpendicular to the maximum medio-lateral diameter of the prosthetic tibial tray and a line connecting the anterior tuberosity with the geometric centre of the tibial bone plate (**f**).*

are less accurate than those derived from second level imaging techniques, such as CT or MRI.

Several studies reported the importance of a correct coronal alignment for the success of TKA, concluding that an alignment outside 3° leads to a decreased survivorship. In conventional TKA, the incidence of malalignment can be as high as 25%, as showed in some series (23, 24). In the last years, a fair number of papers evaluated post-operative alignment of TKAs implanted using patient-specific instrumentations reporting controversial results, as confirmed by recent reviews and meta-analyses (25-29).

The rotational alignment of the femoral and tibial component may play a major role in the long-term survivorship of TKAs as well. Poor outcomes and major complications such as pain, instability, and stiffness after TKA have been linked to errors in rotational alignment of the components. With regard to this specific topic, data on patient-specific instrumentations are divisive. Yoon WhanRoh et al (30) found that the patient-specific instrumentation was unreliable, resulting in a relatively large number of dropouts (16% of 50 TKAs), owing to malrotation of the femoral component. MacDessi et al (31) evaluated with CT the mean rotation of the femoral component in 115 TKAs using PSI, concluding that 90.4% of patients was within 3° of neutral alignment to the surgical epicondylar axis.

Recent literature demonstrated a better accuracy of femoral component alignment (32, 33, 34) and global mechanical alignment with significantly shorter operation times and blood loss (32, 33), at the cost of an increased risk of outliers for the tibial component alignment (32, 35), that could reduce implant longevity. However, the amount of outliers seemed to be lower with MRI-based PSIs when compared with CT-based PSIs that do not match with the cartilaginous surface, resulting in a gap between the guide e the cartilage and an associated poorer fit for the guide (33). In our series, the data concerning prosthetic component positioning planned pre-operatively and relative to coronal, sagittal and axial alignment, were found to be consistent with those evaluated at post-operative CT, with only two outliers in the sagittal orientation of a femoral component and in the rotational alignment of another femoral implant, respectively.

Three-dimensional pre-operative planning, based on CT or MRI, could improve the surgical outcome through an appropriate choice of implant size, but for PSI, even on this issue, available data are in dispute with each other. Stronach et al (36) evaluated the planning and surgery of 66 TKAs performed with patient specific instrumentation recording that the predetermined implant size was changed intra-operatively in 77% of femurs and in 53% of tibias. Yaffe et al (37) studied 111 TKAs using PSI, 30 of which were evaluated with CAN, concluding that the PSI system was both more accurate and more precise than the CAN in predicting femoral component size in TKA (89% vs 43% respectively, $p<0.001$). Chen et al (38) studied the use of PSI in 30 patients and reported that the predictability for implant size remained 100%. In the present study MRI provided

Table III. *Comparison between the pre-operative MRI data, concerning the spatial positioning of implants, and the corresponding post-operative CT values.*

Component	Orientation	Preoperative MRI data	Postoperative CT measurements	Mean difference	Limits of agreement (±1.6 SD)	Number of outliers
Femoral	Coronal*	0±0	0.4±1.5	-0.4	-3.2 - 2.8	0
	Sagittal**	3.4±0.5	3.4±1.0	-0.2	-1.5 - 1.2	1
	Axial***	0±0	0.4±0.7	-0.2	-2.0 - 1.2	1
Tibial	Coronal*	0±0	0.1±1.0	0.0	-2.0 - 2.1	0
	Sagittal**	6.1±0.6	5.8±0.7	0.2	-0.8 - 1.2	0
	Axial***	NA	-11.7±3.1	NA	NA	NA

*Unless otherwise indicated, data are expressed in degrees and presented as mean ± standard deviation. *Positive values stand for valgus deviation, negatives for varus; **Positive values stand for flexion, negatives for extension; ***Positive values stand for extrarotation, negatives for intrarotation.*

***MRI:** magnetic resonance imaging; **CT:** computed tomography; **SD:** standard deviation; **NA:** not applicable.*

the 3D model of an arthritic knee fairly well corresponding to the effective articular anatomy. In fact, the size of the femoral and tibial prosthetic components, hypothesized at pre-operative planning, was confirmed in all cases at the operating theatre.

In contrast with the first data reported on patient specific instrumentation (39), our findings about the thickness of the tibial liners are complying with those reported by Howell et al (16), indicating that the cut plane was set correctly and the amount of bone removal was conservative. Zambianchi et al (40), evaluated the precision of two patient-specific instrumentation systems in 41 patient-specific TKAs, comparing bony resection thickness of the pre-operative planning and intra-operative measurements by a manual caliper, concluding that the two systems were accurate in distal femoral and posterior lateral femoral condyle cuts (90.2-95.1%) and less precise in posterior medial femoral condyle and proximal tibial resections (70.7-75.6%).

In a recent series, the pre-operative prediction of bony resections was reported to be fairly accurate, with the tibial cuts having the lowest proportion of acceptable cuts (defined as ≤1.5 mm, 68.9%) and more outliers (defined as >2.5 mm) than the femur (12.7% *vs* 7.5%) (41). Our study showed good to excellent correlation between the femoral and tibial bone cuts, hypothesized at pre-operative planning, and the corresponding intra-operative measurements; two outliers were detected among the values measured, concerning the thickness of the distal resection of a lateral femoral condyle (11 mm) and the posterior resection of a medial femoral condyle (6 mm), respectively

This study has several limitations. First, the small number of patients with a potential lack of power, even though we did not perform a power-analysis. Pre- and intra- operative measurements were performed exclusively by a single orthopedic surgeon, making it impossible to analyze inter-observer variation. Furthermore, the surgical procedures were performed by the same experienced surgeon that made the bone cuts and was the sole decision maker when assessing the accuracy of the cuts and soft tissue balancing. This is not representative of low volume or inexperienced knee surgeon using this technology. Besides, only the PSI system was assessed and the reported findings might not be applicable to all the patient specific instrumentations currently available on the market. In addition, the CT post-operative measurements did not take into account the contribution of weight bearing on the assessment of coronal alignment.

Finally, this study did not examine the impact of an accurate component positioning and sizing as regards clinical outcomes, only evaluating the reliability of a custom-fit TKA planning in the restoration of optimal component alignment. The long-term survival of an accurately aligned knee resulting from a custom-fit technology can only be presumed to be good but was not proven in our study.

This study showed the feasibility of a 3D MRI-based pre-operative planning in TKA reporting an excellent concordance between the data planned pre-operatively and the intra-operative measurements. The accuracy of this MRI-based custom fit TKA in providing a correct alignment of prosthetic components has been demonstrated through a post-operative CT evaluation. Further studies with an increased number of patients are certainly needed to confirm these findings.

REFERENCES

1. Iorio R, Robb WJ, Healy WL et al. Orthopaedic surgeon workforce and volume assessment for total hip and knee replacement in the United States: preparing for an epidemic. J Bone Joint Surg Am 2008; 90:1598-605.
2. NIH Consensus Statement on total knee replacement December 8-10, 2003. J Bone Joint Surg Am 2004; 86A:1328-35.
3. Cheng T, Pan XY, Mao X, Zhang GY, Zhang XL. Little clinical advantage of computer-assisted navigation over conventional instrumentation in primary total knee arthroplasty at early follow-up. Knee 2012; 19: 237-45.
4. Cheng T, Zhao S, Peng X, Zhang X. Does computer-assisted surgery improve postoperative leg alignment and implant positioning following total knee arthroplasty? A meta-analysis of randomized controlled trials? Knee Surg Sports Traumatol

Arthrosc 2012; 20:1307-22.
5. Ishida K, Matsumoto T, Tsumura N et al. Mid-term outcomes of computer-assisted total knee arthroplasty. Knee Surg Sports Traumatol Arthrosc 2011; 19:1107-12.
6. Conteduca F, Iorio R, Mazza D et al. Evaluation of the accuracy of a patient-specific instrumentation by navigation. Knee Surg Sports Traumatol Arthrosc 2013; 21:2194-9.
7. Bargren JH, Blaha JD, Freeman MA. Alignment in total knee arthroplasty. Correlated biomechanical and clinical observations. Clin Orthop Relat Res 1983; 178-83.
8. Berger RA, Crossett LS, Jacobs JJ, Rubash HE. Malrotation causing patellofemoral complications after total knee arthroplasty. Clin Orthop Relat Res 1998; 144-53.
9. Moreland JR. Mechanisms of failure in total knee arthroplasty. Clin Orthop Relat Res 1988; 49-64.
10. Ng VY, DeClaire JH, Berend KR, Gulick BC, Lombardi AV, Jr. Improved accuracy of alignment with patient-specific positioning guides compared with manual instrumentation in TKA. Clin Orthop Relat Res 2012; 470:99-107.
11. Bonutti PM, Dethmers D, Ulrich SD, Seyler TM, Mont MA. Computer navigation-assisted versus minimally invasive TKA: benefits and drawbacks. Clin Orthop Relat Res 2008; 466:2756-62.
12. Jenny JY, Miehlke RK, Giurea A. Learning curve in navigated total knee replacement. A multi-centre study comparing experienced and beginner centres. Knee 2008; 15:80-84.
13. Barrack RL, Ruh EL, Williams BM, Ford AD, Foreman K, Nunley RM. Patient specific cutting blocks are currently of no proven value. J Bone Joint Surg Br 2012; 94:95-99.
14. Abdel MP, von Roth P, Hommel H, Perka C, Pfitzner T. Intraoperative navigation of patient-specific instrumentation does not predict final implant position. J Arthroplasty 2015; 30(4):564-6.
15. Anderl W, Pauzenberger L, Kölblinger R. Patient-specific instrumentation improved mechanical alignment, while early clinical outcome was comparable to conventional instrumentation in TKA. Knee Surg Sports Traumatol Arthrosc 2016; 24(1):102-11.
16. Howell SM, Kuznik K, Hull ML, Siston RA. Results of an initial experience with custom-fit positioning total knee arthroplasty in a series of 48 patients. Orthopedics 2008; 31:857-63.
17. Klatt BA, Goyal N, Austin MS, Hozack WJ. Custom-fit total knee arthroplasty (OtisKnee) results in malalignment. J Arthroplasty 2008; 23:26-9.
18. Nunley RM, Ellison BS, Zhu J, Ruh EL, Howell SM, Barrack RL. Do patient-specific guides improve coronal alignment in total knee arthroplasty? Clin Orthop Relat Res 2012; 470:895-902.
19. Ollivier M, Tribot-Laspiere Q, Amzallag J, Boisrenoult P, Pujol N, Beaufils P. Abnormal rate of intraoperative and postoperative implant positioning outliers using "MRI-based patient-specific" compared to "computer assisted" instrumentation in total knee replacement. Knee Surg Sports Traumatol Arthrosc 2015; 24(11):3441-7.
20. Parratte S, Blanc G, Boussemart T, Ollivier M, Le Corroller T, Argenson JN. Rotation in total knee arthroplasty: no difference between patient-specific and conventional instrumentation. Knee Surg Sports Traumatol Arthrosc 2013; 21(10):2213-9.
21. Spencer BA, Mont MA, McGrath MS, Boyd B, Mitrick MF. Initial experience with custom-fit total knee replacement: intra-operative events and long-leg coronal alignment. Int Orthop 2009; 33:1571-5.
22. Matziolis G, Krocker D, Weiss U, Tohtz S, Perka C.A prospective, randomized study of computer-assisted and conventional total knee arthroplasty. Three-dimensional evaluation of implant alignment and rotation. J Bone Joint Surg Am 2007; 89:236-43.
23. Mahaluxmivala J, Bankes MJ, Nicolai P, Aldam CH, Allen PW. The effect of surgeon experience on component positioning in 673 Press Fit Condylar posterior cruciate-sacrificing total knee arthroplasties. J Arthroplasty 2001; 16:635-40.
24. Perillo-Marcone A, Barrett DS, Taylor M. The importance of tibial alignment: finite element analysis of tibial malalignment. J Arthroplasty 2000; 15:1020-7.
25. Fu H, Wang J, Zhou S, Cheng T, Zhang W, Wang Q, Zhang X. No difference in mechanical alignment and femoral component placement between patient-specific instrumentation and conventional instrumentation in TKA. Knee Surg Sports Traumatol Arthrosc 2015; 23(11):3288-95.
26. Mannan A, Smith TO. Favourable rotational

alignment outcomes in PSI knee arthroplasty: A Level 1 systematic review and meta-analysis. Knee 2016; S0968-0160(15)00175-1.
27. Sassoon A, Nam D, Nunley R, Barrack R. Systematic review of patient-specific instrumentation in total knee arthroplasty: new but not improved. Clin Orthop Relat Res 2015; 473(1):151-8.
28. Shen C, Tang ZH, Hu JZ, Zou GY, Xiao RC, Yan DX. Patient-specific instrumentation does not improve accuracy in total knee arthroplasty. Orthopedics 2015; 38(3):e178-88.
29. Voleti PB, Hamula MJ, Baldwin KD, Lee GC. Current data do not support routine use of patient-specific instrumentation in total knee arthroplasty. J Arthroplasty 2014; 29(9):1709-12.
30. Roh YW, Kim TW, Lee S, Seong SC, Lee MC. Is TKA using patient-specific instruments comparable to conventional TKA? A randomized controlled study of one system. Clin Orthop Relat Res 2013; 471:3988-95.
31. Macdessi SJ, Jang B, Harris IA, Wheatley E, Bryant C, Chen DB. A comparison of alignment using patient specific guides, computer navigation and conventional instrumentation in total knee arthroplasty. Knee 2014; 21(2):406-9.
32. Thienpont E, Schwab PE, Fennema P. Efficacy of Patient-Specific Instruments in Total Knee Arthroplasty: A Systematic Review and Meta-Analysis. J Bone Joint Surg Am 2017; 99(6):521-530.
33. Schotanus MGM, Thijs E, Heijmans M, Vos R, Kort NP. Favourable alignment outcomes with MRI-based patient-specific instruments in total knee arthroplasty. Knee Surg Sports Traumatol Arthrosc 2017.
34. Mannan A, Smith TO. Favourable rotational alignment outcomes in PSI knee arthroplasty: A Level 1 systematic review and meta-analysis. Knee 2016; 23(2):186-90.
35. Huijbregts HJ, Khan RJ, Fick DP, et al. Component alignment and clinical outcome following total knee arthroplasty: a randomised controlled trial comparing an intramedullary alignment system with patient-specific instrumentation. Bone Joint J 2016; 98-B(8):1043-9.
36. Stronach BM, Pelt CE, Erickson J, Peters CL. Patient-specific total knee arthroplasty required frequent surgeon-directed changes. Clin Orthop Relat Res 2013; 471:169-74.
37. Yaffe MA, Patel A, Mc Coy BW et al. Component sizing in total knee arthroplasty: patient-specific guides vs. computer-assisted navigation. Biomed Tech (Berl) 2012; 57:277-82.
38. Chen JY, Yeo SJ, Yew AK et al. The radiological outcomes of patient-specific instrumentation versus conventional total knee arthroplasty. Knee Surg Sports Traumatol Arthrosc 2014; 22:630-5.
39. Hafez MA, Chelule KL, Seedhom BB, Sherman KP. Computer-assisted total knee arthroplasty using patient-specific templating. Clin Orthop Relat Res 2006; 444:184-92.
40. Zambianchi F, Colombelli A, Digennaro V, et al. Assessment of patient-specific instrumentation precision through bone resection measurements. Knee Surg Sports Traumatol Arthrosc 2015; [Epub ahead of print].
41. Levy YD, An VVG, Shean CJW, Groen FR, Walker PM, Bruce WJM. The accuracy of bony resection from patient-specific guides during total knee arthroplasty. Knee Surg Sports Traumatol Arthrosc 2017; 25(6):1678-85.

COMPARISON BETWEEN DIFFERENT CELL SOURCES AND CULTURE STRATEGIES FOR TENDON TISSUE ENGINEERING

A. DI GIANCAMILLO[1], D. DEPONTI[2], M.T. RAIMONDI[3], F. BOSCHETTI[3,4], F. GERVASO[5], S. MODINA[1], L. MANGIAVINI[4] and G.M. PERETTI[4,6,]

[1]Department of Health, Animal Science and Food Safety, University of Milan, Italy; [2]IRCCS, Ospedale San Raffaele, Milan, Italy; [3]Department of Chemistry, Materials and Chemical Engineering "Giulio Natta", Politecnico di Milano, Milan, Italy; [4]IRCCS Istituto Ortopedico Galeazzi, Milan, Italy; [5]Department of Engineering for Innovation, University of Salento, Italy; [6]Department of Biomedical Sciences for Health, University of Milan, Italy

The aim of this study was to evaluate the effect of an *in vitro* mechanical stimulation by the use of a bioreactor on an engineered tendon for 7 and 14 days and to analyze the effect of the use of different cell sources: tenocytes, dermal fibroblasts or Adipose-Derived Stem Cells (ASCs), isolated from pig tissues. Histology showed a re-organization of the neo-tissue derived from the three cell populations along the direction of the stimulus. At T7, cells morphology was preserved while an increased cellular suffering at T14 was observed for all cell populations. Tenocytes exhibited higher survival than other cells. A stable immunopositivity for collagen type 1 or 3 at both time points was also observed. In conclusion, dermal fibroblasts and ASCs represent an interesting alternative and *in vitro* culture with mechanical stimuli may enhance the maturation of a tendon-like tissue.

Native tendons possess a high cellular content and a remarkable matrix presence necessary to support their growth and development, indispensable phases for maintaining tissue functions. Tissue engineering has developed techniques that combine the use of cell with scaffolds promoting tissue regeneration by stimulating the proliferation of local cells and the production of the structural matrix, fundamental when the implanted scaffold begins to degrade. Autologous cells, such as tenocytes, are the best source to ensure cellular replacement both for structural and functional purpose. Indeed, the isolation and culture of tenoblasts/tenocytes from different anatomic sites is still possible, but this involves loss of tissue.

In recent years, some studies have compared different cell sources, which might be suitable for tendon tissue engineering. Namely, dermal fibroblasts were considered as potential cells due to their ability to adapt and differentiate into a tenocyte-like cells. Dermal fibroblasts are easily accessible, with many characteristics in common with tenocytes because they both originate from mesoderm. In the last few years adipose-derived stems (ASCs) have become another interesting cell source as previous studies have shown their ability to differentiate into tenocytes (1). One of the problems faced by researchers is the lack of mechanical stimuli during the *in vitro* culture that may lead to scaffold structural alterations and to cell de-differentiation (2, 3). Thus, the maintenance of tenocyte phenotype has always been an obstacle to the development of an *in vitro* tendon construct. In this study, we analyzed the benefits of mechanical stimulation during *in vitro* culture. Moreover, the

Key words: tendon, tissue engineering, cell morphology, synthetic profile, bioreactor

Mailing address:
Giuseppe M. Peretti, M.D.,
Department of Biomedical Sciences for Health,
University of Milan,
IRCCS Istituto Ortopedico Galeazzi,
Via R. Galeazzi 4, 20161 Milan, Italy
Tel.: +39 02 5031 9967 - +39 02 6621 4735 - Fax: +39 02 6621 4736
e-mail: gperetti@iol.it

0393-974X (2017)

suitability of the different cellular populations to realize an engineered tendon seeded on scaffold and *in vitro* cultured in the presence of mechanical stimulus was investigated.

MATERIALS AND METHODS

Cell isolation

Tendons, dermis and adipose tissue were collected from Landrace X Large White pigs and processed for cell isolation as previously described (4). Briefly, dermal fibroblasts and tenocytes were aseptically isolated from piglets (10kg) respectively from dermis and Achilles tendons and washed in sterile PBS (Phosphate Buffered Saline) (Celbio, Italy), added with 50 µg/ml of gentamicin (Lonza, Italy), 0.5 µg/ml of amphotericin B (Lonza, Italy), 100 U/ml of Penicillin/Streptomycin solution (Lonza, Italy).

After three washes, samples were finely powdered and subsequently digested in DMEM High Glucose medium (Celbio, Italy), composed of 10% fetal bovine serum (Celbio, Italy), 2mM ultra-glutamine, 0.1% collagenase Type I (DBA-Italia Srl, Italy), 100 U/ml of Penicillin/Streptomycin solution, 50 µg/ml of gentamicin and 0.5 µg/ml of amphotericin B in an incubated oscillating water bath at 37˚C, overnight. All the undigested fragment tissues and debris were gently removed using a 100 microns sterile filter (BD Falcon, USA). The cell suspension was then centrifuged for 10 minutes at 1400 rpm and the obtained pellet was re-suspended in DMEM. Concerning adipose tissue, mesenchymal stem cells were isolated from pig adipose tissue as previously described (4). Briefly, the tissue was digested in DMEM High Glucose medium plus 0.1% collagenase Type I for 1 hour at 37°C; adipose fraction was discharged from the obtained cell suspension by centrifuging at 3200 rpm for 10 minutes and the cell pellet was re-suspended in DMEM and filtered with a 100-micron sterile filter (BD Falcon, USA).

As for dermis and tendon, the cell pellet was re-suspended again in DMEM High Glucose. Cell populations obtained from tendon, dermis and adipose tissue, were seeded in Petri dish and cultured in DMEM High Glucose medium containing 2mM ultra-glutamine, 20% fetal bovine serum, 1mM sodium pyruvate (GIBCO, Italy) and 10mM HEPES (GIBCO, Italy), 100 U/ml of Penicillin/Streptomycin solution, 50 µg/ml of gentamicin, 0.5 µg/ml of amphotericin B.

Scaffold synthesis

Scaffold consisted of sponges made of collagen 1 and fabricated at the Department of Innovation Engineering, University of Salento as described elsewhere (4). Collagen 1 was isolated by pulverizing freeze-dried equine tendon (Antema®, kindly provided by Opocrin S.p.A., Italy). The collagen powder was then suspended in distilled water at 2%, lyophilized and slowly frozen, thus obtaining a scaffold with high pore size. The samples were subsequently heated for 72 h at 121°C in a vacuum stove to crosslink collagen chains. Lastly, scaffolds were treated at 160°C for 2 h vacuum for sterilization (DHS Standard). Dimension of the obtained scaffold was 5 mm wide, 40 mm in length and 3 mm in thickness.

Scaffold seeding

Tenocytes, dermal fibroblasts and ASCs were *in vitro* expanded (4 passages), then re-suspended in a solution with aprotinin (0.2 mg/ml) (Sigma), tranexamic acid (1.5 mg/ml) (Sigma), bovine fibrinogen (110 mg/ml) (Fluka Chemic GmbH, Buchs, SG, Switzerland) and adjusted to a concentration of $80x10^6$ cells/ml. Subsequently, 100 µl of each fibrinogen-cell solution was seeded onto a collagen sponge ($8x10^6$ cells/sponge, as previously described (4).

After the complete cell integration into the scaffolds, 100 µl of thrombin were added (1.37 mg/ml, Chemicon International Inc., Temecula, CA, USA) to form fibrin glue encapsulation (5).

Immediately after polymerization of the fibrin glue (about 30 minutes) scaffolds were collected to evaluate distribution, cell survival and synthetic activity and their morphology at T0 as described below. For each scaffold 5 replicates were performed.

Scaffold in vitro cultured in static and dynamic conditions

Tenocytes, dermal fibroblasts and ASCs scaffolds were *in vitro* cultured both in static and dynamic conditions for 7 and 14 days (T7, T14) in a bioreactor. Each collagen sponge was located in a Petri dish and housed at 37°C in basic culture medium (DMEM High Glucose, 20% fetal bovine serum, 2mM ultra-glutamine, 100U/ml of Penicillin/Streptomycin solution, 50 ug/ml of gentamicin, 0,5 ug/ml of amphotericin B, 1mM sodium pyruvate, 10mM HEPES and 50ug/ml ascorbic acid (Sigma, Italy). Considering that the maintenance of sterility is particularly important in cell culture procedure,

Petri dish had no direct access to the chamber and, in the dynamic conditions, the pulsatile stretch was magnetically applied. In this case, the bioreactor chamber was at an initial pre-loading tension of 3%; the tensional stimulation was then applied with a frequency of 0.5 Hz and a duration of 30 minutes/h, to cyclically stretch the scaffold to a total deformation of 10%. For each scaffold 5 replicates were performed.

Histological analysis

All the scaffolds were fixed in 10% (v/v) phosphate-buffered formaldehyde, dehydrated in a graded ethanol series, embedded in paraffin. After rehydration, 4 μm-thick sections were stained with Haematoxylin/Eosin to evaluate the morphology of the sample. Photomicrographs were taken with an Olympus BX51 microscope (Olympus, Italy) equipped with a digital camera and final magnifications were calculated.

Double immunofluorescence of cell-seeded collagen sponges

After rehydration sections were washed three times in phosphate buffered saline, PBS (pH 7.4), and incubated with a anti collagen type 1 primary antiserum (1:50, Millipore) for 24h at 18°C, washed in PBS, and subsequently treated with the Avidin-Biotin blocking kit solution (Vector Laboratories Inc.). Sections were then washed in PBS for 10 min and incubated with a solution of goat biotinylated anti-rabbit IgG (Vector Laboratories Inc.) 10 mg/mL in Tris-buffered saline (TBS) for 1 h at 18-20°C and after rinsing twice in PBS, they were treated with Fluorescein-Avidin D (Vector Laboratories Inc.), 10 mg/mL in $NaHCO_3$, 0.1 M, pH 8.5, and 0.15M NaCl for 1 h at 18-20°C.

After washing in PBS, section were incubated with 1:50 anti-collagen type-3 antiserum (Chondrex Inc.) and a blocking step with the Avidin-Biotin kit (Vector Laboratories Inc.) was also performed. Successively, the sections were rinsed in PBS for 10 min and incubated with 10 mg/mL goat biotinylated anti-mouse IgG (Vector Laboratories Inc.) for 1 h at 18–20°C, washed twice in PBS, and treated with Rhodamine-Avidin D (Vector Laboratories Inc.), 10 mg/mL in $NaHCO_3$, 0.1 M, pH 8.5, with 0.15M NaCl for 1 h at 18-20°C. Pig Achille tendon was used as a positive control; negative controls were performed by the omission of the secondary antibodies.

Finally, all tissue sections were embedded in

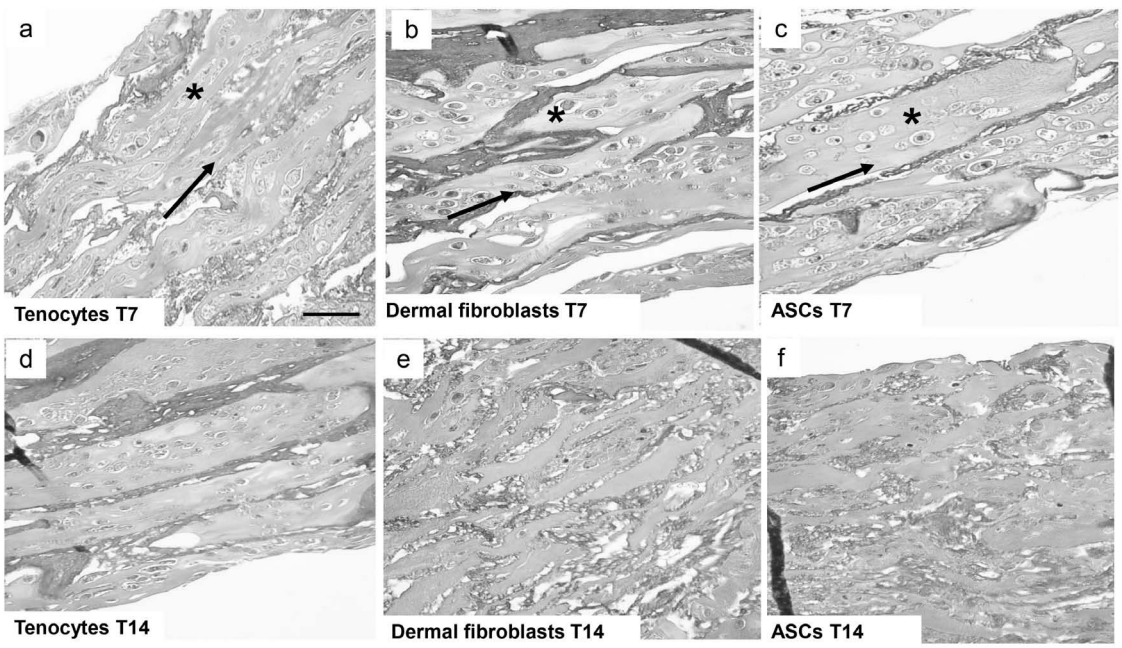

Fig. 1. *H&E. Tenocytes, dermal fibroblasts and ASCs seeded scaffolds with fibrin glue with or without a mechanical stimulus at 7 and 14 days. Scale bar, 200μm.*

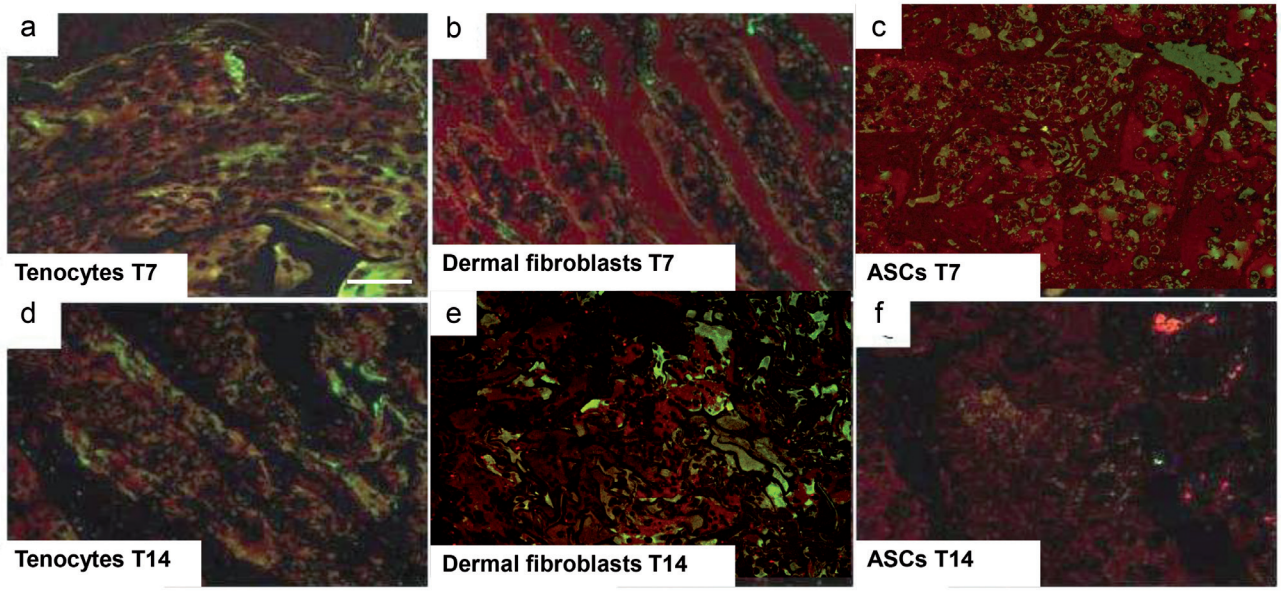

Fig. 2. *Immunofluorescence. Tenocytes, dermal fibroblasts and ASCs seeded scaffolds with fibrin glue with or without a mechanical stimulus at 7 and 14 days. green: collagen type 1; red: collagen type 3. Scale bar: 200 µm.*

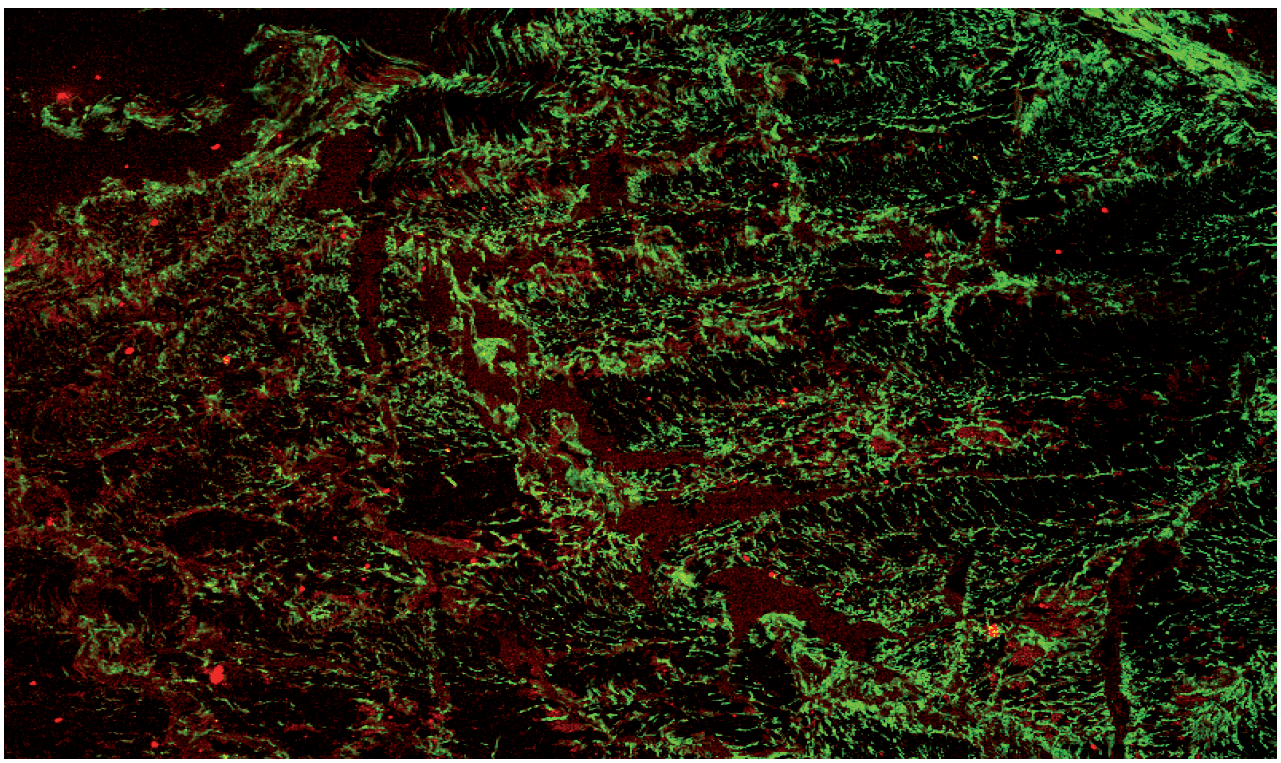

Fig 3. *Double mmunofluorescence of native tendon. green: collagen type 1; red: collagen type 3. Scale bar: 200 µm.*

Vectashield antifade Mounting Medium (Vector Laboratories Inc.) and observed using a Confocal Laser Scanning Microscope (FluoView FV300; Olympus) immunofluororeactive structures were excited using equipped of an Argon/Helio-Neon-Green lasers with excitation and barrier filters set for fluorescein and rhodamine. Images containing superimposition of fluorescence were obtained by sequentially acquiring the image slice of each laser excitation or channel.

RESULTS

Scaffold in vitro cultured in dynamic condition: histological analysis

At T7 the scaffold mechanically stimulated showed organization of the fibers along the direction of the stimulus (Fig. 1a-c) and all the three cell populations were located along the fibers (arrows), which now appeared longitudinally oriented (asterisk). Tenocytes showed a more marked molten appearance than the other two types of cells (Fig. 1a) and mechanical stimulation at T14 enhanced this behaviour (Fig. 1d-f). An increased cellular suffering after 14 days of stimulation compared to stimulated samples for 7 days was observed (Fig. 1. d-f). However, tenocytes exhibit greater survival ability than dermoblasts and mesenchymal cells maintained on scaffolds under the same mechanical stimulus.

Scaffold seeding and culture in dynamic condition: immunofluorescence

Cells seeded on stimulated scaffolds (Fig. 2), were lining along the reorganized fibers of the collagen sponges and these fibers were morphologically similar to the native tissue as collagen 1 and 3 that were homogenously expressed inside the fibres (Fig. 3). This aspect was almost comparable for all the three cell populations. Tenocytes revealed a synthetic profile, which closely resembled the native tissue both a T7 and T14 (Fig 2. a, d), since immunostainings for collagen 1 and 3 along the fibers were comparable. Dermal fibroblasts and ASCs showed a synthetic profile with a higher collagen 3 staining than collagen 1 at both time points when compared to tenocytes culture, and to the native tendon tissue (Fig. 2. b, c e, f).

DISCUSSION

The effect of a mechanical stimulation on a model of engineered tendon was analyzed in this study. This stimulus acts both on the cells and scaffold fibers to orient and align them along the direction of the force, closely resembling the native tendon. However, this stimulus was not sufficient to overcome the problems associated with the static culture of the cellular compounds, as described in a previous study (4): indeed, no effects on collagen type 1 and 3 deposition was observed. In addition, after 14 days of stimulation, a progressive impoverishment of cellular scaffold was observed. Nonetheless, these data show how the mechanical stimulation can direct cells to a precise tissue organization, an indispensable effect for the fabrication of an engineered tendon. This evidence suggests that different stimuli, in frequency and intensity, may further enhance the maturation of an engineered construct towards a tendon-like tissue. Moreover, these data suggest that tenocytes *in vitro* probably need additional stimuli besides the mechanical ones, to reproduce a micro-environment, which more closely resembles the native tendon.

The use of tenocytes in the production of a tendon replacement model represents the optimal choice in terms of cellular competence: they are responsive to the stimuli that normally maintain the function of the tendon in vivo. However, their use in a clinical setting is limited by several factors: the tendon is characterized by the presence of few cells embedded in an abundant matrix; thus, the cellular yield obtained from digestion is therefore low. Moreover, the isolation of autologous cells requires an invasive procedure, which damages healthy tendon portions (6). Thus, the use of an alternative cell source is essential for tendon engineering purposes. Dermal fibroblasts and mesenchymal cells from adipose tissue represent an interesting alternative, as they require a less invasive harvest procedure on the patient. Moreover, such cell populations have been widely used in tissue engineering due to their plasticity (7, 8). Mechanical stimulation is another essential component to obtain an engineered tendon, which can sustain the different types of load.

Reproducing a stimulatory environment as

close as possible to the natural microenvironment of the tendon tissue could allow for an enhancement and an increase in the effects derived from the mechanical stimulation. We observed a beneficial effect of the mechanical stimulus especially after 7 days of culture: scaffold fibers were re-organized, cells were re-distributed along the lined lines in the direction of the stimulus; cell vitality and synthetic activity were also improved, resulting in an engineered construct of better quality.

Concerning the cell source, further studies are needed to understand how to optimize culture with dermal fibroblasts and ASCs, evaluating, in this case, the use of specific growth and differentiation factors, or up-regulating specific proteins involved in the development and regeneration of the tendon tissue. Regarding the mechanical stimulus, the device used in this study is potentially suitable for supporting proper tendon engineering. The stimulus protocol used could be modified by evaluating any variations in the experimental sample response. Based on this model, it will be possible to further optimize the different parameters and experimental conditions to obtain a tendon-like tissue.

REFERENCES

1. Uysal AC, Mizuno H. Differentiation of adipose-derived stem cells for tendon repair. Methods Mol Biol 2011; 702:443-51.
2. Altman GH, Horan RL, Martin I, et al. Cell differentiation by mechanical stress. FASEB J 2002; 16(2):270-2.
3. Wang JH, Yang G, Li Z, Shen W. Fibroblast responses to cyclic mechanical stretching depend on cell orientation to the stretching direction. J Biomech 2004; 37(4):573-6.
4. Deponti D, Di Giancamillo A, Gervaso F, et al. Alternative cell sources for tendon/ligament engineering. J Orthop 2013; 5(3):93-99.
5. Deponti D, Di Giancamillo A, Mangiavini L, Pozzi A, Fraschini G, Sosio C, Domeneghini C, Peretti GM. Fibrin-based model for cartilage regeneration: tissue maturation from in vitro to in vivo. Tissue Eng Part A 2012; 18(11-12):1109-22.
6. Thaker H, Sharma AK. Engaging stem cells for customized tendon regeneration. Stem Cells Int 2012. 2012:309187.
7. Liu W, Chen B, Deng D, Xu F, Cui L, Cao Y. Repair of tendon defect with dermal fibroblast engineered tendon in a porcine model. Tissue Eng 2006; 12(4):775-88.
8. Riboh J, Chong AK, Pham H, Longaker M, Jacobs C, Chang J. Optimization of flexor tendon tissue engineering with a cyclic strain bioreactor. J Hand Surg Am 2008; 33(8):1388-96.

THE ANALYSIS OF DIFFERENT SCAFFOLDS AND THE BENEFIT OF FIBRIN GLUE FOR TENDON TISSUE ENGINEERING AT DIFFERENT CULTURE TIMES

A. DI GIANCAMILLO[1], D. DEPONTI[2], F. GERVASO[3], L. SALVATORE[3], F. SCALERA[3], L. MANGIAVINI[4], R. SCURATI[5], A. SANNINO[3] and G.M. PERETTI[4,5]

[1] Department of Health, Animal Science and Food Safety, University of Milan, Italy; [2]IRCCS, Ospedale San Raffaele, Milan, Italy; [3]Department of Engineering for Innovation, University of Salento, Italy; [4]IRCCS Istituto Ortopedico Galeazzi, Milan, Italy; [5]Department of Biomedical Sciences for Health, University of Milan, Italy

This study evaluated a tendon substitute model. Tenocytes were isolated from pig Achilles tendon, seeded onto scaffolds (Opocrin 2%, Typeone 3% and Symatese 2%) and studied by histology, immunofluorescence for collagen type 1 and 3 and biochemical analysis to assess cellularity. The permeability of these compounds was evaluated in the presence or absence of fibrin glue. Opocrin 2% was the best choice for cellular distribution within the scaffolds, which were then cultured for T0, T4, T7 and T10 days. Fibrin glue has been strongly supportive for the survival of cells with a significant increase in DNA content at T10 ($P<0.05$). Moreover, the synthetic activity of fibrin-free scaffolds was always negative. Lastly, a progressive increase in collagen 1 and 3 with fibrin-glue was observed. However, static culture is not sufficient to support long-term cellular activities and at T10 there is still a lack of organized matrix similar to the native tissue.

A tendon is a fibrous connective tissue, whose role involves the transmission of the forces generated by the muscle to the skeletal apparatus to ensure the joint movement and the maintenance of the posture (1). Every year, millions of people are affected by musculoskeletal damage and 43% of these injuries are due to tendons and/or ligaments. In particular, Achilles tendon, as well as the patellar and the rotator cuff tendons are the most susceptible to injury.

Tendon is a connective tissue characterized by a slow natural healing process (2) leading to the formation of a tissue with structural and functional properties inferior to native tissue (3). Thus, the creation of an engineered tendon arises from multiple clinical needs. To date, many authors developed studies combining different biomaterials with different cellular populations (4) to obtain tissue with properties similar to those of a native tendon. Among the different scaffolds, natural polymers such as collagen derivatives have been proposed for tendon engineering, since they are among the major components of the tendon extracellular matrix. Collagen derivatives are hydrophilic polymers that can support cell adhesion and proliferation (5).

Therefore, cell permeability is an essential parameter to evaluate a promising tendon substitute; however, once cells have colonized the scaffold, they need to be maintained within the material. Several studies evaluated the potential of different hydrogels embedding cells for tissue engineering, including fibrin glue (6). Fibrin glue is a natural polymer which provide a supportive three-dimensional environment, allowing cells to differentiate, proliferate and/or synthesize matrix (7). A crucial point to be evaluated is the determination of the level of *in vitro* maturation of the engineered composite before being

Key words: Tendon, scaffold, fibrin glue, cell morphology, synthetic activity

Mailing address:
Giuseppe M. Peretti, M.D.,
Department of Biomedical Sciences for Health,
University of Milan,
IRCCS Istituto Ortopedico Galeazzi,
Via R. Galeazzi 4, 20161 Milan, Italy
Tel.: +39 02 5031 9967 - +39 02 6621 4735 - Fax: +39 02 6621 4736
e-mail: gperetti@iol.it

0393-974X (2017)

implanted. Assuming that the tendon tissue is unable to repair spontaneously due to acute breakdown or chronic degeneration, this study aims to recreate an engineered tendon by combining a biological scaffold composed mainly by collagen fibres with porcine tenocytes.

In particular, the following aspects were highlighted: 1) comparison of different types of collagen scaffolds with tenocytes in the presence or absence of fibrin glue, to evaluate which type of scaffold is more permeable and suitable for cellular seeding; 2) the utility of fibrin glue, as a suitable tenocytes carrier.

MATERIALS AND METHODS

Cell isolation

Tendons were collected from adult Landrace X Large White pigs and processed for cell isolation as previously described (8). Briefly, tenocytes were aseptically isolated from piglets' Achilles tendons (10kg) and washed in sterile PBS (Phosphate Buffered Saline, Celbio, Italy) with 50 µg/ml of gentamicin (Lonza, Italy), 0.5 µg/ml of amphotericin B (Lonza, Italy) and 100 U/ml of Penicillin/Streptomycin solution (Lonza, Italy). After three washes, samples were finely powdered and subsequently digested in DMEM High Glucose medium (Celbio, Italy), composed of 10% fetal bovine serum (Celbio, Italy), 2mM ultra-glutamine, 0.1% collagenase Type I (DBA-Italia Srl, Italy), 100 U/ml of Penicillin/Streptomycin solution, 50 µg/ml of gentamicin and 0.5 µg/ml of amphotericin B. Samples were incubated overnight in an oscillating water bath at 37˚C.

All the undigested fragment tissues and debris were gently removed using a 100 micron sterile filter (BD Falcon, USA). The cell suspension was then centrifuged for 10 min at 1400 rpm and the obtained pellet was re-suspended in DMEM. Tenocytes were seeded and cultured in DMEM High Glucose medium containing 2mM ultra-glutamine, 20% fetal bovine serum, 1mM sodium pyruvate (GIBCO, Italy) and 10mM HEPES (GIBCO, Italy), 100 U/ml of Penicillin/Streptomycin solution, 50 µg/ml of gentamicin, 0.5 µg/ml of amphotericin B.

Scaffold synthesis

Collagen sponges were made of collagen 1 and fabricated at the Department of Innovation Engineering, University of Salento. At the beginning of our work, we tested the cellular response to 3 different types of collagen scaffolds: Opocrin 2%, Typeone 3% and Symatese 2%. The 2% Opocrin type is composed of collagen type I, isolated from equine tendon through an extraction process characterized by a preliminary step of mechanical treatment of raw tissues and then the use of alkaline hydroxides, sulphates, and enzymatic purification to complete the extraction.

The obtained collagen powder is suspended in distilled water in a percentage equal to 2 and the obtained slurry is cast into aluminium moulds. These moulds are subjected to a lyophilization cycle characterized by a slow freezing step, i.e. the slower the freezing process and the ice crystals grow, the higher the increase in the pore size of the collagen scaffold. Samples are subsequently subjected to heat treatment (DHT) for 72 h in a vacuum stove at 121°C to facilitate crosslinking between the collagen chains. Finally, scaffolds are sterilized at 160°C for 2 h vacuum (DHS Standard).

The result of this process is a porous parallelepiped of 5 mm wide, 40 mm in length and 3 mm in thickness. Typeone 3% collagen is very similar to the Opocrin, as is derived from the same tissue source, showing roughly the same chemical composition; thus, they have to deal with a similar extraction and purification treatment. However, the particular conditions of mechanical and chemical treatment of raw fibres in the extraction phase and the different synthesis parameters of the slurry in the processing phase, lead to the development of porous matrices with structural, mechanical and biodegradation properties sometimes remarkably different. Symatese 2% scaffolds are made of collagen I isolated by dermis of animals (6 months-old). The fundamental difference compared to the tendon derivative collagen relies in the different structure, much lower in the dermal derivative collagen (fewer covalent bonds involved). This leads to easier solubilization and thus a faster degradation of this type of scaffold.

Scaffold choice with or without fibrin glue

Tenocyte cell population was expanded *in vitro* (4 passages), then collected and re-suspended in a solution with aprotinin (0.2 mg/ml) (Sigma), tranexamic acid (1.5 mg/ml) (Sigma), bovine fibrinogen (110 mg/ml) (Fluka Chemic GmbH, Buchs, SG, Switzerland) and adjusted to

a concentration of $80x10^6$ cells/ml. Subsequently, 100 µl of fibrinogen-cell solution was seeded onto three different collagen sponges (8 x 10^6 cells/scaffold, previously described) to choose the best scaffold.

After the complete absorption of the cell solution some scaffolds were cultured as described below, other scaffolds were added with 100 µl of thrombin (1.37 mg/ml, Chemicon International Inc., Temecula, CA, USA) to form fibrin glue encapsulation.

The complete polymerization of the fibrin glue was reached after 30 min and the scaffolds with the tenocytes were immediately collected to evaluate the distribution and survival of the cells within the three different scaffolds and subsequently processed for morphological analysis and described below.

Once the best scaffold was chosen, tenocytes were cultured as already described *in vitro* with or without fibrinogen, for 0, 4, 7 and 10 days in basic culture medium (DMEM High Glucose, 20% fetal bovine serum, 2mM ultra-glutamine, 100 U/ml of Penicillin/Streptomycin solution, 50 µg/ml of gentamicin, 0.5 µg/ml of amphotericin B, 1mM sodium pyruvate, 10mM HEPES and 50 µg/ml ascorbic acid (Sigma, Italy), to evaluate the best cell survival condition. Some samples were collected for morphological analysis as described below.

Histological analysis of cell-seeded collagen sponges

The seeded scaffolds were fixed in 10% (v/v) phosphate-buffered formaldehyde. The samples were then dehydrated in a graded 50% (v/v), 70% (v/v), 95% (v/v) and 100% (v/v) ethanol series, embedded in paraffin and cut into 4 µm-thick sections. After rehydration, sections were stained with Hematoxilyn/Eosin using a standard staining protocol, for the evaluation of the morphology. Photomicrographs were taken with an Olympus BX51 microscope (Olympus, Italy) equipped with a digital camera and final magnifications were calculated.

Double immunofluorescence of cell-seeded collagen sponges

After rehydration, sections were washed thrice in phosphate buffered saline, PBS (pH 7.4). They were subsequently incubated with the first-step primary antiserum, 1:50 anticollagen type I (Millipore) for 24 h at 18-20°C, then washed in PBS, and subsequently treated with the Avidin-Biotin blocking kit solution (Vector Laboratories Inc.). The sections were then washed in PBS for 10 min and incubated with a solution of goat biotinylated anti-rabbit IgG (Vector Laboratories Inc.) 10 mg/mL in Tris-buffered saline (TBS) for 1 h at 18-20°C. After rinsing twice in PBS, the sections were treated with Fluorescein-Avidin D (Vector Laboratories Inc.), 10 mg/mL in $NaHCO_3$, 0.1 M, pH 8.5, and 0.15M NaCl for 1 h at 18-20°C.

The sections were then washed in PBS and subsequently treated with 1:50 anti-collagen type-III antiserum (Chondrex Inc.). A blocking step with the Avidin-Biotin kit (Vector Laboratories Inc.) was performed, and then, the sections were rinsed in PBS for 10 min and incubated with 10 mg/mL goat biotinylated anti-mouse IgG (Vector Laboratories Inc.) for 1 h at 18-20°C. The sections were then washed twice in PBS, and treated with Rhodamine-Avidin D (Vector Laboratories Inc.), 10 mg/mL in $NaHCO_3$, 0.1 M, pH 8.5, with 0.15M NaCl for 1 h at 18-20°C. Finally, the slides with tissue sections were embedded in Vectashield Mounting Medium (Vector Laboratories Inc.) and observed using a Confocal Laser Scanning Microscope (FluoView FV300; Olympus).

The immunofluororeactive structures were excited using Argon/Helio-Neon-Green lasers with excitation and barrier filters set for fluorescein and rhodamine. The images containing superimposition of fluorescence were obtained by sequentially acquiring the image slice of each laser excitation or channel. Pig Achilles tendon was used as a positive control.

Biochemical analysis

Other scaffolds at the same timepoints with or without fibrin glue (T0, T4, T7 and T10) were digested in papain (Sigma) for 16-24 h at 60°C; the digestion solution was composed of 125 mg/mL of papain (Sigma) in 100mM sodium phosphate, 10mM sodium EDTA (Sigma), 10mM cysteine hydrochloride (Sigma), 5mM EDTA adjusted to pH 6.5 and brought to 100mL of solution with distilled water.

After digestion, samples were stored at -80°C. Aliquots of the digested samples were assayed for DNA content with the Quant-iT Picogreen dsDNA Assay Kit (Molecular Probes, Invitrogen) and a fluorescence microplate reader and standard fluorescein wavelengths (excitation 485 nm, emission 538 nm, cut-off 530 nm).

The standard curve for the analysis was generated using the bacteriophage lambda DNA supplied with the kit.

Statistical Analysis

Statistical analysis of the DNA results (collagen scaffold with or without fibrin glue in static condition) was performed using the general linear model of the SAS (version 8.1, Cary Inc., NC). The individual scaffold was the experimental unit of all response variables. The data were presented as least squared means SEM. Differences between means were considered significant at $P < 0.05$.

RESULTS

Scaffolds seeding with or without fibrin glue: Histological analysis

Collagen sponges were seeded with tenocytes as gold standard to evaluate cell distribution and survival within the scaffold and to compare the different scaffolds. At time 0, tenocytes were not homogeneously distributed within the Symatese 2% and Typeone 3% scaffolds both with or without fibroin glue encapsulation (Fig. 1); whereas tenocytes seeded onto Opocrin 2% scaffold showed a homogeneous distribution both with or without fibrin glue (Fig. 1); thus, this latter scaffold was chosen for further timepoint evaluation.

Opocrin 2% scaffold with or without fibrin glue: *Histological analysis*

In Fig. 2, a comparison between opocrin 2% collagenic scaffold with or without fibrin glue was performed at different timepoints. Comparing the two scaffolds at the same timepoints, it was evident a cellular decrease and cluster formation when fibrin glue was not used (Fig. 2a-d), while after 10 days of *in vitro* culture, cell population showed a good morphology and distribution within the scaffolds. Moreover, the tenocytes embedded in the fibrin glue 3D culture were roundish and alive into the scaffold at 7 (Fig. 2C) and 10 days (Fig. 2D), with a decrease of cells and signs of scaffold degradation observed at 10 days. Tenocytes did not appear to have a preferred direction of alignment.

Opocrin 2% scaffold with or without fibrin glue: double immunofluorescence

Fig. 2a1-d1 shows how the fibrin-free scaffold

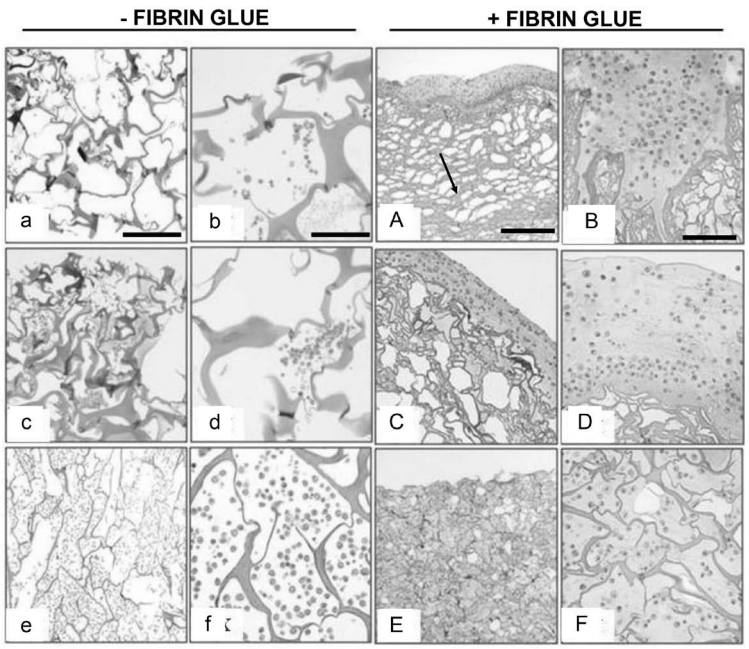

Fig. 1. *Tenocytes seeded in different scaffolds with or without fibrin glue.* ***a, b, A, B****): 2% Symatese seeded scaffold;* ***c, d, C, D****): 3% Typeone seeded scaffold;* ***e, f, E, F****): 2% Opocrin seeded scaffold with fibrin glue with or without a mechanical stimulus at 7 and 14 days;* ***a, c, e, A, C, E****) scale bar, 200μm;* ***b, d, f, B, D, F****): scale bar, 100 m.*

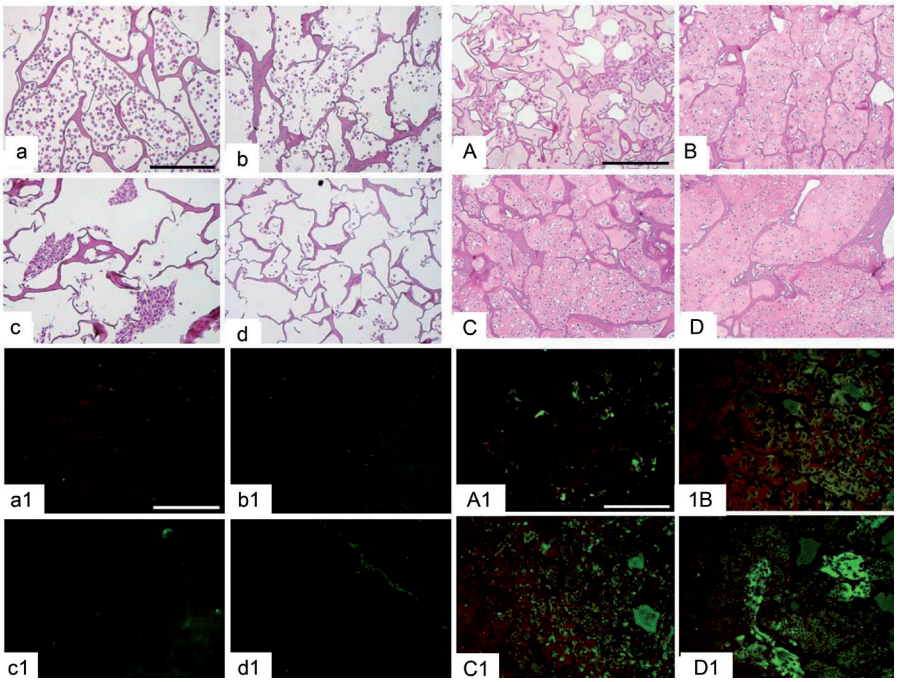

Fig. 2. *Tenocytes seeded in 2% Opocrin scaffolds with or without fibrin glue **HE**): Scaffolds without fibrin glue **a**) at 0 days, **b**) at 4 days, **c**) at 7 days, **d**) at 10 days; Scaffolds with fibrin glue **A**): at 0 days; **B**): at 4 days; **C**); at 7 days; **D**) at 10 days. Double immunofluorescence collagen type 1 (**green**), collagen type 3 (**red**) and co-localization (**yellow**); Scaffolds without fibrin glue **a1**): at 0 days; **b1**): at 4 days; **c1**): at 7 days; **d1**): at 10 days. Scaffolds with fibrin glue **A1**): at 0 days; **B1**): at 4 days; **C1**): at 7 days; **D1**): at 10 days. All the scale bars are the same as the ones located in Fig. 2a, A, a1, A1, 200μm.*

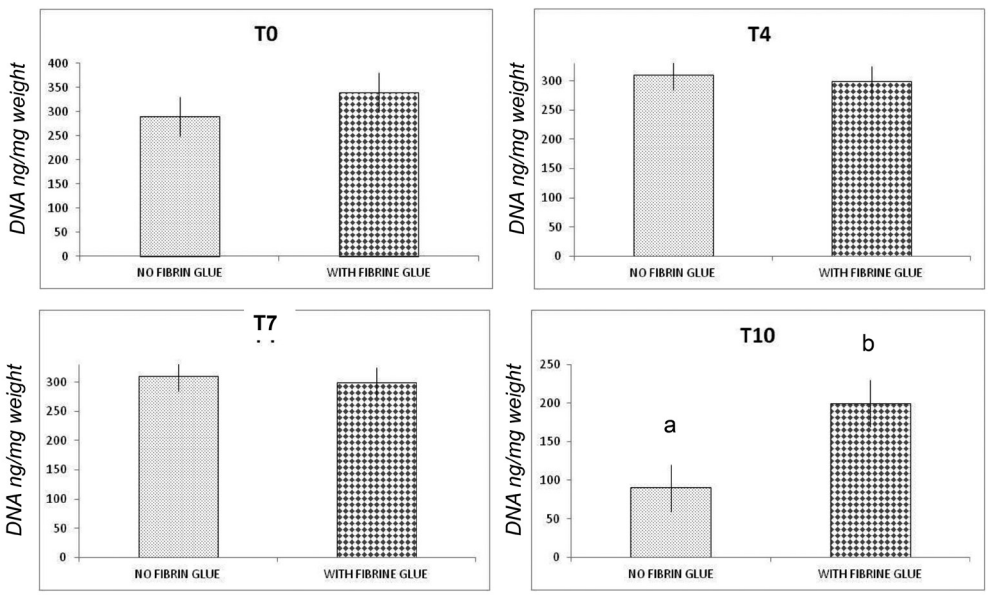

Fig. 3. *In vitro culture at 0, 4, 7, and 10 days. Quantification of DNA normalized to the wet weight (mg/mg). Values with different superscripts (**a**, **b**) differ for $p<0.01$.*

was negative for both immunostainings at different time of analysis. Fig. 2A1-D1, however, highlights the progressive increase in the expression of collagen 1 and collagen 3 secreted by cells on a scaffold with fibrin glue: from time T0 to T10, an increase of both immunostaining can be observed, but still lacking an organized matrix.

Opocrin 2% scaffold with or without fibrin glue: *Biochemical analysis*

DNA content of opocrin 2% scaffold with or without fibrin glue showed no statistical differences at T0, T4 or T7, but fibrin glue opocrin 2% scaffold revealed a statistically higher DNA content than the one with no glue at T10 (Fig. 3, $P<0.05$).

DISCUSSION

The aim of this study was to create a tendon substitute model through the application of tissue engineering techniques that can represent a workable model for the development of an engineered tendon with wide clinical potentials. Therefore, several cellular populations, isolated from different pig tissues were seeded onto different collagen scaffolds, with or without fibrin glue. The use of tissue engineering techniques to create a new tendon is mainly due to the spread of clinical issues and to the inadequacy and inability of the major surgical techniques to fully restore native tissue conditions. In addition, the tendon is poor in vascular tissue characterized by reduced oxygen availability and hence with limited ability to self-generate. Based on these premises, the tendon tissue is well suited to be *in vitro* engineered.

As a preliminary study, the priority of our project was to select the experimental conditions that would lay the foundations for such a model. Initially, attention was focused on scaffolds, as essential support to cell growth: different types of commercial collagen scaffolds were then compared. To date, there are three categories of scaffold which are highly employed: polysaccharides, polyesters, and collagen derivatives (9). In particular, cellular seeding was tested on scaffolds Opocrin 2%, Typeone 3% and Symatese 2%. The permeability of these compounds was also evaluated in the presence of fibrin glue, since this hydrogel was found to be an important support in cartilage engineering both alone and in association with collagen scaffolds (7).

As shown in the results, the 2% Opocrin collagen compound was the best choice in terms of homogeneity of cellular distribution within the scaffold, both in presence and in absence of fibrin glue. Based on this evidence, subsequent experiments were conducted using 2% Opocrin scaffold support. The use of fibrin glue in association with this material has been strongly supportive to the survival and to the synthetic activity of the cells (tenocytes), allowing them to produce matrix within the scaffold and to promote a preliminary maturation of the *in vitro* compound.

Ahmed et al. (10) reviewed the use of fibrin as a versatile biopolymer, which shows a great potential in tissue regeneration and wound healing. However, static culture is not sufficient to support such long-term cellular activities: at 10 days of culture, as a cellular failure is observed in terms of cellularity, suggesting that longer times do not allow proper preservation of the properties acquired.

This result is similar to what observed by Lee et al. (11) who showed that static culture conditions enhanced scaffold degradation in rabbit Achilles tendon. This observation supports the next choice of optimizing culture conditions by introducing the mechanical stimulus determined by the bioreactor to promote cell survival.

REFERENCES

1. Galloway MT, Lalley AL, Shearn JT. The role of mechanical loading in tendon development, maintenance, injury, and repair. J Bone Joint Surg Am, 2013. 95(17):1620-8.
2. Müller SA, Todorov A, Heisterbach PE, Martin I, Majewski M. Tendon healing: an overview of physiology, biology, and pathology of tendon healing and systematic review of state of the art in tendon bioengineering. Knee Surg Sports Traumatol Arthrosc 2015; 23(7):p. 2097-105.
3. Liu CF, Aschbacher-Smith L, Barthelery NJ, Dyment N, Butler D, Wylie C. Spatial and temporal

expression of molecular markers and cell signals during normal development of the mouse patellar tendon. Tissue Eng Part A 2012; 18(5-6):598-608.
4. Bagnaninchi PO, Yang Y, El Haj AJ, Maffulli N. Tissue engineering for tendon repair. Br J Sports Med 2007; 41(8):e10; discussion e10.
5. Zhu J, Marchant RE. Design properties of hydrogel tissue-engineering scaffolds. Expert Rev Med Devices 2011; 8(5):607-26.
6. Jia X, Kiick KL. Hybrid multicomponent hydrogels for tissue engineering. Macromol Biosci 2009; 9(2):140-56.
7. Deponti D, Di Giancamillo A, Mangiavini L, Pozzi A, Fraschini G, Sosio C, Domeneghini C, Peretti GM. Fibrin-based model for cartilage regeneration: tissue maturation from in vitro to in vivo. Tissue Eng Part A 2012; 18(11-12):1109-22.
8. D. Deponti, A. Di Giancamillo, F. Gervaso, et al. Alternative cell sources for tendon/ligament engineering. J Orthop 2013; 5(3):93-99.
9. Liu Y, Ramanath HS, Wang DA. Tendon tissue engineering using scaffold enhancing strategies. Trends Biotechnol 2008; 26(4):201-9.
10. Ahmed TA, Dare EV, Hincke M. Fibrin: a versatile scaffold for tissue engineering applications. Tissue Eng Part B Rev 2008; 14(2):199-215.
11. Lee J, Guarino V, Gloria A, Ambrosio L, Tae G, Kim YH, Jung Y, Kim SH, Kim SH. Regeneration of Achilles' tendon: the role of dynamic stimulation for enhanced cell proliferation and mechanical properties. J Biomater Sci Polym Ed 2010; 21(8-9):1173-90.

DIRECT ANTERIOR APPROACH VERSUS POSTEROLATERAL APPROACH IN TOTAL HIP ARTHROPLASTY: EFFECTS ON EARLY POST-OPERATIVE REHABILITATION PERIOD

C. FALDINI[1], F. PERNA[1], A. MAZZOTTI[1], N. STEFANINI[1], A. PANCIERA[1], G. GERACI[1], P. MORA[1] and F. TRAINA[2]

[1]1st Orthopaedic and Traumatologic Clinic, Istituto Ortopedico Rizzoli, Bologna, Italy; [2]Dipartimento di Ortopedia e Traumatologia, Department of Biomedical Sciences and Morphological and Functional Images, Scuola Ortopedia e Traumatologia, Università di Messina, Italy

Main surgical approaches to the hip have been modified during last decades, in an effort to reduce invasiveness of the surgical procedure and allow a faster rehabilitation. Direct anterior approach is the only approach, which does not require muscle detachment, thus theoretically leading to reduced post-operative pain and allows earlier recovery. The aim of this study was to report a comparison between patients operated with direct anterior approach and postero-lateral approach in terms of immediate post-operative and in-hospital records. Pain, operative time, intra- and post-operative complications, blood loss, hospitalization, motor component of the Functional Independence Measure (M-FIM), timed up and go (TUG) test were measured between the two groups and compared. Direct anterior approach showed better results in M-FIM, TUG, hospitalization and blood loss, without any significant difference for intra- and post-operative complications between the 2 groups. This study shows that early post-operative recovery is influenced by the chosen approach. Direct anterior approach showed better outcomes when compared to postero-lateral approach, limited to hospitalization, blood loss, and functional scores. Further comparisons are needed to evaluate direct anterior approach to maintain advantages over postero-lateral approach on longer follow-up period.

In recent years, less invasive approaches have increasingly been taken into account for primary total hip arthroplasty (THA) with the aim to allow faster recovery. Many surgeons described modified minimally invasive surgical approach for THA with several improvements in terms of blood loss and transfusion requirement, peri-operative pain and recovery times (1, 2). However, advantages and disadvantages have been widely described for each approach hence, the best one is still a matter of debate. It has therefore been noted that, even if the cosmetic issue is gaining importance for both patients and surgeons, when dealing with mini-invasive THA, the length of the incision seems to be less accountable than the grade of muscle disruption, soft tissue impairment and bone preservation on surgical outcome (3). The ideal mini-invasive hip approach for THA should therefore be reliable, allowing surgeons to dominate the pathological anatomy and each possible complication and tissue sparing. Nonetheless, despite a wide literature dealing with this topic, a definitive verdict that allows choosing a surgical approach to another has not yet been defined.

Direct anterior hip approach (DAA) is the only one that develops in a real inter-muscular and inter-nervous interval because it develops between the

Key words: total hip arthroplasty, anterior approach, posterolateral approach, rehabilitation

Mailing address:
Cesare Faldini,
1st Orthopaedic and Traumatologic Clinic,
Istituto Ortopedico Rizzoli,
Via Giulio Cesare Pupilli 1,
40136, Bologna, Italy
e-mail: cesare.faldini@ior.it

0393-974X (2017)

sartorius muscles (femoral nerve) medially and the tensor fasciae latae (superior gluteal nerve) laterally. The muscle-sparing trait of this approach could lead to an earlier post-operative recovery compared with the posterolateral approach (PA) which encompasses the passage through the gluteus maximus and the partial detachment of the short external rotator muscles. In addition, the direct anterior intermuscular approach to the hip has several further advantages over the PA including such as improved dynamic hip stability, and decreased risk of hip dislocation after surgery. However, some disadvantages have also been addressed such as lateral femoral cutaneous nerve neuroapraxia and intraoperative fracture of the femur with a reported incidence of up to 6.5% (4-6).

Despite long-term results seem to be equal when using both DAA and PA (7) due to the differences of soft tissue treatments, we speculated whether there could be differences in the early postoperative period, especially during rehabilitation protocol.

The aim of this paper is to compare early postoperative results between the direct anterior approach and the posterolateral approach for THA in patients with hip osteoarthritis.

MATERIALS AND METHODS

Patients affected by hip osteoarthritis and subjected to THA between January 2014 and January 2017 at our institution were recruited from a consecutive cohort of subjects and retrospectively evaluated by the review of medical and rehabilitation records. Inclusion criteria were: 1) diagnosis of hip osteoarthritis; 2) had either a DAA or a PA; 3) complete rehabilitation records and 4) minimum 6 month-follow-up. Exclusion criteria were: 1) fractures; 2) osteonecrosis; 3) previous lower limb surgery; 4) associate neurological disease; 5) rheumatoid arthritis; 6) anticoagulant treatment; 7) simultaneous bilateral procedure; 8) severe congenital disorders; 9) urinary retention or urinary tract infection; 10) abdominal complications (ileus, gastric ulcer); 11) opioid side effects or allergy. A total of 412 primary THA were performed during the study period. Of these, 127 matched the inclusion and exclusion criteria leaving 127 patients. There were 62 patients in the DAA group and 65 in the PA group. No differences were recorded in demographic data between the two groups (Table I).

For the DAA group, one surgeon (CF) performed all surgeries through an anterior minimally invasive approach using a dedicated mobile leg positioner and a dedicated surgical instrumentation (Medacta, Switzerland). A cementless elliptical hydroxyapatite coated cup (Versafitcup®, Medacta, Switzerland) and a cementless straight hydroxyapatite coated short stem (AMIS® stem, Medacta, Switzerland) were used in all cases. A straight incision starting 1 cm distal and 1 cm lateral to the ASIS was prolonged for about 7 cm toward the lateral border of the patella. The intermuscular plane between the tensor fasciae latae and the sartorious was developed and the lateral circumflex vessels were ligated. The rectus femoris and the iliopsoas tendon were released and an "H" shaped capsulotomy was performed.

Table I. *Demographic data between the two groups.*

Variable	DAA	PA	*p*
Age	64 ± 8.4	65 ± 7.1	0.42
Males/Females	29/33	24/41	0.06
BMI (kg/m^2)	28.7 ± 4.5	30.1 ± 5.2	0.21
VAS	4.6 ± 2.5	5.1 ± 2.2	0.15
HHS (total)	54.8 ± 10.2	56.3 ± 9.7	0.30

The head of the femur was resected *in situ* and then removed. The leg was placed under traction and slight external rotation to improve acetabular exposure, and the cup was then implanted. Femoral exposure was achieved by placing the leg in extension, adduction and external rotation. After the stem was implanted, the hip was reduced using the mobile leg positioner and the capsule was repaired. Standard fascial and skin closure were done over a suction drainage.

For the PA group, one surgeon (FT) performed all surgeries through a posterolateral minimally invasive approach. A cementless hemispherical hydroxyapatite coated cup (Mpact®, Medacta, Switzerland) and a cementless straight hydroxyapatite coated short stem (AMIS® stem, Medacta, Switzerland) were used in all cases. The skin incision was made starting posterior and slightly proximal to the tip of the greater trochanter and distally along the shaft of the femur for about 8 cm. The fascia was divided in line with the skin incision over the center of the greater trochanter and the gluteus maximum was bluntly divided in line with its fibers. Using a periosteal elevator, the piriformis tendon was exposed and the troachanteric bursa was retracted posteriorly to expose the short external rotators and the posterior edge of the gluteus medius. The short external rotators were released as a single flap from the greater trochanter and the lateral portion of the femoral neck.

A "Z" shaped capsulotomy was performed. The hip was dislocated posteriorly using gentle flexion, adduction, and internal rotation and the femoral head was resected. Then the leg was placed in neutral position on a surgical trolley and the cup was implanted. The hip was internally rotated, slightly flexed, and adducted. After the stem was implanted, the hip was reduced by traction, slightly extension and external rotation and the capsule was repaired. The piriformis tendon was reattached. Standard fascial and skin closure were done over a suction drainage.

The same rehabilitation protocol was followed for both groups. However, patients receiving the PA were imposed to avoid a combination of flexion with adduction and internal rotation for 6 weeks. No hip precautions were enforced to those receiving DAA.

A daily-based record of recovery was made for each patient measuring: pain using visual analog scale (VAS) and narcotic consumption. Operative time, intra- and early post-operative complications, blood loss and length of hospital stays were recorded. Independence on motor component of the Functional Independence Measure (M-FIM)(8), the timed up and go test (TUG)(9) were measured on preoperative and on the 3rd and 6th post-operative days, or earlier if discharged. M-FIM score was measured related to the ability to walk 50 meters, go up and down one flight of stairs (12 stairs) and sit and get up from standing position from a chair. Maximum achievable M-FIM is 7 for each item. Post-operative radiographs were executed in the recovery room and afterwards at 6 weeks and 1-year follow-up.

Pre- and post- operative score measurements were compared using matched-pairs analysis. A p-value threshold < 0.05 was chosen to define statistical significance.

RESULTS

At 3rd postoperative day patients in the DAA achieved better M-FIM score compared to PA (respectively 7.5±0.97 and 61.15) with statistically significant difference (p=0.006). Differences were maintained at the 6th postoperative day (respectively 18±2.0 and 15.8±1.75) with statistically significant difference (p=0.009) (Table II). TUG test results were significantly better with DAA compared to PA at the 3rd postoperative day (respectively 42.212.96 and 51.5±10.37) with statistically significant difference (p=0.047) and at the 6th postoperative day (respectively 23.4±5.38 and 27.1±7.32) (p=0.11) (Table III). Mean VAS at 3rd postoperative day was 2.9±0.9 and 3.1±1.0 (p=0.51), and 1.25±0.71 and 1.16±0.75 (p=0.83) at the 6th postoperative day respectively for DAA and PA group. Mean operative time was significantly lower for PA group compared to DAA group, respectively 64.2±14.74 minutes and 77.1±17.37 minutes (p=0.04). Mean hospital length of stay was lower for DAA group compared to PA group of an average of 1 day less with statistically significant difference, respectively 6.5±0.97 days and 7.5±0.71 days (p=0.02). Mean blood loss measured by the difference between the preoperative hemoglobin values and the 2nd postoperative day were similarly in both group, respectively 2.3±0.38 for the DAA and 2.61±0.4 for the PA group (p=0.09) (Table IV). One patient in DAA group and two in

the PA group required two units of PRBC transfusion and were not considered for blood loss measurements above.

No significant differences were recorded on complications rate between the groups. Two patients in the DAA group experienced lateral femoral cutaneous nerve (LFCN) neuroapraxia during recovery; however complete recovery was recorded respectively at 3- and 6-month follow-up. One patients developed an undisplaced greater trochanter fracture during DAA without clinical relevance on the recorded outcome. One patients in the PA reported groin pain with complete resolution at 3 months follow-up and one patient sustained a posterior hip dislocation which required a revision.

DISCUSSION

The aim of this paper was to compare early postoperative results between the direct anterior approach and the posterolateral approach for THA in patients with hip osteoarthritis. Based on our results

Table II. *M-FIM differences between the two groups at the 3th and 6th postoperative day.*

M-FIN	3rd day post-op		*p*	6th day post-op		*p*
	DAA	PA		DAA	PA	
Walk	2.9 ± 0.87	2.2 ± 0.92	0.098	5.8 ± 1.0	4.8 ± 1.23	0.322
Stairs	1.5 ± 0.70	1.4 ± 0.52	0.722	6 ± 1.1	5.1 ± 1.0	0.698
Standing	3.1 ± 0.74	2.4 ± 0.84	0.064	6.2 ± 0.63	5.9 ± 0.74	0.998
Total	7.5 ± 0.97	6 ± 1.15	**0.006**	18 ± 2.0	15.8 ± 1.75	**0.009**

Table III. *TUG test results between the two groups at the 3th and 6th postoperative day.*

TUG (sec)	3rd day post-op		*p*	6th day post-op		*p*
	DAA	PA		DAA	PA	
	42.2 ± 12.96	51.5 ± 10.37	**0.047**	23.4 ± 5.38	27.1 ± 7.32	0.11

Table IV. *Operative time, Length of hospital stay, Blood loss and VAS between the two groups.*

Variable	DAA			PA		*p*
Operative time (minutes)	77.1 ± 17.37			64.2 ± 14.74		**0.04**
Length of hospital stay (days)	6.5 ± 0.97			7.5 ± 0.71		**0.02**
Blood loss (mg/dl)	2.3 ± 0.38			2.61 ± 0.4		0.09
VAS	3rd day	6th day	*p*	3rd day	6th day	*p*
	2.9 ± 0.9	3.1 ± 1.0	0.51	1.25 ± 0.71	1.16 ± 0.75	0.83

the DAA showed significantly improved early results compared to PA in almost all the categories measured. We found significantly better results during in-hospital recovery in case of DAA for M-FIM and TUG both at 3rd and at 6th postoperative day.

The comparison between DAA and PA in THA in terms of early functional recovery have been matter of the debate in the recent literature. A wide number of studies have evaluated the outcomes of the two different surgical approaches. According to Meermans et al, comparing the clinical results of DAA and PA by means of well validated scores such as Harris hip score, Western Ontario and McMaster Universities Artrhirtis index the mean scores were better for DAA for the first six weeks post-operatively. Subsequently there was no differences between DAA and PA (10). Similarly, Barrett et al found that DAA subjects performed well in the immediate post-operative period; they had lower VAS pain scores on the first post-operative day, more subjects climbing stairs normally and walking unlimited at 6 weeks, and higher HOOS Symptoms scores at 3 months. No differences were observed at later time points (3).

These findings, in line with our results, highlighted the impressive performance of the muscle sparing DAA in the immediate post-operative period and the subsequent loss of advantage with respect to PA over time. The immediate benefits for the DAA approach are testified by Bergin et al., that compared DAA and PA based on inflammation and markers of muscle damage. They found that levels of serum creatine kinase and tumor necrosis factor alpha were slightly decreased in the DAA group, thus concluding that the DAA caused lesser muscle damage compared to PA (11).

One of the more advocated advantages of the DAA is the lower duration of in hospital stay. In our cohort of patients, a slight reduction on length of hospitalization were found in DAA group with a recorded main duration of 6.5 days, diversely to PA, which remained in hospital on average 1 day longer with statistically significant difference ($p=0.02$). Similarly to our results, Martin et al found a shorter hospital stay in patients undergone DAA compared to PA (2.9 ± 4 days, $p=0.001$) (12). Petis et al found similar results, with a reported length of stay in hospital of 2.28 and 3.02 days respectively for DAA and PA (13).

Longer operative time required to perform THA through a DAA are reported in the current literature. According to a recent review by Meermans et al, most studies evaluated found that the operating time is significantly longer when the DAA was employed, with a steep learning curve reported by many (10). Operative time for DAA proved to be higher compared to PA of an average of 12.9 minutes in our study. This finding is consistent with the current literature. In addition, we believe that this measure could be underestimated because it considered time from incision to complete suture without evaluating time to prepare patients on bed, which is, in our experience, much longer for DAA due to the use of a dedicated mobile leg positioner. Nonetheless, the higher costs, secondary to the longer operative room occupancy time could be overcome by the lower hospital length of stay of DAA as reported by many authors (5, 12, 14-17).

Blood loss following DAA represent a controversial topic. According to several authors, blood loss is higher in DAA when compared to traditional PA (18, 19). In our study however, no differences were observed regarding blood loss between the 2 groups. This is consistent to the case series presented by Alecci et al and Matta et al (16, 20).

This study aimed to evaluate differences between the DAA and the PA in the early postoperative recovery therefore, one of the main limit of the present study is the short follow-up period and the absence of records regarding the functional status at a longer follow-up. This could have hidden a possible leveling of the differences reported on the early postoperative reports on a longer follow-up as reported by several authors (12, 16, 17, 20-23). Indeed, similarly to our results a faster functional recovery in patients undergone DAA on TUG and M-FIM for up to 2 weeks were found by Rodriguez et al (17).

Another limit of the present study is the absence of correlation between the radiographic parameters and the functional outcome. However, due to its nature we believe that differences in cup and stem positioning could not interfere with the clinical outcome in such a limited period of evaluation like

the early postoperative recovery. Moreover, in our study patients undergone PA were advised to take some hip movements precautions that could have interfere with the ability to reach higher results on M-FIM and TUG test. However, such limitations have been taken also from other authors reporting differences between DAA and PA because of the well-known risks of dislocation in case of PA especially during the early postoperative recovery (17).

Others limits of the present study are related to the small number of patients, which might reduce its statistical power and the retrospective nature or the lack of a gait analysis evaluation performed in the early post-operative period before discharging the patient. Maffiuletti et al, reported results on spatiotemporal parameters of gait after THA with either a DAA or a PA founding higher stiffness in patients subjected to PA but similar pain and function at 6-month follow-up (24). It would be interesting to perform an early gait analysis evaluation in order to assess differences between the 2 groups.

In conclusion, our results suggest that the surgical approach can influence the early postoperative recovery with a significant improvement in case of DAA compared to PA measured M-FIM, TUG, and hospital length of stay. However, prospectively randomized controlled study with larger populations are required in order to assess if the differences recorded in this study are maintained on longer follow-up period and to evaluate correlation between clinical and radiological results, if any.

REFERENCES

1. Nanni M, Perna F, Calamelli C, et al. Wound drainages in total hip arthroplasty: to use or not to use? Review of the literature on current practice. Musculoskelet. Surg 2013; 97(2):101-7.
2. Trevisan C, Compagnoni R, Klumpp R. Comparison of clinical results and patient's satisfaction between direct anterior approach and Hardinge approach in primary total hip arthroplasty in a community hospital. Musculoskelet Sur 2017.
3. Barrett WP, Turner SE, Leopold JP. Prospective randomized study of direct anterior vs postero-lateral approach for total hip arthroplasty. J Arthroplasty 2013; 28(9):1634-8.
4. Homma Y, Baba T, Sano K, et al. Lateral femoral cutaneous nerve injury with the direct anterior approach for total hip arthroplasty. Int Orthop 2016; 40(8):1587-93.
5. Faldini C, Perna F, Pilla F, et al. Is a minimally invasive anterior approach effective in old patients? A pilot study. J Biol Regul Homeost Agents 2016; 30(4S1):193-9.
6. Trevisan CL, Klumpp R, Recalcati W, et al. Influence of personality psychology on outcome of total hip arthroplasty: a cross-sectional study on 69 patients. Musculoskelet Surg 2015; 99(3):231-6.
7. Malek IA, Royce G, Bhatti SU, et al. A comparison between the direct anterior and posterior approaches for total hip arthroplasty: the role of an 'Enhanced Recovery' pathway. Bone Jt J 2016; 98B(6):754-60.
8. Granger CV, Hamilton BB, Linacre JM, et al. Performance profiles of the functional independence measure. Am J Phys Med Rehabil 1993; 72(2):84.
9. Hershkovitz A, Brill S. Get up and go--home. Aging Clin. Exp. Res. 2006; 18(4):301-6.
10. Meermans G, Konan S, Das R, et al. The direct anterior approach in total hip arthroplasty: a systematic review of the literature. Bone Jt J 2017; 99(6):732-40.
11. Bergin PF, Doppelt JD, Kephart CJ, et al. Comparison of minimally invasive direct anterior versus posterior total hip arthroplasty based on inflammation and muscle damage markers. J Bone Joint Surg Am 2011; 93(15):1392-8.
12. Martin CT, Pugely AJ, Gao Y, et al. A Comparison of Hospital Length of Stay and Short-term Morbidity Between the Anterior and the Posterior Approaches to Total Hip Arthroplasty. J Arthroplasty 2013; 28(5):849-54.
13. Petis S, Howard JL, Lanting BL, et al. Surgical approach in primary total hip arthroplasty: anatomy, technique and clinical outcomes. Can J Surg 2015; 58(2):128-139.
14. Joseph NM, Roberts J, Mulligan MT. Financial impact of total hip arthroplasty: a comparison of anterior versus posterior surgical approaches. Arthroplasty Today 2016; 3(1):39-43.
15. Cadossi M, Chiarello E, Savarino L, et al. A comparison of hemiarthroplasty with a novel

polycarbonate-urethane acetabular component for displaced intracapsular fractures of the femoral neck: A randomised controlled trial in elderly patients. Bone Jt J 2013; 95:609-15.
16. Alecci V, Valente M, Crucil M, et al. Comparison of primary total hip replacements performed with a direct anterior approach versus the standard lateral approach: perioperative findings. J Orthop Traumatol 2011; 12(3):123-9.
17. Rodriguez JA, Deshmukh AJ, Rathod PA, et al. Does the direct anterior approach in THA offer faster rehabilitation and comparable safety to the posterior approach? Clin Orthop 2014; 472(2):455-63.
18. Woolson ST, Pouliot MA, Huddleston JI. Primary total hip arthroplasty using an anterior approach and a fracture table: short-term results from a community hospital. J Arthroplasty 2009; 24(7):999-1005.
19. Jewett BA, Collis DK. High complication rate with anterior total hip arthroplasties on a fracture table. Clin Orthop 2011; 469(2):503-7.
20. Matta JM, Shahrdar C, Ferguson T. Single-incision anterior approach for total hip arthroplasty on an orthopaedic table. Clin Orthop 2005; 441:115-24.
21. Faldini C, Pilla F, Fenga D, et al. Isolate acetabular cup revision through the direct anterior hip approach: surgical technique, early experience and review of the literature. J Biol Regul Homeost Agents 2016; 30(4S1):201-206.
22. Abouel-Enin S, Fraig H, Griffiths J, et al. Intra-pelvic migration of femoral head trial in total hip arthroplasty, a rare intra-operative complication: a systematic literature review. Musculoskelet Surg 2016; 100(2):77-81.
23. Chillemi M, Placella G, Caraffa A, et al. Serologic and radiographic outcome of total hip arthroplasty with CoCr modular neck at mid-term follow-up. Musculoskelet Surg 2016.
24. Maffiuletti NA, Impellizzeri FM, Widler K, et al. Spatiotemporal parameters of gait after total hip replacement: anterior versus posterior approach. Orthop Clin North Am 2009; 40(3):407-15.

MODIFIED MINIMALLY INVASIVE DIRECT ANTERIOR APPROACH THROUGH A BIKINI INCISION FOR TOTAL HIP ARTHROPLASTY: TECHNIQUE AND RESULTS IN YOUNG FEMALE PATIENTS

C. FALDINI[1], A. MAZZOTTI[1], F. PERNA[1], N. STEFANINI[1], A. PANCIERA[1], F. PILLA[1], A. RUFFILLI[1], E.M. NEONAKIS[2] and F. TRAINA[3]

[1]1st Orthopaedic and Traumatologic Clinic, Istituto Ortopedico Rizzoli, Bologna, Italy; [2]Orthopaedic Department, Aghia Sophia Children's Hospital, Athens, Greece; [3]Dipartimento di Ortopedia e Traumatologia, Department of Biomedical Sciences and Morphological and Functional Images, Scuola Ortopedia e Traumatologia, Università di Messina, Italy

Direct anterior approach for THA has gained popularity over the last years. However, concerns have been raised regarding the cosmetic, related to the incision that does not respect the Langer's skin tension line and may produce hypertrophic scars. The aim of this study was to analyze the preliminary results in 22 young female patients undergoing THA through a minimally invasive direct anterior approach using a modified oblique bikini incision. Clinical evaluations showed an improvement of WOMAC, UCLA and Harris Hip Score at 5-month follow-up. The technique ensured proper implant positioning and showed advantages in terms of complications, transfusion rates, hospital length of stay and functional recovery. From the aesthetic point of view, the expected cosmetic results were obtained. Minimally invasive direct anterior approach using a modified oblique bikini incision represent a viable option for THA, combining both the advantages of a minimal invasive procedure with a better aesthetic appearance.

Over the last years, minimally invasive surgical techniques in total hip arthroplasty (THA) have become more attractive. The direct anterior approach (DAA) for THA is considered a tissue sparing procedure which allows to reach the hip joint capsule through the interval between the Sartorius and Rectus Femoris medially and the Tensor Fasciae Latae laterally, without muscle detachment. This intermuscular and internervous procedure was first described by Hueter (1) and later popularized by Smith-Petersen (2) and Judet (3, 4). In the past decade, the DAA has progressively gained popularity among orthopedic surgeons for its theoretical advantages over other techniques (5, 6): minimal soft tissue dissection with no muscle detachment (7), faster functional recovery (8), reduced postoperative loss of hip muscle mass and force (9), reduced blood loss (10), less pain (11), fewer complications (10,12-14), lower dislocation rate (15) and shorter hospital stay (16). However, despite these potential advantages, some drawbacks associated with the DAA remain.

The technique requires a steep learning curve; inexperienced surgeons (17, 18) have reported several complications. Other limitations include the restricted indications (19), the possible injury to the lateral femoral cutaneous nerve (LFCN) (20), the need for further release of tendon and capsule (12, 21), and the difficulty in intraoperative leg-length assessment when using a mobile leg positioner (14).

In addition, similar concerns have been argued regarding the cosmetic related to the incision: the classic anterior approach longitudinal skin incision, which starts 1 inch lateral and inferior to the external edge of the anterior superior iliac spine and then runs

Key words: Total hip arthroplasty, anterior approach, minimally invasive surgery, bikini incision, young female patients

Mailing address:
Cesare Faldini,
1st Orthopaedic and Traumatologic Clinic,
Istituto Ortopedico Rizzoli,
Via Giulio Cesare Pupilli 1,
40136, Bologna, Italy
e-mail: cesare.faldini@ior.it

0393-974X (2017)

obliquely downward and slightly outward toward the fibular head (14) does not respect the Langer's skin tension line (22) of the inguinal and thigh regions (23, 24). Langer's line ideally correspond to the natural orientation of dermis collagen fibers, which are parallel to the orientation of the underlying muscle fibers. Incisions made parallel to Langer's lines usually heal better and produce less scarring and better regeneration.

Conversely, incisions that cut across Langer's lines have a tendency to produce hypertrophic and obvious scars. Therefore, the scar widening that may occur after a classic DAA can cause patient discomfort and poor satisfaction ratings, especially when dealing with young and fit women. In order to overcome this issue, short oblique skin incisions following the skin crease of the groin (the bikini line) have been proposed (23, 24). This new approach should theoretically provide a better incision healing and allow to hide the surgical scar when wearing underwear or swimwear.

The aim of this study was to analyze the results in 22 young female patients undergoing THA through a modified minimally invasive DAA using a bikini incision. In particular, we wanted to evaluate whether the incision leads to satisfactory scar results, allows for good clinical outcomes and is safe with regard to possible early complications (implant malpositioning, LFCN damage, blood loss, early implant dislocation).

MATERIALS AND METHODS

Twenty-five young female patients who underwent cementless THA through a modified minimally invasive DAA, with a bikini incision for end stage hip osteoarthritis between January 2015 and January 2017 were included in this study.

Two patients were lost at follow-up and one patient did not complete the post-operative self-assessment questionnaire and were therefore excluded from the study. The remaining 22 patients provided written informed consent after receiving a detailed explanation of the study and agreed to data publication.

Diagnosis was primary osteoarthritis in 20 patients and secondary osteoarthritis in 2 patients. Surgery was performed in 8 cases on the left hip and in 14 cases on the right hip. The average patients age at the time of surgery was 37.72 years (range 19-48); average body max index (BMI) was 26.23 (range 23.3-31.4).

During the study period, the senior author performed all THA through a modified minimally invasive DAA with a bikini incision, using a specific surgical instrumentation (Medacta International SA, Switzerland). All patients received a ceramic on ceramic coupling with a cementless hydroxyapatite-coated elliptical press-fit cup (Versafitcup®, Medacta) and a cementless hydroxyapatite-coated straight short stem (AMIS stem®, Medacta).

All intraoperative and postoperative complications were recorded. Operating time was assessed. The need for transfusion and patients preoperative and postoperative hemoglobin levels (at first postoperative day and at the discharge) were recorded. Eventually, the presence of hypoesthesia and dysesthesia in the distribution of the LFCN or LFCN lesions were also considered. Clinical assessments were performed preoperatively, 1 month and 5 months after surgery and were determined by the Western Ontario and McMaster Universities Arthritis Index (WOMAC), the University of California, Los Angeles activity scale (UCLA) and the Harris Hip Score (HHS). The patients completed a satisfaction questionnaire related to the scar using a numeric rating scale (from 0 = completely dissatisfied to 10 = very satisfied) 5 months after surgery. Lengths of scars were also measured. Radiographic evaluation was made preoperatively, at 1 month and at the last follow-up on antero-posterior and lateral view X-rays. Cup inclination and stem orientation were evaluated at the last follow-up. Cup inclination was measured on pelvis anteroposterior X-rays as the angle between the inter-teardrop line and the edge of the cup; a stem was considered varus or valgus if the angle described by the intersection of the axis of the stem and the axis of the femoral shaft was higher than 5 degrees.

Surgical technique

Patient is placed supine on specific operative table, with the operated leg secured on a mobile leg positioner (AMIS mobile leg positioner®). Surgical field should include only the operated leg, extended proximally to the umbilicus and distally to the rotula.

The rotula should be positioned at the zenith, with the foot in internal rotation and the hip in slight flexion and

abduction. The skin cut of the bikini incision is oblique, following the skin crease at the level of the inguinal fold, two third laterally and one third medially in respect to the ASIS. Before the incision, it is advisable to perform some slight hip flexion and extension movements to better detect the skin crease location.

After skin incision, all the other steps are performed longitudinally. Subcutaneous tissues are excised and muscolaris fascia is reached, identifying the intermuscular space between Sartorius and Tensor Fasciae Latae muscle. To protect the LFCN the fascia is sharply incised more lateral than classic Hueter's approach, over Tensor Fasciae Latae muscle belly. Intermuscular space is then bluntly developed, with the operated leg in slight flexion and abduction, to decrease tension of the fascia. By retracting Tensor Fasciae Latae and Sartorius muscles, the deep layer is reached. The head of the Rectus Femoris is identified and bluntly displaced without detaching the muscle origin. Below that, the underlying deep aponeurosis is exposed and the vascular bundle of the lateral circumflex femoral artery is identified, passing from posterior to anterior at this level; its ascending branch, which runs in the intertrochanteric line, is then ligated and cut, to avoid bleeding and to achieve a clean surgical field. Capsulotomy is performed with a "Delta-shape" incision, tagging the lateral capsular flap, to facilitate the exposure of the acetabulum and the suture at the end of the surgery. Femoral neck osteotomy is then performed; correct orientation of the osteotomy is verified with respect to the position of the intercondylar axis.

After completing the osteotomy, leg is put in slight traction and external rotation, obtaining a widening of the osteotomy space, and the femoral head is removed. The acetabulum is exposed using curved Hohmann retractors. Reamer is inserted into the acetabulum freely and then a specific offset handle is connected to start reaming to avoid impingement against soft-tissues and leverage effect. First reaming is performed by medializing the center of rotation, and then progressive reaming is performed to a reamer size, which have macroscopic stability. Trial cup is impacted into the acetabulum to assess orientation and stability. When optimal stability is achieved, definitive cup (Versafitcup®, Medacta) is inserted. To expose the femur, the leg must be placed in external rotation and hyperextension and is adducted until the leg passes underneath the non-operated one.

In order to reduce the risk of femoral fracture during broaching, the posterior aspect of the capsula should be released. Femoral canal is then identified and prepared for broaching using a box osteotome. The canal is opened and its integrity is checked with a curved spoon. Progressive broaching is then executed until stability is reached. Even for femoral broaching is necessary to use specific offset handle to avoid impingement against soft tissues. After placing trial components for the femoral stem and head, definitive components (AMIS stem®, Medacta) are then inserted. The hip is reduced and the surgical field is closed by multiple layers suturing.

Partial weight-bearing was started with two crutches the day after surgery and allowed for three weeks after surgery; then full weight bearing was permitted.

RESULTS

No intraoperative or early post-operative complications occurred. The average total surgical time was 70.4 minutes (range 63-78). All patients but one were able to partially weight bear the operated hip on the first post-operative day. The average length of stay in our clinic was 4.9 days (range 4-7).

Only 4 patients (18.18%) required a blood transfusion. The average preoperative hemoglobin levels were 13.65 g /dl (range 11.8-15.5); 1 day after surgery were 9.85 g /dl (range 7.1-10.6) whereas at the discharge were10.77 g /dl (range 9.80-11.40). In 9 patients (40.9%) a mild hypoesthesia in the distribution area of the LCFN was found: in all cases symptoms resolved during the first postoperative month except in 2 patients where the hypoesthesia persisted until 3 and four 4 months respectively.

Clinical assessments were performed at one month (average 31.18 days) and at 5-month follow-up (average 157.04 days) in all patients. Pre-operative WOMAC score averaged 53.55 (range 35.21-80.81) pre-operatively, 84.33 (range 77.5-88.4) at one month follow-up and 92.48 (range 85.5-98.4) at the last follow-up. The average UCLA score at one month follow-up was 4.27 (range 3-5) and 7.9 (range 6-9) the latest follow-up was, while in the pre-operative was 4.4 (range 3-6). Harris Hip Score improved from 43.17 (range 14.55-74) to 83.49 (range 70-92.95) at 1 month postoperatively and 92.03 (range 84.2-98) after 5 months. The

scores related to patients satisfaction questionnaire about the scar showed an overall satisfaction with the following results: average score 5 months after surgery was 8.86 (range: 6-10), 7 patients (31.8%) reported a value of 10 points (very satisfied) and 8 patients (36.3%) a value of 9 points.

Scar length was measured by the same operator (not involved in the surgery) at the last follow-up: average scar length was 9.6cm (range 8.7-11) (Fig. 1, 2). No early implants dislocation were recorded, nor migration and periprosthetic osteolysis were observed at follow-ups. Radiographic evaluation on antero-posterior and lateral views at the last follow-ups showed an average cup inclination of 48.79° (range 41-60.5); stem orientation was evaluated as neutral in all patients apart from 3 patients (13.6%) in which the stem showed a slightly varus alignment.

DISCUSSION

Over the last years the DAA for THA has gained popularity (5-6) for its theoretical advantages in terms of minimal soft tissue dissection, reduced surgical complications, pain and risk of dislocation (7, 9, 10, 11, 12-16). For these features, the DAA is usually reserved to young and active patients in which a tissue sparing procedure should allow for faster mobilization and better functional recovery (8). Despite that, the longitudinal skin incision performed in DAA (14), which does not respect the Langer's skin tension line (22), can represent an issue for the formation of hypertrophic scars, thus resulting in patient discomfort and dissatisfaction, particularly when facing young female patients. In the attempt to improving the cosmetic aspect of the surgery, different incisions along the physiological skin crease, have been proposed (23).

In this study, we reported the results of 22 young female patients who underwent THA through a modified minimally invasive DAA with a bikini incision. Short-term clinical outcomes were excellent with no major complications. The DAA for THA ensured minor surgical trauma and showed many advantages in terms of complications, transfusion rates, hospital length of stay and functional recovery. In addition, from the aesthetic point of view, the

Fig. 1. *Twenty-eight years old patient at 5-month follow-up after THA through a minimally invasive DAA using the oblique bikini incision.*

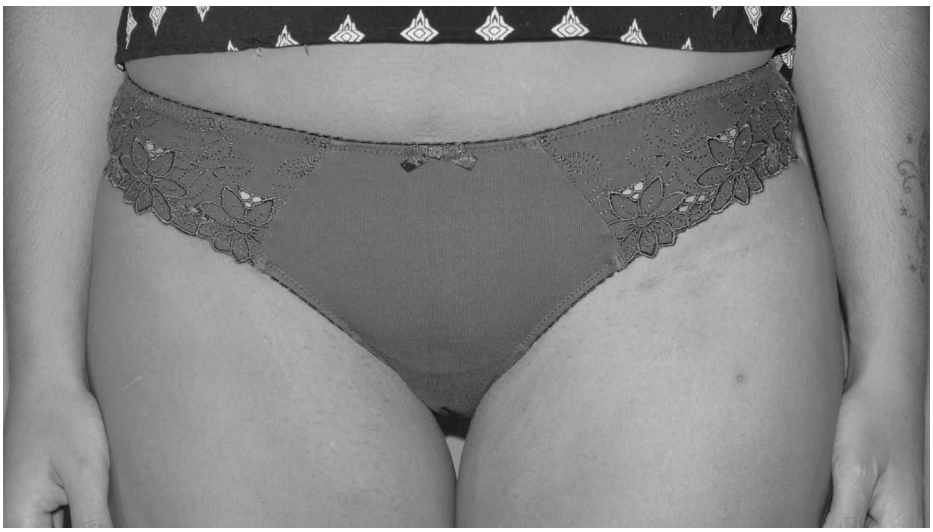

Fig. 2. *Surgical scar at 5-month follow-up showing the good cosmetic outcomes.*

satisfaction questionnaire related to the scar using a numeric rating scale average score confirmed the expected cosmetic result. The scar was nearly undetectable in the majority of patients at 5-month follow-up.

Our results reflects the good outcomes reported by Leunig et al, who popularized the bikini incision in 2013 (23). The approach we described presents some differences if compared to the one proposed by Leunig. The use of a specific mobile leg positioner offers several advantages. It gives a more stable position to the femur and allows for a better exposure. When performing the capsulotomy, we prefer not to detach Rectus Femoris reflected head with the capsule, thus theoretically reducing postoperative pain and peri and postoperative bleeding. Osteotomy of the femoral neck is achieved with the head in situ, without previous dislocation, in order to reduce the stress on the femur.

Finally, since we use a monoblock femoral stem, we perform acetabulum-first surgery to have better visualization of the acetabulum and no impingement from the femoral trunnion when reaming and positioning prosthetic cup. This allowed for proper implant positioning in most cases of both stem and cup.

Only few complications were observed in our series. The incision did not interfere with a proper prosthetic components positioning. No major lesions to the LCFN occurred. A mild hypoesthesia in the LCFN distribution area were observed in the 40.9% of cases with a spontaneous resolution over time. The incidence of this complication were lower if compared to the results reported by Leunig et al (23) who described an objective hypoesthesia in 60% of patients with the same incision. The incidence of LCFN injuries however may vary depending on several factors such as incision position and dissection plane (24, 25). Our technique indeed performs a more lateral incision on muscle fascia, over the tensor fascia lata muscle belly, in order to reduce the incidence of injuries to the LCFN, which runs superficially and more medially in the intermuscular space. In any case several paper have shown that dysesthesia or hypoesthesia after DAA, regardless of the incision type (20, 25) tend to resolve spontaneously over time without complications.

The results reported in our series may in particular be related to the patient's choice: young and slim patients represent the ideal candidates for this procedure, (23) while obesity and significant joint deformity generally described as less suitable for DAA (23).

Main limitations of the study are represented by the small sample size and by the short-term follow-up considered. Despite that, the 5-month follow-up was enough to determine the effectiveness of the procedure in terms of fast recovery and good cosmetic outcomes. Another limitation is the

absence of a control group, which would allow for comparative analysis with other approaches.

Although our findings need to be validated by larger and comparative studies in the future, DAA through a bikini incision represent a viable option for THA in young female patients, combining both the advantages of a minimal invasive procedure with a better aesthetic appearance.

REFERENCES

1. Hueter C. Grundriss der Chirurgie. 2. Leipzig: FCW Vogel; 1883:129-200.
2. Smith-Petersen MN, Larson CB, et al. Complications of old fractures of the neck of the femur; results of treatment of vitallium-mold arthroplasty. J Bone Joint Surg Am 1947; 29(1):41-48.
3. Judet J, Judet H. Anterior approach in total hip arthroplasty. Presse Med 1985; 14:1031-3.
4. Rachbauer F, Kain MS, Leunig M. The history of the anterior approach to the hip. Orthop Clin North Am 2009; 40:311-20.
5. Masonis J, Thompson C, Odum S. Safe and accurate: learning the direct anterior total hip arthroplasty. Orthopedics 2008; 31(12S2):1417-26.
6. Zhao HY, Kang PD, Xia YY, Shi XJ, Nie Y, Pei FX. Comparison of Early Functional Recovery After Total Hip Arthroplasty Using a Direct Anterior or Posterolateral Approach: A Randomized Controlled Trial. J Arthroplasty 2017; S0883-5403(17)30496-5.
7. Yakovlev AE, Resch BE, Karasev SA. Treatment of intractable hip pain after THA and GTB using peripheral nerve field stimulation: a case series. WMJ 2010; 109:149-52.
8. Nakata K, Nishikawa M, Yamamoto K, Hirota S, Yoshikawa H. A clinical comparative study of the direct anterior with miniposterior approach: two consecutive series. J Arthroplasty 2009; 24:698-704.
9. Clark BC. In vivo alterations in skeletal muscle form and function after disuse atrophy. Med Sci Sports Exerc 2009; 41:1869-75.
10. Faldini C, Perna F, Pilla F, Stefanini N, Pungetti C, Persiani V, Traina F. Is a minimally invasive anterior approach effective in old patients? A pilot study. J Biol Regul Homeost Agents 2016; 30(4S1):193-9.
11. Goebel S, Steinert AF, Schillinger J, Eulert J, Broscheit J, RudertM, Nöth U. Reduced postoperative pain in total hip arthroplasty after minimal-invasive anterior approach. Int Orthop 2012; 36:491-8.
12. Barrett WP, Turner SE, Leopold JP. Prospective randomized study of direct anterior vs postero-lateral approach for total hip arthroplasty. J Arthroplasty 2013; 28:1634-8.
13. Mirza AJ, Lombardi AV Jr, Morris MJ, Berend KR. A mini-anterior approach to the hip for total joint replacement: optimizing results. Improving hip joint replacement outcomes. Bone Joint J. 2014; 96-(11S):32-5.
14. Cadossi M, Sambri A, Tedesco G, Mazzotti A, Terrando S, Faldini C. Anterior Approach in Total Hip Replacement. Orthopedics 2017; 40(3):e553-e6.
15. Matta JM, Shahrdar C, Ferguson T. Single-incision anterior approach for total hip arthroplasty on an orthopaedic table. Clin Orthop Relat Res 2005; 441:115-24.
16. Bremer AK, Kalberer F, Pfirrmann CW, Dora C. Soft-tissue changes in hip abductor muscles and tendons after total hip replacement: comparison between the direct anterior and the transgluteal approaches. J Bone Joint Surg Br 2011; 93:886-9.
17. Yi C, Agudelo JF, Dayton MR, Morgan SJ. Early complications of anterior supine intermuscular total hip arthroplasty. Orthopedics 2013; 36(3):e276-e81.
18. De Geest T, Vansintjan P, De Loore G. Direct anterior total hip arthroplasty: complications and early outcome in a series of 300 cases. Acta Orthop Belg 2013; 79(2):166-73.
19. Nam D, Sculco PK, Abdel MP, Alexiades MM, Figgie MP, Mayman DJ. Leg-length inequalities following THA based on surgical technique. Orthopedics 2013; 36:395-400.
20. Goulding K, Beaulé PE, Kim PR, Fazekas A. Incidence of lateral femoral cutaneous nerve neuropraxia after anterior approach hip arthroplasty. Clin Orthop Relat Res 2010; 468(9):2397-404.
21. Liberati A, Altman DG, Tetzlaff J, et al. The PRISMA statement for reporting systematic reviews and meta-analyses of studies that evaluate health care interventions: explanation and elaboration. J Clin Epidemiol 2009; 62:1-34.
22. Karl Langer, "Zur Anatomie und Physiologie der Haut. Über die Spaltbarkeit der Cutis". Sitzungsbericht der

Mathematisch-naturwissenschaftlichen Classe der Wiener Kaiserlichen Academie der Wissenschaften Abt. 44 (1861).
23. Leunig M, Faas M, von Knoch F, Naal FD. Skin crease 'bikini' incision for anterior approach total hip arthroplasty: surgical technique and preliminary results. Clin Orthop Relat Res. 2013; 471(7):2245-52.
24. Lanting BA, Hartley KC, Raffoul AJ, Burkhart TA, Sommerville L, Martin GR, Howard JL, Johnson M. Bikini versus traditional incision direct anterior approach: is there any difference in soft tissue damage? Hip Int. 2017; 27(4):397-400.
25. Bhargava T, Goytia RN, Jones LC, Hungerford MW. Lateral femoral cutaneous nerve impairment after direct anterior approach for total hip arthroplasty. Orthopedics 2010; 33:472.

DIRECT VERTEBRAL ROTATION AND DIFFERENTLY SHAPED DUAL RODS TRANSLATION TECHNIQUE IN ADOLESCENT IDIOPATHIC SCOLIOSIS

C. FALDINI[1], F. PERNA[1], R. BORGHI,[1] M. CHEHRASSAN[1], N. STEFANINI[1], A. RUFFILLI[1], A. MAZZOTTI[1], K. MARTIKOS[2] and F. TRAINA[3]

[1]1st Orthopaedic and Traumatologic Clinic, Istituto Ortopedico Rizzoli, Bologna, Italy; [2]Department of Spinal Deformity Surgery, Istituto Ortopedico Rizzoli di Bologna, Bologna, Italy; [3]Dipartimento di Ortopedia e Traumatologia, Department of Biomedical Sciences and Morphological and Functional Images, Scuola Ortopedia e Traumatologia, Università di Messina, Italy

Direct vertebral rotation (DVR) is widely used to correct the axial deformity in adolescent idiopathic scoliosis (AIS). Indirect rotation techniques may help DVR in order to improve outcome. Vertebral translation technique combined with the use of two differently shaped rods resulted effective in reducing the rib hump deformity. The aim of this study is to describe the technique and evaluate the efficacy of combined DVR and vertebral translation technique on axial deformity correction. Mean follow-up was 2.7 years. Cobb angle, kyphosis angle, apical vertebrae axial rotation angle, SRS-22 questionnaire of 30 AIS patients treated with combined DVR and differently shaped dual rods translation technique were collected and compared preoperatively and postoperatively. At the last follow-up no screw pull-out, nonunion or loss of correction were recorded. The combination of DVR and differently shaped dual rods translation technique in AIS can provide good three-dimensional correction and improvement of patient's quality of life.

Adolescent Idiopathic Scoliosis (AIS) is a three-dimensional deformity on the frontal, sagittal and axial planes. The vertebral rotation is an important component of scoliosis and described as rib hump when the apical vertebra is placed in thoracic spine. Historically, frontal plane deformity correction was the only aim of surgical procedure before the correction on sagittal and axial planes were taken into consideration. Scoliosis correction on frontal plane heralded by Hibbs as *in situ* fusion and, later on, with the implant designed by Harrington.

The first attempt of a three-dimensional correction was proposed by Cotrel-Dubousset at the beginning of the 1980's with the aid of two rods, without satisfactory results on the axial plane. Roy-Camille and Suk introduced and extended the use of pedicle screws, which provided the correction force on all three columns of the spine, providing more effective corrective maneuver. (1, 2).

In order to obtain a better correction of the deformity also on the axial plane, in 2004, Lee et al. introduced the direct vertebral rotation (DVR) technique in witch pedicles screws were applied as foothold to directly correct the rotation of vertebrae (3). DVR can be performed in different ways with the same concept to reduce the rib hump. Indirect vertebral rotation techniques may help DVR in order to improve the results.

Vertebral translation technique combined with the use of two differently shaped rods has demonstrated

Key words: direct vertebral rotation, pedicle screws, scoliosis correction, surgical technique

Mailing address:
Cesare Faldini,
1st Orthopaedic and Traumatologic Clinic,
Istituto Ortopedico Rizzoli,
Via Giulio Cesare Pupilli 1,
40136, Bologna, Italy.
e-mail: cesare.faldini@ior.it

0393-974X (2017)

to be effective to reduce the rib hump deformity (4, 5). The aim of this study is to describe the surgical technique and eventually evaluate the efficacy of combined DVR and vertebral translation technique on axial deformity correction.

MATERIALS AND METHODS

Thirty patients including 26 females and 4 males affected by adolescent idiopathic scoliosis (AIS), surgically treated from January 2010 to January 2015 were enrolled in this study and evaluated retrospectively. Mean patient age was 14.8 years. One surgeon performed all surgery. Acording to Lenke classification for AIS the number of patients was as follow: 17 main thoracic (Lenke type 1), 2 double thoracic (Lenke type 2), 6 double major (Lenke type 3), 2 thoracolumbar/lumbar (Lenke type 5) and 3 thoracolumbar/lumbar main thoracic (Lenke type 6) (6). Inclusion criteria were: patients affected by AIS, minimum two years of follow-up.

Exclusion criteria included congenital, syndromic and neuromuscular scoliosis and scoliosis with more than 100° on coronal Cobb angle. Applied surgical technique for all patients was DVR and differently shaped dual rods translation using pedicle screws-only construct. Evaluation parameters on X-rays were coronal Cobb angle, T5-T12 thoracic kyphosis angle and sagittal vertical axis (SVA), which was used to evaluate the sagittal balance, whereas the distance from the C7 coronal plumb line (C7PL) to the central sacral vertical line (CSVL) was used for global coronal balance assessment. These measures were evaluated on standing long-cassette postero-anterior and lateral radiograph before and after surgery and during last follow up control.

Before surgery, supine bending radiographs were performed for each patient in order to evaluate the rigidity of the curve and to classify the deformity according to Lenke (6). Magnetic resonance imaging (MRI) was pre-operatively evaluated in all patients in order to exclude neurological problems. In addition, MRI was used to measure apical vertebrae axial rotation (AVAR) before surgery. Post-operatively computer tomography (CT) scans was performed to control the position of the pedicle screws and measure AVAR (7, 8). All patients were asked to complete the Scoliosis Research Society 22 Questionnaire (SRS-22), before surgery and at 1 year follow-up, in order to investigate function, pain, self-image, mental health and treatment satisfaction (9). Statistical analysis: all data were analysed with SPSS software (SpSS, version 18.0; SpSS Chicago, Il). P-value of <0.005 was considered as being statistically significant.

Surgical Technique

Patients were placed in a prone position and a standard posterior approach of the spine was performed. The level of fusion was planned according to Lenke et al. and pedicle screws were inserted accordingly using the drill-assisted

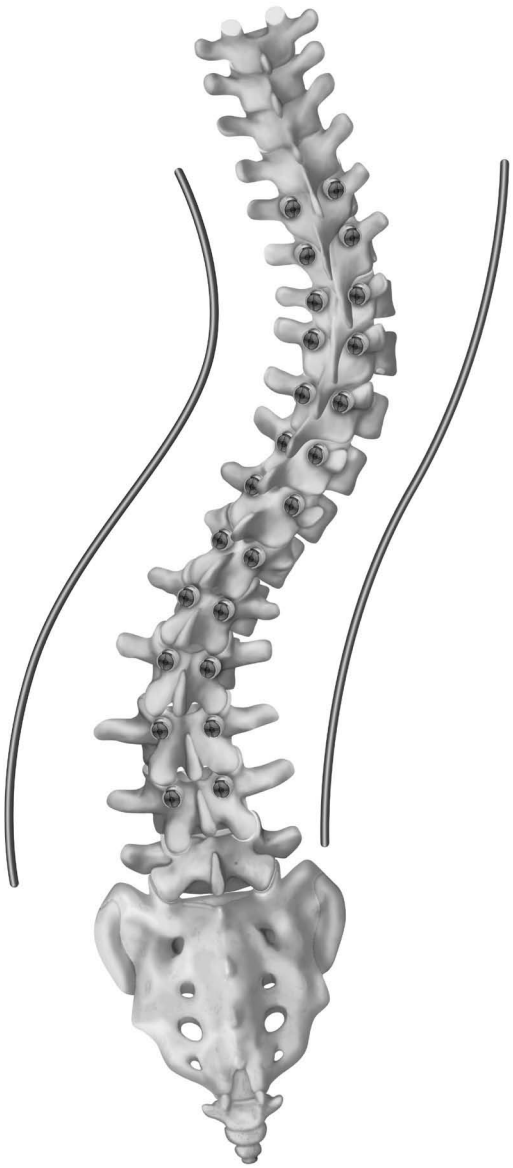

Fig. 1. *Different rods contouring.*

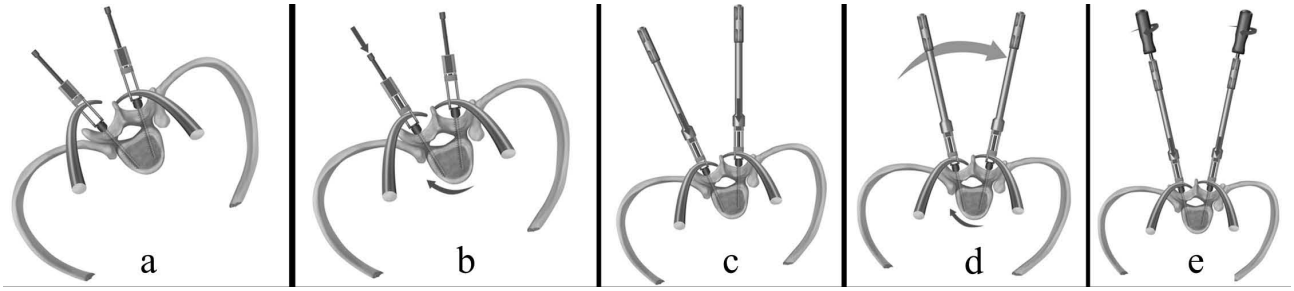

Fig. 2. *schematic representations of: rods rotations (**a**); concave rods reduction (**b**); application of implant extender (**c**); direct vertebral rotation (**d**); rods tightening on the screw heads (**e**).*

technique (6, 10). In order to identify the pedicles entry points at the level of thoracic spine and to perform posterior release to improve the deformity correction, the posterior facet joints were removed at all levels of thoracic spine in the fusion area.

The facet joint was preserved at the upper most level to avoid proximal junction kyphosis. Uniplanar pedicle screws were used at all levels. High-density system was applied in all cases in order to distribute applied forced at the moment of translation and consequently DVR on more pedicles. Two 5.5 mm Cobalt-chrome alloy rods were shaped differently as over-shaped and under-shaped according to necessary kyphosis and lordosis (Fig. 1).

After the insertion of the rods and application of reduction jacks rods fixator (specific instrumentation, which progressively allows to pull the vertebrae toward the rods) both rods were rotated from convex to concave side (counter clockwise in case of right thoracic curve) in order to partially correction of the deformity on frontal plane (Fig. 2a). As a general concept the under-shaped rod placed adjacent to, but not in contact with the screw head in the same side of the rotation of the vertebral body and over-shaped rod far distant on the other side. In this way, at the time of rod reduction, while the force is applied to reduce the rod on the screws' head on the concave side, vertebral bodies rotate toward the concave side and so the vertebral rotation on the axial plane is achieved consequently (Fig. 2b). In case of main thoracic scoliosis curve (Lenke 1), on the concave side an over-shaped rod is applied, while an under-shaped rod on the convex side. In case of a double thoracic curve (Lenke 2), each rod will be over-shaped on the concave side, and under-shaped on the convex side. During the shaping of the rods, care should be taken considering the thoracic kyphosis, which is reduced proximally.

In case of double curve at the level of thoracic and lumbar spine, including Lenke 3 and Lenke 6 scoliosis curve, the over-shaped rod (both as kyphosis and lordosis) is applied on the concave side of the thoracic curve, and convex side of the lumbar curve, while the under-shaped rod is applied on the convex side of the thoracic spine and concave side of the lumbar spine (Fig. 1). In case of a single lumbar curve (Lenke 5) the over-shaped rod is used on the convex side and the under-shaped rod on the concave siThe rods were leaned onto pedicle screws with the aid of reduction jacks anchored on screws heads to perform translation. The reduction jacks were reduced partially. This maneuver should be performed sequentially in order to distribute the force on several screws to avoid screw pullout. Translation can potentially correct the deformity in all three planes. Due to the fact that the rods are shaped differently, during this procedure the vertebral body rotates toward the concave side and the vertebral rotation on the axial plane will be reduced consequently. The more proximal and distal screws were fully tightened to create a fix foundation in order to maintain achieved coronal correction.

DVR was then performed, using implant extenders (Fig. 2c, d). When desired axial correction was achieved, the rod was tighten on the screw heads (Fig. 2e). Final modeling of rods was performed with in situ bender.

In all patients, decortication was performed, and in all cases, morselized bone was used as bone graft mixed with the obtained local bone from facet joints removal. All patients were operated with the use of cell saver and spinal cord monitoring of somatosensory evoked potentials (SEPs) and motor evoked potentials (MEPs).

RESULTS

Patients were reviewed at an average follow-up of 2.7 years (range 2-4 years). The mean Cobb angle decreased from a preoperative value of 67.1°±10.4° to a postoperative value of 14.3°±4.0° ($p<0.005$). The mean T5-T12 kyphosis angle was 16.1°±5.6° preoperatively and 23.0°±3.0° after surgery. Among patients with hypo-kyphosis scoliosis T5-T12 kyphosis angle was 13.2°±4.7° preoperatively, and 21.4°±2.7° after surgery, with significant gain of a mean of 8.2° ($p<0.005$). The sagittal and coronal balance evaluated respectively with the SVA and the C7PL from the CSVL did not show statistically significant changes between pre- and post-operative values. Pre-operatively, the mean AVAR angle measured on MRI was 25.5°±2.7°. The mean AVAR angle measured on CT post-operatively was 10.3°±1.75°, with a correction rate of 59.3% ($p<0.005$). The mean evaluation SRS-22 questionnaire was 2.4±0.5 before surgery and 3.8±0.5 after surgery.

No major intraoperative complications occurred. Post-operative complications were one superficial wound infection and one deep wound infection. Both cases were surgically treated with debridement and then with a specific antibiotic therapy. There was no loss of correction or screws pullout comparing post-operative and last follow-up X-rays.

DISCUSSION

The aim of this study is to present a comprehensive description and evaluate the results of DVR and differently shaped dual rods translation technique in adolescent idiopathic scoliosis that combines these methods in order to improve three dimensional correction of the deformity. The rib hump deformity caused by the axial rotational of the vertebrae is an important pattern of AIS that is strictly related to the self-image of the patient. (11) Several techniques, such as thoracoplasty, translation and DVR, have been proposed in order to obtain a better correction on the axial plane. Some authors believe that thoracoplasty may be associated with increased of blood loss, surgical time, pain and long term pulmonary effects (12, 13).

The DVR is now used worldwide for the surgical treatment of AIS. This technique was introduced first by Lee et al. and provided an axial correction of 42.5% on the axial plane, and a coronal Cobb correction of 80% (3).

Suk et al. defined the important role of DVR in reducing the rib hump, but suggest combining DVR to other techniques, such as thoracoplasty, in order to get a better rib hump correction (14). In literature, the derotational correction obtained with only DVR technique, measured through the apical vertebral rotation compared to the sagittal plane (Rasag), is between 37% and 63 (15-18). However, to correct scoliosis on frontal and sagittal planes, DVR should be combined with other techniques.

The idea of translation for the correction of AIS was first described by Luque. He performed this technique using sublaminar wires cerclages. However, the application of sublaminar wire cerclages was associated with neurological risks; in addition, introducing more efficient instruments to correct the AIS such as sublaminar hooks and consequently pedicle screws with different techniques, limited the use of translation for a few decades. (19, 20, 21). Recently Clement et al. reproduced translation technique by using pedicle screws without differently shaped rods. They reported good results on frontal and sagittal planes compared to the cantilever reduction in hypo-kyphotic AIS patients without any correction on axial plane (22, 23). Like the aforementioned study, among the hypo-kyphotic AIS we observed good kyphosis restoration using this combined technique which can play an important role to provide sagittal balance. The purpose of the combination of the translation technique with differently shaped rods and DVR is to obtain a good three-dimensional correction of the deformity while reducing the risk of screw pullout at the time of DVR. Wang et al. using computerized patient-specific biomechanical models, demonstrate that using two differently shaped rods improves axial deformity correction, but consequently it can increase the screws pullout forces. Due to the latter, they suggest using this procedure in combination with the DVR (5). According to our results, this technique can provide good correction on all planes which is comparable with the study performed previously by Seki et al

(24). They performed a rod rotation and differential rod contouring correction, followed by DVR in AIS Lenke Type I, II and V. A cone-beam CT scanner with C-arm was used intra-operatively to evaluate axial correction after rod rotation (average correction: 6.2°) and after DVR (average correction: 4.2°). The apical vertebral body rotation reduction was 60%, in line with our results, but the mean Cobb angle before surgery (52°) was inferior to our group of patients (24). In our experience, the use of reduction jacks, anchored on screws heads, helps to distribute the corrective forces along the curve, reducing the pullout risk, and increasing the axial forces that determine correction. In addition, long reduction jacks provide stronger lever arms at the time of DVR and bigger reduction space to host the over shaped rod.

Pre-operative MRI in addition to exclude the possible neurological problems can provide an axial view of the spine in order to evaluate the apical vertebrae axial rotation (AVAR) before surgery without radiation exposure in patients which are particularly in growing age. Post-operatively computer tomography (CT) scans was performed to control the accurate position of the pedicle screws and measure AVAR (7, 8, 25).

In conclusion, according to our results the combination of DVR and differently shaped dual rods translation technique in adolescent idiopathic scoliosis can provide good three-dimensional correction and improve the patient quality of life and self imaging. However, for better understanding, the efficacy of this method should be compared separately with two different groups of patient who are treated by DVR and differently shaped rods alone.

REFERENCES

1. Hasler CC. A brief overview of 100 years of history of surgical treatment for adolescent idiopathic scoliosis. J Child Orthop 2013; 7:57-62.
2. Kim YJ, Lenke LG, Kim J, et al. Comparative Analysis of Pedicle Screw Versus Hybrid Instrumentation in Posterior Spinal Fusion of Adolescent Idiopathic Scoliosis. Spine 2006; 31:291-8.
3. Lee S-M, Suk S-I, Chung E-R. Direct vertebral rotation: a new technique of three-dimensional deformity correction with segmental pedicle screw fixation in adolescent idiopathic scoliosis. Spine 2004; 29:343-9.
4. Faldini C, Perna F, Chehrassan M, et al. Simultaneous double rod and en-bloc direct vertebral rotation technique for correction of main thoracic adolescent idiopathic scoliosis: retrospective analysis of 14 cases. J Biol Regul Homeost Agents 2016; 30:181-6.
5. Wang X, Boyer L, Le Naveaux F, et al. How does differential rod contouring contribute to 3-dimensional correction and affect the bone-screw forces in adolescent idiopathic scoliosis instrumentation? Clin Biomech Bristol Avon 2016; 39:115-21.
6. Lenke LG, Betz RR, Harms J, et al. Adolescent idiopathic scoliosis: a new classification to determine extent of spinal arthrodesis. J Bone Joint Surg Am 2001; 83-A:1169-81.
7. Lam GC, Hill DL, Le LH, et al. Vertebral rotation measurement: a summary and comparison of common radiographic and CT methods. Scoliosis 2008; 3:16.
8. Birchall D, Hughes DG, Hindle J, et al. Measurement of vertebral rotation in adolescent idiopathic scoliosis using three-dimensional magnetic resonance imaging. Spine 1997; 22:2403-07.
9. Monticone M, Baiardi P, Calabrò D, et al. Development of the Italian version of the revised Scoliosis Research Society-22 Patient Questionnaire, SRS-22r-I: cross-cultural adaptation, factor analysis, reliability, and validity. Spine 2010; 35:E1412-7.
10. Perna F, Borghi R, Pilla F, et al. Pedicle screw insertion techniques: an update and review of the literature. Musculoskelet Surg 2016; 100:165-9.
11. Carrasco MIB, Ruiz MCS. (Perceived self-image in adolescent idiopathic scoliosis: an integrative review of the literature). Rev Esc Enferm U P 2014; 48:748-58.
12. Lenke LG, Bridwell KH, Blanke K, Baldus C Analysis of pulmonary function and chest cage dimension changes after thoracoplasty in idiopathic scoliosis. Spine 1995; 20:1343-50.
13. Gitelman Y, Lenke LG, Bridwell KH, et al. Pulmonary function in adolescent idiopathic scoliosis relative to the surgical procedure: a 10-year follow-up analysis. Spine 2011; 36:1665-72.

14. Suk S-I, Kim J-H, Kim S-S, et al. Thoracoplasty in thoracic adolescent idiopathic scoliosis. Spine 2008; 33:1061-7
15. Abul-Kasim K, Karlsson MK, Ohlin A. Increased rod stiffness improves the degree of deformity correction by segmental pedicle screw fixation in adolescent idiopathic scoliosis. Scoliosis 2011; 6:13.
16. Asghar J, Samdani AF, Pahys JM, et al. Computed tomography evaluation of rotation correction in adolescent idiopathic scoliosis: a comparison of an all pedicle screw construct versus a hook-rod system. Spine 2009; 34:804-7.
17. Di Silvestre M, Lolli F, Bakaloudis G, et al. Apical vertebral derotation in the posterior treatment of adolescent idiopathic scoliosis: myth or reality? Eur Spine J Off Publ Eur Spine Soc Eur Spinal Deform Soc Eur Sect Cerv Spine Res Soc 2013; 22:313-23
18. Rushton PRP, Grevitt MP. Do vertebral derotation techniques offer better outcomes compared to traditional methods in the surgical treatment of adolescent idiopathic scoliosis? Eur Spine J 2014; 23:1166-76.
19. Luque ER. Segmental spinal instrumentation for correction of scoliosis. Clin Orthop 1982; 192-8.
20. Songer MN, Spencer DL, Meyer PR, Jayaraman G. The use of sublaminar cables to replace Luque wires. Spine 1991; 16:S418-421.
21. Muschik M, Schlenzka D, Robinson PN, Kupferschmidt C. Dorsal instrumentation for idiopathic adolescent thoracic scoliosis: rod rotation versus translation. Eur Spine J. 1999; 8(2):93-9.
22. Clement J-L, Chau E, Geoffray A, Suisse G. Restoration of thoracic kyphosis by simultaneous translation on two rods for adolescent idiopathic scoliosis. Eur Spine J 2014l; 23(Suppl) 4:S438-45.
23. Clement J-L, Chau E, Geoffray A, Vallade M-J. Simultaneous translation on two rods to treat adolescent idiopathic scoliosis: radiographic results in coronal, sagittal, and transverse plane of a series of 62 patients with a minimum follow-up of two years. Spine 2012; 37:184-92.
24. Seki S, Kawaguchi Y, Nakano M, et al. Rod rotation and differential rod contouring followed by direct vertebral rotation for treatment of adolescent idiopathic scoliosis: effect on thoracic and thoracolumbar or lumbar curves assessed with intraoperative computed tomography. Spine 2016; 16:365-71.
25. Ozturk C, Karadereler S, Ornek I, et al. The role of routine magnetic resonance imaging in the preoperative evaluation of adolescent idiopathic scoliosis. Int Orthop 2010; 34:543-6.

CORRELATION BETWEEN GAMMA GLUTAMYLTRANSFERASE FRACTIONS AND BONE QUALITY

M.FRANZINI[1], A.NESTI[2], D.PANETTA[3], V. FIERABRACCI[1], S. MARCHETTI[2], P.D. PARCHI[2], L. CAPONI[1], A. PAOLICCHI[1], V. MUSETTI[4], P. SALVADORI[3], M. EDMIN[5,6], A. PUCCI[7], E. BONICOLI[2], M. SCAGLIONE[2] and N. PIOLANTI[2]

[1]Department of Translational Research and New Technologies in Medicine and Surgery, University of Pisa, Italy; [2]Department of Orthopaedics and Traumatology I, University of Pisa; [3]Institute of Clinical Physiology of National Research Council (IFC-CNR) of Pisa; [4]Department of Laboratory Medicine, Fondazione Toscana Gabriele Monasterio, Pisa, Italy; [5]Institute of Life Sciences, Scuola Superiore Sant'Anna, Pisa, Italy; [6]Cardiology Division, Fondazione Toscana Gabriele Monasterio, Pisa, Italy; [7]Histopathology Department, University Hospital, Pisa, Italy

Gamma-glutamyltransferase (GGT) has been recently identified as a bone-resorbing factor. The aim of this study was to investigate the association between plasma GGT fractions levels and bone quality. Plasma GGT fractions were analysed by gel-filtration chromatography. Bone quality was established quantitatively by two micro-CT derived microarchitectural parameters: the BV/TV (mineralised bone volume/total volume), and the SMI (structure model index) that describes the rod-like (low resistant) or plate-like (high-resistant) shape of bone trabeculae. We enrolled 93 patients hospitalised for elective total hip replacement (group Arthrosis, n=46) or for proximal femoral fracture (group Fracture, n=47). Patients within the first quartile of BV/TV (Q_1, osteoporotic patients, n=6) showed higher levels of b-GGT fraction [median (min-max): 3.37 (1.42–6.81)] compared to patients with normal bone density (fourth quartile Q_4, n=10; 1.40 (0.83–4.36); p=0.0393]. Also, according to SMI, b-GGT value was higher in the subgroup with bone fragility [Q_1, n=8: 1.36 (0.43–4.36); Q_4, n=8: 5.10 (1.4 –7.60); p=0.0117]. In conclusion, patients characterised by fragile bone structure showed specifically higher levels of plasma b-GGT activity thus suggesting fractional GGT analysis as a possible biomarker in the diagnosis of osteoporosis.

Gamma-glutamyltransferase (GGT), an enzyme of the cell membrane present at the surface of virtually all human cells, is mainly expressed in tissues with secretory or absorptive function, such as liver - in correspondence of bile canaliculi and bile ducts - and kidney (1). GGT catalyses the transfer of a gamma-glutamyl groups to acceptors such as aminoacids and dipeptides (2), and its main physiological substrates are glutathione (gamma-glutamylcysteinylglycine, GSH) (3), leukotriene C4 (4) and nitrosoglutathione (5). Due to its role in GSH metabolism, GGT is viewed primarily as an antioxidant enzyme (3), but it has also a potent pro-oxidant action at the cell surface: in fact, in the presence of copper (Cu^{2+}) or iron (Fe^{3+}) ions, GGT promotes the formation of reactive oxygen species in the extracellular space (6, 7).

GGT is found in human blood, and its values are a well-known biomarker of liver disease and alcohol abuse (2); during the last decades, GGT

Keywords: Osteoporosis, gamma-glutamyltransferase, GGT fraction, micro-CT, biomarker

Mailing address:
Piolanti Nicola
Department of Orthopaedics and Traumatology I,
University of Pisa,
Pisa, PI, Italy
Tel.: +393397566410 - Fax: +39050996501
e-mail: nicpio@hotmail.it

0393-974X (2017)

elevation has been increasingly associated with the risk of death for cardiovascular disease, the onset diabetes and the metabolic syndrome (2) and recently with bone resorption (8-10). Serum and urinary GGT levels were found to be inversely correlated with bone mineral density (11-13), and the bone resorption associated to bile duct ligation is reversed by the administration of anti-GGT antibodies (14).

Bone resorption is the unique function of osteoclast cells, which derive from the monocyte/macrophage lineage (15). Osteoclasts differentiation is regulated by osteoblast cells through the expression of RANK-ligand (RANKL) protein, which binds to the osteoclast's receptor RANK, thus promoting their differentiation and ultimately leading to bone resorption (16). Osteoprotegerin (OPG) inhibits RANK activation and the subsequent bone remodelling binding RANKL. *In vivo* studies in mice highlighted the importance of the OPG/RANK/RANKL system; in fact, RANKL gene knockout animals lack osteoclasts, while OPG gene knockout mice present a severe osteoporosis (16).

GGT is thought to interfere with this mechanism as a ligand rather than as an enzyme, since independently of catalytical action it promotes bone remodelling by stimulating osteoblasts activity increasing the expression of RANKL, apparently acting as a cytokine (8-10). This hypothesis is supported by the finding that the GGT molecule presents a CX3C chemokine domain (disulphide bridges between Cys 191 and 195, (17) which is the signature motif for one class of chemokines, the only known member of which is fractalkine (18). A more recent study suggest GGT has also an inhibitory effect on bone formation (14).

Recently, 4 different molecular forms of GGT have been found in blood, i.e. big-GGT (b-GGT, M.W >2000 kDa), medium-GGT (m-GGT, M.W 1000 kDa), small-GGT (s-GGT, M.W 240 kDa), free-GGT (f-GGT, M.W 70 kDa), each one with different physical-chemical properties, biogenesis (19, 20), and pathophysiological correlations (21-25) and despite all show similar catalytic properties, it is likely that the profound structural differences among them influence their ligand properties and thus the epidemiological association with bone resorption.

This study was aimed to establish if the serum levels of each GGT fraction show a different association with cancellous bone structure and density.

MATERIALS AND METHODS

Patient selection

From February 2014 to August 2015, we selected two groups of patients, aged between 60 and 85 years, who were admitted to our Orthopaedic Unit. The group "Arthrosis" included patients suffering from primary osteoarthritis of the undergoing hip replacement; the group "Fracture" included patients experiencing a proximal femoral fragility fracture undergoing total or partial hip replacement or reduction and synthesis of the fracture. The exclusion criteria for the Arthrosis group were the positive anamnesis for liver diseases, alcohol abuse, osteoporosis (treated or not) or therapy with drugs that may have modified the quality of osseous tissue (for example chronic corticosteroid therapy). In the Fracture group, the unique exclusion criteria was the positive anamnesis for liver diseases or alcohol abuse. Before enrolment, each patient signed an informed consent form. In addition, a data collection form was filled-in for each patient.

Surgery

Patients suffering from primary localized arthritis of the hip (Arthrosis Group) underwent a total hip replacement. During surgery, femoral head and neck were removed and preserved. The femoral head, fixed in formalin and subsequently embedded in paraffin, was sent to our laboratory of anatomic pathology where it was subjected to morphological analysis (on sections stained with haematoxylin and eosin). The femoral neck specimen, fixed in formalin, was analysed with Micro-CT in the laboratories of Institute of Clinical Physiology of National Research Council (IFC-CNR) of Pisa. In patients with a fragility femoral fracture (Fracture Group), a hip replacement was performed in case of a medial fracture and femoral head and neck were sent to laboratories. Lateral fractures of the femoral neck were reduced and fixed by means of endomedullary nail, without any collection of bone tissue.

Micro-CT scanning and image analysis

Bone samples obtained from femoral neck were formalin fixed (4% v/v) immediately after excision. Samples were analysed by high-resolution micro-computed tomography (micro-CT) scanning system (XALT) as already described (26). All scans were performed with the following settings: 50 kV, 0.6 mA, 2 mm Al filtration 920 projections over 360°, with a total scan time of 46 min per sample. Volumetric images for each scan have been reconstructed using cone-beam filtered backprojection (FBP) algorithm with an isotropic voxel size of 49 micron. For quantitative analysis of the trabecular component, subvolumes of 8x8x4 mm^3 have been cropped from the central part of the sample image, thus avoiding cortical bone. The cropped volumes have then been sent to the BoneJ plugin of the ImageJ software (27-28).

Quantitative analysis of trabecular microarchitecture was based on 2 parameters: the BV/TV (Bone Volume/Total Volume) representing the volume of mineralised bone per unit volume of the sample, and the structure model index (SMI) that describes the shape of bone trabeculae (rod-like or plate-like) (29). Along with the total SMI, both the convex component (SMI+) and the concave component (SMI-) of the SMI have been calculated. The results obtained were employed to stratify the patients on the basis of the calculation of quartiles distribution of BV/TV or SMI.

Fractional GGT analysis

During the preoperative phase, a blood sample of 3 ml was collected from each patient in a test tube containing EDTA (ethylenediamine tetraacetic acid). Analysis of fractional GGT activity was performed on the obtained plasma as previously described (19). Samples (0.02 ml) were processed by size exclusion chromatography (column: Superose 6 HR 10/300 GL, GE Healthcare). Fractional enzymatic activity was quantified by post-column injection of the fluorescent substrate gamma-glutamyl-7-amido-4-methylcoumarin (gGluAMC, 0.030 mmol/). Enzymatic reaction proceeded for 4.5 min in a reaction coil kept at the 37°C in a water bath. The signal produced by the reaction was detected by means of a fluorescence detector operating at excitation/emission wavelength of 380/440 nm; the intensity of the fluorescence signal was expressed in arbitrary fluorescence units.

Under these reactive conditions, the area under curve is proportional to GGT activity. Fractional GGT area was calculated with the aid of a computer program (MATLAB Version 7 MathWorks, Inc.) to resolve overlapping peaks as described (21).

Laboratory analyses and reference values

Standard assay of all blood tests were simultaneously performed according to the standard clinical laboratory procedures by automated analysers (Beckman Synchron CX 9- PRO analyser, Beckman Coulter, Brea, CA, USA) on preoperative blood samples. Reference values were: creatinine 0.5-0.9 mg/dl for women and 0.7-1.2 mg/dl for men; aspartate aminotransferase (AST) 0.45 U/l; alanine aminotransferase (ALT) 0.40 U/l; fibrinogen 200-400 mg/dl. Fractional GGT reference values have been published (21).

Statistical analysis

Data are presented as median (25^{th}-75^{th} percentile). The statistical comparisons between two groups were carried out with the Mann-Whitney's test; an alpha level of $p<0.05$ was considered significant. Statistical analysis was performed with the MedCalc Statistical Software version 14.12.0.

RESULTS

Patients' characteristics

Between February 2014 and August 2015, we enrolled 93 patients, 61 females and 32 males: 46 patients where included in the Arthrosis group and 47 in the Fracture group. When possible, a specimen from femoral head (n=39) was collected for the morphological analysis and confirmed the clinical suspicions, i.e. patients in the Arthrosis group presented a remodelled osseous tissue with an irregular cortical bone and an altered articular cartilage. Whereas patients included in the Fracture group had an evident osteoporotic bone tissue with haemorrhagic areas and associated bone remodelling near the fractured area.

The main characteristics of the two groups are reported in Table I. The Fracture group included older patients than the Arthrosis group, ($p<0.0001$) while no differences were observed in the renal and liver functions parameters, which were within the

normality range in both groups.

Plasma levels of total GGT activity of all patients where within the reference values. As concerns fractional GGT analysis (Table I), we did not observe any differences between the two groups except for f-GGT fraction that was significantly higher in the Arthrosis subgroup.

Micro-CT analysis

Thirty bone samples obtained from femoral neck were further characterize by micro-CT to evaluate the fraction of bone volume (BV/TV) and the structure model index (SMI), allowing the intragroup image-based identification of osteoporotic patients as described below (Fig. 1a, b).

Based on BV/TV, patients in the first quartile (Q_1, n=6) were classified as osteoporotic, while patients in the forth quartile (Q_4, n=10) had a normal bone density. Patients in the second and third quartiles of BV/TV values could not be reliably classified, thus we compared total and fractional GGT activities between the first and fourth quartile. Patients within BV/TV-Q_1 failed to show higher total GGT values [median (min-max), BV/TV-Q_1: 19.67 (13.46-48.60); BV/TV-Q_4: 14.47 (10.45- 41.90); p=0.1289]. Fractional GGT analysis (Fig. 2) showed that b-GGT fraction activity was significantly higher in the BV/TV-Q_1 compared to BV/TV-Q_4 subgroups [Q_1:3.37 (1.42-6.81); Q_4:1.40 (0.83- 4.36); p=0.0393]. No differences were observed in the other GGT fractions.

To measure trabecular bone fragility, we first verified if the bone samples were predominantly convex, as required for reliable usage of the SMI (30). The ratio of SMI-/SMI+ was always small [0.063 (0.016-0.211)], which allowed us to consider the SMI as a good indicator of trabecular morphology and aspect ratio.

According to the SMI, patients within the Q_1 (n=8) mostly presented plate-like trabeculae which are associated with a highly resistant bone structure, while patients in the Q_4 (n=8) were characterized by rod-like trabeculae which are associated with a fragile bone structure. Also, in this case median total GGT value was insignificantly higher in the subgroup with bone fragility [Q_1: 14.17 (10.29 – 41.90); Q_4: 23.92 (13.46-48.60); p=0.0742]. Fractional GGT analysis (Fig. 3), confirmed that b-GGT activity was significantly higher in the SMI-Q_4 subgroup [Q_1:1.36

Table I. *Characteristics of the enrolled patients.*

	Arthrosis group	Fracture group	p value
N	46	47	
Males; Females	20; 26	12; 35	
Age, years	72 (68-77)	81 (76-89)	<0.0001
Creatinine, mg/dl	0.87 (0.78-1.07)	0.87 (0.69-1.12)	0.9168
AST, U/l	17.0 (14.5-20.0)	17.5 (15.0-22.0)	0.5216
ALT, U/l	15.0 (12.0-20.0)	12.0 (9.5-16.0)	0.0281
Fibrinogen, mg/dl	337 (296-387)	367 (289-445)	0.3712
Total GGT, U/l	16.4 (13.0-21.1)	15.56 (11.5-21.5)	0.4491
b-GGT, U/l	1.65 (1.13-3.17)	1.72 (1.15-3.68)	0.8386
m-GGT, U/l	0.35 (0.21-0.47)	0.39 (0.22-0.71)	0.3234
s-GGT, U/l	4.01 (2.62-8.11)	5.07 (2.92-8.79)	0.3585
f-GGT, U/l	9.73 (7.59-12.33)	7.80 (6.17-9.33)	0.0005

*Data are expressed as median (25th-75th percentile). **AST**: aspartate aminotransferase; **ALT**; alanine aminotransferase. Statistical comparison was performed by Mann-Whitney test.*

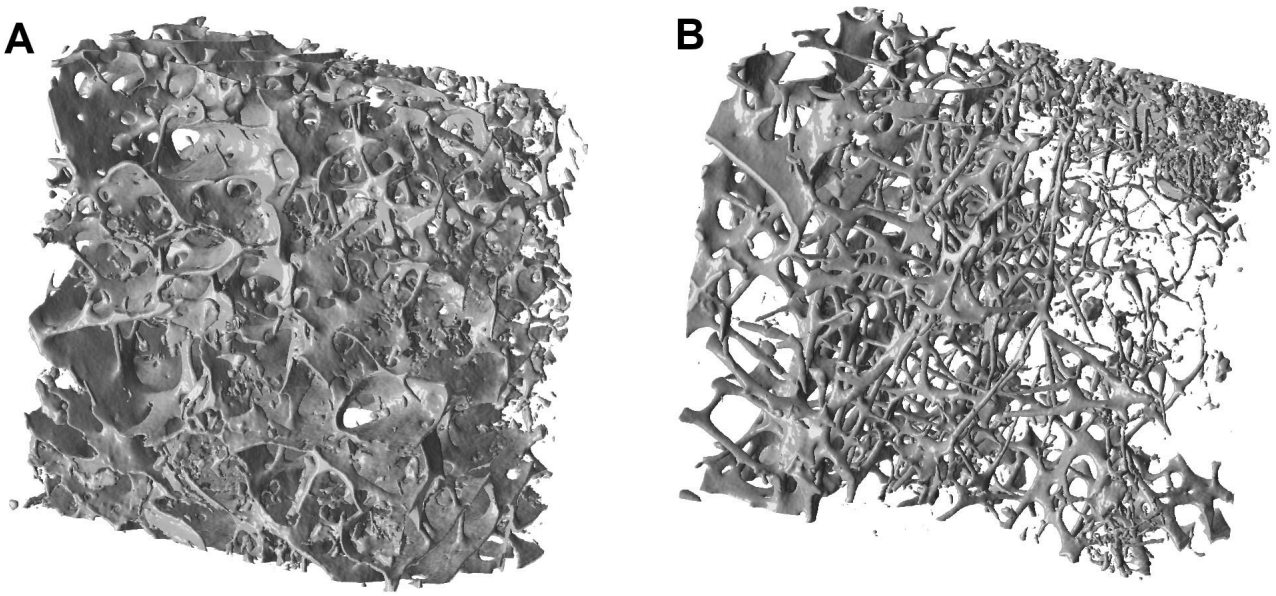

Fig. 1. *Images obtained by micro-CT scan analysis of femoral neck specimens representative of a normal* ***(panel A)*** *or osteoporotic bone* ***(panel B)****.*

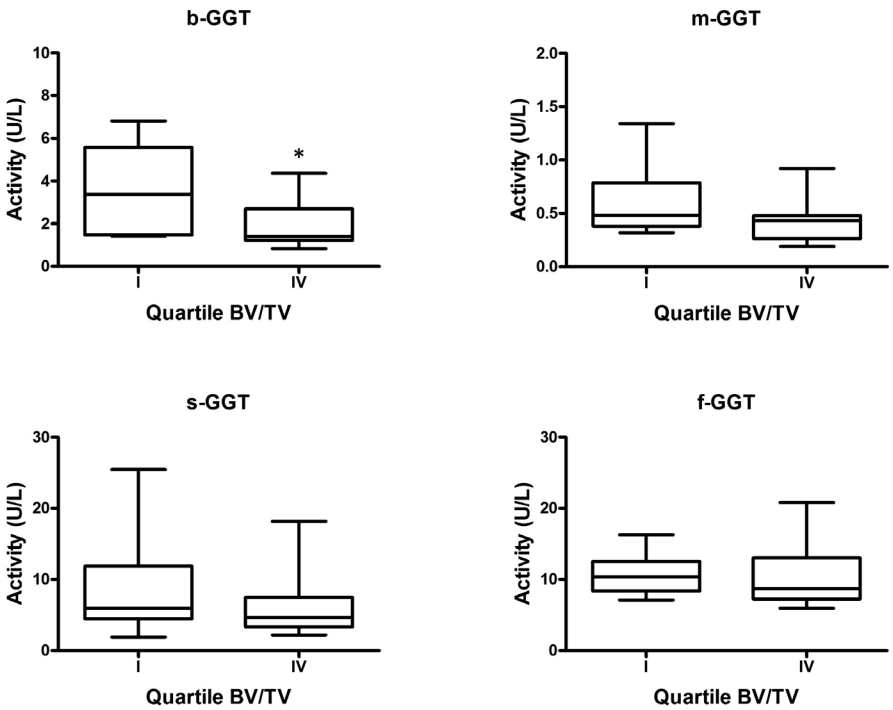

Fig. 2. *Distribution of fractional GGT activity in patients within the first or the fourth quartile of the BV/TV parameter. The box represents the 25th and 75th percentiles and the line the median value. Whiskers correspond to minimum and maximum values. Statistical comparison was performed by Mann-Whitney test.* *******: $p<0.05$.

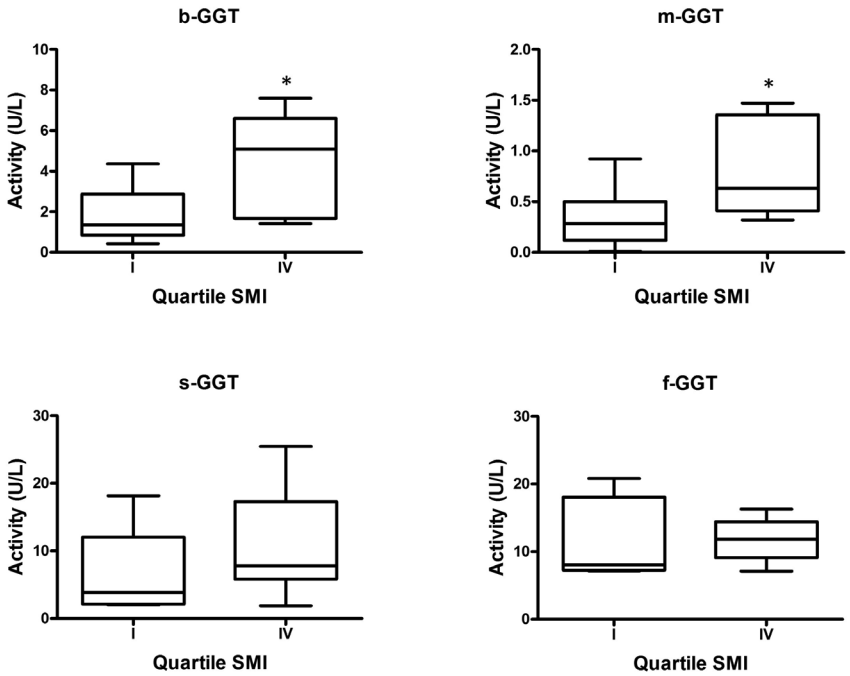

Fig. 3. *Distribution of fractional GGT activity in patients within the first or the fourth quartile of the SMI parameter. The box represents the 25th and 75th percentiles and the line the median value. Whiskers correspond to minimum and maximum values. Statistical comparison was performed by Mann-Whitney test. *: p<0.05.*

(0.43–4.36); Q_4: 5.10 (1.42–7.60); p = 0.0117]. The m-GGT fraction was also significantly different between SMI-Q_1 and Q_4 [Q_1: 0.29 (0.01–0.92); Q_4: 0.63 (0.32–1.47); p=0.0357].

DISCUSSION

In the last years GGT is coming to the attention of researchers as a regulator of bone turnover (11, 31), as both serum (11, 13) and urinary (12) GGT activity were found to be inversely correlated with bone mineral density. In the present study, we investigated the association between bone structure parameters, obtained by micro-CT analysis, and circulating levels of GGT fractions, to establish if a specific fraction(s) is associated with bone resorption. We found that patients characterised by a fragile bone structure showed also selectively higher levels of plasma b-GGT activity in comparison with patients having normal bone parameters at micro-CT.

In the Fracture group, patients were enrolled on the basis of clinical suspicion for the presence of bone fragility, we do not used standard diagnostic methods such as Dual-energy X-ray absorptiometry or bone turnover markers due to patient selection (patients with hip fracture). For the Arthrosis group the diagnosis was made with preoperative X-rays and anamnesis. In both groups, the diagnosis was confirmed by histological analysis.

Comparing these two groups, we did not find significant differences in total or fractional GGT values, except for f-GGT fraction which was slightly higher in the Fracture group. Our data apparently disagree with previous findings (11, 13); this might depend on several reasons, including the low diagnostic sensitivity of the inclusion criteria we used.

To increase the sensitivity and specificity of patient classification we performed micro-CT analysis to quantify the volume of mineralized bone per unit volume of the sample (BV/TV) and

the structure model index (SMI). High values of SMI are associated with the presence of rod-like trabeculae, which have a low mechanical resistance. Thus, low BV/TV (first quartile of the distribution) or high SMI (fourth quartile of the distribution) values identify patients with bone fragility. Despite the recent criticisms to the SMI parameter due to the confounding effect of the concave component (SMI) having non negligible values in certain cancellous bone samples [30], we have found in our sample that the SMI is a very small fraction of the convex component (SMI^+). We believe that this is sufficient to allow us to use the SMI as a reliable metrics of trabecular morphology, which in turn is linked to bone fragility. According to BV/TV or SMI-based reclassification of patients, fractional GGT analysis showed an association between bone fragility and higher levels of plasma b-GGT activity.

The possible mechanisms linking the GGT levels to bone turnover have been investigated in several *in vitro* and *in vivo* studies. The published studies agree that GGT promotes and inhibits the differentiation and activity of osteoclasts and osteoblasts, respectively, resulting in a decreased rate of bone formation. Furthermore, all the studies highlighted a new biological function of GGT, which regulates bone metabolism independently of its enzymatic activity, acting as a cytokine. Crystallographic studies on human GGT protein showed the presence of disulphide bridges exposed on the surface of the heavy subunit following the CX3C scheme (Cys 191-195) (17), which is the structural elements characterising the fractalkine chemokine family (18). It is not known yet if this disulphide bridge is responsible for the cytokine function of GGT but the hypothesis agrees with the findings that only GGT heavy subunit has an osteoclastogenesis activity (32) that can be neutralised by antibodies against the GGT heavy subunit (9,14).

The role of GGT protein in the pathological of bone resorption is supported also by immunohistochemistry studies which revealed GGT expression is up regulated in inflamed tissues where GGT positive osteoclasts, macrophages, lymphocytes, plasma cells were detected (9, 33). Our studies showed that b-GGT fraction, which consists of GGT-positive exosomes (20), can be released from activated neutrophils (30) and pro-inflammatory M1-like macrophages (35). Besides b-GGT is the only fraction detectable in inflamed tissues such as stenotic valves (33) and atherosclerotic plaques (36). Interestingly in both types of lesion, GGT activity was negatively associated with the extent of calcification (33, 36) and in the atherosclerosis model, intra-plaque b-GGT activity was positively correlated with plasma b-GGT levels (36).

Bone turnover is likely to be regulated by locally produced and released GGT protein, anyway a contribution from circulating GGT can not be excluded. In fact *in vivo* studies on animal models showed on one hand that systemic elevation of GGT expression was associated with osteopenia (10,14), on the other hand osteopenia was reduced by systemic treatment with a monoclonal antibody against GGT able to neutralise its cytokine-related effects (9,14).

On the base of our previous studies we proposed that fractional GGT analysis has a higher diagnostic potentiality than total GGT evaluation in that it may distinguish a liver functional derangement associated with inflammatory conditions or hepatocyte damage, the first being detected by b-GGT (22) and the second by s-GGT increase (24, 25). In line with this hypothesis, the present study showed a selective association of bone structure with b-GGT and not with s-GGT, confirming the exclusive association of the latter with liver damage and not with inflammation.

In conclusion, our data highlight an association between plasma b-GGT fraction and bone quality. Further studies will be aimed at evaluating if fractional GGT analysis could become a new diagnostic instrument in order to make faster the diagnostic process for osteoporosis.

ACKNOWLEDGEMENTS

The authors wish to dedicate the present manuscript to the memory of Prof. Lisanti who greatly worked to the scientific design of the present study.

REFERENCES

1. Hanigan MH, Frierson HF. Immunohistochemical

detection of gamma-glutamyl transpeptidase in normal human tissue. J Histochem Cytochem Off J Histochem Soc 1996; 44(10):1101-8.
2. Whitfield JB. Gamma glutamyl transferase. Crit Rev Clin Lab Sci. 2001;38(4):263–355.
3. Meister A. Glutathione metabolism. Methods Enzymol 1995; 251:3-7.
4. Lewis RA, Austen KF, Soberman RJ. Leukotrienes and other products of the 5-lipoxygenase pathway. Biochemistry and relation to pathobiology in human diseases. N Engl J Med 1990; 323(10):645-55.
5. Hogg N, Singh RJ, Konorev E, Joseph J, Kalyanaraman B. S-Nitrosoglutathione as a substrate for gamma-glutamyl transpeptidase. Biochem J 1997; 323(Pt2):477-81.
6. Dominici S, Paolicchi A, Lorenzini E, Maellaro E, Comporti M, Pieri L, Minotti G, Pompella A. Gamma-glutamyltransferase-dependent prooxidant reactions: a factor in multiple processes. BioFactors Oxf Engl 2003; 17(1-4):187-98.
7. Paolicchi A, Minotti G, Tonarelli P, et al. Gamma-glutamyl transpeptidase-dependent iron reduction and LDL oxidation--a potential mechanism in atherosclerosis. J Investig Med 1999; 47(3):151-60.
8. Niida S, Kawahara M, Ishizuka Y, et al. Gamma-glutamyltranspeptidase stimulates receptor activator of nuclear factor-kappaB ligand expression independent of its enzymatic activity and serves as a pathological bone-resorbing factor. J Biol Chem 2004; 279(7):5752-6.
9. Ishizuka Y, Moriwaki S, Kawahara-Hanaoka M, et al. Treatment with anti-gamma-glutamyl transpeptidase antibody attenuates osteolysis in collagen-induced arthritis mice. J Bone Miner Res Off J Am Soc Bone Miner Res 2007; 22(12):1933-42.
10. Hiramatsu K, Asaba Y, Takeshita S, et al. Overexpression of gamma-glutamyltransferase in transgenic mice accelerates bone resorption and causes osteoporosis. Endocrinology 2007; 148(6):2708-15.
11. Choi HS, Kim KJ, Rhee Y, Lim SK. Serum γ-Glutamyl Transferase Is Inversely Associated with Bone Mineral Density Independently of Alcohol Consumption. Endocrinol Metab Seoul Korea 2016; 31(1):64-71.
12. A. saba Y, Hiramatsu K, Matsui Y, et al. Urinary gamma-glutamyltransferase (GGT) as a potential marker of bone resorption. Bone 2006; 39(6):1276-82.
13. Kim B-J, Baek S, Ahn SH, et al. A higher serum gamma-glutamyl transferase level could be associated with an increased risk of incident osteoporotic fractures in Korean men aged 50 years or older. Endocr J 2014; 61(3):257-63.
14. Kawazoe Y, Miyauchi M, Nagasaki A, et al. Osteodystrophy in Cholestatic Liver Diseases Is Attenuated by Anti-γ-Glutamyl Transpeptidase Antibody. PloS One 2015; 10(9):e0139620.
15. Teitelbaum SL. Bone resorption by osteoclasts. Science 2000; 289(5484):1504-8.
16. Boyle WJ, Simonet WS, Lacey DL. Osteoclast differentiation and activation. Nature 2003; 423(6937):337-42.
17. West MB, Chen Y, Wickham S, Heroux A, Cahill K, Hanigan MH, Mooers BHM. Novel insights into eukaryotic γ-glutamyltranspeptidase 1 from the crystal structure of the glutamate-bound human enzyme. J Biol Chem 2013; 288(44):31902-13.
18. Stievano L, Piovan E, Amadori A. C and CX3C chemokines: cell sources and physiopathological implications. Crit Rev Immunol 2004; 24(3):205-28.
19. Franzini M, Bramanti E, Ottaviano V, et al. A high performance gel filtration chromatography method for gamma-glutamyltransferase fraction analysis. Anal Biochem 2008; 374(1):1-6.
20. Fornaciari I, Fierabracci V, Corti A, et al. Gamma-glutamyltransferase fractions in human plasma and bile: characteristic and biogenesis. PloS One 2014; 9(2):e88532.
21. Franzini M, Ottaviano V, Fierabracci V, et al. Fractions of plasma gamma-glutamyltransferase in healthy individuals: reference values. Clin Chim Acta Int J Clin Chem 2008; 395(1-2):188-9.
22. Franzini M, Fornaciari I, Fierabracci V, et al. Accuracy of b-GGT fraction for the diagnosis of non-alcoholic fatty liver disease. Liver Int Off J Int Assoc Study Liver 2012; 32(4):629-34.
23. Franzini M, Fornaciari I, Rong J, Larson MG, Passino C, Emdin M, Paolicchi A, Vasan RS. Correlates and reference limits of plasma gamma-glutamyltransferase fractions from the Framingham Heart Study. Clin Chim Acta 2013; 417:19-25.

24. Franzini M, Fornaciari I, Vico T, et al. High-sensitivity γ-glutamyltransferase fraction pattern in alcohol addicts and abstainers. Drug Alcohol Depend 2013; 127(1-3):239-42.
25. Elawdi HA, Franzini M, Paolicchi A, et al. Circulating gamma-glutamyltransferase fractions in cirrhosis. Liver Int Off J Int Assoc Study Liver 2014; 34(7):e191-199.
26. Panetta D, Belcari N, Del Guerra A, Bartolomei A, Salvadori PA. Analysis of image sharpness reproducibility on a novel engineered micro-CT scanner with variable geometry and embedded recalibration software. Phys Med 2012; 28:166-173.
27. Doube M, Klosowski MM, Arganda-Carreras I, et al. BoneJ: free and extensible bone image analysis in ImageJ. Bone 2010;47(6):1076
28. Rasband WS, Eliceiri KW. NIH Image to ImageJ: 25 years of image analysis. Nat Methods 2012; 9(7):671-5.
29. Hildebrand T, Rüegsegger P. Quantification of bone microarchitecture with the structure model index. Comput. Methods Biomech Biomed Engin 1997; 1:15-23. doi:10.1080/01495739708936692.
30. Salmon PL, Ohlsson C, Shefelbine SJ, Doube M. Structure model index does not measure rods and plates in trabecular bone. Frontiers in Endocrinology 2015; 6:162. doi:10.3389/fendo.2015.00162.
31. Levasseur R, Barrios R, Elefteriou F, Glass DA, Lieberman MW, Karsenty G. Reversible skeletal abnormalities in gamma-glutamyl transpeptidase-deficient mice. Endocrinology 2003; 144(7):2761-4.
32. Kim J, Jang S, Kim A, Su H, Gunawardhana N, Jeon Y-E, Bak EJ, Kim J-H, Cha J-H. Role of bacterial γ-glutamyltranspeptidase as a novel virulence factor in bone-resorbing pathogenesis. J Microbiol Seoul Korea 2016; 54(5):396-402.
33. Cappelli S, Epistolato MC, Vianello A, et al. Aortic valve disease and gamma-glutamyltransferase: accumulation in tissue and relationships with calcific degeneration. Atherosclerosis 2010; 213(2):385-91.
34. Corti A, Franzini M, Cianchetti S, et al. Contribution by polymorphonucleate granulocytes to elevated gamma-glutamyltransferase in cystic fibrosis sputum. PloS One. 2012; 7(4):e34772.
35. Belcastro E, Franzini M, Cianchetti S, Lorenzini E, Masotti S, Fierabracci V, Pucci A, Pompella A, Corti A. Monocytes/macrophages activation contributes to b-gamma-glutamyltransferase accumulation inside atherosclerotic plaques. J Transl Med 2015; 13:325.
36. Pucci A, Franzini M, Matteucci M, et al. b-Gamma-glutamyltransferase activity in human vulnerable carotid plaques. Atherosclerosis 2014; 237(1):307-13.

USE OF AUTOLOGOUS BONE MARROW CELLS CONCENTRATE ENRICHED WITH PLATELET-FIBRIN ON EXTENSOR MECHANISM ALLOGRAFT RECONSTRUCTION FOR EXTENSOR MECHANISM FAILURE FOLLOWING TOTAL KNEE ARTHROPLASTY

S. GIANNOTTI[1], P.D. PARCHI[2], G.B. COLASANTI[1], G. AGOSTINI[2], F. MORESCHINI[1], C. CATALDI[1], P. FERRATA[1] and R. CAPANNA[2]

[1]U.O.C. Ortopedia e Traumatologia Università degli Studi di Siena; [2]U.O. Ortopedia e Traumatologia Università degli Studi di Pisa

Allografts techniques remain the best reconstructive strategy for chronic extensor mechanism lesions after total knee arthroplasty (3) but outcomes depend strictly on the host tissue-allograft junctions healing. The purpose of this study is to evaluate if modern techniques of adding autologous bone marrow cells concentrate enriched with platelet-rich fibrin, provide better healing of the allograft. We present the case of an 86 years old patient affected by patellar tendon rupture after TKA. A whole extensor mechanism allograft was performed adding a bone marrow cells concentrate enriched with platelet-rich fibrin on the host tissue-allograft junctions. Preoperatively and at each follow-up the value of Knee Society Score and radiographic consolidation signs were recorded. Radiographic controls showed clear signs of consolidation already at 1 months follow-up and a solid fusion at 3 months. This case report describes a valid method to improve healing using a tissue-construct engineered with stem cells and growth factors.

Extensor mechanism disruption is a devastating complication of total knee arthroplasty (TKA), with a incidence of 0.1-2.5% (1). Disruption of the extensor mechanism may result in patellar fractures and ruptures of quadriceps or patellar tendons. Moreover, disruption of the extensor mechanism results in extension lag, limited range of motion (ROM), weakness, difficulties in walking and pain (2). The aetiology of this lesion can be both traumatic or atraumatic. Traumatic ruptures may be due to a direct trauma or induced by surgical acts. Atraumatic ruptures may occur in degenerated tendons, often secondary to immunocompromised conditions such as rheumatoid arthritis, lupus erythematosus, diabetes mellitus, infections or inadequate positioning of prosthetic component (3). There are different surgical options such as primary repair, reconstructive techniques using autograft augmentation (semitendinousus tendon), synthetic mesh, gastrocnemius rotational flaps or allografts (4).

Primary repair techniques, employed in traumatic non-arthroplasty cases, have shown unsatisfactory results in chronic lesions after TKA (4). Among these techniques, Achilles tendon allograft and whole extensor mechanism allograft (EMA) allow better restoration of the anatomy. Different cases of allograft failure are mentioned in literature, with an incidence between 10 and 31% (1, 5, 6). Allograft failure can usually occur both at distal end (tibial) of the grafts that at proximal side (quadriceps tendon rupture); therefore critical points of this technique are the host tissue-allograft junctions, where the impaired healing leads to a failure of the allograft and delays active knee flexion. Based on previous

Key words: total knee arthroplasty, patellar tendon, extensor mechanism allograft, platelet rich-fibrin, bone marrow

Mailing address:
Giannotti Stefano MD,
Associate Professor,
Orthopedic Division University of Siena,
Siena, SI, Italy
e-mail: stefano.giannotti@unisi.it

0393-974X (2017)

experiences of C.G. Park (7), G. Vadalà (8) and Johnson (9) we decided to use stem cells added with platelet rich-fibrin (PRF) to improve allograft healing. The purpose of this paper was to evaluate if adding growth factors and stem cells by autologous bone marrow concentrate enriched with PRF could provide better healing of the allograft.

MATERIALS AND METHODS

We present the case of an 86-year-old female affected by patellar tendon rupture after TKA. A whole extensor mechanism allograft was performed with addiction of bone marrow cells concentrate enriched with PRP on the host tissue-allograft junctions. The operative technique included the use of fresh-frozen, non-irradiated full extensor mechanism allograft tensioned tightly in full extension as described by Nazarian and Booth (10).

Before starting the surgical procedure, we obtained 60 ml of bone marrow aspirate from anterior iliac crest using a trocar connected with a syringe and we centrifuged in the operating room. This procedure allowed separation of mononuclear cells from red cells. At the same time, 120 ml of the patient's own blood were drawn and processed to obtain platelet-rich fibrin (11). Using the previous skin incision, we reached the knee joint by a midline incision through the quadriceps and patellar tendon, splitting the host EM into medial and lateral halves and exposing the entire extensor mechanism injured. The osteotomised patella was shelled out and carefully removed (the midline incision was carried into the host quadriceps proximally and distally over the host tibial tubercle). Simultaneously, on the back table we harvested the allograft tibial bone block fashioned with a proximal-reverse dovetail shape in order to ensure a better press-fit.

A groove was later created on the tibia (4 cm long x 2.5 cm wide x 1 cm deep), distal and medial to the patellar tendon insertion, using a high speed saw to provide a rectangular cavity with a corresponding dovetail shape for stable fixation of the tibial bone block. At the same time, the bone marrow cell concentrate was combined with PRF to form a gel-like tissue that we applied between allograft and the tibial cavity (Fig. 1). The construct was stabilized with two metal cerclage wires. The allograft is drawn proximally under the host quadriceps using heavy, non-absorbable suture.

Proximally, the allograft quadriceps tendon was stitched with Krakow-type non-absorbable suture to tighten the allograft on the host tendon in knee full extension (10). We also applied the PRF membranes stitching together the allograft tendon and the host quadriceps (12). The allograft patella was not resurfaced. Postoperatively, the knee was placed in full extension in a brace for 6 weeks with

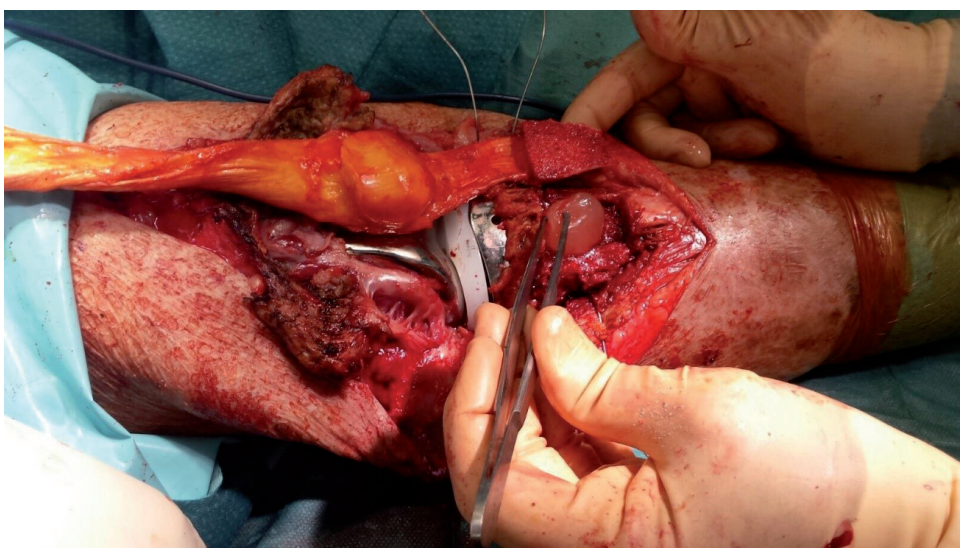

Fig 1. *Bone marrow cell concentrate combined with PRF applied in the tibial cavity.*

a touchdown weight bearing only. Isometric quadriceps exercises were granted, forbidding active flexion-extension of the hip. After 6 weeks, a gradual passive assisted flexion from 30° to 90° was allowed in order to reach, within 6 weeks, a hinged knee brace.

Preoperatively and at each follow-up (1, 3 and 6 months) the value of Knee Society Score (KSS), radiographic consolidation signs, ultrasound tendon integrity and height of the patella were recorded. We considered the height of the patella, obtained by measuring the perpendicular distance of the distal pole of patellar to joint line, as a sign of quadriceps' tendon suture strength. Moreover, we assessed quadriceps tendon integrity with ultrasound study of the junction. The radiographic results were evaluated according to the radiographic scoring system described by Taira et al. (13) that includes periosteal reaction, host-graft union, graft appearance and graft complications like fracture or absorption.

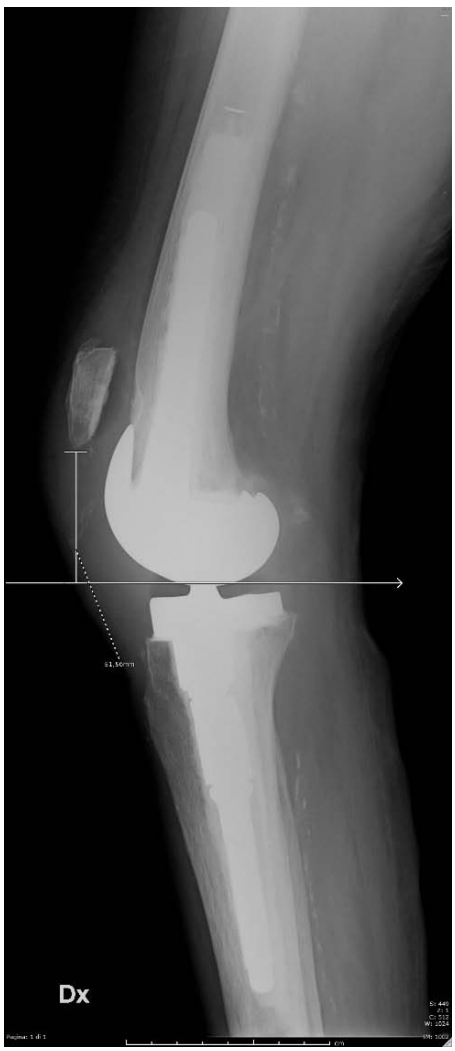

Fig 2. *Extensor mechanism failure. Radiographic height measurement of the patella.*

RESULTS

There were no significant intraoperative complications or adverse effects. We observed a dehiscence of the wound successfully treated with antibiotic therapy, local debridement and a rotating skin flap. Preoperative extensor lag was 20° and the Knee Society Score was of 30 points. The height of the patella was 51.5 mm (Fig 2).

At 1 month, KSS score was not evaluable in all its voices, but the height of patella reduced drastically at 21.1 mm and the radiograph showed already clear signs of consolidation (Fig 3). At 3 months, we registered an increase of the KSS compared to the preoperative value with a score of 48 and a lag extension value of 15°. After 6 months from surgery, the extensor lag decreased from 15° to 0° and the KSS improved from 48 to 75 points. The radiographic check at 1 month already showed clear consolidation signs of the tibial tubercle and a solid fusion at 3-month follow-up. No sign of tearing or laceration were detected through ultrasound evaluation in each follow-up.

DISCUSSION

The healing of junctions points among host and allograft is crucial to start rehabilitation safely and with minimum delay. The homologous bone of the tibial block and the allograft tendon have both bioconductive and bioinductive capacities (14).

Bioconductivity refers to a graft's passive ability to act as a framework on which host growth may occur. Bioinductivity, on the other hand, refers to the ability to actively stimulate host growth. In fact, during its reabsorption after implant, it exposes the collagen matrix containing morphogenetic proteins; these proteins are responsible for the process of bioinduction that allows osteointegration of the tibial block and the healing of the allograft tendon

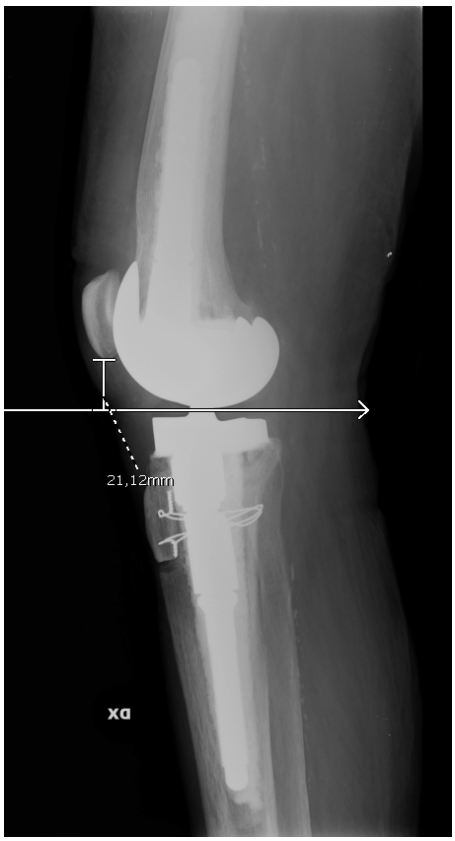

Fig 3. *First month after surgery. Height of patella reduced and radiographic signs of consolidation.*

on the host quadriceps tendon (14, 15). Despite this, processed structural allograft, due to its lack in viable cells, have reduced bioinductive proprieties that can result in junctional non-union, fracturing of the graft, and post-procedural infections (16). Osteoporosis, systemic illnesses, vascular insufficiency and bad tissues quality also have an adverse impact on fusion and healing of the allograft. It is critical to have a rapid healing of the host tissue-allograft junctions for the success of this kind of surgery. For this reason, in order to improve the healing we added the biologic stimulus of growth factors and stem cells inside bone marrow and PRF. We started this work based on the experience of C.G. Park (7) on bone allograft healing in rabbits and G. Vadalà (8) and Johnson (9) in spine surgery where they demonstrate a better healing of the graft when provided with stem cells and growth factors. Bone marrow is composed of a variety of cells, including mesenchymal stem cells that contribute to the regeneration of mesenchymal tissues, capable of self-renewal and differentiation into various cell types such as bone, muscle, tendon and ligament (17). These properties have a positive influence on bone formation, neoangiogenesis and graft inclusion.

In addition, PRF is a source of a variety of growth factor such as platelet-derived growth factor (PDGF), transforming growth factor (TGF-b1 and -b2), vascular endothelial growth factor (VEGF), platelet derived endothelial cell growth factor (PDEGF), interleukin-1 (IL-1), basic fibroblast growth factor (bFGF), platelet activating factor-4 (PAF-4) and insulin like growth factor (15). PRF stimulates bone and tendon graft incorporation giving a biological support to the normal healing process and promoting the osteoblastic differentiation of pluripotential bone marrow stem cells (18). Numerous experiences in literature have shown the effectiveness of the use of bone marrow cells and platelet-rich plasma with bone or tendon allograft to induce healing (7, 8, 9, 19, 20, 21). This study has limitations such as its retrospective nature, the size of our sample and the lack of a control group. However, relying on results of previous experiences (7, 8, 9), it is plausible to conclude that the favourable process of allograft healing observed in our patient was enhanced by the presence of the concentrated marrow cells addicted with PRF. In this case report, we describe the positive outcome of this technique that in the future could also be applied in other surgical contexts.

REFERENCES

1. Lim CT, Amanatullah DF, Huddleston JI 3rd, Harris AHS, Hwang KL, Maloney WJ, Goodman SB. Reconstruction of disrupted extensor mechanism following total knee arthroplasty. J Arthroplasty 2017;32(10):3134-40.
2. Lamberti A, Balato G, Summa PP, Rajgopal A, Vasdev A, Baldini A. Surgical options for chronic patellar tendon rupture in total knee arthroplasty. European Society of Sports Traumatology, Knee Surg Sports Traumatol Arthrosc. 2016. [Epub ahead of print].
3. Cottino U, Deledda D, Rosso F, Blonna D, Bonasia DE, Rossi R. Chronic knee extensor mechanism

lesions in total knee arthroplasty: a literature review. Joints 2016; 4(3):159-64.
4. Bonnin M, Lustig S, Huten D. Extensor tendon ruptures after total knee arthroplasty. Orthop Traumatol Surg Res 2016; 102(1S):S21-31.
5. Ricciardi BF, Oi K, BS, Trivellas M, Lee YY, Della Valle AG, Westrich GH. Survivorship and prognostic factors for extensor mechanism allograft reconstruction after total knee replacement. J Arthroplast 2017; 32:(1)183-8.
6. Emerson RH Jr, Head WC, Malinin TI. Reconstruction of patellar tendon rupture after total knee arthroplasty with an extensor mechanism allograft. Clin Orthop Relat Res 1990; 260:154-61.
7. Park CG, Joo MW, Jeong J, Kang YK, Lee DR. Evaluation of the effects of the combination of autologous mesenchymal stem cells and platelet-rich plasma on structural allograft healing. Cell Tissue Bank 2017; 18(2):229-38.
8. Vadalà G, Di Martino A, Tirindelli MC, Denaro L, Denaro V. Use of autologous bone marrow cells concentrate enriched with platelet-rich fibrin on corticocancellous bone allograft for posterolateral multilevel cervical fusion. J Tissue Eng Regen Med 2008; 2(8):515-20.
9. R.G. Johnson, MD. Bone marrow concentrate with allograft equivalent to autograft in lumbar fusion. Spine (Phila Pa 1976) 2014; 39(9):695-700.
10. Nazarian DG, Booth RE Jr. Extensor mechanism allograft in total knee arthroplasty. Clin Orthop Relat Res 1999; (367):123-9.
11. Trombi L, Danti S, Savelli S, Moscato S, D'Alessandro D, Ricci C, Giannotti S, Petrini M. Mesenchymal Stromal Cell Culture and Delivery in Autologous Conditions: A Smart Approach for Orthopedic Applications. J Vis Exp 2016; (118):54845.
12. Giannotti S, Dell'Osso G, Bottai V, Ghilardi M, Bugelli G, Lazzerini I, Guido G. Treatment of Tendon Injuries of the Lower Limb with Growth Factors Associated with Autologous Fibrin Scaffold or Collagenous Scaffold. Surgic Techno Inter 2015; 26:324-8.
13. Hirofumi Taira, Jose Moreno, Purificacion Ripalda, Francisco Forriol. Radiological and histological analysis of cortical allograft: an experimental study in sheep femora. Arch Orthop Trauma Surg 2004; 124(5):320-5.
14. R. Capanna, P. De Biase, A. Piccioli. Clinical applications of scaffolds engineered with stem cells and growth factors. G.I.O.T. 2010; 36:78-182.
15. Eagan MJ, McAllister DR. Biology of allograft incorporation. Clin Sports Med 2009; 28(2):203-14.
16. Mankin HJ, Gebhardt MC, Jennings LC, Springfield DS, Tomford WW. Long-term results of allograft replacement in the management of bone tumors. Clin Orthop Relat Res 1996; (324):86-97.
17. Pereira RF, Halford KW, O'Hara MD, Leeper DB, Sokolov BP, Pollard MD, Bagasra O, Prockop DJ. Cultured adherent cells from marrow can serve as long-lasting precursor cell for bone, cartilage, and lung in irradiated mice. Proc Natl Acad Sci U S A 1995; 92(11):4857-61.
18. Giannotti S, Bottai V, Ghilardi M, Dell'osso G, Fazzi R, Trombi L, Petrini M, Guido G. Treatment of pseudoarthrosis of the upper limb using expanded mesenchymal stem cells: a pilot study. Eur Rev Med Pharmacol Sci 2013; 17(2):224-7.
19. Dell'Osso G, Bugelli G, Celli F, Petrini M, Trombi L, Guido G, Giannotti S. Grafting of Expanded Mesenchymal Stem Cells without Associated Procedure in a Healed Case of Ulna Pseudarthrosis: A Case Report. Surg Technol Int 2016; 28:289-92.
20. Giannotti S, Trombi L, Bottai V, Ghilardi M, D'Alessandro D, Danti S, Dell'Osso G, Guido G, Petrini M. Use of autologous human mesenchymal stromal cell/fibrin clot constructs in upper limb non-unions: long-term assessment. PLoS One 2013; 8(8):e73893.
21. Pacini S, Carnicelli V, Trombi L, Montali M, Fazzi R, Lazzarini E, Giannotti S, Petrini M. Constitutive expression of pluripotency-associated genes in mesodermal progenitor cells (MPCs). PLoS One 2010; 5(3):e9861.

ONE-STEP CARTILAGE REPAIR WITH MINCED CHONDRAL FRAGMENT ONTO A COMPOSITE SCAFFOLD: AN *IN VITRO* HUMAN STUDY AT LOW OXYGEN TENSION

A.G. MARMOTTI[1], G.M. PERETTI[2,3], S. MATTIA[1], L. MANGIAVINI[3], D.E. BONASIA[1], F. DETTONI[1], E. BELLATO[1] S. SCHWIENBACHER[4] and F. CASTOLDI[1]

[1]Department of Orthopaedics and Traumatology, University of Turin, Turin, Italy; [2]Department of Biomedical Sciences for Health, University of Milan, Milan, Italy; [3]IRCCS Istituto Ortopedico Galeazzi, Milan, Italy; [4]Department of Orthopaedics Surgery and Traumatology, Inselspital, University of Bern, Bern, Switzerland

Minced cartilage fragments are a viable cell source for one stage cartilage repair. However, the joint surface is a low oxygen tension microenvironment and little evidence is present in literature regarding the behaviour of cartilage fragments in this peculiar condition. The aim of the study is i) to verify if low oxygen tension could negatively influence chondrocyte outgrowth from cartilage fragments into a Hyaluronic-Acid(HA)/fibrin scaffold and ii) to evaluate its effects on the behaviour of migrating chondrocyte, compared to normoxic condition. A slight decrease in chondrocyte migration and proliferation was observed in low oxygen tension cultures. Conversely, an increase in the expression of SOX9, β-catenin, HIFs, collagen-I and II ($p<0.05$) in migrating chondrocytes from low oxygen tension cultures was present. Thus, a long term- exposure at low oxygen tension seems to improve the chondrocytic phenotype expression of cell outgrowing from cartilage fragments onto a HA/fibrin scaffold.

Cartilage defects are a common and often incidental finding during knee and ankle reconstructive surgery (1, 2). The present surgical techniques, such as bone marrow stimulation (i.e., microfractures), osteochondral autograft or allograft transplantation and autologous chondrocyte implantation (ACI) have some well-known limitations (2, 3). One-step off-the-shelf techniques by tissue engineering are therefore suggested as promising alternatives to the previously mentioned procedures, to allow for ameliorating the efficiency and the efficacy of the cartilage repair process.

The use of chondral fragments is becoming an appealing alternative for one-step cartilage repair, due to the ease of performing the procedure and the low cost related to this technique. Autologous cartilage fragments may be harvested from non-weight bearing area of the knee joint at no cost, as initially shown by one of the first pioneer study of this technique (3). Furthermore, in the presence of a detached *in situ* large chondral fragments, the healthy cartilage of the fragment has been proposed as a source of chondral chips to cover the original cartilage lesion, as recently suggested by Salzmann et al. (4) and Guillen Garcia et al. (5).

Fragments are minced in small pieces of less than 1 mm^3 (6) to obtain the largest contact area with the surrounding environment to allow for improving chondrocyte "escape" and outgrowth. A recent *in vitro* study by Bonasia et al. has defined the dimension of less than 1 mm^3 as the best size for the procedure, approximately corresponding to a "cartilage paste". A recent descriptive clinical paper by Salzmann et al. (7) has also confirmed this observation. In preclinical studies, encouraging result have been obtained with the use of minced

Key words: one-step cartilage repair, minced cartilage fragments, low oxygen tension, composite scaffold

Mailing address:
GAntonio Marmotti,
Department of Orthopaedics and Traumatology
University of Turin, Turin, Italy
Via Paolini 20, 10138 Turin, Italy
e-mail: antonio.marmotti@inwind.it

0393-974X (2017)

cartilage combined with a hyaluronic acid derivative felt named HYAFF-11, as recently shown in a rabbit and in a goat models (1, 8, 9).

Compared to autologous chondrocyte implantation (ACI) and membrane-ACI (MACI), this technique has the advantage of requiring a single-step surgery. Furthermore, similar scaffolds and membrane may be used to seal the defect, but the lack of a first surgery to obtain the cartilage harvest and the lack of a prolonged culture of the autologous chondrocytes may considerably reduce the final costs of the procedure, making it attractive for widespread use (10). Thus, the evidence from literature allows for conceiving the use of minced cartilage fragments as a promising off-the-shelf, culture-free, one-step therapy for cartilage lesions. Indeed, it does not need any major cell manipulation or specific devices, it may be a viable solution for any hospital setting, provided there is availability of simple tools such as fibrin glue and a commercial scaffold and it is theoretically cost effective and simpler than the two stages approaches as ACI and MACI.

However, when implanting the chondral fragments at the cartilage defect site, the procedure implies that this source of cells is placed in a low oxygen tension environment. The joint microenvironment and the cartilage surface are physiologically held at a low oxygen pressure. While at the upper layer facing the synovial fluid and the joint space, where the repair process takes place, oxygen tension is approximately 10%, this value drops to close to 1% at the lowest level of cartilage, close to subchondral bone (11). Thus, the aim of our study is to assess the effects of a low oxygen tension environment on the behavior of chondrocytes migrating from human minced cartilage fragments and outgrowing onto a HYAFF-11-fibrin glue composite scaffold.

MATERIALS AND METHODS

Approval was obtained from the Ethical Committee of Mauriziano Hospital for the use of human tissue. Informed consent was obtained from each human donor.

Construct cultures

Constructs were prepared with human cartilage fragments. Human cartilage explants were harvested from the intercondylar notch of 20 young donors undergoing anterior cruciate ligament reconstruction. Initially, fragments were rinsed, transferred to a Petri dish and minced into small cuboidal fragments (less than 1 mm^3) in sterile conditions with a sharp scalpel (Fig. 1). Cartilage fragments were loaded onto scaffolds made by non-woven esterified HA derivative felt (Hyaff-11, FIDIA Advanced Biopolymers, Italy).

Scaffolds were then cut to pieces of 0.5 cm^2. 10-15 mg of cartilage fragments were evenly seeded onto the membrane and retained with a coating of approximately 200 µl fibrinogen and thrombin. A commercial fibrin glue (Tisseel, Baxter, AG, Vienna, Austria) was used as a source of fibrinogen and thrombin (Fig. 1) thrombin that was previously diluted 1:4 with calcium chloride. Constructs

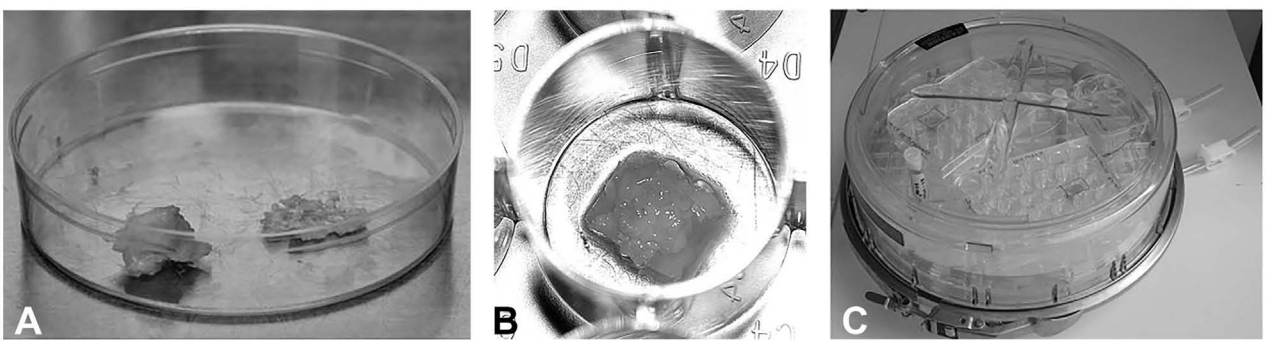

Fig. 1. *Constructs were prepared with minced cartilage fragments (A) loaded onto a non-woven esterified Hyaluronic-Acid-derivative felt (Hyaff-11) and retained with a coating of fibrin glue (B). Constructs were cultured either in normoxic or low oxygen tension (10% O_2) conditions. The hypoxia incubator chamber is shown in (C).*

were cultured at 37°C in a humidified atmosphere containing 5% CO_2 and 21% or 10% O_2 (respectively "normoxic" and "low oxygen tension" conditions). The growth medium contained DMEM high glucose (4500 mg/l) with 10% fetal bovine serum, HEPES (10 mM), non-essential amino acids (0,1 mM), L-proline (20 ng/ml), ascorbic acid (50 μg/ml), penicillin/streptomycin (100 u/ml each). After 5 weeks of culture, constructs were fixed in formalin, included in paraffin and sectioned with a microtome.

Achievement of the low oxygen level culture condition

To stimulate a low oxygen environment, we used a hypoxia incubator chamber (Stemcell Technologies). We connected the chamber to a gas cylinder containing O_2 3% set at 20 l\min flow. Through this system, inside the chamber environment 4 minutes of O_2 oxygen flow would reach 3% of O_2 concentration while, following the gas expansion curve, in the intermediate phase (considered as a linear phase),10% O_2 concentration is reached approximately after a 2:30 minutes exposure (Fig. 1). This time lapse of 2:30 minutes was used to obtain a low oxygen tension condition for construct cultures.

Cell counting technique

Cell counting was performed to quantify migration and outgrowth of chondrocytes from cartilage fragments onto the scaffold. After 5 weeks of culture, sections of cartilage constructs were stained for haematoxylin/eosin (H/E) and examined under light microscopy. Three different areas in 2 different sections per construct were examined by 2 independent observers using light microscopy. The areas where examined at 20x magnification. The number of migrating cells for each single area was defined by the arithmetical mean of the cell counts from both observers. Mean numbers of migrating cells from every area were statistically compared and graphed with GraphPad Prism®.

Scaffold immunofluorescence technique

Expression of SOX-9 (Merck Millipore, Milano, Italy), collagen type II (Merck Millipore, Milano, Italy), collagen type I (Merck Millipore, Milano, Italy), β-catenin (Merck Millipore, Milano, Italy), PCNA (Santa Cruz Biotechnology, Dallas, TX, USA), HIF-1α and HIF-2α (Abcam, Cambridge, MA, USA) was assessed using immunofluorescence techniques, as described in our previous study (12).

Evaluation of fluorescence intensity

We have evaluated the difference of intensity of fluorescence between different cartilage constructs, using ImageJ program, as previously described (12).

Statistical analysis

All data in text and figures are provided as means±standard deviation (SD). Statistical analysis was carried out with the statistical software package GraphPad Prism 5.0.

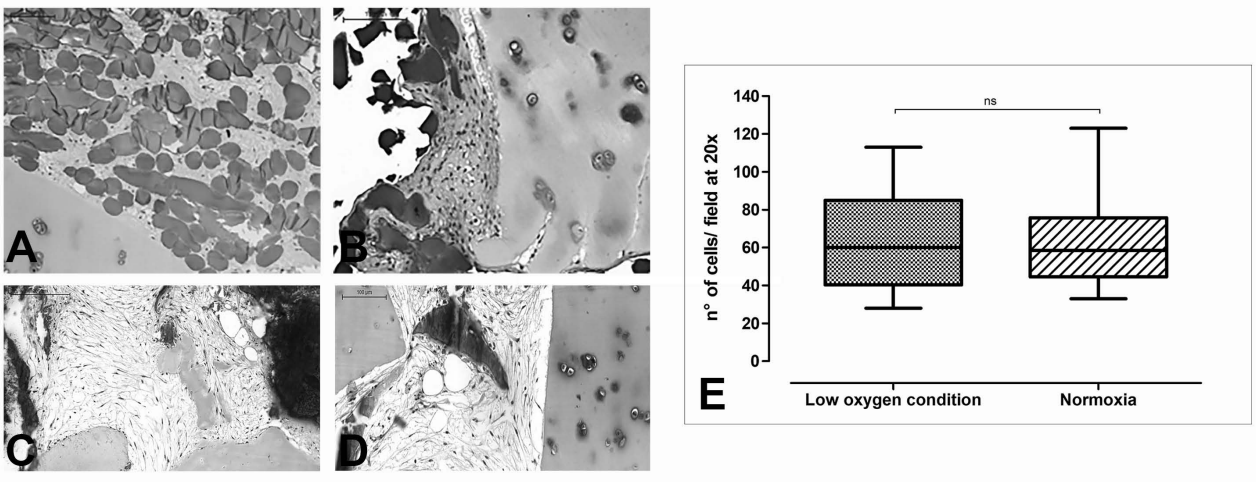

Fig. 2. *Migrating cells predominantly showed a roundish shape when embedded into the scaffold (**A, B**) and a spindle-like shape when close to the fragments (**C, D**). A slight decrease in chondrocyte migration and proliferation was observed in low oxygen tension cultures, albeit not statistically significant (**E**).*

RESULTS

Cell migration from cartilage fragments

H&E staining of the constructs after 5 weeks of *in vitro* culture is shown in Fig. 2. The migration and outgrowth of the chondrocyte into the HYAFF-11 scaffolds was evident both in normoxic and low oxygen conditions. The histological appearance of chondrocytes migrated from the fragments was identifiable in two different subtypes: the cells close to the fragments showed a predominantly spindle-

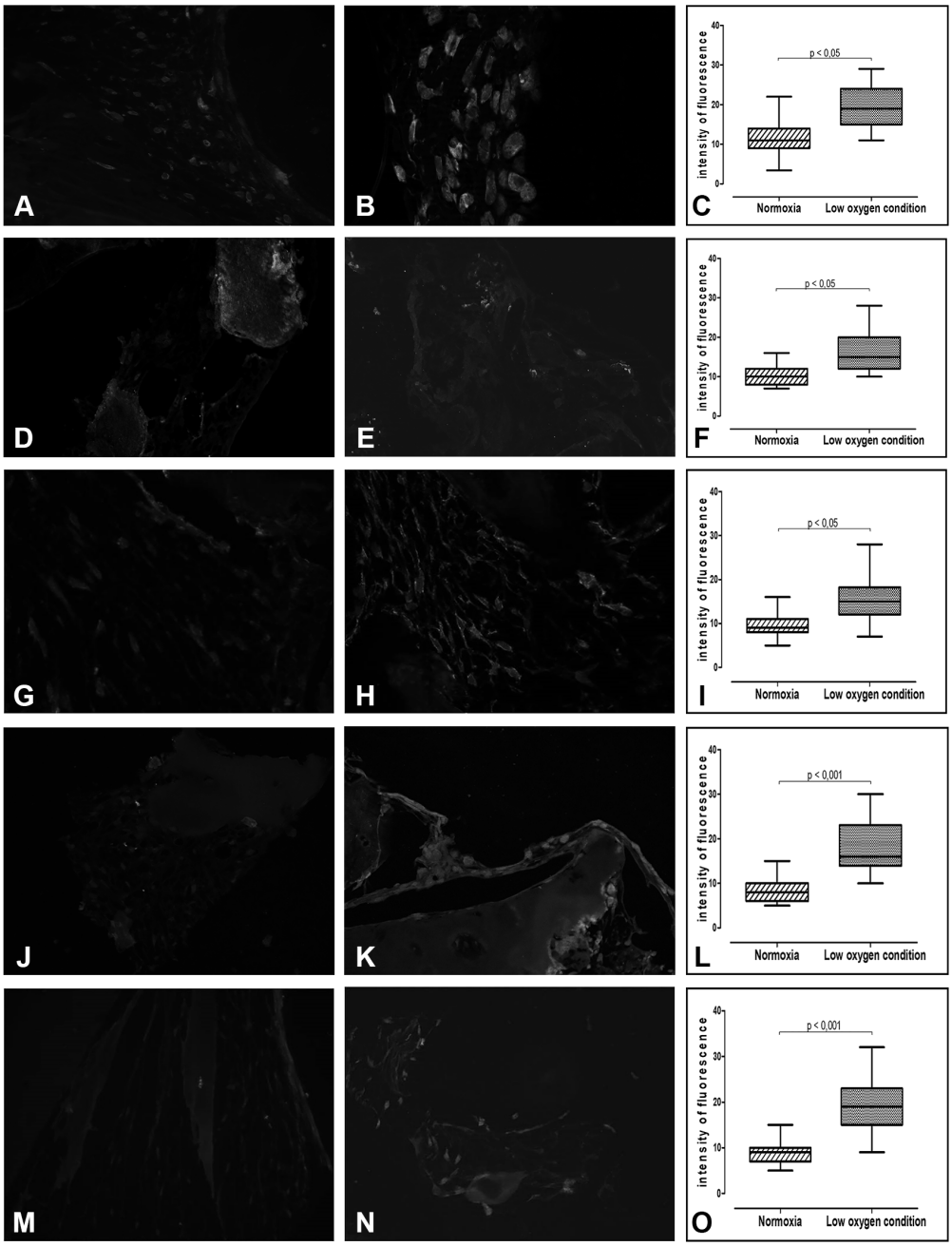

Fig. 3. *Expression of SOX-9 (**A-C**), β-catenin (**D-F**), collagen type II (**G-I**), HIF-1α (**J-L**) and HIF-2α (**M-O**) in migrating chondrocytes from normoxia (**A, D, G, J, M**) and low oxygen tension (**B, E, H, K, N**) cultures is shown. Graphs showing the mean values of fluorescence intensity are displayed in (**C, F, I, L, O**).*

like shape, while those that were embedded into the scaffold showed a more roundish shape. A slight decrease in chondrocyte migration and proliferation was observed in hypoxic cultures after 5 weeks of culture, albeit not significant (Fig. 2).

Immunofluorescence analysis

Immunofluorescence analysis was positive for SOX-9 both in low oxygen and in normoxic conditions. The analysis of the quantification of fluorescence intensity showed a statistically significant difference between low oxygen condition and normoxia (Fig. 3).

The same trend was observed for collagen type II, β-catenin, collagen type I. Indeed, collagen type II was expressed both in low oxygen condition than in normoxia cultures; the fluorescent signal was significantly higher at low oxygen tension. Similarly, immunofluorescence of the constructs was positive for proliferative marker β-catenin both in low oxygen cultures than in normoxia cultures. The difference in intensity of fluorescence was again statistically significant. Collagen type I expression was observed in both culture conditions, with a statistically significant difference.

A greater statistical difference was detected for the hypoxic markers HIF-1α and HIF-2α expressions between the two cultures groups ($p < 0.001$).

DISCUSSION

The ability and the mechanisms by which chondrocytes migrate from cartilage fragments and proliferate into the surrounding environment is not hampered by construct culture at low oxygen tension. Rather, a long-term exposure at low oxygen tension seems to improve the chondrocytic phenotype expression of cell outgrowing from cartilage fragments onto a HA/fibrin scaffold. Moreover, the absence of negative effect of low oxygen tension on chondral fragments may represent a relevant clue for a possible *in vivo* clinical use of cartilage fragments in a HA/fibrin scaffold for one-step cartilage repair.

In our study, the *in vitro* effect of low oxygen on chondrocyte migrating from chondral fragments has been investigated to provide further evidences to the surgical procedure of one step cartilage repair with minced chondral fragments and cartilage paste. In our knowledge, this is the first study providing specific data of the behaviour of human cartilage fragments in a low oxygen tension environment. The low oxygen tension value used in our study was chosen to simulate the oxygen tension conditions found at the surface of a cartilage defect, where the repair site is exposed to the joint microenvironment (11).

The cartilage chips were obtained from a young population corresponding to that usually amenable for cartilage repair surgery. As previously demonstrated in literature, chondral fragments from this subset of patients show a better migration efficiency compared to that of fragments harvested from an older population. Indeed, both Bonasia et al. and Marmotti et al. have observed a greater outgrowth potential of juvenile and young donors' chondral chips than fragments harvested from adult donor both in an *in vitro* (13) and in a preclinical (14) rabbit studies. More recently, an *in vitro* study of Andjelkov et al (15) has also shown the lower repairing potential of adult fragments, thus confirming the age-dependence of chondrocyte migration from chondral fragments. These observations may have a clinical relevance making this one-step technique suitable for a young population.

The scaffold and the fibrin glue used in our study correspond to those of previous experimental settings and they are also commonly available for clinical use. Indeed, previous *in vitro* and preclinical models have shown the favourable effect of the hyaluronic acid derivative felt towards chondrocyte migration from minced cartilage chips (8, 9, 13).

The first result observed in our study was the absence of any significant difference in cell migration between the normoxic and the low oxygen tension cultures. This suggests the lack of any negative effect of low oxygen on the mechanism by which chondrocyte outgrow from the fragments and it gives further evidences of the possible *in vivo* use of this principle of chondral lesion repair. Migrating chondrocytes have a fibroblast-like phenotype near the fragment and a more roundish appearance when included into the scaffold. This may reflect

a different stages of chondrocyte activation. The former seems closer to a motile and proliferative phenotype similar to that of chondrocyte at the early stage of chondrogenesis as well as that of superficial zone (SFZ) chondrocytes. This observation has been proposed in a recent study by Marmotti et al. (13), suggesting a possible phenotypic shift of migrating chondrocytes towards a peculiar proliferative precursor state similar to that of early stage of chondrogenesis (16) and similar to that shown by SFZ chondrocytes, as observed by Yasuhara et al. (17) The expression of β-catenin seems a specific feature of that particular stage of differentiation. On the other hand, chondrocytes included into the scaffold show a more roundish form, closer to the shape of mature chondrocytes.

A significant difference was perceived with the semi-quantitative comparative analysis of fluorescence intensity for chondrocytic, hypoxic and proliferative markers, that are markedly more expressed under low oxygen tension than in normoxic environment. The increased in HIF expression, particularly HIF-2α, may be partially responsible to the observed increase in SOX-9 expression. Several evidences in literature show a direct correlation between HIF-2α and SOX-9 (18), likely through a direct binding of HIF-2α to a specific site in the regulator gene SOX-9 (19-22). A molecular mechanism linking HIF-2α and the over-expression of β-catenin may also be supposed, paralleling a known interaction of these factors observed in different cell populations as described by Choi et al. (23) and Genetos et al. (24). Moreover, a direct link between HIF-1α and collagen production may be suggested by the recent observations on Mouse Epiphyseal Growth Plate Chondrocytes and their hypoxic environment by Aro et al. (25). An anti-catabolic role of HIF-1α has also been described in human chondrocytes in a recent *in vitro* study of Thoms et al. (22), who observed a HIF-1α dependent down-regulation of catabolic enzyme MMP-13 (matrix metalloproteinase 13) and up-regulation of TIMP-3 (tissue inhibitor of metalloproteinases 3). Further studies on our specific chondrocyte population may allow for confirming these molecular mechanisms also for chondrocytes migrating from minced chondral fragments.

However, the over-expression of SOX-9 is certainly a key factor involved in the increased collagen type I and II production observed at low oxygen tension, as observed in our study through semi-quantitative evaluation of immunofluorescence intensity. These data are consistent with the expression of proliferative markers and the increase in β-catenin and PCNA production in our low oxygen tension environment. Indeed, the peculiar phenotype of migrating chondrocyte may allow for the presence of both i) proliferating cells, likely the ones directly outgrowing out of the minced chondral fragment, showing a more distinct pre-chondrogenic precursor state and expressing β–catenin, and ii) non-proliferating cells, embedded in the scaffold at the end of the migration process, showing features more similar to stationary pre-chondrocyte and end-stage chondrocytes, as the production of collagen I and II. All these effects are promoted by the presence of low oxygen tension, suggesting a positive role of the joint microenvironment towards this specific mechanism of cartilage repair by means of minced chondral fragments.

Some drawbacks are present in this study. First, the experiments are performed *in vitro*; thus, the presence of different mediators in the joint microenvironment and their interaction with the outgrowing chondrocytes cannot be reproduced. Nevertheless, preclinical animal trials previously performed by our study group allowed for confirming an overall efficacy of this procedure to obtain a stable repair tissue (8, 9, 14). A second limitation is the short-term culture period (i.e. 5 weeks) implied in the *in vitro* setting of our experiments. This allows for assessing the effects of the low oxygen tension only in a short time lapse but it does not allow for observing the evolution of the neo-formed tissue derived from the outgrowing chondrocytes. Such an assessment in humans may only be achieved by a clinical study that may represent the next logical step of this research.

Furthermore, in future, the interaction between migrating chondrocyte and bone marrow mesenchymal stem cells needs to be investigated. Indeed, the *in vivo* close proximity of these two

cell populations during the repair process has to be considered, as the surgical technique involves a "preparation" of the defect site either by debridement or by drilling (4, 7, 26). Moreover, a synergy of these two subtypes of cells has been recently demonstrated *in vitro* by Abbas M (27) and in a phase one clinical study by de Windt TS et al (28), using an association of allogeneic mesenchymal stem cells and autologous chondrons. Thus, a supplementation of bone marrow concentrate may be hypothesized as a possible adjuvant to facilitate the repair process leaded by minced cartilage fragments in a composite HA-fibrin scaffold.

REFERENCES

1. Bonasia DE, Marmotti A, Rosso F, Collo G, Rossi R.Use of chondral fragments for one stage cartilage repair: A systematic review. World J Orthop 2015; 6(11):1006-11.
2. Looze CA, Capo J, Ryan MK, Begly JP, Chapman C, Swanson D, Singh BC, Strauss EJ. Evaluation and management of osteochondral lesions of the talus. Cartilage 2017; 8(1):19-30.
3. Cole BJ, Farr J, Winalski CS, Hosea T, Richmond J, Mandelbaum B, De Deyne PG. Outcomes after a single-stage procedure for cell-based cartilage repair: a prospective clinical safety trial with 2-year follow-up. Am J Sports Med 2011; 39(6):1170-9.
4. Salzmann GM, Baumann GA, Preiss S. Spontaneous minced cartilage procedure for unexpectedly large femoral condyle surface defect. Case Rep Orthop 2016; 2016:1498135.
5. Guillén-García P, Rodríguez-Iñigo E, Guillén-Vicente I. Viability of pathologic cartilage fragments as a source for autologous chondrocyte cultures. Cartilage 2016; 7(2):149-56.
6. Frisbie DD, Lu Y, Kawcak CE, DiCarlo EF, Binette F, McIlwraith CW. In vivo evaluation of autologous cartilage fragment-loaded scaffolds implanted into equine articular defects and compared with autologous chondrocyte implantation. Am J Sports Med 2009; 37(S1)71S-80S.
7. Salzmann GM, Calek AK, Preiss S. Second-generation autologous minced cartilage repair technique. Arthrosc Tech 2017; 6(1):e127-e131.
8. Marmotti A1, Bruzzone M, Bonasia DE. One-step osteochondral repair with cartilage fragments in a composite scaffold. Knee Surg Sports Traumatol Arthrosc 2012; 20(12):2590-601.
9. Marmotti A, Bruzzone M, Bonasia DE. Autologous cartilage fragments in a composite scaffold for one stage osteochondral repair in a goat model. Eur Cell Mater 2013; 26:15-31; discussion 31-2.
10. Zhang C, Cai YZ, Lin XJ. One-step cartilage repair technique as a next generation of cell therapy for cartilage defects: biological characteristics, preclinical application, surgical techniques, and clinical developments. Arthroscopy 2016; 32(7):1444-50.
11. Pfander D, Gelse K. Hypoxia and osteoarthritis: how chondrocytes survive hypoxic environments. Curr Opin Rheumatol 2007; 19(5):457-62.
12. Marmotti A, Mattia S, Mangiavini L. Tranexamic acid effects on cartilage and synovial tissue: an in vitro study for a possible safe intra-articular use. J Biol Regul Homeost Agents 2016; 30(4S1):33-40.
13. Marmotti A, Bonasia DE, Bruzzone M, et al. Human cartilage fragments in a composite scaffold for single-stage cartilage repair: an in vitro study of the chondrocyte migration and the influence of TGF-beta1 and G-CSF. Knee Surg Sports Traumatol Arthrosc 2013; 21(8):1819-33.
14. Bonasia DE, Martin JA, Marmotti A, Kurriger GL, Lehman AD, Rossi R, Amendola A.The use of autologous adult, allogenic juvenile, and combined juvenile-adult cartilage fragments for the repair of chondral defects. Knee Surg Sports Traumatol Arthrosc, 2016; 24(12):3988-96.
15. Andjelkov N, Hamberg H, Bjellerup P. No outgrowth of chondrocytes from non-digested particulated articular cartilage embedded in commercially available fibrin matrix: an in vitro study. J Orthop Surg Res 2016; 11:23.
16. Ryu JH, Kim SJ, Kim SH, Oh CD, Hwang SG, Chun CH, Oh SH, Seong JK, Huh TL, Chun JS. Regulation of the chondrocyte phenotype by beta-catenin. Development 2002; 129(23):5541-50.
17. Yasuhara R, Ohta Y, Yuasa T, Kondo N, Hoang T, Addya S, Fortina P, Pacifici M, Iwamoto M, Enomoto-Iwamoto M. Roles of beta-catenin signaling in phenotypic expression and proliferation

of articular cartilage superficial zone cells. Lab Invest 2011; 91(12):1739-52.
18. Thoms BL, Murphy CL. Inhibition of hypoxia-inducible factor-targeting prolyl hydroxylase domain-containing protein 2 (PHD2) enhances matrix synthesis by human chondrocytes. J Biol Chem 2010; 285(27):20472-80.
19. Lafont JE, Talma S, Murphy CL. Hypoxia-inducible factor 2alpha is essential for hypoxic induction of the human articular chondrocyte phenotype. Arthritis Rheum 2007; 56(10):3297-306.
20. Mariani E, Pulsatelli L, Facchini A. Signaling pathways in cartilage repair. Int J Mol Sci 2014; 15(5):8667-98.
21. Murphy CL, Thoms BL, Vaghjiani RJ, Lafont JE. Hypoxia. HIF-mediated articular chondrocyte function: prospects for cartilage repair. Arthritis Res Ther 2009; 11(1):213.
22. Thoms BL, Dudek KA, Lafont JE, Murphy CL. Hypoxia promotes the production and inhibits the destruction of human articular cartilage. Arthritis Rheum 2013; 65(5):1302-12.
23. Choi H, Chun YS, Kim TY, Park JW. HIF-2alpha enhances beta-catenin/TCF-driven transcription by interacting with beta-catenin. Cancer Res 2010; 70(24):10101-11.
24. Genetos DC, Toupadakis CA, Raheja LF, Wong A, Papanicolaou SE, Fyhrie DP, Loots GG, Yellowley CE. Hypoxia decreases sclerostin expression and increases Wnt signaling in osteoblasts. J Cell Biochem 2010; 110(2):457-67.
25. Aro EE, Khatri R, Gerard-O'Riley R, Mangiavini L, Myllyharju J, Schipani E. Hypoxia-inducible factor-1 (HIF-1) but not HIF-2 is essential for hypoxic induction of collagen prolyl 4-hydroxylases in primary newborn mouse epiphyseal growth plate chondrocytes. J Biol Chem 2012; 287(44):37134-44.
26. Riboh JC, Cole BJ, Farr J. Particulated articular cartilage for symptomatic chondral defects of the knee. Curr Rev Musculoskelet Med 2015; 8(4):429-35.
27. Abbas M. Combination of bone marrow mesenchymal stem cells and cartilage fragments contribute to enhanced repair of osteochondral defects. Bioinformation 2017; 13(6): p.196-201.
28. de Windt TS, Vonk LA, Slaper-Cortenbach IC, et al. Allogeneic Mesenchymal Stem Cells Stimulate Cartilage Regeneration and Are Safe for Single-Stage Cartilage Repair in Humans upon Mixture with Recycled Autologous Chondrons. Stem Cells 2017; 35(1):256-64.

BONE CEMENT IMPLANTATION SYNDROME (BCIS): A THROMBOELASTOGRAPHIC (TEG) STUDY OF THE EFFECT OF BONE CEMENT ON COAGULATION

M. MORDÀ[1], S. PINI[2], F. CELLI[1], F. CASELLA[1], P. PARCHI[1], N. PIOLANTI [1], S. MARCHETTI[1] and M. SCAGLIONE[1]

[1]Orthopaedic Clinic, University of Pisa, Pisa, Italy; [2]Anesthesiology & Reanimation, AOUP, Pisa, Italy

Bone cement implantation syndrome (BCIS) is a rare form of intraoperative pulmonary embolism (EP) that occurs during cementation. It can be explained by two main theories: the monomer mediated model and the mechanic model. Our goal is to evaluate thromboelastographic changes in patients undergoing surgery for femoral neck fractures. We recruited 32 patients with a femoral neck fracture. The average age was 81.91 years (range 62-95). The patients were divided in two different groups: cemented hip arthroplasty (CC, 13 patients) and other surgical non-cemented techniques (SC, non-cemented hip arthroplasty, osteosynthesis). The coagulation was evaluated by TEG in the early pre-operatory (time A) and post-operatory (time B), both on native blood and on blood added with Heparinase. We used the *t*-test to compare the differences between the two groups. The coagulation index CI was modified on hypercoagulability by surgery in both groups, but without statistical significance between the two groups ($p>0.05$). R parameter decreases between time A and time B in the same way in both groups ($p>0.05$). Parameter MA had no major variations between time A and B, without statistical significance ($p>0.05$). From our study it is evident that although the surgery would result in a change in the layout of the TEG toward hypercoagulability, this is similar both in cemented and non-cemented surgical interventions for femoral neck fractures in elderly patients. An altered coagulation does not appear to be the cause or a factor in determining the BCIS.

Bone cement implantation syndrome (BCIS) is a rare form of intraoperative pulmonary embolism (PE) that occurs during cemented hip arthroplasty. BCIS is massive and fatal, and most likely underestimated (1, 2).

The etiopathogenetic model is not yet well understood. Some studies (2, 3, 4, 5, 6, 7, 8) suggest a direct action of the cement on vascular wall and probably on coagulation. Our goal is to evaluate and compare the changes of blood coagulation pattern caused by the use of cement during surgery in elderly patients with femoral neck fracture.

Our study used the thromboelastography (TEG), a little-used method in orthopedic trauma field, which allows obtaining quantitative and qualitative information on the visco-elastic characteristics of patient clot (9). Analyzing a blood sample, immediately before and after the surgical procedure, this tool is able to tell us if the surgery has brought about a change in the patient's blood coagulation pattern and, eventually, the extent of such alteration.

MATERIALS AND METHODS

Thirty-two patients were recruited, 6 males and 26 females. All of them reported a fracture of the proximal femur following a trauma; patients who had serious

Key words: thrombelastography, bone cement implantation syndrome, prosthesis

Mailing address:
Prof. Michelangelo Scaglione,
via Paradisa 2,
56124, Pisa, Italy
Tel.: 050996527
Fax: 050992027
e-mail: michelangelo.scaglione@gmail.com

0393-974X (2017)

comorbidities or did not undergo surgery within 48 h, which is the threshold recommended by international guidelines, were excluded from the study. The age of patients ranges between 62 and 95 years, and had an average 81.91 years; the average age was 82.27 of female patients and 80.33 years for males.

The patients were divided into two different groups: Group 1 included the ones treated with cemented prosthesis (CC) (13 patients, age range 67-95 years, average age 82.46, 9 females, 4 males), and Group 2, operated without cementing techniques (SC) such as cementless prosthesis or osteosynthesis (19 patients, age range 62-91 years, average age 81.53, 17 females and 2 males). Two blood samples of 1cc were taken from all patients. The first one, just before entering the operating theatre (PRE), and the second one right after the patient left the operating theatre (POST).

Blood samples were taken by specialized nurses from a peripheral vein of the arm, with a non-heparinized syringe. A quantity of 1cc of blood was transferred to a test tube containing Kaolin and two 0.36cc samples were taken and placed inside the TEG device, the first in a baseline cuvette, the second in a cuvette containing the Heparinase enzyme.

The TEG parameters taken into account were the R parameter ("reaction time", v. n 4-8 min), MA ("maximum amplitude", v.n. 54-72 mm) and CI ("coagulation index", v.n. -3, +3). By using a Student's *t*-test for independent samples, we compared the differences between the two groups, CC and SC.

Teg exam description

Thromboelastography is a method to register the viscoelastic properties of a whole blood sample through 3 main phases: clot formation, clot retraction and clot lysis. A big difference between standard coagulation laboratory tests and TEG® is that the first one measures the coagulation on centrifuged plasma, while TEG® is performed on whole blood. This method is therefore able to show the interactions between platelets, fibrin and proteins of the coagulation cascade (9, 10, 11, 12).

TEG® takes into account four basic parameters, called R, K, Alpha angle and MA. The coagulation index (CI) is then calculated starting from these basic parameters. Given the scarcity of data in the literature regarding the parameters K and Alpha angle, we decided to take into account in our study only the parameters R, MA and CI.

R (Reaction time): This line goes from the beginning of the graph until it reaches the width of 2 mm. This parameter gives us information about the speed of fibrin clot formation. It is measured in minutes and its normal duration is 4-8 min, corresponding to 19-28 mm in the graph. A 'short' R value indicates hypercoagulability (9, 10, 11) (Fig. 1).

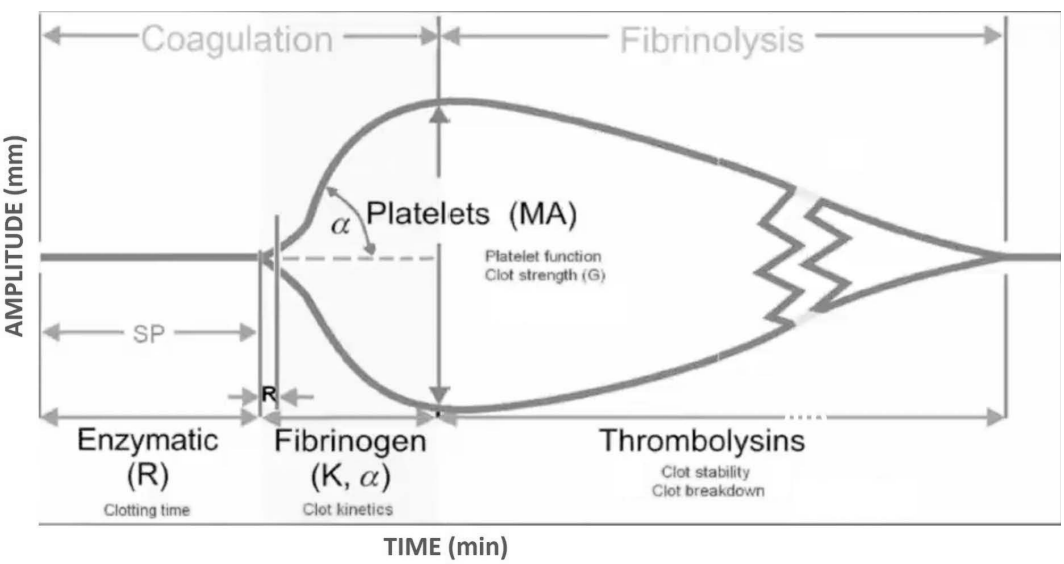

Fig. 1. *The thromboelastogram, showing R and MA parameters.*

MA (Maximum Amplitude): this parameter corresponds to the maximum extent that reaches the graph, and correlates with the strength of the blood clot. It is strictly dependent on the number and function of platelets and on their interaction with fibrin. The normal values are 54-72 mm and its increase is a sign of hypercoagulability (9, 10, 11) (Fig. 1).

CI (Coagulation Index): this index is a linear combination of kinetic parameters of clot development and clot strength (R, K, Alpha angle and MA), its normal values range from -3 to +3. CI is a benchmark that sums up the situation of the patient's blood; a more positive value suggests a state of hypercoagulability (9, 10, 11).

The (TEG®) allows to analyze the patient's whole blood sample unchanged, but by adding certain reagents, it is possible to study other particular features of the clot. In particular, by combining the Heparinase enzyme (9, 13), it allows to study the patient's blood eliminating the anticoagulant action of EBPM, such as in a patient not protected by its prophylactic action.

RESULTS

Coagulation patter was assessed in all 32 patients with blood samples taken both preoperatively and in the immediate postoperative period. The thromboelastographic study was performed on all samples, both with unfortified blood and with blood containing heparinase. Table I and II show the arithmetic average for the R, MA and CI parameters for the two groups of patients (Table I, II).

As shown in the Table I, relative to the pre-operative values, patients faced the surgery with an R parameter in the normal range (4-8 mm), closed to its lower limit, the two groups do not show statistically relevant differences. The difference between unfortified blood and blood with heparinase was minimal. Preoperatively, the MA parameter was at the upper limit of normality and it remained almost unchanged for the post-operative sampling, with no differences between the two groups. In this case, the values measured in the blood with heparinase were higher than in the non-added blood, without difference between the pre- and post-operative time and between the two groups. The normal range of CI parameter is -3/+3. For both groups, for the unfortified blood, it tends towards the upper part of the range, meaning a certain hypercoagulability. The CI values measured on blood with heparinase were above normal limit of the range already in the pre-operative sample. The CI then increased postoperatively up to the upper limit of the normal range for both groups of patients in the unfortified blood, whereas it exceeded the normal limit in both groups when the blood was treated with heparinase. Table III sums up the statistical analysis. The *t*-test was not significant ($p>0.05$) in the comparison between CC and SC group for all parameters (Table III).

DISCUSSION

The aim of our study is to shed light on the pathogenetic model of the bone cement implantation syndrome that occurs during cementing operations.

Table I. *Arithmetic average for the pre-operative period.*

PRE-OPERATIVE SAMPLE				
PARAMETER	Group CC		Group SC	
	Basal	Eparinase	Basal	Eparinase
R	4,32	4,03	4,86	4,55
MA	71,12	76,80	71,59	77,03
CI	2,42	3,44	2,17	3,07

Table II. *Arithmetic average for the post-operative period.*

POST-OPERATIVE SAMPLE				
PARAMETER	Group CC		Group SC	
	Basal	Eparinase	Basal	Eparinase
R	4,09	4,18	3,55	3,6
MA	71,69	76,98	69,47	74,68
CI	2,90	3,53	3,05	3,49

Table III. *Statistical study with Student's t test for independent samples for all parameters.*

PARAMETER	PRE-OPERATIVE SAMPLE		POST-OPERATIVE SAMPLE	
	basal	eparinase	basal	eparinase
R	p=0,38	p=0,38	p=0,42	p=0,36
MA	p=0,85	p=0,94	p=0,40	p=0,42
CI	p=0,65	p=0,57	p=0,81	P=0,9

Typically, this is a respiratory distress syndrome which manifests with: hypoxia, hypotension, arrhythmia, increased resistance of pulmonary circulation and cardiac arrest. BCIS can occur during acetabular or femoral cementation, prosthesis positioning and joint reduction (1, 2, 14, 16, 17). There are two principal etiopathogenetic theories (1, 2):

1. the Monomer Mediated model, where polymethyl methacrylate (PMMA) acts as a modulator of the vascular smooth muscle cells and a procoagulant agent;
2. The Embolic model, according to which the high pressure of the cement at the time of its use results in the release of several blood clots in the bloodstream.

The Monomer Mediated model is supported by *in vitro* studies (18, 19), in which polymers of methyl methacrylate lead to vasodilation, although unconfirmed by *in vivo* experiments (20, 21).

A functional study performed on 15 patients monitoring blood pressure, pulmonary pressure, left ventricular tele-diastolic volume and right ventricular ejection fraction during cementation, showed that the cement implant caused a pronounced vasoconstriction of the pulmonary vascular bed and a functional reduction of the right ventricle. Moreover, an alteration of the ventilation/perfusion ratio was reported, typical of pulmonary embolism.

To support the Embolic model instead, there are some studies with transesophageal echocardiography showing a release of blood clots in the bloodstream during cementation. (22, 23, 24) This phenomenon is due to the high intramedullary pressure generated during the cementing operation and the implantation of the prosthesis; PMMA produces an exothermic reaction, expanding in the space between the prosthesis and the bone of the patient, trapping air and bone marrow content, which is thus pushed

towards the venous circulation.

In literature, there are some autopsy (25, 26, 27) reports where typically, multiple occlusive thrombi composed of fat and bone marrow amorphous material are found at the level of the pulmonary circulation and sometimes also in other districts, such as renal and pancreatic. A study on dogs (21) reported that the use of cement could cause a release of emboli 10 times greater than surgery without cementation. At necropsy, fat and medullary material emboli were found in the pulmonary microcirculation. A recent study (28) showed a reduction of blood pressure and oxygen partial pressure falls after cementation in patients with *vena cava* filter; at intraoperative ultrasound monitoring, the cava filter seems to prevent the arrival of emboli in atrial cavity.

The two hypothesis may not be mutually exclusive, resulting in a cumulative effect that would explain why this type of embolism has never occurred in cementless prosthesis, although even in these, emboli release during the surgery has been documented (1, 2). In addition to mechanical obstruction, in fact, a direct effect of emboli on the blood vessels and mediators release may occur, (1, 2, 4, 6, 29), such as thrombin and tissue thromboplastin.

Furthermore, the same symptoms that characterize this syndrome have been reported in other practices using cement, such as vertebroplasty (5, 30) and total knee arthroplasty (31, 32) during which however. significant release of microemboli has not been observed. Probably, other less known alterations are implicated, such as acute alteration of coagulation, caused by the contact between the PMMA and the bloodstream. This may explain why techniques like the vertebroplasty may present clinical signs similar to cement syndrome, without however using high pressure cementation (5, 30).

Our study demonstrates that surgical procedure has a procoagulant effect because the coagulation index increases between the pre and post-operative in both groups. CI normal value ranges from -3 to + 3, the higher the CI, the more the patient has an increased risk of developing a thromboembolic complication. In our cohort, the patients had pre-operative CI value close to upper limit of standard range (+3) and this value increased after surgery. This variation is the same for the group treated with cemented prosthesis and the control group ($p>0.05$). Even better, the coagulation index does not appear totally altered in the comparison between the two groups, evidence that the clotting is not altered by the cement. The values of CI and MA relating to blood added with heparinase were higher than natural blood, while the values of R remained almost unchanged in the two blood samples. This shows that the EBPM is important to protect against hypercoagulability on trauma and surgery, in fact the lowest values of CI found in unfortified blood expresses this protective efficacy.

These data also show that probably this hypercoagulability can to be found especially in the MA parameter rather than R parameter, where the contribution of platelet phase is higher than enzymatic phase of coagulation. The procoagulant effect of PMMA in contact with vascular endothelium is therefore absent or non-significant, so it cannot be recognized as a cause or as a contributing factor of the constellation of symptoms of cement bone syndrome. Our results confirm the embolic model that is the more accredited theory today.

CONCLUSION

Investigating the possible causes for typical clinical manifestations of bone cement syndrome, our study demonstrates that cement does not have an impact on coagulation in elderly patients undergoing surgery for fractured neck of femur. We believe that more studies are necessary to clarify the pathogenic mechanisms of those serious and often fatal complications in order to prevent their occurrence in the operating room.

REFERENCES

1. Donaldson AJ, Thomson HE, Harper NJ, Kenny NW. Bone cement implantation syndrome. Br J Anaest. 2009; 102(1):12-22.
2. Razuin R, Effat O, Shahidan MN, Shama DV, Miswan MF. Bone cement implantation syndrome. Malays J Pathol 2013; 35(1):87-90.
3. Modig J, Busch C, Olerud S, Saldeen T, Waernbaum

G. Arterial hypotension and hypoxaemia during total hip replacement: the importance of thromboplastic products, fat embolism and acrylic monomers. Acta Anaesthesiol Scand 1975; 19(1):28-43
4. Modig J, Busch C, Waernbaum G. Effects of graded infusions of monomethylmethacrylate on coagulation, blood lipids, respiration and circulation. An experimental study in dogs. Clin Orthop Relat Res 1975; 113:187-97.
5. Vasconcelos C, Gailloud P, Martin JB, Murphy KJ. Transient arterial hypotension induced by polymethylmethacrylate injection during percutaneous vertebroplasty. J Vasc Interv Radiol 2001; 12(8):1001-2.
6. Motobe T, Hashiguchi T, Uchimura T, Yamakuchi M, Taniguchi N, Komiya S, Maruyama I. Endogenous cannabinoids are candidates for lipid mediators of bone cement implantation syndrome. Shock 2004; 21(1):8-12.
7. Duncan JA. Intra-operative collapse or death related to the use of acrylic cement in hip surgery. Anaesthesia 1989; 44(2):149-53.
8. Ten Hagen A, Doldersum P, van Raaij T. Anaphylactic shock during cement implantation of a total hip arthroplasty in a patient with underlying mastocytosis: case report of a rare intraoperative complication. Patient Saf Surg 2016; 10:25.
9. Manduca M, Saporito EF, Giardina A. [Thrombo-elastography in intensive care]. Acta Chirurgica Mediterranea 2006; 22:145.
10. Shen L, Tabaie S, Ivascu N. Viscoelastic testing inside and beyond the operating room. J Thorac Dis 2017; 9(S4):S299-S308.
11. Wilson D, Cooke EA, McNally MA, Wilson HK, Yeates A, Mollan RA. Changes in coagulability as measured by thrombelastography following surgery for proximal femoral fracture. Injury 2001; 32(10):765-70.
12. Bolliger D, Seeberger MD, Tanaka KA. Principles and practice of thromboelastography in clinical coagulation management and transfusion practice. Transfus Med Rev 2012; 26(1):1-13.
13. Coppell JA, Thalheimer U, Zambruni A, Triantos CK, Riddell AF, Burroughs AK, Perry DJ. The effects of unfractionated heparin, low molecular weight heparin and danaparoid on the thromboelastogram (TEG): an in-vitro comparison of standard and heparinase-modified TEGs with conventional coagulation assays. Blood Coagul Fibrinolysis 2006; 17(2):97-104.
14. Kotyra M, Houltz E, Ricksten SE. Pulmonary haemodynamics and right ventricular function during cemented hemiarthroplasty for femoral neck fracture. Acta Anaesthesiol Scand 2010; 54(10):1210-6.
15. Rothberg DL, Kubiak EN, Peters CL, Randall RL, Aoki SK. Reducing the risk of bone cement implantation syndrome during femoral arthroplasty. Orthopedics 2013; 36(4):e463-7.
16. Park HJ, Kang H, Lee JW, Baek SM, Seo JS. Comparison of hemodynamic changes between old and very old patients undergoing cemented bipolar hemiarthroplasty under spinal anesthesia. Korean J Anesthesiol 2015; 68(1):37-42.
17. Byrick RJ. Cement implantation syndrome: a time limited embolic phenomenon. Can J Anaesth 1997; 44(2):107-11.
18. Karlsson J, Wendling W, Chen D, Zelinsky J, Jeevanandam V, Hellman S, Carlsson C. Methylmethacrylate monomer produces direct relaxation of vascular smooth muscle in vitro. Acta Anaesthesiol Scand 1995; 39(5):685-9.
19. Peebles DJ, Ellis RH, Stride SD, Simpson BR. Cardiovascular effects of methylmethacrylate cement. Br Med J 1972; 1(5796):349-51.
20. McLaughlin RE, Di Fazio CA, Hakala M, Abbott B, MacPhail JA, Mack WP, Sweet DE. Blood clearance and acute pulmonary toxicity of methylmethacrylate in dogs after simulated arthroplasty and intravenous injection. J Bone Joint Surg Am 1973; 55(8):1621-8.
21. Orsini EC, Byrick RJ, Mullen JB, Kay JC, Waddell JP. Cardiopulmonary function and pulmonary microemboli during arthroplasty using cemented or non-cemented components. The role of intramedullary pressure. J Bone Joint Surg Am 1987; 69(6):822-32.
22. Koessler MJ, Fabiani R, Hamer H, Pitto RP. The clinical relevance of embolic events detected by transesophageal echocardiography during cemented total hip arthroplasty: a randomized clinical trial. Anesth Analg 2001; 92(1): 49-55.
23. Lafont ND, Kalonji MK, Barre J, Guillaume C, Boogaerts JG. Clinical features and echocardiography

of embolism during cemented hip arthroplasty. Can J Anaesth 1997; 44(2):112-7.
24. Lafont ND, Kostucki WM, Marchand PH, Michaux MN, Boogaerts JG. Embolism detected by transoesophageal echocardiography during hip arthroplasty. Can J Anaesth 1994; 41(9):850-3.
25. Sevitt S. Fat embolism in patients with fractured hips. Br Med J 1972; 2(5808):257-62.
26. Parvizi J, Holiday AD, Ereth MH, Lewallen DG. The Frank Stinchfield Award. Sudden death during primary hip arthroplasty. Clin Orthop Relat Res 1999; 369:39-48
27. Pietak S, Holmes J, Matthews R, Petrasek A, Porter B. Cardiovascular collapse after femoral prosthesis surgery for acute hip fracture. Can J Anaesth 1997; 44(2):198-201.
28. Wangang G, Qiansung Z, Bingling L, Xiaoqin S, Dingcheng X, Chen W. An Experimental Study to Determine the Role of Inferior Vena Cava Filter in Preventing Bone Cement Implantation Syndrome. Iran J Radiol 2015; 12(3):e14142
29. Modig J, Busch C, Olerud S, Saldeen T, Waernbaum G. Arterial hypotension and hypoxaemia during total hip replacement: the importance of thromboplastic products, fat embolism and acrylic monomers. Acta Anaesthesiol Scand 1975; 19(1):28-43.
30. Chen HL, Wong CS, Ho ST, Chang FL, Hsu CH, Wu CT. A lethal pulmonary embolism during percutaneous vertebroplasty. Anesth Analg 2002; 95(4):1060-2
31. Orsini EC, Richards RR, Mullen JM. Fatal fat embolism during cemented total knee arthroplasty: a case report. Can J Surg. 1986; 29(5):385-6.
32. Byrick RJ, Forbes D, Waddell JP. A monitored cardiovascular collapse during cemented total knee replacement. Anesthesiology 1986; 65(2):213-6.

HISTOLOGICAL CHANGES OF THE MENISCUS FOLLOWING AN OSTEOCHONDRAL LESION

G.M. PERETTI[1,2], I. TESSARO[2], L. MONTANARI[3], U. POLITO[4], A. DI GIANCAMILLO[4], M. DI GIANCAMILLO[5], A. MARMOTTI[6], A. MONTARULI[1], E. ROVEDA[1] and L. MANGIAVINI[2]

[1]Department of Biomedical Sciences for Health, University of Milan, Italy; [2]Laboratory of Tissue Engineering and Biomaterials, IRCCS Istituto Ortopedico Galeazzi, Milan, Italy; [3]Residency Program in Orthopaedics and Traumatology, University of Milan, Milan, Italy; [4]Department of Health, Animal Science and Food Safety, University of Milan, Italy; [5]Department of Veterinary Medicine, University of Milan, Italy; [6]Department of Orthopaedics and Traumatology, University of Turin, Turin, Italy

In the last few years, different tissue engineering strategies have been developed for the repair of osteochondral lesions. When the osteochondral scaffold is implanted on the femoral condyle, the meniscus might be affected by the implant and might undergo a progressive degeneration. The aim of our study is to analyze the morphological changes of the meniscus following an osteochondral lesion and the implant of a biphasic scaffold. A critical osteochondral defect was generated in the medial femoral condyle of mature sheep. Three defects were left untreated, the remaining lesions were divided into three groups and treated with a biphasic substituted formed by collagen type I and Wollastonite or Wollastonite/Hydroxyapatite. Animals were sacrificed after 6 months and menisci were isolated and analyzed by arthro-CT, macroscopic evaluation and histology. The results demonstrated that the osteochondral lesion negatively affects meniscus morphology and that the osteochondral substitute only partially mitigates the meniscus degeneration.

The knee is one of the biggest synovial joints and its unique biomechanical properties are the result of a complex anatomy. The bony surfaces, femoral condyles and tibial plateaus, are covered by a thick layer of articular cartilage, which has the essential function to absorb and distribute the loads onto the subchondral bone and to provide a large range of joint motion with excellent lubrication (1).

The load transfer is also provided by another essential structure: the meniscus. Meniscus is a fibrocartilaginous tissue mainly composed of water and few highly differentiated cells surrounded by an abundant extracellular matrix. Meniscus morphology varies in the different regions. Its periphery is highly fibrous, abundant in cells and collagen I, while the inner portion of the tissue is more cartilaginous with fewer cells, a higher proteoglycan content and the presence of collagen II. In addition, the spatial distribution of the collagen fibers differs in the different areas and it creates an extremely effective mechanism of load sharing among the body and horns of the meniscus (2-5).

Both articular cartilage and meniscus possess a scarce self-healing potential: thus, these tissues frequently undergo progressive degeneration when damaged leading to osteoarthritis.

In the last years, countless tissue engineering techniques have been introduced in the attempt to regenerate both hyaline cartilage and meniscus (6-11). However, few studies have focused on the

Key words: meniscus, histology, osteochondral lesion, animal model

Mailing address:
Laura Mangiavini, M.D.,
IRCCS Istituto Ortopedico Galeazzi,
Via R. Galeazzi 4, 20161, Milan, Italy
Tel.: +39 02 5031 4930
Fax: +39 02 6621 4736
e-mail: lauman82@hotmail.it

0393-974X (2017)

tight relationship between cartilage and meniscus degeneration and almost no papers have investigated meniscal changes in response to an osteochondral lesion and to an implant of an osteochondral scaffold.

Indeed, when a cartilaginous lesion is localized on the femoral condyle or on the tibial plateau, the load distribution is altered. Moreover, chondrocytes surrounding the lesion start secreting several pro-inflammatory cytokines, which in turn trigger the activation of several pathways that may affect the cell viability and the production of extracellular matrix by the chondrocytes themselves and by the meniscal cells (12-15).

In our study, we carefully investigated the morphological changes that occur in the meniscus of a sheep model following an osteochondral lesion and the implant of a biphasic acellular scaffold.

At the end of the experimental time, we observed that the presence of the osteochondral lesion progressively leads to a decrease of cell viability and matrix production and to the disruption of the collagen architecture. The presence of the osteochondral scaffold only partially prevented the onset of these degenerative phenomena.

MATERIALS AND METHODS

Animal study

Eighteen sheep (100 kg of body weight), were anesthetized as previously described (16), and placed in the supine position. A longitudinal paramedian incision was made in the medial aspect of the right knee. Subsequently, the articular capsule was opened and a critical osteochondral defect was generated in the medial femoral condyle.

The size of the lesion was 11 mm in diameter and 9 mm in depth and it was created with custom-made instruments. The animals were divided into 4 groups: in one group, the defect was left untreated (CTRL group) and in the other groups 3 different osteochondral biphasic scaffolds (BWS, HWS or HMG) were tested as previously described (17).

Animals were sacrificed after 6 months under anesthesia with a lethal injection of KCl. The right knees were then harvested and further analyzed as described below.

Radiological evaluation

Arthro-CT scans were performed on the harvested knees at Department of Veterinary Medicine (DIMEVET), Università degli Studi di Milano, Ospedale Didattico Universitario Az. Polo Veterinario di Lodi.

For arthrography, each limb underwent a spiral CT examination (16 slices CT scanner - GE Brightspeed®, GE Healthcare, Milano - Italy) before and after the intraarticular injection of contrast medium. A 22-gauge needle was inserted into the joint, medial to the mid-point of the patellar tendon. To ensure correct positioning of the needle, synovial fluid was aspirated. 25 ml of nonionic triiodinated contrast (Iomeprol - Iomeron® 150 mg/ml, Bracco, Italy) were then injected into the articular space through paraligamentous technique (18).

The joint was repeatedly flexed and extended to achieve satisfactory distribution of the contrast medium throughout the joint. The following parameters were used for CT scanning: slice thickness=1.25 mm; pitch=0.9375; kVp=120; mA=220. The limbs were exanimated cranio-caudally and scanned from the distal femoral diaphysis to the proximal tibial diaphysis.

Multiplanar reconstructions were performed with a dedicated image analysis software (Aycan Osirix Pro®).

Macroscopic evaluation

The skin and the articular capsule were opened and macroscopic evaluation of the knees was performed. The assessment of the articular cartilage and of the osteochondral repair was achieved following the International Cartilage Repair Society (ICRS) Macroscopic score, as previously described (17). Menisci were isolated, the presence and the site of a lesion was assessed by three independent observers. Subsequently, menisci were divided into three portions: anterior horn, intermediate portion (body) and posterior horn.

Histological evaluation

Samples were then fixed in 10% phosphate-buffered Formaldehyde and then processed for paraffin embedding. The pieces were dehydrated in a graded 50% (v/v), 70% (v/v), 95% (v/v), and 100% (v/v) ethanol series, embedded in paraffin, and cut into 10-mm-thick sections. Subsequently, some slides were stained with Hematoxylin & Eosin following standard protocols to analyze cell morphology. Other sections were stained with Safranin/

Fast Green to evaluate the presence and distribution of Glycosaminoglycans (16, 19). All the sections were examined by three independent observers and several parameters were evaluated: surface smoothness (surface score) on femoral side, tibial side and inner border; cellularity and matrix staining (Safranin O-Fast Green) (20).

RESULTS

At the end of the experimental time, a contrast agent was injected into the synovial space of few samples and they underwent a radiological evaluation by CT scanning (Fig. 1), as Computed Tomographic Arthrography allows for an excellent visualization of intra-articular structures. On the dorsal plane (Fig. 1A), the narrowing of the medial intra-articular space associated to the consequent thinning of the medial meniscus caused a non-homogeneous distribution of the contrast medium around this structure that impedes a distinct characterization of the anterior horn profile. Transverse images showed that contrast medium outline both menisci, but differently (Fig. 1B). Lateral meniscus (arrow, corresponding to the control femoral condyle) is completely surrounded by the contrast medium, that depicts the entire structure and allows for the identification of all the meniscal components (anterior horn, body and posterior horn). Medial meniscus (corresponding to the treated femoral condyle) is not entirely outlined by the contrast medium; in particular, the anterior horn is not completely identifiable. Finally, sagittal arthrografic images (Fig. 1C, D) showed a normal distribution of the contrast medium within the intra-articular space of the lateral compartment and a fully depiction of the lateral meniscus (Fig. 1C); whereas, the anterior horn and the body of the medial meniscus are not fully recognizable (Fig. 1D).

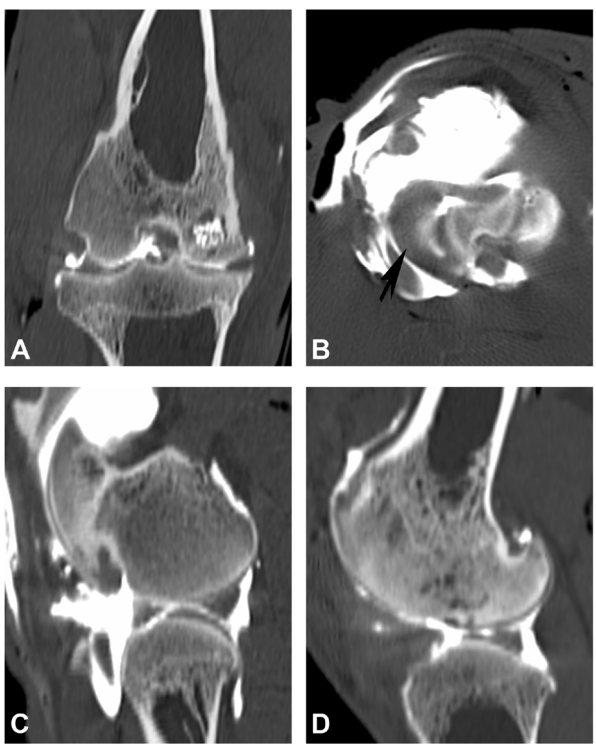

Fig. 1. *Radiological evaluation of the menisci. Arthro-CT scans of a representative sample: dorsal (**A**), transverse (**B**) and sagittal (lateral side: **C**; medial side: **D**) are shown. Note the presence of the biphasic scaffold in (**A**). The arrow in (**B**) points at the lateral meniscus.*

Subsequently, knees were dissected and a careful macroscopic evaluation was performed. The assessment of the overall joint and of the articular cartilage was achieved following the ICRS macroscopic scale as previously described (17). Both medial and lateral menisci were evaluated and the presence of meniscal degeneration was quantified with a numeric scale (0=total degeneration; 4=no degeneration); the lateral meniscus of each joint was used as a control. Overall, the lateral meniscus appeared in good conditions in almost all the samples, whereas different degrees of degeneration were present in the medial menisci (Fig. 2:1). Lesions were concentrated in the anterior horn and in the body, they mirrored the corresponding osteochondral defect and were characterized by fibrillation, delamination and, in the worst cases, calcification. In all groups, the medial meniscus was significantly worse than the lateral meniscus (Fig. 2:2).

The presence of the biphasic osteochondral construct did not prevent the progressive degeneration; in particular, the addition of wollastonite in the scaffold appeared to worsen not only cartilage repair, as previously described (17), but also meniscus integrity (Fig. 2. B, D).

Microscopically, several parameters were examined; smoothness of the tibial, femoral surface and inner border, cellularity and matrix staining. For each criterion, a numeric scale was applied as

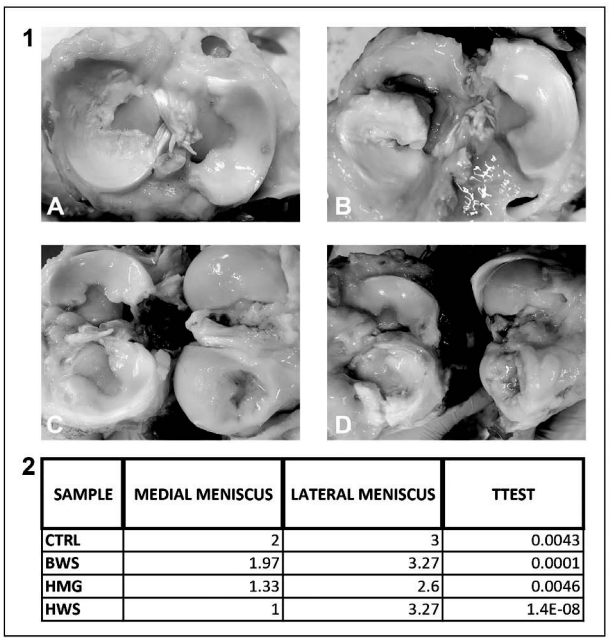

2

SAMPLE	MEDIAL MENISCUS	LATERAL MENISCUS	TTEST
CTRL	2	3	0.0043
BWS	1.97	3.27	0.0001
HMG	1.33	2.6	0.0046
HWS	1	3.27	1.4E-08

Fig. 2. *Macroscopic assessment of the menisci.* ***1)*** *Macroscopic images of representative untreated (**A** and **C**) and BWS (**B** and **D**) sample; Medial menisci are shown on the left side in (**A** and **B**) and on the bottom side in (**C** and **D**); Note the osteochondral lesions in (**C** and **D**).* ***2)*** *Macroscopic score of the medial and lateral menisci of the different groups: mean values are shown. Test t values are reported on the right side ($p<0.05$).*

described in a previous work (20) and the lateral meniscus was used as reference. In the samples left untreated, the surfaces were mostly fibrillated and sometimes completely disrupted; sections were characterized by a reactive hypercellularity and by a moderate production of Glycosaminoglycans (GaGs) as shown by the moderate Safranin O staining. In the BWS and HWS groups, the degeneration worsened when compared to the untreated group as shown by the increase in fibrillation, the progressive hypocellularity and the decrease in Safranin O staining, which reflects the disruption in matrix content and the inability of the cells to repair the damage (Fig. 3. C, D). In BWS group, all the three scores were significantly worse than the untreated samples; whereas in the HMG group we noticed a partial but significant amelioration in the surface score when compared to the CTRL group (Fig. 3:2).

DISCUSSION

In this study, we analyzed the morphological changes of the meniscus in a sheep model subjected to the implant of an osteochondral substitute. In particular, we generated a critical osteochondral defect in the medial condyle of the right knee and we subsequently implanted a biphasic scaffold made of collagen type I and Hydroxyapatite or Hydroxyapatite/Wollastonite; as control, few defects were left untreated. The aim was to evaluate the effects of the osteochondral lesion and of the implant on the meniscus. The sheep were sacrificed after six months and the knees were analyzed radiologically, macroscopically and histologically. At the end of the experimental time, animals did not show any sign

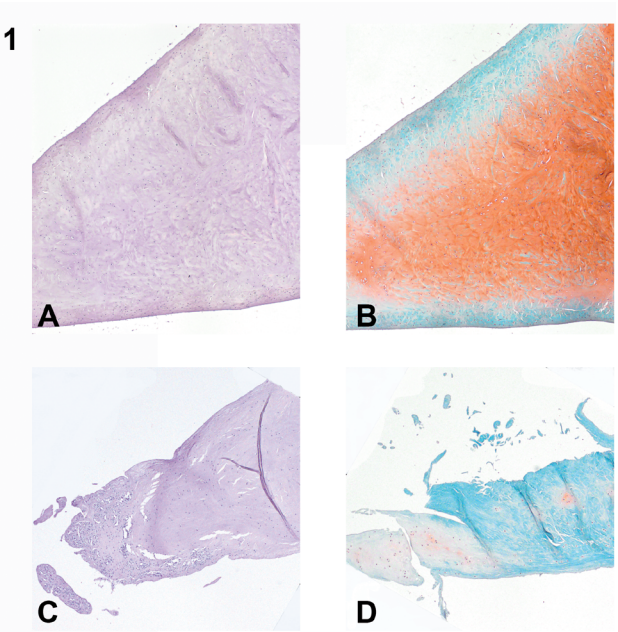

2

Samples	Surface score			Cellularity	Matrix staining
	Femoral side	Tibial side	Inner border		
LATERAL VERSUS CTRL	**1.03E-08**	**1.61E-10**	0.85	0.09	**0.01**
BWS VERSUS CTRL	0.54	0.73	**0.004**	**0.012**	**0.036**
HWS VERSUS CTRL	0.69	0.60	0.29	0.09	0.06
HMG VERSUS CTRL	0.06	**0.0002**	**4.18E-07**	0.86	0.40

Fig. 3. *Histologic evaluation of the menisci.* ***1)*** *H&E and Safranin-O pictures of a representative lateral meniscus (**A** and **B**) and a treated (**C** and **D**) sample.* ***2)*** *Histologic score of the medial menisci of the different groups: mean values are shown. The CTRL group was compared to the lateral meniscus; **BWS**, **HWS** and **HMG** samples were compared to the untreated group (**CTRL**). Test t values are reported on the right side, significant values are highlighted in bold ($p<0.05$).*

of infection or joint impairment. Generally, all the medial menisci showed signs of degeneration in the anterior horn and in the body; whereas the posterior horn was preserved.

Menisci play a fundamental biomechanical role in distributing load from the femoral to the tibial compartment and in absorbing shocks (1). When articular cartilage of the condyles is damaged, the knee biomechanics is altered and also menisci are obviously affected by this degenerative process (13). In a previous study by Pauli C. et al. (20), authors carefully analyzed the morphological changes of the meniscus during aging: they demonstrated that the degenerative process during osteoarthritis (OA) starts within the meniscal tissue rather than on the surface, differently from articular cartilage where the initial damage is represented by superficial fibrillation (21). They also showed that the posterior horn is the most affected area of the degenerative process, thus speculating that the anterior horn may be more resistant to degeneration (22). However, in this study, authors described the natural history of meniscal deterioration, but they did not analyze meniscal changes in traumatic conditions. In our study, we analyzed a sheep model of osteochondral repair in the femoral condyle: differently from the above-mentioned study (20), meniscal degeneration started with a superficial fibrillation and progressive loosening of glycosaminoglycans. Moreover, medial menisci were characterized by different degree of calcification and tears; in our traumatic model, the lesion was focused on the anterior horn and on the body, whereas the posterior horn was almost unaffected in all the samples. The implant of our biphasic scaffolds only partially prevented meniscal degeneration. Samples treated with the hydroxyapatite/Wollastonite biphasic substitute showed the worst results, as the macroscopic and the histologic scores were consistently lower than the untreated samples: this result is consistent with our previous findings, where we speculated that probably Wollastonite is detrimental for osteochondral repair (17). Osteochondral lesions treated with the HMG scaffold showed a partial but significant better surface score when compared to the untreated lesions; however, cellularity and matrix staining were not significantly ameliorated. This finding again supports our previous outcomes, suggesting that this type of biphasic scaffold is the most appropriated to treat osteochondral lesions (17).

In conclusion, the implant of the osteochondral scaffold did not prevent meniscal degeneration, but this apparent bad result has several explanations. First, the sheep model does not allow for a proper post-operative rehabilitation protocol: in the first 4-6 weeks after the implant, the weight bearing should be avoided to favor the integration and the repair of the lesion. Sheep were obviously allowed to graze immediately after surgery: thus, the altered biomechanics of the operated knee lead to initial meniscal degeneration.

Moreover, in our preliminary study we decided to generate a critical-size defect (9 x 11 mm) to avoid its spontaneous repair; however, the lesion was probably too big to allow for an appropriate reparative process and therefore also menisci were negatively affected by the lack of cartilage repair.

Thus, further studies with other animal models and with smaller osteochondral lesions are required to fully analyze the morphological changes of the meniscus following the implant of an osteochondral scaffold.

REFERENCES

1. Song Y, et al. Meniscectomy alters the dynamic deformational behavior and cumulative strain of tibial articular cartilage in knee joints subjected to cyclic loads. Osteoarthritis Cartilage 2008; 16(12):1545-54.
2. Di Giancamillo A, et al. Meniscus maturation in the swine model: changes occurring along with anterior to posterior and medial to lateral aspect during growth. J Cell Mol Med 2014; 18(10):1964-74.
3. Di Giancamillo A, Mangiavini L, Tessaro I, Marmotti A, Scurati R, Peretti GM. The meniscus vascularization: the direct correlation with tissue composition for tissue engineering purposes. J Biol Regul Homeost Agents, 2016; 30(4S1):85-90.
4. Kambic HE, McDevitt CA. Spatial organization of types I and II collagen in the canine meniscus. J Orthop Res 2005; 23(1):142-9.

5. McDevitt CA, Webber RJ. The ultrastructure and biochemistry of meniscal cartilage. Clin Orthop Relat Res 1990(252):8-18.
6. Mandal BB, Park SH, Gil ES, Kaplan DL. Multilayered silk scaffolds for meniscus tissue engineering. Biomaterials 2011; 32(2):639-51.
7. Niu W, Guo W, Han S, Zhu Y, Liu S, Guo Q. Cell-Based Strategies for Meniscus Tissue Engineering. Stem Cells Int 2016; 2016:4717184.
8. Peretti GM, Caruso EM, Randolph MA, Zaleske DJ. Meniscal repair using engineered tissue. J Orthop Res 2001; 19(2):278-85.
9. Peretti GM, Gill TJ, Xu JW, Randolph MA, Morse KR, Zaleske DJ. Cell-based therapy for meniscal repair: a large animal study. Am J Sports Med 2004; 32(1):146-58.
10. Peretti GM, Randolph MA, Caruso EM, Rossetti F, Zaleske DJ. Bonding of cartilage matrices with cultured chondrocytes: an experimental model. J Orthop Res 1998; 16(1):89-95.
11. Scotti C, Pozzi A, Mangiavini L, Vitari F, Boschetti F, Domeneghini C, Fraschini G, Peretti GM.Healing of meniscal tissue by cellular fibrin glue: an in vivo study. Knee Surg Sports Traumatol Arthrosc 2009; 17(6):645-51.
12. Bijlsma JW, Berenbaum F, Lafeber FP. Osteoarthritis: an update with relevance for clinical practice. Lancet 2011; 377(9783):2115-26.
13. Englund M, Guermazi A, Lohmander LS. The meniscus in knee osteoarthritis. Rheum Dis Clin North Am 2009; 35(3):579-90.
14. Musumeci G, Szychlinska MA, Mobasheri A. Age-related degeneration of articular cartilage in the pathogenesis of osteoarthritis: molecular markers of senescent chondrocytes. Histol Histopathol 2015; 30(1):1-12.
15. Verdonk R, Madry H, Shabshin N, et al. The role of meniscal tissue in joint protection in early osteoarthritis. Knee Surg Sports Traumatol Arthrosc 2016; 24(6):1763-74.
16. Sosio C, Di Giancamillo A, Deponti D. Osteochondral repair by a novel interconnecting collagen-hydroxyapatite substitute: a large-animal study. Tissue Eng Part A 2015; 21(3-4):704-15.
17. Gervaso F, Mangiavini L, Di Giancamillo A. Comparison of three novel biphasic scaffolds for one-stage treatment of osteochondral defects in a sheep model. J Biol Regul Homeost Agents 2016; 30(4S1):24-31.
18. Vandeweerd JM, Kirschvink N, Muylkens B. A study of the anatomy and injection techniques of the ovine stifle by positive contrast arthrography, computed tomography arthrography and gross anatomical dissection. Vet J 2012; 193(2):426-32.
19. Scotti C, Buragas MS, Mangiavini L, Sosio C, Di Giancamillo A, Domeneghini C, Fraschini G, Peretti GM. A tissue engineered osteochondral plug: an in vitro morphological evaluation. Knee Surg Sports Traumatol Arthrosc 2007; 15(11):1363-9.
20. Pauli C, Grogan SP, Patil S, Otsuki S, Hasegawa A, Koziol J, Lotz MK, D'Lima DD. Macroscopic and histopathologic analysis of human knee menisci in aging and osteoarthritis. Osteoarthritis Cartilage 2011; 19(9):1132-41.
21. Pritzker KP, Gay S, Jimenez SA, Ostergaard K, Pelletier JP, Revell PA, Salter D, van den Berg WB. Osteoarthritis cartilage histopathology: grading and staging. Osteoarthritis Cartilage 2006; 14(1):13-29.
22. Katsuragawa Y, Saitoh K, Tanaka N, et al. Changes of human menisci in osteoarthritic knee joints. Osteoarthritis Cartilage 2010; 18(9):1133-43.

THE TREATMENT OF LOW-GRADE SEPTIC NON-UNIONS

F.VERDONI[1], R.D. D'AMATO[2], L.MANGIAVINI[1], M.D. LOMBARDO[2] and G.M. PERETTI[1,3]

[1]IRCCS Istituto Ortopedico Galeazzi, Milan, Italy; [2]Residency Program in Orthopaedics and Traumatology, University of Milan, Milan, Italy; [3]Department of Biomedical Sciences for Health, University of Milan, Italy

Non-union (or pseudoarthrosis) is defined as a fracture that fails to consolidate after 6 months from the trauma. Current conservative treatments consist of biological (i.e. with calcium, Vitamin D) and mechanical stimulation. Moreover, surgical approaches include the use of endomidollar nail osteosynthesis, compression plates that are often associated with bone grafts. External fixation is a valid surgical alternative especially in case of septic non-unions. Indeed, compression-distraction osteosynthesis results in a significant improvement in bone vascularisation and exerts a powerful osteoinductive stimulus on the non-union site. In this review, we will describe a cohort of patients affected by low-grade septic non-unions and treated with external fixation.

Non-union (or pseudoarthrosis) is defined as a failure in fracture consolidation after at least 6 months from the trauma, and is characterized by the presence of fibrocartilaginous tissue within the two bony segments (1).

The percentage of fractures which undergo non-union is between 2% and 7% (1). Based on several studies, the most common sites of non-unions are tibia, femur, humerus or forearm (2), whereas other authors report the tibia as the predominant affected area (3). In addition, the incidence of non-union is higher in exposed diaphysis fractures.

Non-union aetiology is not yet well defined, but several systemic and local factors are involved. Indeed, pseudoarthrosis is classified as non-infected (aseptic) or infected non-union. The diagnosis is based on anamnestic data, clinical features (pain, functional impotence, bone movements and creeps) and radiographic signs (persistence of the fracture line, bone sclerosis, hypertrophic callus, atrophic bone resorption). The treatment is mainly surgical and involves several options depending on the type of pseudoarthrosis.

New therapeutic perspectives are represented by the use of the circular external fixation and by the effects it exerts on bone regeneration.

Etiopathogenesis

To date, non-union aetiology is still unclear. Multiple systemic or local factors influence the process of fracture consolidation. Among the systemic factors, we can mention age, nutritional status, systemic diseases, corticosteroid therapy, bone metabolic diseases, tumours, antineoplastic drugs. Among the local factors, we can cite blood supply, fracture site, reduction, immobilization, soft tissue injury and infection (4, 5).

Classification

- Aseptic non-unions

According to Weber and Cech's classification (6), aseptic pseudoarthrosis is divided into hypertrophic and atrophic, based on the vitality of bone fragments.

Key words: non-union, infection, external fixation

Mailing address:
Giuseppe M. Peretti, M.D.
Department of Biomedical Sciences for Health,
University of Milan, IRCCS Istituto Ortopedico Galeazzi,
Via R. Galeazzi 4, 20161, Milan, Italy
Tel.: +39 02 5031 9967 - +39 02 6621 4735 - Fax: +39 02 6621 4736
e-mail: gperetti@iol.it

0393-974X (2017)

Hypertrophic/hypervascular pseudoarthrosis are further subdivided into:

• Elephant paw pseudoarthrosis: largely hypertrophic and rich in bone callous. They usually follow an unstable fixation or a premature load.

• Horse's hoof pseudoarthrosis: moderately hypertrophic and with low bone callus. Typically, they follow a moderately unstable immobilization.

• Oligotrophic pseudoarthrosis: non-hypertrophic and with no bone callus. They generally follow a fracture shift.

Atrophic/avascular pseudoarthrosis are further subdivided into:

• Dystrophic pseudoarthrosis: characterized by the presence of an interposed fragment with decreased blood supply.

• Necrotic pseudoarthrosis: characterized by the presence of one or more necrotic interposed fragments.

• Pseudoarthrosis with loss of substance: characterized by loss of bone fragments in diaphysis.

• Atrophic pseudoarthrosis: characterized by the absence of interposed fragments; the terminal parts of the fragments are osteoporotic and atrophic.

- *Septic non-unions*

Infected or septic pseudoarthrosis follows the classification of Cierny (7), which subdivides osteomyelitis into 4 anatomic types, based on the extent of infection:

• Type 1: bone marrow osteomyelitis

• Type 2: superficial osteomyelitis

• Type 3: localized osteomyelitis

• Type 4: widespread infection

Each type is further subdivided into three physiological classes, based on systemic features:

• A: physiologically normal subject

• B: subject with local or systemic impairment to healing of fracture and wound;

• C: subject with high risk of complications in case of surgical procedure.

Diagnosis

The diagnosis of non-union is primarily based on a detailed history of patient's nutritional status, systemic disease, body weight, fracture type (affected bone, fracture dynamics, soft tissue damage, type and duration of treatment, pain, neurovascular complications, and possible infection).

The physical examination provides information on callus stability (movements and creepy bones), pain, functional impotence, swelling, heat and redness.

For diagnostic purposes, the determination of serum albumin levels and total lymphocyte count are essential. Moreover, electrolyte values may indicate nutritional deficiencies. In addition, VES can remain elevated for several months after a fracture. A concomitant increase in white blood cells count and Reactive C Protein are typical of infected non-unions (8).

The radiographic examination (according to the four projections: antero-posterior, lateral and oblique views) is mandatory to diagnose and to evaluate long bone pseudoarthrosis. In septic non-unions, a few weeks after the onset of septicaemia, a radiotransparent area can be visualized at the X-rays as sign of osteopenia; then, in the late phase, there is an impoverishment of the bone matrix (Fig. 1) (9).

In selected cases, a CT-scan may be useful to identify and to quantify bone loss, fluid or haemorrhagic masses (10).

Magnetic Resonance Imaging (MRI) accurately displays vascularization of long bones, allowing for the evaluation of surgical accessibility and for the choice of the best treatment (11). MRI also allows for precise measurement of the extent and location of the inflammatory process within the bone (11).

MATERIALS AND METHODS

Twelve patients affected by post-traumatic non-union who had undergone previous treatments at other nosocomial sites were retrospectively evaluated from 2010 to 2017. In all cases, there was low-grade septic pseudoarthrosis. Eight patients were males, 4 patients were females with an average age of 35 years (range 24-61 years). All the non-unions were localized at the lower limbs; 9 at the level of the tibia (6 right, 3 left) and 3 at the femur level (1 left, 2 right). In one case, it was type 1 septic non-union according to Cierny classification, 8 cases of type 2 and 3 cases of type 3. We did not observe any case of type 4 septic non-unions.

All patients had undergone antibiotic drug therapy, debridement of the fracture site, and application of circular external fixator in monofocal compression-distraction according to the Ilizarov method. In some cases, the use of biophysical stimulation with pulsed magnetic fields was also used.

RESULTS

All patients were clinically evaluated and they were periodically checked for up to 2 years. Treatment with external fixator lasted 5 months in Type 1 non-unions, from 4 to 8 months in Type 2 and from 6 to 9 months in Type 3 non-unions (Fig. 1, 2). Under no circumstances intraoperative complications have been observed. Bone scintigraphy was used to examine the evolution of the treatment.

In 5 patients, a superficial infection occurred around one or two k-wires, treated and resolved by antibiotic therapy. In 1 patient 1 or 2 k-wires failed and required the replacement of the wires.

Overall results (distinguished in functional results and bone results) were evaluated according to Paley's classification as: excellent, good or sufficient.

The type 1 patient had a satisfactory result from the bone point of view and good result from a functional one. In type 2, 3 patients had a good bone result and an excellent function score. 5 patients had a good result both from a functional and bone point of view (Fig. 3).

In the cluster of patients with type 3 non-union, 1 patient reported a sufficient bone and functional outcome, 1 patient had a good functional and bone result and 1 patient reported an excellent bone score and a good one from the functional point of view.

DISCUSSION

Non-union treatment is mainly based on prevention, proper reduction and immobilization of the fracture to allow for a correct consolidation, but also on the accurate reconstruction of soft tissues, on the functional load as early as possible, and on careful monitoring of possible infections (12).

Regarding treatment, non-surgical methods include pharmacological therapy (calcium, vitamin

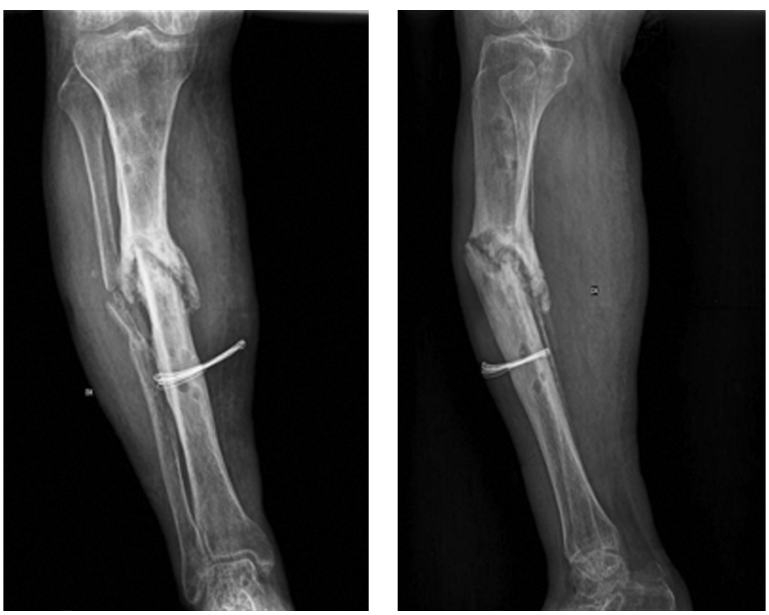

Fig. 1. *A representative example of low-grade septic non-union of the tibia. Note the radiotransparent area at the site of infection.*

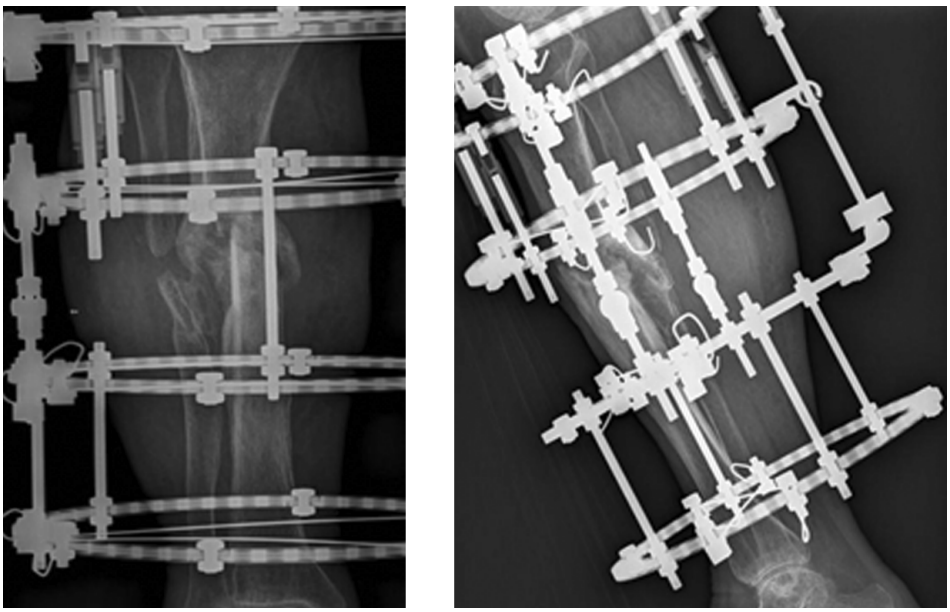

Fig. 2. *A representative image of the ongoing treatment with external fixation of the septic non-union shown in Fig. 1.*

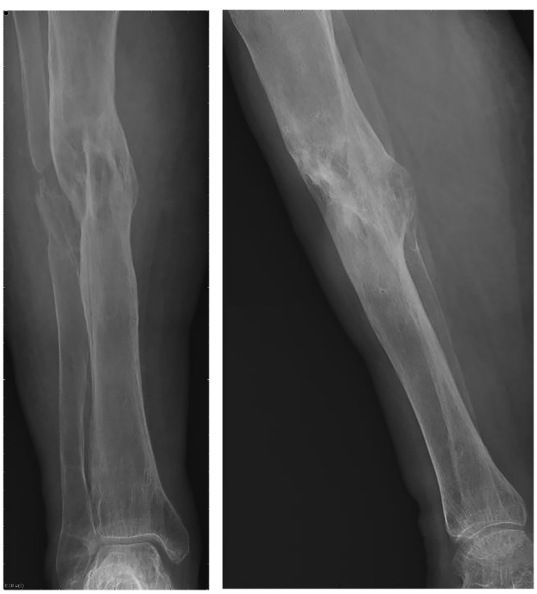

Fig. 3. *Healing of the low-grade septic non-union after the treatment with external fixation.*

D3, bisphosphonates), mechanical stimulation (increased functional stability associated with the focal stability), biophysical stimulation (electric or electromagnetic fields and low intensity pulsed ultrasounds) (13, 14).

Surgical treatment of hypertrophic non-unions is based on a stable immobilization by endomidollar nail osteosynthesis, which allows for a partial load, but it may cause alteration of the endosteal blood supply, which can be fully restored in about 12 weeks (15). Compression plates also provide a stability of the bony callus but do not give adequate

osteogenic stimulation; thus, this surgical alternative is often associated with a bone graft (16-18). Hypertrophic non-unions are frequently associated with arterial disorders or angular deformity, resulting in shortening of the involved limb. This specific complication is treated by a distanced monolayer osteosynthesis, which involves the gradual removal of the bony extremities, with simultaneous correction of associated deformities by guiding a circular external fixation (19).

Normotrophic pseudoarthrosis needs an increased biological stimulation to determine an osteogenic stimulus for proper fracture consolidation. For this purpose, a monofocal compression-distraction osteosynthesis with circular external fixation is used. The advantages are represented by a rigid immobilization of bone fragments, the absence of synthetic media, and the respect of bone marrow. The disadvantages are due to a minimal axial load, the risk of infection of the fiches and the lack of dynamization of the bony segments (19-21).

Atrophic pseudoarthrosis requires a greater biological stimulation, which can be obtained with bone grafts or growth factors, which nowadays are mimicked by several recombinant drugs, such as Bone Morphogenetic Proteins (22, 23); however, this pharmacological approach has some disadvantages, such as the high costs and the possible adverse reactions.

For septic non-unions, surgical treatment consists of the use of external fixators after careful debridement, with complete removal of all the fistula paths, the necrotic and infected tissues, and subsequent washing with antibiotic solution (24).

Compression-distraction osteosynthesis results in a significant improvement in bone vascularisation and has a stimulating effect on soft dystrophic tissues. In almost all cases, patients well tolerated the circular external fixator throughout the treatment, maintaining good joint function.

These data support the use of circular external fixation rather than axial systems. Indeed, the stability of the circular external fixator allows for early load on the limbs from the firsts post-operative days. In addition, during the treatment, the device may allow for the change of the position of affected segments, as needed.

Regarding tolerability, the soft tissue morbidity is low, even in case of extensive bone transport. These advantages are obtained not only with the Ilizarov fixation, but also with all circular external fixation systems.

In our low-grade septic non-unions, characterized by negative clinical signs, negative inflammatory indexes but topographically limited positivity to scintigraphy with marked leukocytes, the use of the circular external compression-distraction fixator, proved to be particularly effective in terms of functional outcomes, representing an optimal treatment option, if used by expert hands, in the management of septic non-unions.

It is well known that the tension of the tissues obtained with an external device is the most effective motor to stimulate osteogenesis as "the infection burns in the fire of regeneration". Indeed, infection itself slows down, but does not stop bone repair, as long as septic processes are characterized by a low-grade activity.

External fixation, guarantees ease of application, reduced time, reduced bone loss, reduced interference with the affected fracture site and at the same time gives the correct anabolic stimulus, as well as an elastic synthesis but without any impairment of stability.

Thus, this treatment can be applied to selected patients affected by septic non-unions with excellent outcomes. Indeed, the use of an external fixator allows for a reduction in bone loss, reduction in treatment time and thus less psychological impact on the patient himself.

REFERENCES

1. Milgram JW. Nonunion pseudarthrosis of fracture healing. A histopathologic study of 95 human specimens. Clin Orthop Relat Res 1991; 268:203-13.
2. Boyd HB, Symposium: Treatment of Ununited Fractures of the Long Bones; Introduction. J Bone Joint Surg Am 1965; 47:167-8.
3. Pneumaticos SG, Panteli M, Triantafyllopoulos GK, Papakostidis C, Giannoudis PV. Management outcome of diaphyseal aseptic non-unions of the lower limb: a systematic review. Surgeon 2014;

12(3):166-75.
4. Heiple KG, Herndon CH. The pathologic physiology of nonunion. Clin Orthop Relat Res 1965; 43:11-21.
5. Rodriguez-Merchan EC, Forriol F. Nonunion: general principles and experimental data. Clin Orthop Relat Res 2004; 419:4-12.
6. Segmuller G, Bekier A, Cech O. 85Sr uptake study in non-union in man. Eur Surg Res 1970; 2(3):226-32.
7. Cierny G, Mader JT 3rd, Penninck JJ. A clinical staging system for adult osteomyelitis. Clin Orthop Relat Res 2003; 414:7-24.
8. Roesgen M, Hierholzer G, Hax PM. Post-traumatic osteomyelitis. Pathophysiology and management. Arch Orthop Trauma Surg 1989; 108(1):1-9.
9. Tumeh SS, Aliabadi P, Weissman BN, McNeil BJ. Disease activity in osteomyelitis: role of radiography. Radiology 1987; 165(3):781-4.
10. Ochsner PE, Sokhegyi A, Petralli C. The value of computerized tomography in the assessment of chronic osteomyelitis. (A radiological, histological and clinical correlation study). Z Orthop Ihre Grenzgeb 1990; 128:(3)313-8.
11. Mason MD, Zlatkin MB, Esterhai JL, Dalinka MK, Velchik MG, Kressel HY. Chronic complicated osteomyelitis of the lower extremity: evaluation with MR imaging. Radiology 1989; 173(2):355-9.
12. Kostenuik P, Mirza FM. Fracture healing physiology and the quest for therapies for delayed healing and nonunion. J Orthop Res 2017; 35(2):213-23.
13. Larsson S, Fazzalari NL. Anti-osteoporosis therapy and fracture healing. Arch Orthop Trauma Surg 2014; 134(2):291-7.
14. Sibai T, Morgan EF, Einhorn TA. Anabolic agents and bone quality. Clin Orthop Relat Res 2011 469(8):2215-24.
15. Rhinelander FW. Tibial blood supply in relation to fracture healing. Clin Orthop Relat Res 1974; 105:34-81.
16. Jewell E, Merrell G. The use of a sliding bone graft in the upper extremity for long bone nonunions. J Hand Surg Am 2015; 40(5):1025-7.
17. Egol KA, Nauth A, Lee M, Pape HC, Watson JT, Borrelli J Jr. Bone Grafting: Sourcing, Timing, Strategies, and Alternatives. J Orthop Trauma 2015; 29(S12):10-4.
18. Brinker MR, O'Connor DP. Management of Aseptic Tibial and Femoral Diaphyseal Nonunions Without Bony Defects. Orthop Clin North Am 2016; 47(1):67-75.
19. Paley D, Catagni MA, Argnani F, Villa A, Benedetti GB, Cattaneo R. Ilizarov treatment of tibial nonunions with bone loss. Clin Orthop Relat Res 1989; (241):146-65.
20. Cattaneo R, Catagni M, Johnson EE. The treatment of infected nonunions and segmental defects of the tibia by the methods of Ilizarov. Clin Orthop Relat Res 1992; 280:143-52.
21. Garcia-Cimbrelo, E. J.C. Marti-Gonzalez, Circular external fixation in tibial nonunions. Clin Orthop Relat Res 2004; 419:65-70.
22. Glass GE, Jain A. Cochrane corner: bone morphogenetic protein (BMP) for fracture healing in adults. J Hand Surg Eur Vol 2013; 38(4):447-9.
23. Virk MS, Lieberman JR.,Biologic adjuvants for fracture healing. Arthritis Res Ther 2012; 14(6):225.
24. Kuzin MI, Kostiuchenok BM, Matasov VM, Kuz'menko VV, Umiarov GA. (Treatment of open fractures with extensive soft tissue injury in a controlled abacterial environment). Ortop Travmatol Protez 1980; 11:1-4.

AUTOLOGOUS LIPOTRANSFER VERSUS STROMAL VASCULAR FRACTION ENRICHED LIPOINJECTION FOR DIABETIC FOOT WOUNDS HEALING: A PILOT STUDY

G. VICENTI, G. SOLARINO, V. PESCE, L. MORETTI, A. NOTARNICOLA, M. CARROZZO, F. RIFINO and B. MORETTI

Department of Basic Medical Sciences, Neuroscience and Sense Organs, Section of Human Anatomy and Histology, School of Medicine-University of Bari, Italy

Chronic ulcers of the lower limbs represent a significant social and economic burden. Diabetes is a strong risk factor for development of chronic lesions. Adult stem cells and growth factors derived from the adipose tissue are among the most promising therapeutic strategies for hard to heal wounds. Fat grafts have been used for several decades to treat soft tissue deformities, but despite its excellent characteristics, the outcome was unpredictable, due to partial necrosis and resorption of the graft. Stem cells' enrichment of these grafts or their injection into the edges of the ulcers have shown encouraging results in various experimental settings. In this pilot study, we compared the standard of care to autologous lipotransfer and stromal vascular fraction (SVF) enriched lipoinjection in 30 patients with diabetic foot ulcers, showing clear superiority of SVF enriched lipoinjection in terms of percentage of reduction of ulcers size and healing time.

Chronic wounds of the lower limbs affect up to 3% of the adult population and represent a significant social and economic burden (1). Diabetes, whose prevalence is swiftly increasing, is one of the major causes of chronic lower limbs ulcers because it makes foot injuries more likely, due to diabetic neuropathy and impairs healing processes by reducing neovascularization and tissue oxygenation, granulocytic function, collagen synthesis and extracellular matrix integrity (2).

Among the different emerging therapeutic strategies for hard to heal lesions, the use of stem cells holds great promise of damaged tissue repair (1). Considering the several issues regarding the use of embryonic stem cells, the scientific community has focused their attention on adult stem cells, usually resident in most of the tissues of the human body to ensure the physiological cycle of death of old cells and their replenishment (1). The accessibility and abundance of the adipose tissue have made adipose-derived stem cells a particularly interesting tool for regenerative medicine. The digestion of a sample of adipose tissue generates several cell types which are referred to as the stromal vascular fraction (SVF) and include adipose-derived stem cells (ASCs), fibroblasts, vascular smooth muscle cells, endothelial cells, macrophages and lymphocytes. ASCs account for approximately 30% of the cells composing the SVF. These multipotent cells are characterized by the ability to differentiate in cells not only from the mesodermal lineage, but also from the ectodermal (i.e. neuron-like cells) and endodermal (i.e. hepatic cells, pancreatic cells) lineages. Classically, upon adequate induction, ASCs are able to differentiate in adipocytes, chondrocytes and osteoblasts (3). Moreover, adipose-derived stem cells have great

Key words: stem cells, chronic ulcers, regenerative medicine, adipose tissue, stromal vascular fraction, autologous lipotransfer

Mailing address:
Vicenti Giovanni, MD, PhD,
University of Bari,
Piazza Giulio Cesare 11,
70124 Bari, Italy
Tel.: +39 3480128360
e-mail: dott.gvicenti@gmail.com

0393-974X (2017)

proliferative potential maintaining their genome stable throughout long-term cultures (3).

Specifically, the two main mechanisms by which ASCs enhance wound repair are differentiation in other cell types and paracrine activities. By both these mechanisms, ASCs stimulate re-epithelialization, angiogenesis and vascular stability, increasing blood and oxygen flow to the wound site, as demonstrated in studies conducted on animal and human models in which ASCs were intra-arterially, intra-venously, intramuscularly or topically delivered (1). Marino and colleagues showed that ASCs injection in the edge of the ulcers led to reduction in their depth and diameter and consequently pain attenuation in 20 patients affected from peripheral arterial disease (4).

In a mice model, Nambu et al. demonstrated that autologous ASCs transplantation was able to repair skin ulcers even in the presence of diabetes (5), which is known to impair ASCs efficacy in wound healing (6).

Fat grafting has been widely used since 1980 in both aesthetic and reconstructive medicine to treat deformities due to aging and different types of diseases. Fat is readily available, biocompatible, inexpensive and harvesting it does not provoke detectable scars on the donor site. All these characteristics make the adipose tissue the standard against which other regenerating strategies have to be compared (7). Despite the well-known efficacy of autologous fat injection on scarred tissue recovery (8), its use in chronic ulcers associated to the most common clinical conditions had been so far sporadic (9), therefore it is still difficult to draw conclusions. Interestingly, a prospective cohort study conducted on 30 diabetic patients showed that autologous lipotransfer improved diabetic foot wounds healing, when standard of care failed (9).

Nonetheless, autologous lipotransfer is still saddled with the partial necrosis of the injected adipose tissue and the following unpredictability of the outcome (10). Enriching the fat graft with adipose stem cells is supposed to enhance its survival and its healing properties (11). In particular, it has been recently demonstrated that autologous fat grafting for soft tissue defects had a better outcome if enriched with stromal vascular fraction (11).

In 2001, Zuk and colleagues were the first to come up with a protocol for ASCs isolation from an adipose tissue sample obtained during a liposuction procedure (12). Since then, a whole new field of the scientific research was dedicated to investigate the feasibility and safety of the several potential clinical applications of these adult stem cells; a significant number of clinical trials have been conducted, many of which are still ongoing (13).

Raposio et al. described a method of ASCs isolation from adipose tissue involving mechanical and enzymatic means (14). According to the Good Manufacturing Practice Guidelines this is considered minimal manipulation and is not restricted in Europe (15). This is not true in the United States, where the use of collagenase is not regarded as minimal manipulation and the ASCs isolated according to this protocol are considered a drug and their use regulated by the Food and Drug Administration (1). Hence, the need for isolation protocols requiring minimal handling and avoiding the enzymatic digestion step. Several automated and semi-automated systems are currently under development, with only a few already commercially available (16).

Recently, the scientific community has questioned the regenerative potential of the SVF compared to ASCs alone. For example, in one of the few research works describing a head-to-head comparison between them, SVF has shown a significantly better improvement of erectile function in a rat model of cavernous nerve injury (17). Notably, SVF is easier to obtain because it does not require any cell separation nor specific culturing conditions (16). Moreover, the heterogeneity of the cells composing the stromal vascular fraction might provide the explanation for SVF better immunomodulatory, angiogenetic and anti-inflammatory activities (16). Chae et al. underlined that human SVF cells, obtained from subcutaneous fat of healthy donors, exhibited higher expression of wound healing or epithelium development related genes and higher cell migration compared to cultured ASCs (18).

Despite the broad healing potential of the SVF of the adipose tissue, little is known in literature about its effects on chronic wounds in diabetic patients. Therefore, we decided to compare the standard of

care to autologous lipotransfer and SVF enriched lipoinjection.

MATHERIALS AND METHODS

From January 2016 to January 2017, 30 diabetic patients admitted to the orthopedic ward for refractory foot ulcers were recruited to this pilot study. All the patients gave informed consent to participate.

The study population was composed of 21 men and 9 women, aged between 43 and 82, 14 patients were obese and the others were overweight (Table I).

Eligibility criteria were acceptable glycemic control (glycated hemoglobin <8%), grade IID ulcers according to the University of Texas Diabetic Wound Classification System (19), chronic foot ulcer refractory to at least two months of standard of care consisting of offloading, debridement, advanced wound dressings, vacuum-assisted closure and revascularization. Exclusion criteria were an ulcer surface area larger then 10 cm^2, feasibility of other standard procedures, uncontrolled diabetes. Average wound size was 6.27±2.31 cm^2. Ulcer debridement was the first step in every treatment group. Ten patients were randomly assigned to continue the standard of care (Group 1), ten patients were treated with autologous lipotransfer (Group 2) and the remaining ten patients underwent SVF enriched lipoinjection (Group 3). Wound swab and biopsy were taken when necessary, to rule out the presence of infection and cancerous tissue.

Autologous lipotransfer (20) consisted in transferring the lipoaspirate harvested from the upper thigh or the lower abdomen into the ulcer bed. The harvested amount of fat accounted for approximately 2 ml of lipoaspirate for each square centimeter of the wound surface. The donor area was first infiltrated with a tumescence solution composed of lidocaine and sodium chloride 0.9%, in order to avoid hemorrhages and perioperative pain. Fat harvesting was then performed with a blunt cannula connected to a 20

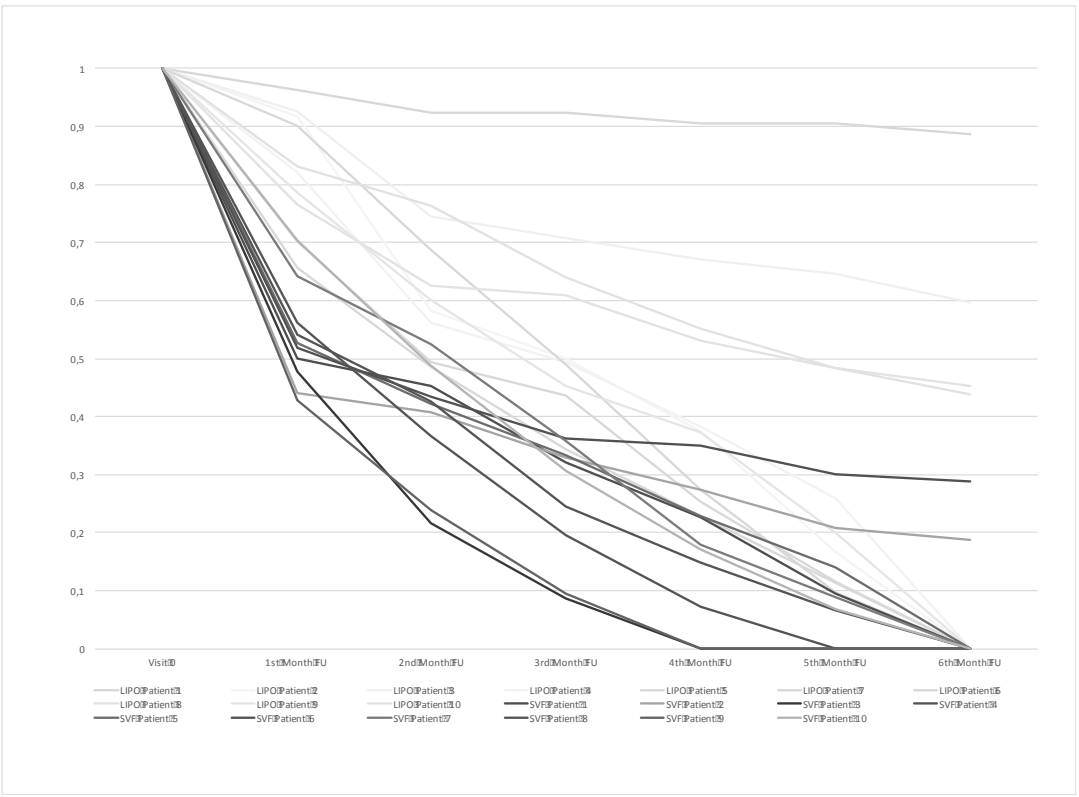

Fig. 1. *Comparison of percentage of wound size reduction over the 6 month-follow-up period in Group 2 and Group 3.*

Table I. *Characteristics of patients in Group 1, Group 2 and Group 3.*

Patient	Age (years)	BMI (kg/m^2)	Initial Wound Area (cm^2)	6-Month FU Wound Area
Group 1: Standard of Care				
1. Man	48	26	5.8	7
2. Woman	77	33	8.3	9
3. Man	68	29	2.8	2.6
4. Man	43	27	6.7	8.3
5. Woman	71	38	7.9	8.9
6. Man	52	30	8.1	9.5
7. Man	69	28	3.5	3.2
8. Man	80	34	5.3	7.8
9. Woman	65	27	2.1	0
10. Man	76	32	9.6	11.5
Group 2: Autologous Lipotransfer				
1. Woman	71	31	5.3	4.7
2. Man	62	34	2.4	0
3. Man	54	37	8.2	4.9
4. Man	81	26	7.3	0
5. Man	53	27	5.1	0
6. Man	57	26	8.7	0
7. Man	60	32	3.5	0
8. Woman	82	41	6.4	2.9
9. Woman	66	27	7.5	0
10. Man	73	26	8.9	3.9
Group 3: Stromal Vascular Fraction Enriched Lipoinjection				
1. Man	70	38	8.4	0
2. Man	69	40	9.1	1.7
3. Woman	55	26	2.3	0
4. Man	49	29	4.1	0
5. Woman	72	36	5.7	0
6. Man	68	34	8.3	2.4
7. Man	63	27	7.8	0
8. Man	56	26	6.1	0
9. Man	80	28	4.2	0
10. Woman	67	29	8.8	0

ml Luer Lock syringe, with the plunger of the syringe pulled at the top during the procedure, to generate a slightly negative pressure to ease the lipoaspiration. The cannula was advanced and retracted with radial movement inside the harvesting area. The fat was then centrifuged at 3000 rpm for 3 min. The intermediate layer obtained with centrifugation is the only one with therapeutic applications. This layer was in fact transferred to 2.5 ml syringes using a closed system and injected into the borders and the bottom of the ulcers. Finally, a vacuum-assisted closure dressing was applied.

In this study, MyStem® kit (MyStem LLC, Wilmington, Del.) was used to enrich the autologous lipoaspirate with the stromal vascular fraction. This already commercially available kit allows a fast, one-step, non enzymatic procedure for SVF isolation. Four ml of adipose tissue for each square centimeter of the wound area, instead of two ml, was harvested because of the waste product obtained with this technique. Fat was collected with the same procedure described above, using the dedicated cannula provided in the kit and then infused in a sterile closed device. This device is composed of a fluidic system with mesh filters, flexible collection bags, Luer Lock connectors for syringes from which the washing buffer solution and the separated tissue fraction are collected. This process doesn't require centrifugation or other time consuming procedures, it has a low risk of contamination and it's highly reproducible (21).

A study conducted by Cicione and colleagues confirmed that MyStem® was able to retrieve a lipoaspirate fluid rich of adipose stem cells and trophic factors (21). This lipoaspirate was then injected into the ulcers. The ulcers were clinically evaluated monthly for up to 6 months. The primary objective of the study was complete wound closure; the secondary objective was reduction of the ulcer diameter.

RESULTS

The groups were quite homogeneous regarding demographic and clinical features. All patients completed the study and participated to every follow-up visit.

Among the patients who continued the standard of care, only one achieved wound healing. Instead, two of them made no improvement, whereas in the rest of the patients the wound area increased of averagely 1.5 cm^2 (Table I). Notably, the only patient in which an improvement was recorded was the one with the smaller wound size.

Far better results were achieved in the group receiving autologous lipotransfer. Six patients reached complete wound closure and four displayed reduction of the wound area of -3.1 ± 1.8 cm^2. According to previous works, a 50% reduction of the ulcer size was observed approximately after two months in most of the patients (Fig. 1).

Finally, patients undergoing SVF enriched lipoinjection showed the most encouraging results. All patients exhibited entirely closed wounds at the last visit of the follow up period, except two patients who still showed significant reduction of the ulcer area (-6.65 ± 1.1 cm^2). A 50% reduction of the wound size was recorded after one month from the procedure (Fig. 1).

DISCUSSION

Discovery of new and appropriate treatment strategies for hard to heal wounds is mandatory given their high social and economic costs and the widespread diffusion of predisposing chronic diseases such as diabetes. Non healing ulcers may require amputation, thus leading to reduced quality of life, increased risk of ailments and, finally, mortality (22).

Tissue engineering and regenerative medicine are the scientific fields aiming to resolve this issue. Being broadly available for harvesting, adult stem cells derived from the adipose tissue are among the most promising tools for wound healing.

In fact, the regenerative potential of fat grafts might be explained by the presence of these adipose stem cells and adipokines like leptin and adiponectin, as it can be inferred from studies concerning their topical application on full-thickness wounds in animal models (9, 23).

Accordingly to Stasch and collegues (9), the outcome of autologous lipotransfer was satisfactory, but the results obtained with the SVF enriched lipoinjection were even more exciting. Therefore, it should be advisable to appeal to SVF or adipose stem cells at least in the most complicated cases.

Is it not yet clear whether it is more convenient to use adipose stem cells or the whole stromal vascular fraction, to exploit its growth factors and immunomodulatory abilities (16).

For merely practical reasons, we chose to use an already available kit able to isolate the adipose stromal vascular fraction. As far as our knowledge goes this is the first time a comparison between this system and autologous lipotransfer has been made concerning their efficacy in treating diabetic foot ulcers. As predictable, despite the scarce sample size, adipose SVF has been compared to standard of care and to fat graft transfer with outstanding results.

New devices providing fast, safe and inexpensive isolation of stem cells are highly anticipated, in order to extend these treatment strategies to the vast majority of patients and therefore reduce complications and costs associated with diabetic foot and chronic ulcers.

Further studies are needed to compare SVF and ASCs in this setting and in many others and investigate the use of adipose stem cells and stromal vascular fraction combined with different scaffolds or platelet rich plasma in the same experimental conditions.

REFERENCES

1. Bertozzi N, Simonacci F, Grieco MP, Grignaffini

E, Raposio E. The biological and clinical basis for the use of adipose-derived stem cells in the field of wound healing. Ann Med Surg 2017; 20:41-8.
2. Tsourdi E, Barthel A, Rietzsch H, Reichel A, Bornstein SR. Current aspects in the pathophysiology and treatment of chronic wounds in diabetes mellitus. Biomed Res. Int. 2013; 2013:385641.
3. Lindroos B, Suuronen R, Miettinen S. The Potential of Adipose Stem Cells in Regenerative Medicine. Stem Cell Rev 2011; 7(2):269-91.
4. Marino G, Moraci M, Armenia E, et al. Therapy with autologous adipose-derived regenerative cells for the care of chronic ulcer of lower limbs in patients with peripheral arterial disease. J Surg Res 2013; 185:36-44.
5. Nambu M, Kishimoto S, Nakamura S, et al. Accelerated Wound Healing in Healing-Impaired db/db Mice by Autologous Adipose Tissue-Derived Stromal Cells Combined With Atelocollagen Matrix. Ann Plast Surg 2009; 62:317-21.
6. Cianfarani F, Toietta G, Di Rocco G, Cesareo E, Zambruno G, Odorisio T. Diabetes impairs adipose tissue-derived stem cell function and efficiency in promoting wound healing. Wound Repair Regen 2013; 21:545-53.
7. Kakagia D, Norbert P. Autologous Fat Grafting. Surg Innov 2014; 21:327-36.
8. Wazer DE. 4-45 Clinical treatment of radiotherapy tissue damage by lipoaspirate transplant: a healing process mediated by adipose-derived adult stem cells. Breast Dis 2008; 18:393-4.
9. Stasch T, Hoehne J, Huynh T, De Baerdemaeker R, Grandel S, Herold C. Débridement and autologous lipotransfer for chronic ulceration of the diabetic foot and lower limb improves wound healing. Plast Reconstr Surg 2015; 136(6):1357-66.
10. Matsumoto D, Sato K, Gonda K, et al. Cell-assisted lipotransfer: supportive use of human adipose-derived cells for soft tissue augmentation with lipoinjection. Tissue Eng 2006; 12:3375-82.
11. Yoshimura K, Sato K, Aoi N, et al. Cell-assisted lipotransfer for facial lipoatrophy: Efficacy of clinical use of adipose-derived stem cells. Dermatologic Surg 2008; 34:1178-85.
12. Zuk, PA E Al. Multilineage cells from human adipose tissue: implications for cell-based therapies. Tissue Eng 2001; 7:211-28.
13. De Francesco F, Ricci G, D'Andrea F, Nicoletti GF, Ferraro GA. Human adipose stem cells: from bench to bedside. Tissue Eng - Part B Rev 2015; 21:572-84.
14. Raposio E, Caruana G, Petrella M, Bonomini S, Grieco MP. A standardized method of isolating adipose-derived stem cells for clinical applications. Ann Plast Surg 2015; 0:1.
15. Banyard DA, Salibian AA, Widgerow AD, Evans GRD. Implications for human adipose-derived stem cells in plastic surgery. J Cell Mol Med 2015; 19:21-30.
16. Bora P, Majumdar AS. Adipose tissue-derived stromal vascular fraction in regenerative medicine: a brief review on biology and translation. Stem Cell Res Ther 2017;
17. You D, Jang MJ, Kim BH, et al. Comparative study of autologous stromal vascular fraction and adipose-derived stem cells for erectile function recovery in a rat model of cavernous nerve injury. Stem Cells Transl Med 2015; 4:351-8.
18. Chae DS, Han S, Son M, Kim SW. Stromal vascular fraction shows robust wound healing through high chemotactic and epithelialization property. Cytotherapy 2017; 19(4):543-54.
19. Armstrong DG, Lavery LA, Harkless LB. Validation of a diabetic wound classification system. Diabetes Care 1998; 21:855-9.
20. Klinger M, Lisa A, Klinger F, et al. Regenerative approach to scars, ulcers and related problems with fat grafting. Clin Plast Surg 2015; 42:345-52.
21. Cicione C, Di Taranto G, Barba M, et al. In vitro validation of a closed device enabling the purification of the fluid portion of liposuction aspirates. Plast Reconstr Surg 2016; 137:1157-67.
22. Wilbek TE, Jansen RB, Jorgensen B, Svendsen OL. The diabetic foot in a multidisciplinary team setting number of amputations below ankle level and mortality. Exp Clin Endocrinol Diabetes 2016; 124:535-40.
23. Shibata S, Tada Y, Asano Y, et al. Adiponectin regulates cutaneous wound healing by promoting keratinocyte proliferation and migration via the ERK signaling pathway. J Immunol 2012; 189:3231-41.

SCANNING ELECTRON, 3D-CONFOCAL AND STEREOTACTIC MICROSCOPIES MORPHO-STRUCTURAL ANALYSIS OF ANTIBIOTIC-LOADED CEMENT POROSITY IN THREE DIFFERENT FORMULATIONS

D. FENGA[1], A. CANTIVALLI[1], O.D. JOAQUIN[1], A. FAVALORO[2], G. VERMIGLIO[2] and M.A. ROSA[1]

[1]Department of Biomedical and Dental Sciences and Morphofunctional Imaging, Orthopaedic and Traumatology Section, Policlinico Universitario "G. Martino", Messina, Italy; [2]Department of Biomedical and Dental Sciences and Morphofunctional Imaging, Anatomy section, Policlinico Universitario "G. Martino", Messina, Italy

Chronic osteoarticular infections such as osteomyelitis or periprosthetic joint infection (PJI) have become a growing problem over the years. The "gold standard" in local antibiotic administration is still the antibiotic-loaded acrylic bone cement (ALABC) which is used in both prophylaxis, because it has been shown it can reduce the risk of infection and used in therapy during a "two-stage surgery" in PJI or in chronic osteomyelitis. We performed morphological analysis of three different formulations of antibiotic-loaded cement (ALABC) using techniques of light microscopy, scanning electron microscopy (SEM) and 3D immunofluorescence, in order to explain how the morphological aspects of cement could influence and modulate antibiotic elution.

One of the most common complications in orthopedic surgery is represented by deep bacterial infection such as chronic osteoarticular infections such as osteomyelitis or periprosthetic joint infection (PJIs) (1, 2). The presence of implants or prosthesis facilitate bacterial infection mainly in open surgery procedures and the local antibiotic administration in association with a systemic antibiotic therapy represents the most useful instrument against infection (1, 2)..

The "gold standard" in local antibiotic administration is the antibiotic-loaded acrylic bone cement (ALABC) which is widely used in surgical practice both in prophylaxis and therapy of PJIs because it has been shown that its use can reduce the risk of infection (2- 5).

The success of ALABC mainly depends on its morphological feature as its porosity that increases the exchange surface enhancing the antibiotic release (6, 7).. Moreover, ALABC has important mechanical properties such as resistance to strength compression, so it is also used as a temporary spacer in infected arthroplasty (7-9). In fact, in PJIs, the gold standard is the two-step surgery, which consists of replacing the infected implant with an antibiotic-loaded spacer and after 8-12 weeks, removing the spacer in order to use a definitive prosthesis (5)..

Recently, several modifications in ALABC properties, such as changing the mixing method, the environmental conditions at mixing (temperature, humidity etc.), the type of antibiotic and methods to modify the porosity have been proposed with the aim of enhancing and accelerate antibiotic elution capability (10-13).. Although several studies have focused on these modifications, it is universally recognized that viscosity, porosity and antibiotic

Key words: cement, antibiotic, elution, microscopical analysis

Mailing address:
Prof. Michele Attilio Rosa
Via Consolare Valeria 1,
98122 Messina, Italy
Tel.: +39 3386629847
Fax: +39 0902213052
e-mail: mattilio51@gmail.com

0393-974X (2017)

concentration are the keys to change the amount of antibiotic released (6, 14, 15)..

Most of the works are performed with biochemical and mechanical analysis in order to evaluate the amount of the antibiotic released, the inhibition of bacterial growth and the mechanical property of the cement, but few reports focused on morphological and structural aspects of ALABC (16-20).

In the present study, we performed morphological analysis of three different formulations of antibiotic-loaded cement (ALABC) using techniques of light microscopy, scanning electron microscopy (SEM) and 3D immunofluorescence, in order to explain how the morphological aspects of cement could influence and modulate antibiotic elution.

MATERIALS AND METHODS

Samples preparation

The 3 different formulations were obtained by changing the order of mixing of the parts which usually make up the cement and using the Vancomicin antibiotic (Hospira, ABBOT), 1 g powder. The cement used was G1-40 (G21 Srl), 40 g, standard viscosity. Within each individual pack of cement there is a phial consisting of methyl methacrylate (MMA) and N.N dimethyl-P-toluidine (DMPT) along with a bag of powder made from polymethyl-methacrylate (PMMA) and benzoyl peroxide (BPO). Sample preparation took place in the operating room in order to maintain maximum sterility of the compounds.

The various components were added in a bowl through 3 different mixing methods. Each sample was modeled using a 5 ml syringe mold and then cut into a cylindrical shape. All samples had equal shape and size. The three samples were mixed in this sequence (14):

sample #1: vancomycin (powder) 4 g + solvent (MMA+DMPT) + cement powder (PMMA+BPO) 40 g.

sample #2: vancomycin (powder) 4 g + saline (4ML) + cement powder (PMMA+BPO) 40 g + solvent (MMA+DMPT)

sample #3: vancomycin (powder) 4g + cement powder (PMMA+BPO) 40 g + solvent (MMA+DMPT)

Stereotactic Optical microscopy

Samples were broken through brittle fractures and the obtained pieces were observed at OM-Hirox digital microscope KH 8700. During the observation of the three specimens, we focused our attention on micro and macro-pores measuring the diameter in μm.

Scanning electron microscopy

The fractured surfaces of the cement were mounted onto stub supports (Tousimis, Rockville, MD, USA) and platinum coated with a Plasma Sciences CrC-100 Turbo-Pumped sputtering system (Electron Microscopy Sciences, Hatfield, PA, USA). Samples were observed using a Phenom G2 Pro scanning electron microscope (Phenom-World B.V., Eindhoven, Netherlands) and the selected images were captured at high resolution (21).

Immunofluorescence

Indirect immunofluorescence reaction was performed on 50μm section of cement obtained by LEICA RM2265 microtome. Single localization reactions have been performed using mouse monoclonal anti-Vancomycin antibody (1:250 dilution; Thermo Scientific). The samples were incubated with primary antibody at room temperature for 2 h; after three rinses with PBS, primary antibody was demonstrated with Texas-Red-conjugated IgG anti mouse (1:100 dilution; Jackson ImmunoResearch Laboratories, West Grove, Pa) and applied for 1 h at room temperature. Finally, the slides were washed in PBS and sealed with mounting medium. Samples were observed with a Zeiss LSM 510 confocal microscope equipped with Argon laser (458 nm and 488 nm λ) and 2 HeNe laser (543 nm and 633 nm λ).

All images were digitized at a resolution of 8 bits into an array of 2048 x 2048 pixels. Optical sections of fluorescence specimens were obtained at 488 nm λ, at 62/s scanning shipped with up to 8 repetitions on average. The pinhole was set for optimal resolution.

RESULTS

Sample #1

Results obtained by optical microscopy observation shows that the sample of cement #1 is characterized by a structure made up of microporosity and the pores are not well defined even by high magnification (Fig. 1A, B). Scanning electron microscopy allowed to observe an irregular

surface with the presence of dust conglomerates which were not be blended with the mixture and the presence of small size pores (Fig. 2A).

Immunofluorescence results and confocal microscopy 3D image reconstructions show a cement structure characterized by small size pores that are connected by medium size canals. Fluorescence pattern for vancomycin antibody was detected at high level within the pores and canals systems (Fig. 3A)

Sample #2

Through optical microscopy, the structure of the cement of sample #2 appears to have a regular surface and big size macropores (Fig. 1C) with an average size of 235 micrometers (Fig. 1D, blue arrow). Scanning electron microscopy images confirm the existence of a regular surface and of big size pores along cement surface (Fig. 2B). Even in these samples, non-blended dust conglomerates are detectable. Immunofluorescence results and confocal microscopy 3D image reconstruction show the presence of big size pores that are connected by medium size channels. Vancomicyn staining pattern was mainly localized inside the pores and the channels (Fig. 3B).

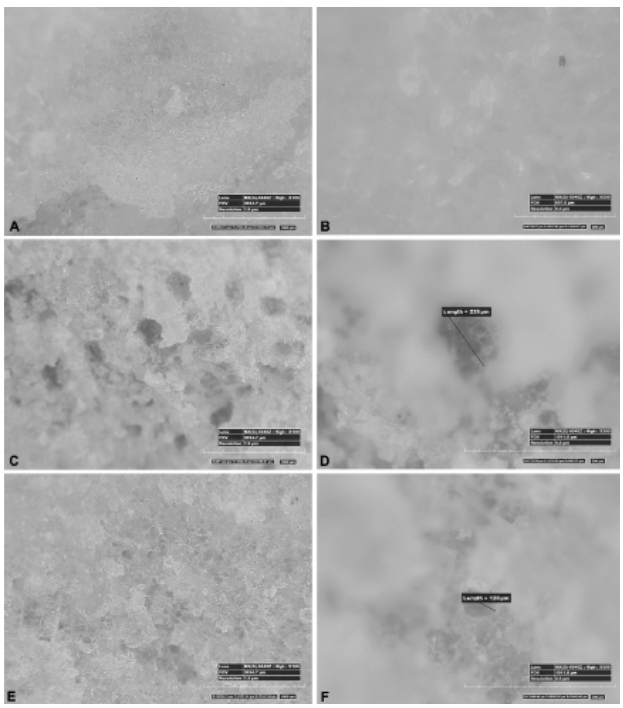

Fig. 1.. *Compound panel of six images of cement obtained by optical microscopy. The **A** image shows sample **#1** which appears very compact with a tight ultrastructural net; the pores are difficult to define by this technique even by high magnification (**B**). Sample **#2** image shows the presence of evident macro-pores (**C**) and the mean size of the pore is 235 micrometers (blue arrow-**D**). Sample **#3** image shows the presence of pores which are bigger than sample **#1** but that are smaller than sample **#2** (**E**); the mean size of the pore is 120 micrometer (**F**).*

Sample #3

Optical microscopy results of sample #3 show a regular surface of cement and the presence of medium size pores which are smaller than the pores of sample #2 (Fig. 1E, F). Scanning electron microscopy results show compact and regular structure within which are located pores (Fig. 2C). Immunofluorescence results and confocal microscopy 3D image reconstruction highlight the presence of pores that are bigger than sample #1 and which are connected with each other without a well-defined canal structures. The fluorescence pattern of vancomycin antibody within the pores appears to be lower than sample #1 (Fig. 3C).

DISCUSSION

It is now accepted in the scientific community that ALABC porosity is the most important feature capable of modifying the release of antibiotic and that the increase of porosity determines an increase of drug release (15, 9, 13).

For this reason, over time, many studies were carried out in order to create a more porous dough capable of releasing more antibiotic for as long as possible (10). Through this study, we want to evaluate the microscopic structure of three different methods to find out why different mixture techniques change the drug elution and moreover, we want to show the different pore sizes that we can obtain by modifying the dough.

In the images obtained by the different microscopy techniques, we discovered peculiar features of the 3 samples. Sample number 1 has a marked microporosity, few compact areas and the texture is extremely irregular. The pores, observed through SEM technique, are very small but extremely numerous, this creates an abnormal increase of

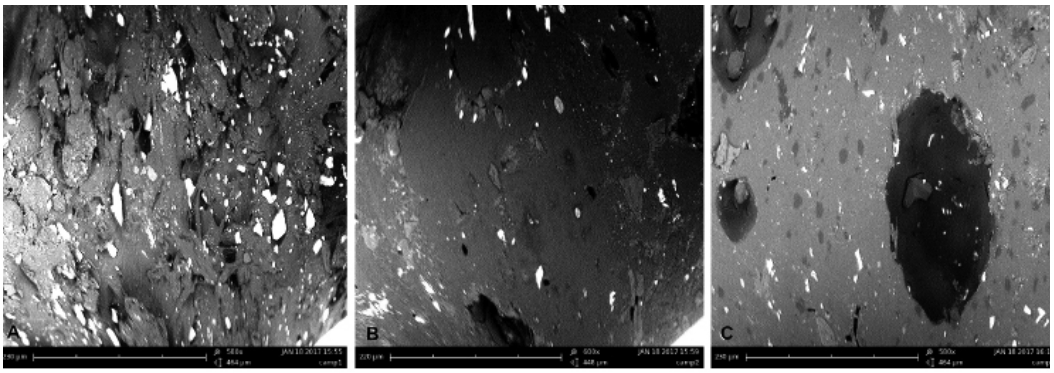

Fig. 2.. *Compound panel of 3 images of cement obtained by scanning electron microscopy. Image of sample* ***#1*** *show that the cement is characterized by microporosity and by the presence of irregular surface; it is also possible to observe conglomerates of dust which are not well blended with the mixture* ***(A)****. In the sample* ***#2*** *it is possible to observe macropores which are bigger than sample* ***#1*** *and it is also evident the presence of dust conglomerates* ***(B)****. Macropores of sample* ***#3****, which are smaller than sample* ***#2*** *and conglomerates of not blended dust* ***(C)****.*

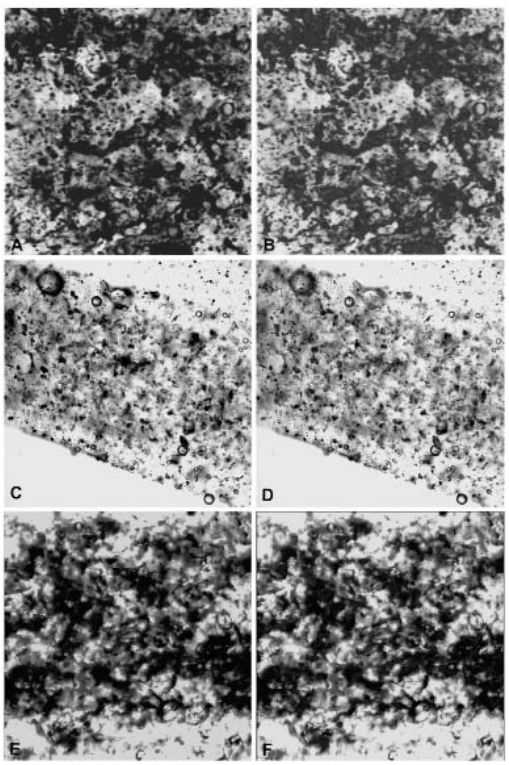

Fig. 3.. *Compound panel of 6 images of cement obtained by immunofluorescence technique.* ***(A)*** *3D image of sample* ***#1*** *shows structure of the cement that is characterized by the presence of micropores that are connected by medium sized canals; in* ***B*** *vancomycin antibody fluorescence pattern (red channel) is mainly localized inside pores and canals at high level.* ***(C, D #2)****.* ***(E)*** *3D image of sample* ***#3*** *show a structure characterized by macropores that seem to communicate directly with each other without a well-defined canals structure; it is possible to observe a weak fluorescence pattern for vancomycin antibody (red channel) inside pores* ***(F)***

exchange surface and *in vitro* it could determine the increasing of elution of antibiotic (14)..

Sample number 2 shows a macroporosity (pore diameter >200 micrometers) but also lots of compact areas which probably do not release antibiotic according to immunofluorescence images in which we can see Vancomycin monoclonal antibody bound to these areas, and not in the channels. Sample number 3 follows the conditions of sample number 2 even though porosities are smaller and the areas of compactness larger, as is evident by light microscope..

All this is explained through the mixing technique. In fact, sample 2 contains Vancomycin solubilized with saline solution that, once evaporated even through heat generated by polymerization reaction, leaves more porosity. In fact, sample 2 has dimensionally greater porosity than sample 3, in addition to the smaller extension of the areas of compactness. For sample 1, the most plausible explanation is that by dissolving the Vancomycin in monomer (solvent) we create intermediate compounds with hydrogen bonds or Wan der Waals bonds that steal monomer to polymerization reaction. This could be confirmed with the solidification time of sample 1 that is up to 5 min longer than sample 2 and 3.

This is due to the fact that having fewer monomer initiator, the reaction starts slower although it, too polymerizes after a longer time. After the

polymerization, both the heat released from the compound and the immersion in PBS (*in vitro*) to evaluate the elution or in bone (*in vivo*), could break bonds and create a progressive cleavage of the cement, exposing more and new dispersant surface and free the antibiotic released from the bond-breaking. This is also evident from a macroscopic analysis because the sample shows internal exfoliation, macro-galleries and a rougher look.

The results obtained by the pictures shows how the mixture tecnique deeply changes the ultrastructure of ALABC. In the first sample in fact, the microporosity and the alteration of the surface could explain the greater elution of antibiotics while minor macro-porosity in the other 2 samples could explain why they have a lower elution.

It is important to highlight how this could be due not only to the areas of porosity, but also to the compactness of areas that could negatively influence the antibiotic elution, trapping it without possibility of release. This can be confirmed by immunofluorescence images that show us how the antibiotic is released only through the channels that we, in section, see as pores. It is essential, in the future, considering the biomechanical characteristics of cement to ensure an optimal use *in vivo*..

REFERENCES

1. Zalavras CG, Patzakis MJ, Holtom P. Local antibiotic therapy in the treatment of open fractures and osteomyelitis. Clin Orthop 2004; (427):86-93.
2. Hanssen AD: Local antibiotic delivery vehicles in the treatment of musculoskeletal infection. Clin Orthop Relat Res 200; (437):91-6.
3. Bourne RB.. Prophylactic use of antibiotic bone cement: an emerging standard--in the affirmative. J Arthroplasty 2004; 19:69-72.
4. Bistolfi A, Massazza G, Verné E, et al. Antibiotic-loaded cement in orthopedic surgery: a review. ISRN Orthop 2011; 2011:290851
5. Philadelphia_Consensus.pdf.
6. Shiramizu K, Lovric V, Leung A, Walsh WR. How do porosity-inducing techniques affect antibiotic elution from bone cement? An in vitro comparison between hydrogen peroxide and a mechanical mixer. J Orthop Traumatol 2008; 9:17-22.
7. Persson C, Baleani M, Guandalini L, Tigani D, Viceconti M. Mechanical effects of the use of vancomycin and meropenem in acrylic bone cement. Acta Orthop 2006; 77:617-21.
8. Pelletier MH, Malisano L, Smitham PJ, Okamoto K, Walsh WR. The compressive properties of bone cements containing large doses of antibiotics. J Arthroplasty 2009; 24:454-60.
9. Paz E, Sanz-Ruiz P, Abenojar J, Vaquero-Martín J, Forriol F, Del Real JC. Evaluation of Elution and Mechanical Properties of High-Dose Antibiotic-Loaded Bone Cement: Comparative "In Vitro" Study of the Influence of Vancomycin and Cefazolin. J Arthroplasty 2015; 30:1423-9.
10. Chang Y, Tai C-L, Hsieh P-H, Ueng SWN. Gentamicin in bone cement: A potentially more effective prophylactic measure of infectionin joint arthroplasty. Bone Jt Res 2013; 2:220-6.
11. Chang YH, Tai CL, Hsu HY, Hsieh PH, Lee MS and Ueng SWN: Liquid antibiotics in bone cement: an effective way to improve the efficiency of antibiotic release in antibiotic loaded bone cement. Bone Jt Res 2014; 3:246-51.
12. Chen DW, Chang Y, Hsieh P-H, Ueng SWN, Lee MS. The influence of storage temperature on the antibiotic release of vancomycin-loaded polymethylmethacrylate. ScientificWorldJournal 2013; 573526:2013.
13. Lee AJC, Ling RSM, Gheduzzi S, Simon J-P, Renfro RJ. Factors affecting the mechanical and viscoelastic properties of acrylic bone cement. J Mater Sci Mater Med 2002; 13:723-33.
14. Fenga D, Currò M, Rosi M, Ortolà DJ, Cantivalli A, Ientile R, Rosa MA.. Quantitative study on Vancomycin release from cement in 3 different formulations: preliminary results and antimicrobial activity. J Biol Regul Homeost Agents 2016; 30:229-35.
15. McLaren AC, McLaren SG, Hickmon MK. Sucrose, xylitol, and erythritol increase PMMA permeability for depot antibiotics. Clin Orthop 2007; 461:60-3.
16. Chang Y, Chen W-C, Hsieh P-H, Chen DW, Lee MS, Shih H-N, Ueng SWN. In Vitro Activities of Daptomycin-, Vancomycin-, and Teicoplanin-Loaded Polymethylmethacrylate against Methicillin-

Susceptible, Methicillin-Resistant, and Vancomycin-Intermediate Strains of Staphylococcus aureus. Antimicrob Agents Chemother 2011; 55:5480-84.
17. Gasparini G, De Gori M, Calonego G, Della Bora T, Caroleo B, Galasso O. Drug elution from high-dose antibiotic-loaded acrylic cement: a comparative, in vitro study. Orthopedics 2014; 37:e999-1005.
18. Bunetel L, Segui A, Cormier M, Percheron E, Langlais F. Release of gentamicin from acrylic bone cement. Clin Pharmacokinet 1989; 17:291-7.
19. Andollina A, Bertoni G, Bertoni F, et al. Vancomycin and meropenem in acrylic cement: elution kinetics of in vitro bactericidal action. Chir Organi Mov 2008; 91:153-8.
20. Cerretani D, Giorgi G, Fornara P, et al. The in vitro elution characteristics of vancomycin combined with imipenem-cilastatin in acrylic bone-cements: a pharmacokinetic study. J Arthroplasty 2002; 17:619-6.
21. Rosa MA, Gugliandolo P, Favaloro A, Vermiglio G, Centofanti A, Bruschetta D, Rizzo G. Morpho-structural alterations of sub-chondral bone tissue in patients with osteoarthritis: a scanning electron microscopy study. Ital J Anat Embryol Arch Ital Anat Ed Embriologia 2015; 120:71-81.

POSTEROLATERAL BUNDLE RECONSTRUCTION OF THE ANTERIOR CRUCIATE LIGAMENT TO RESTORE ROTATIONAL STABILITY OF THE KNEE

G. VADALÀ, S. PETRILLO, F. BUSCHINI, R. PAPALIA and V.DENARO

Department of Orthopaedic and Trauma Surgery, Università Campus Bio-Medico di Roma, Italy

Only 5-10% of partial tears of the anterior cruciate ligament (ACL) are symptomatic, especially in high demand individuals or in patients practicing sports requiring rotational motions.. A certain preoperative diagnosis of this condition is challenging and often needs the combination of clinical examination, magnetic resonance imaging (MRI) and knee-laxity tool measurements. However, the arthroscopic examination of the torn ACL bundle is the most important factor in decision-making. Evidence in various studies have shown that the preservation of the ACL remnant and its surgical augmentation can bring important advantages in terms of vascularity and proprioception, resulting in better outcomes. The purpose of our paper was to describe the surgical technique of arthroscopic posterolateral (PL) bundle reconstruction with the preservation of the anteromedial (AM) bundle for ACL partial tears. Moreover, we reported the current knowledge about rationale, diagnosis and treatment of partial tears of ACL.

Partial tears of the anterior cruciate ligament (ACL) are common in the population, accounting for 10-28% of all ACL tears (1). However, only 5-10% of these lesions are symptomatic, especially in young patients involved in sports requiring jumping or rotational motions (1). The diagnosis of this type of lesion of the ACL is often difficult and still challenging, requiring a combination of careful clinical examination, adequate magnetic resonance imaging (MRI), and knee-laxity tool measurements. However, a certain diagnosis can be achieved only through arthroscopy (2).

The ACL is made of two bundles, the anteromedial (AM) and the posterolateral (PL) (2). Each bundle contributes separately toward stabilizing the knee and injure separately, depending on the knee flexion angle at the time of trauma and the different reciprocal tension pattern between the two bundles (3). From a biomechanical viewpoint, the AM bundle fibres are tight between 30 and 130° of knee flexion and are the primary restraint against anterior tibial translation in flexion; PL bundle fibres are completely tight in full extension and play a role controlling rotational stability. Although both bundles contribute to anterior-posterior stability, only the PL bundle controls the rotational stability of the knee (4).

In case of ACL tear, a standard arthroscopic reconstruction is usually carried out sacrificing the residual portion of the ACL, to avoid intercondylar notch overstuffing and to prevent impingement or extension lag (5). However, in the last decades, several anatomical and biomechanical studies provided better knowledge about correct knee ligament insertions and the functions of the two ACL bundles (5). Modifications in the technique of ACL reconstruction with the emergence of double-bundle and anatomical reconstruction were then

Key words: ACL reconstruction, knee rotational stability, partial ACL tears, postero-lateral bundle, ACL augmentation.

Mailing address:
Gianluca Vadalà, MD, PhD,
Department of Orthopedic and Trauma Surgery,
Università Campus Bio-Medico di Roma
Via Alvaro del Portillo 200,
00128 Rome, Italy
Tel.: +39 06 22 54 11613 - Fax: +39 06 22 54 11638

0393-974X (2017)

developed. Furthermore, a selective single bundle reconstruction with preservation of the intact ACL bundle (selective augmentation technique) in case of partial tears was described (6). In particular, since the restoration of the biomechanical function is essential for the knee kinematic, keeping ACL intact bundle and reconstructing only the injured bundle could be advantageous in restoring knee stability and maintaining the proprioceptive function of the ligament. Excellent results have been reported in literature after selective anteromedial (AM) bundle reconstruction but only few studies reported the outcomes of PL bundle reconstruction with preservation of the AM remnant (7, 8).

The purpose of this study was to describe the surgical technique of arthroscopic PL bundle reconstruction with the preservation of the AM bundle for ACL partial tears. Moreover, we reported the current knowledge about rationale, diagnosis and treatment of partial tears of ACL.

Surgical technique

Under spinal anaesthesia, the patient is placed supine on the operating table and a tourniquet is positioned on the proximal region of the thigh. The lower limb is fixed in a leg holder allowing full extension-flexion range of motion of the knee.

Diagnostic arthroscopy

The diagnostic arthroscopy should start performing a standard anterolateral portal close to patellar tendon and a low AM portal.. A careful inspection of the knee can be easily made through these portals using a probe, looking for meniscal/chondral lesions, or capsular deficiencies. A debridement of the anterior fat pad could allow a better visualization of the intercondylar notch with increased knee flexion. The ACL evaluation started confirming the presence of the continuous AM bundle fibres connecting femoral and tibial footprints, and should be done either in a semiflexed position either in a "figure 4" position of the knee while assessing tension of intact AM bundle fibres by palpation with the probe and via clinical tests. The PL bundle has some specific features; often its direct observation through the anterolateral portal is difficult and the best way is to switch the scope to the anteromedial portal to have a direct view of its insertions. The best leg position to explore the PL bundle is in flexion close to 80° and combined to a varus with an external rotation of the hip (Cabot's position) (9).

Graft harvesting

Our chosen graft for the reconstruction of the PL bundle is the semitendinosus tendon (ST) which is harvested by a 4 cm longitudinal incision located 1-2 cm medial to the tibial tuberosity, at the level of the pes anserinum.. The graft is harvested using an open-ended tendon stripper and then is looped in doubled conformation over a traction suture device and the distal ends are whipstitched with no. 2 vicryl or no-absorbable sutures so that over 2 cm of doubled ST graft could lie in the femoral and tibial fixation tunnels. Then, the graft is looped over a 15-25 mm Endobutton CL-ultra (Smith and Nephew Endoscopy, Andover, MA) for femoral fixation, depending on lateral femoral condyle length.

Since ACL remnant augmentation technique may increase the risk for cyclops syndrome, special attention must be paid to the graft size because a large graft can result in a loss of full extension postoperatively and pain due to overstuffing in the intercondylar notch. The goal is to obtain a graft with a diameter of 6-8 mm.

Bone tunnels

Before drilling bone tunnels, tibial and femoral footprints of the PL bundle are carefully identified and debrided while preserving the intact AM bundle. A careful protection of the remnant fibres of the ACL is crucial, and can be easily made using a probe. Then, the bone tunnels are drilled according to the size of the graft in order to obtain a good tendon-to-bone press fit.

We prefer to perform a selective PL bundle reconstruction using transtibial technique for creating the femoral tunnel. First, we perform tibial tunnel using a tibial guide set to 45-48°, placed approximately 3 cm medial to the tibial tuberosity with a tilt of 40-45° to the tibial axis and with the intra-articular tip of the drill guide positioned

immediately posterolateral to the fibres of the AM bundle, at the centre point of the PL bundle and at an average 4 to 5 mm anterior to the posterior root of the lateral meniscus. A 2 mm Kirschner wire is inserted using the drill guide and then advanced by a conventional cannulated reamer to create the tibial bone tunnel, which is then drilled according to the same diameter of the harvested graft. At the same time, intact AM bundle fibres are retracted with a probe or a curette through the AM portal to protect them during the tibial tunnel drilling.

The femoral PL bone tunnel is then marked with the knee at 110° of flexion because in this position the PL bundle insertion is horizontal to the AM bundle, at an average of 4 to 5 mm posterior to the articular cartilage of lateral femoral condyle. At this time, resident's ridge is also outlined. Through the AM portal, a flexible guidewire is advanced at the centre of PL femoral bundle footprint behind the resident's ridge and then exited outside through the distal femur and thigh. In case of PL bundle rupture, the goal is to position the central portion of the femoral tunnel between 9:30 and 10 o'clock (right knee) and between 2 o'clock and 2:30 o'clock (left knee). The length of tunnel is calculated after increasing the diameter to 4,5 mm with the Endobutton drill,

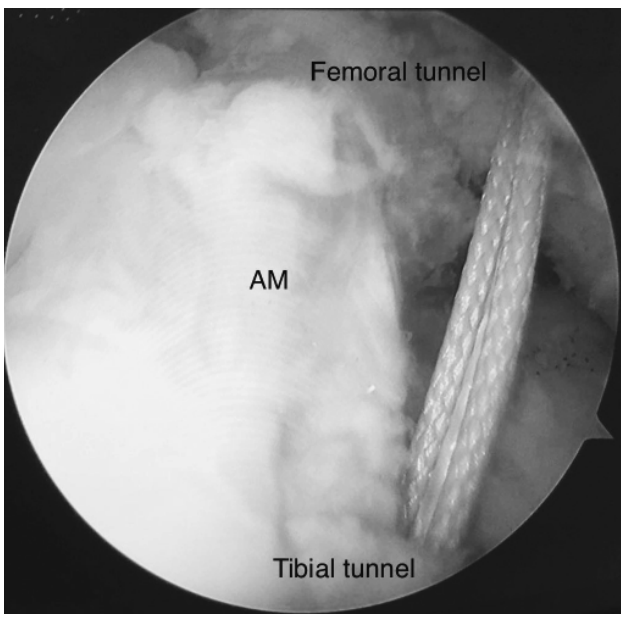

Fig. 1. *Graft passing through tibial tunnel.* ***AM****: anteromedial bundle;* ***PL****: posterolateral bundle).*

then the femoral socket is created using a cannulated reamer of the same diameter of the harvested graft to a depth of approximately 30 mm.

Graft passing and fixation

Once completed both bone tunnels, the graft is routed from the tibia to the femur (Fig.. 1). On the tibial side, graft fixation is performed using a bio-absorbable interference screw in 20° of knee flexion, because it has been shown that both bundles carry the same load within this degree of motion (10).. After selecting the appropriate size of Endobutton CL-ultra for the femoral side, the graft is passed through the tibial tunnel and femoral tunnel, fixed to the lateral femoral cortex by flipping the Endobutton and pulling the graft distally (Fig. 2). Finally, the graft is tensioned on the femoral side and cycled through several flexion-extension movements. Once stable fixation is confirmed, the excess distal ends of the graft are sharply dissected..

DISCUSSION

The reconstruction of ACL is a very common procedure with good to excellent results reported over the years (11). The primary purpose of performing an ACL reconstruction is to restore the biomechanical stability of the knee, therefore reducing the incidence of associated lesions such as meniscal tears, collateral ligaments injuries or cartilage damage (11). Standard ACL reconstruction often involves the resection of the remaining ligament fibres from both the tibial and femoral footprint, to avoid overstuffing into the intercondylar notch and to prevent impingement of soft tissues, which can produce decreased range of motion and extension lag (12). However, it was shown that the preservation of the ACL remnant and of the intact bundle could bring advantages in terms of vascularity and proprioception (12), resulting in improved recovery of joint stability and position, enhanced revascularization, integration and remodelling of the graft (13).

From a biological viewpoint, remnant ACL fibres can maintain blood supply preserving the synovial sheet, and providing support to the healing process of the graft (14). Consequently, preserving

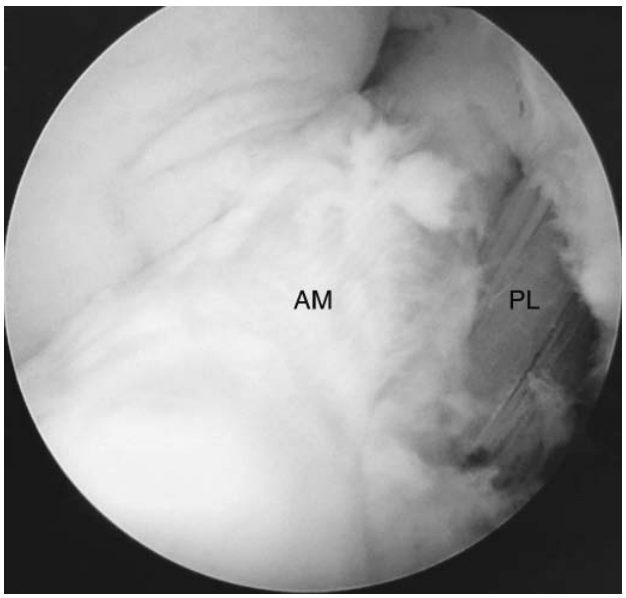

Fig. 2.. *Final result of selective posterolateral.* ***PL****: bundle reconstruction* ***AM****: anteromedial).*

ACL remnants and any eventual uninjured bundle during an ACL reconstruction is very important and can lead to significant biomechanical, vascular and proprioceptive advantages (15). Moreover, these ACL remaining fibres may serve as a guide and landmark for ensuring a better placement and orientation of the graft at the ACL native insertion sites, adding biomechanical strength and stability to the reconstructed bundle in the immediate postoperative period (15).

A preoperative diagnosis of partial tears of the ACL is often challenging and the decision of whether the ACL tear is partial or complete is made based on clinical, MRI and final arthroscopic evaluation. Siebold and Fu (16) pointed out that clinical presentation of partial ACL tears shows significant variations according to the injury pattern of the AM and PL bundles. Depending on the injury mechanism, there is a wide range from asymptomatic to symptomatic elongation or rupture of 1 or 2 bundles. Zantop (17) et al. focused on the correlation between injury mechanism and the injury pattern of the 2 ACL bundles and showed that an AM bundle tear seems to involve a more explosive type trauma to the knee, predominantly in the anterior direction, whereas an injury to the PL bundle might involve a less energetic pivoting injury, with a predominantly rotational component. Patients with symptomatic PL bundle tears usually tend to complain of rotational instability with pivoting sports showing only slightly positive anterior drawer and Lachman test while presenting a positive pivot shift test. On the other hand, patients with AM bundle tears show an accentuated anterior instability with a significantly increased anterior drawer at 90° and Lachman test at 30° of knee flexion.

Besides clinical examination, instrumental exams could also make a valuable contribution to getting accurate diagnosis; however, conventional MRI is not sensitive enough to diagnose a partial ACL tear (18). The double bundle structure of the intact ACL and its specific injury pattern is usually seen on T1 and or T2 weighted 0,2 T MRI on standard views in the sagittal and coronal planes but a clear definition of the two bundles remains often very difficult. Starman et al (18) reported that the AM bundle was detected in most standard viewing planes with high frequency and reliability, while the PL bundle identification was less frequent and had a lower associated reliability in MRI. These data confirmed the difficulty to reliably detect both bundles using a low-field strength 0.2 T MRI with standard planes of view.

We have already demonstrated that partial tears of ACL can predictably be recognized on oblique sagittal (in case of AM bundle tear) and oblique coronal planes (in case of PL bundle tear) using a 3T MRI, allowing a more precise description of ACL rupture patterns and consequently a more distinctive approach for reconstructive surgery (19).

Nevertheless, since the use and the development of better adapted MRI protocols may allow a certain diagnosis of this type of lesion, direct arthroscopic examination of the preserved fibres remains the most important factor in the surgical decision (19, 20). The evaluation of the quality of the PL bundle fibres is better done with the knee in the “figure four” position (Cabot’s position) because in this setting a stretched-out PL bundle cannot show an increase in tension normally seen (9). Moreover, an isolated PL bundle rupture can be easily missed when viewing from standard anterolateral portal and because the presence of the AM bundle which overlies the PL

bundle.

Mott et al. (21) were the first to describe an ACL augmentation surgery in acute ACL tear, pointing out that this type of reconstruction gives back an optimal ligament strength compared to normal ACL. Other authors have reported good clinical outcomes in terms of reduced laxity and better joint stability and proprioception after partial reconstruction of either the AM bundle or the PL bundle (22). Adachi et al (23) described that the remnant preservation during reconstruction may contribute to improve postoperative proprioceptive function of the knee joint, better restoration of knee kinematics and the potential enhancement of graft biological integration. Ochi et al (24) demonstrated that proprioception and healing was effective after single bundle reconstruction in a series of 45 patients who underwent selective augmentation reconstruction with a follow-up of 2 years.. Buda et al (25) reported good or excellent clinical outcomes correlated with integration of the graft with the remaining fibres and with the presence of a signal on postoperative magnetic resonance imaging, while Pujol et al (26) rated a better control on anterior laxity test in patients who underwent selective single bundle augmentation on a prospective, randomized multicentre study.

In conclusion, the reconstruction of the PL bundle of the ACL is a challenging procedure requiring an experienced arthroscopic surgeon and a reproducible technique to place the PL bone tunnel in the anatomic insertion while preserving the AM remnant. Correct tunnel placement and a careful preservation of the intact bundle are critical for achieving successful short and long-term outcomes after this type of ACL reconstruction.

Based on literature evidence and our experience, we recommend this surgical technique that proves to be effective and shows good to excellent clinical outcomes, especially regarding joint proprioception and stability. However, more prospective and randomized controlled studies including large sample of patients and with objective methods of outcome assessment are necessary to evaluate the results about healing, remodelling of the graft, proprioception and biomechanics of the knee, after augmentation surgery for partial ACL tears.

REFERENCES

1. Colombet P, Dejour D, Panisset JC, Siebold R. The French Arthroscopic Society. Current concept of partial anterior cruciate ligament ruptures. Orthop Traumatol Surg Res 2010; 96(8):S109-18.
2. Amis AA. The functions of the fibre bundles of the anterior cruciate ligament in anterior drawer, rotational laxity and the pivot shift. Knee Surg Sports Traumatol Arthrosc 2012; 20:613-620.
3. Zantop T, Herbort M, Raschke MJ, Fu FH, Petersen W. The role of the anteromedial and posterolateral bundles of the anterior cruciate ligament in anterior tibial translation and internal rotation. Am J Sports Med 2007; 35:223-7.
4. Adachi N, Ochi M, Uchio Y, Iwasa J, Ryoke K, Kuriwaka M.. Mechanoreceptors in the anterior cruciate ligament contribute to the joint position sense. Acta Orthop Scand 2002; 73(3):330-4.
5. Rizzello G, Longo UG, Petrillo S, Lamberti A, Khan WS, Maffulli N, Denaro V. Growth factors and stem cells for the management of anterior cruciate ligament tears. Open Orthop J 2012; 6:525-30.
6. Sonnery-Cottet B, Lavoie F, Ogassawara R, Scussiato RG, Kid- der JF, Chambat P. Selective anteromedial bundle recon- struction in partial ACL tears: a series of 36 patients with mean 24 months follow-up. Knee Surg Sports Traumatol Arthrosc 2010; 18(1):47-51.
7. DeFranco MJ, Bach Jr BR. A comprehensive review of partial anterior cruciate ligament tears. J Bone Joint Surg Am 2009; 91:198-208..
8. Torabi M, Fu F, Luo J, Costello J. Clinical relevance and imaging features of isolated single bundle anterior cruciate tear and single bundle augmentation. Clin Imaging 2013; 37(5):830-5.
9. Amis AA, Dawkins GP. Functional anatomy of the anterior cruciate ligament. Fibre bundle actions related to ligament replacements and injuries. J Bone Joint Surg Br 1991; 73(2):260-7.
10. Pujol N, Colombet P, Cucurulo T, et al. Natural history of partial anterior cruciate ligament tears: a systematic literature review. Orthop Traumatol Surg Res 2012; 98(8S):S160-64.
11. Beaufils P, Pujol N. Management of traumatic meniscal tear and degenerative meniscal lesions. Save

the meniscus. Orthop Traumatol Surg Res 2017; pii: S1877-0568(17)30231-1.
12. Sonnery-Cottet B, Panisset JC, Colombet P, et al. French Arthroscopy Society (SFA). Partial ACL reconstruction with preservation of the posterolateral bundle. Orthop Traumatol Surg Res 2012; 98(8S):S165-70.
13. Takazawa Y, Ikeda H, Kawasaki T, et al. ACL Reconstruction Preserving the ACL Remnant Achieves Good Clinical Outcomes and Can Reduce Subsequent Graft Rupture. Orthop J Sports Med 2013; 1(4):2325967113505076.
14. Hong L, Li X, Zhang H, Liu X, Zhang J, Shen JW, Feng H. Anterior cruciate ligament reconstruction with remnant preservation: a prospective, randomized controlled study. Am J Sports Med 2012; 40(12):2747-55.
15. Sonnery-Cottet B, Bazille C, Hulet C, et al. French Arthroscopic Society. Histological features of the ACL remnant in partial tears. Knee 2014; 21(6):1009-13.
16. Siebold R, Fu FH. Assessment and augmentation of symptomatic anteromedial or posterolateral bundle tears of the anterior cruciate ligament. Arthroscopy 2008; 24(11):1289-98.
17. Zantop T, Brucker PU, Vidal A, Zelle BA, Fu FH. Intraarticular rupture pattern of the ACL. Clin Orthop Relat Res 2007; 454:48-53.
18. Starman JS, Vanbeek C, Armfield DR, Sahasrabudhe A, Baker CL 3rd, Irrgang JJ, Fu FH. Assessment of normal ACL double bundle anatomy in standard viewing planes by magnetic resonance imaging. Knee Surg Sports Traumatol Arthrosc 2007; 15(5):493-9.
19. Steckel H, Vadala G, Davis D, Musahl V, Fu FH. 3-T MR imaging of partial ACL tears: a cadaver study. Knee Surg Sports Traumatol Arthrosc 2007; 15(9):1066-71.
20. Steckel H, Vadala G, Davis D, Fu FH. 2D and 3D 3-tesla magnetic resonance imaging of the double bundle structure in anterior cruciate ligament anatomy. Knee Surg Sports Traumatol Arthrosc. 2006; 14(11):1151-8.
21. Mott HW. Semitendinosus anatomic reconstruction for cruciate ligament insufficiency. Clin Orthop Relat Res 1983; 172:90-2.
22. Kazusa H, Nakamae A, Ochi M. Augmentation technique for anterior cruciate ligament injury. Clin Sports Med 2013; 32(1):127-40.
23. Adachi N, Ochi M, Uchio Y, Sumen Y. Anterior cruciate ligament augmentation under arthroscopy: a minimum 2 year follow up in 40 patients. Arch Orthop Trauma Surg 2000; 120(3-4):128-33.
24. Ochi M, Adachi N, Uchio Y, Deie M, Kumahashi N, Ishikawa M, Sera S. A minimum 2-year follow-up after selective anteromedial or posterolateral bundle anterior cruciate ligament reconstruction. Arthroscopy 2009; 25(2):117-22.
25. Buda R, Di Caprio F, Giuriati L, Luciani D, Busacca M, Giannini S. Partial ACL tears augmented with distally inserted hamstring tendons and over-the-top fixation: an MRI evaluation. Knee 2008; 15(2):111-6.
26. Pujol N, Colombet P, Potel JF, et al. French Arthroscopy Society (SFA).. Anterior cruciate ligament reconstruction in partial tear: selective anteromedial bundle reconstruction conserving the posterolateral remnant versus single-bundle anatomic ACL reconstruction: preliminary 1-year results of a prospective randomized study. Orthop Traumatol Surg Res 2012; 98(8S):S171-7.

A NEW SURGICAL POSITIONING SYSTEM FOR ROBOTIC ASSISTED MINIMALLY INVASIVE SPINE SURGERY AND TRANSPEDICULAR APPROACH TO THE DISC

G. VADALÀ[1], D. ACCOTO[2], F. RUSSO[1], I. PORTACCIO[2], M. ROSSINI[2], S. VALENTINI[2], R. PAPALIA[1] and V. DENARO[1]

[1]Department of Orthopaedic and Trauma Surgery, Università Campus Bio-Medico di Roma; [2]Laboratory of Biomedical Robotics and Biomicrosystems, Università Campus Bio-Medico di Roma

Minimally Invasive Spine Surgery (MISS) procedures for the treatment of spinal pathologies have experienced exponential growth due to improved techniques and decreased trauma to the patient. Several MISS procedures that require the use of a trans-pedicular cannula as a guiding tool for pedicle screw placement, delivery of biomaterials to the vertebral body or injection of biologics to the disc space have been described. Although these are clear advantages of MISS, the limited dissection and exposure may reduce the accuracy and stability of operation and make spine surgeons rely heavily on intraoperative fluoroscopy, raising concerns over the level of radiation exposure. Robot-assisted minimal invasive surgery has aroused more attention for its high precision and stability, minimizing risks of damage to neurovascular structures and diminishing harmful exposure to ionizing radiation. The aim of this paper is to describe and characterize a new surgical positioning system for for robotic assisted MISS. The system is conceived to be integrated in a surgical platform capable of supporting the surgeon in a new procedure to treat degenerative intervertebral disc disease. For this purpose, it is necessary to orientate a cannula in order to guide the bone drill along a planned route, to access the intervertebral disc through the pedicle and endplate. In particular, we describe a mechanism that percutaneously guides a cannula towards the intervertebral disc based on the acquisition of few fluoroscopic images. The design of the positioning system, with its features and constrains imposed by the presence of instrumentation and medical staff in the operating room, as well as the software for trajectory planning during surgery, are here described.

Back pain is one of the major source of chronic disability (1) and it has an important socioeconomic impact due to its treatment costs and related loss of work days (2). Although open techniques of surgical repair and augmentation of the spine are widely practiced with good success, the comorbidities of open back surgery are serious and well documented. First of all, extensive soft tissue dissection during open surgery has been shown to trigger short term damage and affect long term degenerative changes (3), which increase the patient's susceptibility to re-injury (4) determining long recovery time and extended loss of work days (2, 5).

With the evolution of modern spine surgery, the use of Minimally Invasive Spine Surgery (MISS) procedures for the treatment of spinal pathologies has experienced exponential growth due to improved techniques and decreased trauma to the patient (6). Indeed, these techniques are associated with decreased intraoperative blood loss, operative time and morbidity. Moreover, these procedures enable earlier mobilization, decreased hospital stay, decreased pain, and an earlier return to baseline function when compared with conventional open procedures. In the past decades, MISS has been widely used in

Key words: minimally invasive spine surgery, MISS, transpedicular approach, intervertebral disc regeneration, spinal fusion

Mailing address:
Dino Accoto, PhD.,
Laboratory of Biomedical Robotics and Biomicrosystems,
Campus Bio-Medico University of Rome,
Via Alvaro del Portillo 200, 00128 Rome, Italy
Tel: +39 06 22 54 11613 - Fax: +39 06 22 54 11638
e-mail: d.accoto@unicampus.it

0393-974X (2017)

deformity, trauma spinal tumor, degenerative disease and spondylolisthesis. Moreover, several MISS procedures that require the use of a trans-pedicular cannula as a guiding tool for pedicle screw placement, delivery of biomaterials to the vertebral body or injection of biologics to the disc space have been described. These procedures are performed in close contact to nervous structures and therefore need high precision.

Although there are clear advantages in MISS, the limited dissection and exposure may reduce the accuracy and stability of operation and make spine surgeons rely heavily on intraoperative fluoroscopy, raising concerns over the level of radiation exposure for all the people in the operating room. Therefore, during the last few decades, robot-assisted minimal invasive surgery has aroused increasing attention for high precision and high stability. Indeed, robotics may help minimize the risk of damage to neurovascular structures maintaining a high degree of accuracy and consistency; furthermore, it may facilitate surgeon access and operating room dynamics, diminishing harmful exposure to ionizing radiation in patients and the operative team. Several surgical robotic platforms have been developed to guarantee an effective surgical technique and assistance to surgeons (7, 8) and are being used to deal with different procedures such as minimally invasive and percutaneous repair and treat a wide variety of orthopedic disorders, such as degenerative disc disease or spinal fractures.

The aim of this paper is to describe and characterize a new surgical positioning system for robotic assisted MISS. This system is conceived for integration in a surgical platform able to support the surgeon in a new procedure to treat degenerative intervertebral disc disease. The surgical procedure involves a transpedicular approach to access the intervertebral disc, which can be performed percutaneously, overcoming the disadvantages of open surgery (9-12). However, this approach bring the risks of nerve root damage and dural tear (13). For this purpose, it is necessary to orientate a cannula to guide the bone drill along a planned route, in order to access the intervertebral disc through the pedicle and endplate. The design of the positioning system, with its features and constrains imposed by the presence of instrumentation and medical staff in the operating room, as well as the software for trajectory planning during surgery, are here described.

The surgical platform

In order to mitigate the risk of injuries during the execution of the transpedicular procedure, a surgical platform has been developed to support the surgeon in defining and following the proper route to the nucleus pulposus during the drilling of the vertebrae. The platform consists of a positioning system and a drilling-trajectory-planning software that work together. The positioning system is clamped to both sidebars of the operating table (Fig. 1) and it slides along them. The clamping mechanism is mounted below the operating table, while the positioning system is situated on one side of it. This allows the medical staff more freedom of movement around the operating table, as well as the use of the platform together with other instruments in the operating room, namely the C-arm.

The Positioning System

The positioning system supports the surgical tools used to drill the vertebras. Its mechanical architecture has 5 Degrees of Freedom (DoF) for freely positioning the surgical tool in the space. The missing degree of freedom corresponds to the rotation around the axis of the tool, which is indeed not necessary considering that most tools are axisymmetric (e.g, cannulae to create a percutaneous access). The 5 DoFs are manually actuated by the surgeon through knobs (Fig. 1). Rotational joints are equipped with an encoder (RLS, RM22) to measure the angular amplitude (Resolution 0.35°). Each joint is kinematically irreversible, so that it locks in the specific configuration defined by the surgeon.

An additional l-DoF allows the translation of the surgical tool along the direction of intervention. The kinematic architecture (Fig.. 2) can be divided into three sub-modules: i): a mechanical device for rough positioning of the surgical tools (joints d_0, j_0 and d_1); ii): a double planar parallelogram (joints $j_{1\text{-}8}$) that creates a remote center of motion (RCM) centered on the tip of the surgical tool; iii): a support for a linear guide (joint d_4) on which the surgical tool can slide.

Such architecture provides a large workspace (755x600x311 mm^3) outside the patient's body (13) and once all joints are locked, only the advancement of the surgical tool along the drilling direction must be taken care of by the surgeon. Materials used are aluminum (EN AW 6060), stainless steel (EN 1.4404) and carbon fiber (HS). The overall weight is 64.7 Kg.

Software for trajectory planning during surgery

The trajectory-planning algorithm relies on the possibility of reconstructing the three-dimensional orientation of a segment using its projections on two orthogonal planes. In the case of the described surgical procedure, such projections are provided by two perpendicular fluoroscopic images of the operating site [antero-posterior (AP) and medio-lateral (ML) views of the lumbar spine], acquired through a C-arm.

The software developed and implemented in MATLAB (Mathworks, Natick MA, USA) allows to: i): determine the current orientation of the cannula and the related configuration of the positioning system (14); ii): plan a safe route to reach the intervertebral space; iii): return the joint parameters j_1 and j_2 to update the configuration of the positioning system so that the driller can reach the IVD space following the planned route. A global reference frame, O-x-y-z, is adopted for the resolution of the problem (Fig. 3). The calculation of current of orientation and trajectory planning requires the following steps:

a) Identifying on both images the same detail (e.g. vertebra thickness, cannula length) and scaling the two views so that such detail has the same dimensions in ML and AP views. In this way, scale changes, due to accidental shifts of the rotation center of C-arm during the acquisition, are compensated.
b) Identifying two points of the cannula on ML and AP views (e.g. the tip and the distal point) in order to: i): operate a registration of the images (along the y-direction); ii): evaluate the current orientation of the cannula and the corresponding configuration of the positioning system (Fig. 3).
c) Choosing on both projections the desired entry point on the vertebra end plate. At this point the software draws a line representing the transpedicular route projected on the two views (Fig. 3).
d) Once the transpedicular trajectory is defined, the software returns the joint parameters according

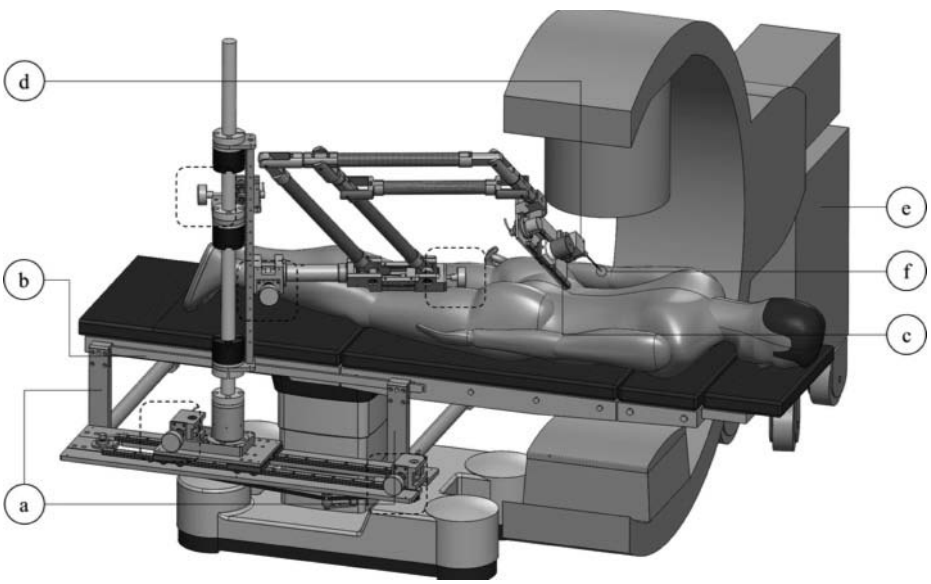

Fig. 1. *The surgeon can adjust the kinematic configuration of the positioning system by manually operating the knobs (highlighted with dashed square);* ***a****): clamping bars;* ***b****): side bar of the operating table;* ***c****): linear guide;* ***d****): surgical tool;* ***e****): C-arm;* ***f****): RCM of the double planar parallelogram.*

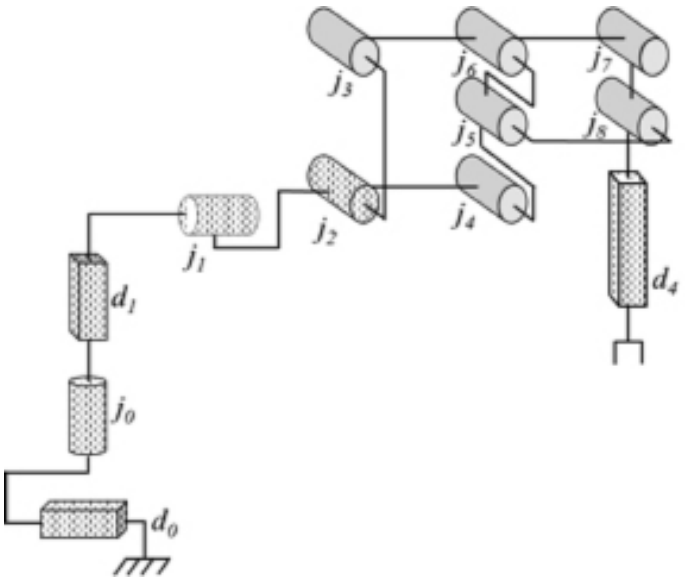

Fig. 2. *Kinematic architecture of the positioning system. Dash ed joints are manually actuated.*

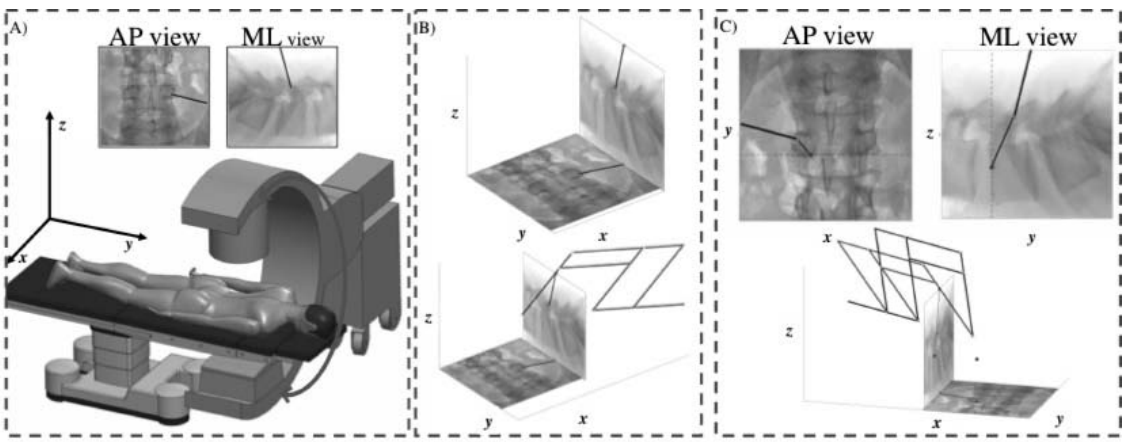

Fig. 3. *Software operating scheme: **A**): acquisition of the medio-lateral (ML) and antero-posterior (AP) fluoroscopic projections; **B**): the surgeon identifies the cannula ends on both images and the software reconstructs the current positioning system configuration; **C**): the surgeon chooses the entry point on the end plate (blue dots) on both **AP** and **ML** views. The software evaluates the joints parameter to be set so that the positioning system can guide the drilling tool along the selected route.*

to which the operator can manually adjust the configuration of the positioning system (Fig. 3).

DISCUSSION

In this paper, a new device for MISS has been developed. We designed and described a surgical positioning system able to percutaneously guide the cannula orientation towards the intervertebral disc based on the acquisition of a few fluoroscopic images. Starting from the identification of the insertion point and trajectory to the intervertebral disc drawn on two perpendicular C-arm fluoroscopic images by the surgeon, the software can guide the insertion through the regulation of the system joints

configuration.

Different robotic-assisted MISS procedures have been previously described and two different approaches can be identified in image-guided navigation. Indeed, a distinction can be made between systems that enable navigation on preoperatively acquired 3D MR- or CT- scans (15-20) and approaches based on intraoperatively fluoroscopic images (21-24). The first approach provides 3D insight and no further radiation during surgery.. However, the 3D image-guided navigation procedure can still be quite invasive and time consuming since the most commonly used image-to-patient registration technique in MR- or CT-guided navigation requires touching anatomic landmarks and therefore removal of soft tissue. The second approach, which is based on intraoperatively acquired fluoroscopic data, does not require an extra image-to-patient registration step, limits radiation and can guide in the procedure by displaying the instrument in multiple projection directions simultaneously. However, it does not provide true 3D information to the surgeon. In clinical practice, commercial systems for the preoperative planning in 3D virtual environment based on CT scan are used. The SpineAssist (MAZOR Surgical Technologies, Caesarea, Israel) is an image-based mechanical guidance system used for spinal fusion. During surgery, two fluoroscopic images are acquired and matched to the pre-operative CT information to guide a surgical robot.. (25, 26)

We propose a surgical positioning system for orienting the insertion of a surgical cannula during MISS that is characterized by a unique set of features, which is not exhibited by other solutions. Indeed, the new system is characterized by low invasiveness, as no mechanical fixtures onto the bones is necessary; low cost; ease of installation, since it can be used in any standard or hybrid surgical room equipped with a C-arm. Moreover, the system has been designed and dimensioned to be compatible with the size of C-arm workspace and interfere minimally with the surgical procedure and medical staff.

The designed system includes a software for the identification of the target cannula orientation, starting from the desired insertion point, and from the pre-planned insertion direction, and a mechanical support handling the cannula and orienting it as required. Starting from two perpendicular fluoroscopic images, the software can assist the surgeon to plan a safe route to reach the intervertebral space. Thus, the software developed for the transpedicular route planning aims to reduce the number of fluoroscopic images, considerably decreasing the absorbed dose for the patient. Furthermore, the SPS simplifies the cannula insertion procedure: the route planning does not require the use of an additional optoelectronic system, but it is only based on fluoroscopic images captured with a C-arm fluoroscope.

In the final prototype, a dedicated position sensor measures the advancement of the drill. In such configuration, the couple of initial images is theoretically sufficient to assure the correct positioning of the cannula. Nonetheless, we expect that a few additional images should be acquired for redundancy and safety reason.

CONCLUSION

This new surgical positioning system represents a promising robotic device for use in various minimally invasive interventional procedures of the spine such as vertebral biopsy, vertebroplasty, paraspinal abscess drainage, spinal fusion, discectomy and regenerative approaches decreasing the radiation exposure to the attending staff and increasing precision. However, further experiments, especially in vivo studies are needed to establish this application in the clinical routine.

ACKNOWLEDGEMENTS

This work was supported by Università Campus Bio-Medico di Roma within the project START-Disc (Smart Surgical platform for the Transpedicular delivery of Advanced Regenerative Therapies into the intervertebral DISC space), and by the Research Grant for Young Investigator of the Italian Minister of Health (GR-2010-2318448).

REFERENCES

1. Vadala G, Russo F, Di Martino A, Denaro V.

Intervertebral disc regeneration: from the degenerative cascade to molecular therapy and tissue engineering. J Tissue Eng Regen Med 2015; 9:679-90.
2. Deyo RA, Cherkin D, Conrad D, Volinn E. Cost, controversy, crisis: low back pain and the health of the public. Annu Rev Public Health 1991; 12:141-56.
3. Cleary K, Clifford M, Stoianovici D, Freedman M, Mun SK, Watson V. Technology improvements for image-guided and minimally invasive spine procedures. IEEE Trans Inf Technol Biomed 2002; 6(4):249-61.
4. Gejo R, Matsui H, Kawaguchi Y, Ishihara H, Tsuji H. Serial changes in trunk muscle performance after posterior lumbar surgery. Spine 1999; 24(10):1023-8.
5. Deyo RA, Cherkin DC, Loeser JD, Bigos SJ, Ciol MA. Morbidity and mortality in association with operations on the lumbar spine. The influence of age, diagnosis, and procedure. J Bone Joint Surg Am 1992; 74(4):536-43.
6. Spetzger U, Von Schilling A, Winkler G, Wahrburg J, Konig A. The past, present and future of minimally invasive spine surgery: a review and speculative outlook. Minim Invasive Ther Allied Technol 2013; 22(4):227-41.
7. DiGioia AM, 3rd, Jaramaz B, Colgan BD. Computer assisted orthopaedic surgery. Image guided and robotic assistive technologies. Clin Orthop Relat Res 1998; 354:8-16.
8. Shweikeh F, Amadio JP, Arnell M, Barnard ZR, Kim TT, Johnson JP, et al. Robotics and the spine: a review of current and ongoing applications. Neurosurg Focus 2014; 36(3):E10.
9. Russo F, Hartman RA, Bell KM, Vo N, Sowa GA, Kang JD, et al. Biomechanical Evaluation of Transpedicular Nucleotomy With Intact Annulus Fibrosus. Spine 2017; 42(4):E193-E201.
10. Vadala G, Russo F, Pattappa G, et al. A Nucleotomy Model with Intact Annulus Fibrosus to Test Intervertebral Disc Regeneration Strategies. Tissue Eng Part C Methods 2015; 21(11):1117-24.
11. Vadala G, De Strobel F, Bernardini M, Denaro L, D'Avella D, Denaro V. The transpedicular approach for the study of intervertebral disc regeneration strategies: in vivo characterization. Eur Spine J 2013; 22(S6):S972-8.
12. Vadala G, Russo F, Pattappa G, et al. The transpedicular approach as an alternative route for intervertebral disc regeneration. Spine 2013; 38(6):E319-24.
13. Le Fournier L, Fusellier M, Halgand B, et al. The transpedicular surgical approach for the development of intervertebral disc targeting regenerative strategies in an ovine model. Eur Spine J 2017;
14. Portaccio I. Design of a positioning system for orienting surgical cannulae during Minimally Invasive Spine Surgery. Biomedical Robotics and Biomechatronics (BioRob) 6th IEEE International Conference on IEEE2016.
15. Arand M, Kinzl L, Hartwig E. [Combined posterior and anterior endoscopic supported instrumentation of the thoracic and lumbar spine. Arguments, concepts and first clinical results]. Zentralbl Chir 2002; 127(6):490-6.
16. Assaker R, Reyns N, Pertruzon B, Lejeune JP. Image-guided endoscopic spine surgery: Part II: clinical applications. Spine 2001; 26(15):1711-8.
17. Assaker R, Cinquin P, Cotten A, Lejeune JP. Image-guided endoscopic spine surgery: Part I. A feasibility study. Spine 2001; 26(15):1705-10.
18. Kim KD, Johnson JP, Babbitz JD. Image-guided thoracic pedicle screw placement: a technical study in cadavers and preliminary clinical experience. Neurosurg Focus 2001; 10(2):E2.
19. Richter M, Amiot LP, Neller S, Kluger P, Puhl W. Computer-assisted surgery in posterior instrumentation of the cervical spine: an in-vitro feasibility study. Eur Spine J 2000; 9(S1):S65-70.
20. Schlenzka D, Laine T, Lund T. [Computer-assisted spine surgery: principles, technique, results and perspectives]. Orthopade 2000; 29(7):658-69.
21. Foley KT, Simon DA, Rampersaud YR. Virtual fluoroscopy: computer-assisted fluoroscopic navigation. Spine 2001; 26(4):347-51.
22. Fritsch E, Duchow J, Seil R, Grunwald I, Reith W. [Accuracy of fluoroscopic navigation of pedicle screws. CT-based evaluation of bone screw placement]. Orthopade 2002; 31(4):385-91.
23. Hofstetter R, Slomczykowski M, Sati M, Nolte LP. Fluoroscopy as an imaging means for computer-assisted surgical navigation. Comput Aided Surg 1999; 4(2):65-76.
24. Nolte LP, Slomczykowski MA, Berlemann U, Strauss MJ, Hofstetter R, Schlenzka D, et al. A new approach

to computer-aided spine surgery: fluoroscopy-based surgical navigation. Eur Spine J 2000; 9(S1):S78-88.
25. Joseph JR, Smith BW, Liu X, Park P. Current applications of robotics in spine surgery: a systematic review of the literature. Neurosurg Focus 2017; 42(5):E2.
26. Dreval ON, Rynkov IP, Kasparova KA, Bruskin A, Aleksandrovskii V, Zil'bernshtein V. [Results of using Spine Assist Mazor in surgical treatment of spine disorders]. Zh Vopr Neirokhir Im N N Burdenko 2014; 78(3):14-20.

BIOMATERIALS AS BONE GRAFT SUBSTITUTES FOR SPINE SURGERY: FROM PRECLINICAL RESULTS TO CLINICAL STUDY

G. BARBANTI BRÒDANO[1], C. GRIFFONI[1], A. NATALONI[2], M. MANFRINI[3], G. GIAVARESI[4], S. BANDIERA[1], A. GASBARRINI[1], S. TERZI[1], R. GHERMANDI[1], G. TEDESCO[1], M. GIROLAMI[1], M. TOGNON[5] and M. FINI[4]

[1]Department of Oncological and Degenerative Spine Surgery, Istituto Ortopedico Rizzoli, Bologna, Italy; [2]Finceramica SpA, Faenza (RA), Italy; [3]Department of Experimental, Diagnostic, and Specialty Medicine, University of Bologna, Bologna, Italy; [4]Laboratorio Studi Preclinici e Chirurgici, Istituto Ortopedico Rizzoli, Bologna, Italy; [5]Department of Morphology, Surgery and Experimental Medicine, School of Medicine, University of Ferrara, Ferrara, Italy

Vertebral fusion is performed in order to stabilize the spine in the presence of degenerative, traumatic or oncological pathologies that alter its stability. The autologous bone, harvested from the patient's iliac crest or from the lamina during surgery, is still considered the "gold standard" for spine fusion due to its osteogenic, osteoinductive and osteoconductive properties. However, several biological and synthetic bone substitutes have been introduced as alternatives for regenerating bone tissue. We have studied in particular the use of ceramic biomaterials prepared from hydroxypatite (HA), starting from *in vitro* analysis, through an *in vivo* study on ovine animal model and a post-market surveillance analysis, to finally design and perform a clinical study, which is ongoing in our Department. In the first step, HA-derived biomaterials were tested *in vitro* in the presence of bone marrow-derived human mesenchymal stem cells (hMSCs) and evaluated for their ability to activate precursor cells. In the second step, the biomimetic bone graft substitute SintLife® putty (MgHA) was evaluated *in vivo*. A posterolateral fusion procedure was applied on 18 sheep, where a fusion level was treated with MgHA, while the other level was treated with autologous bone. Microtomography and histological/histomorphometric analysis were performed six months of after surgery. In the third step, we reported the results of a post-market surveillance study conducted on 4 independent cohorts of patients (total 115 patients), in which HA-derived biomaterials were used as bone graft substitutes or extenders. Finally, a clinical study has been designed and approved by the Ethics Committee of our Institute and is currently ongoing. This study aims to evaluate the efficacy of the ceramic biomaterial SintLife® putty for bone replacement in patients treated by posterolateral fusion for degenerative spine disorders. HA biomaterials were effective in promoting the *in vitro* growth of hMSCs and their osteogenic differentiation. In the animal model, SintLife® putty has been effective in generating neo-formed bone tissue with morphological and structural features similar to those of the pre-existing bone. The post-market surveillance analysis has not reported any intra-operative nor early or late post-operative adverse events. Seven patients are currently recruited for the clinical trial designed to evaluate Sintlife efficacy for spine fusion (FU range: 1-7 months). No adverse events have been recorded. The first CT analysis performed at 6 months FU showed a good spine fusion. The study is ongoing. Our

Key words: autologous bone, spine fusion, synthetic bone graft substitutes, hydroxyapatite, biomaterials

Mailing address:
Dr. Giovanni Barbanti Brodano,
Department of Oncological and Degenerative Spine Surgery,
Istituto Ortopedico Rizzoli, Via G.C. Pupilli 1,
40136 Bologna, Italy
Tel.: +39-051-6366971 - Fax: +39-051-6366337
e-mail: giovanni@barbantibrodano.com

0393-974X (2017)

results, obtained from *in vitro*, preclinical and clinical studies, suggest that biomaterials derived from hydroxyapatite could be a valid alternative to autologous bone graft for vertebral fusion. This would potentially avoid or reduce the need of autologous bone harvesting and therefore, the risk of drawback-related side effects.

Spinal fusion (or arthrodesis) is the most common surgical approach to fuse two or more vertebrae together in order to improve spine column stabilization and relieve discomfort (1). In the last decades, this procedure has significantly increased to treat a variety of spinal disorders, such as deformities of the spine column (e.g. scoliosis and kyphosis), degenerative disc disease with instability (e.g. osteoporosis, disc degeneration, spondylosis, disc herniation, discopathy), but also traumatic injuries (e.g., fractures, spinal cord injuries) and tumours (2, 3).

Despite this, bone union failures (non-union or pseudoarthrosis) still occur in approximately 5 to 35% of patients, mainly because of systemic factors (chronic inflammation, inflammatory diseases, autoimmune deficiencies) and metabolic processes (smoking, diabetes, osteoporosis, previous failed fusions) which have demonstrated to limit the bone healing. This could cause continued pain to patients and reduce activity, produce poor clinical outcomes and require multiple revision surgeries and thus greater medical costs (3-5).

Nowadays, the most common surgical approach to prevent non-unions is represented by the use of internal fixations (including hooks, screws, plates and rods), which however have not completely eliminated the problem. Indeed, a number of physiologic, biologic and molecular events involved in bone healing, together with the presence of side factors (infection, poor vascularity, malnutrition, substantial bone loss) which can impede effective osteosynthesis and lead to symptomatic non-unions, occurring in 10-15% of patients (3, 4-7). Yet even with the efficacy of modern internal fixation techniques, it is generally assumed that instrumentation without intact osseous support will not lead to a complete bone fusion, therefore the need arises to provide new biological strategies for bone healing resolution and new bone tissue formation.

Modern bone grafts, bone substitutes and bioactive factors attempt to facilitate and enhance the healing process when suboptimal conditions exist. Depending on their properties, preparation and application, bone grafts augment natural healing via osteoinductive, osteoconductive and/or osteogenic mechanisms.

An ideal bone graft should possess 3 main features for proper integration: osteoinduction, osteoconduction and osteogenesis which are, respectively, the ability to stimulate precursors cells to migrate into the graft site and differentiate into osteoblasts; the capacity to serve as scaffold for vascular invasion, cellular infiltration and new bone ingrowth formation; the ability to directly lay down new bone matrix (5). In addition, the ideal bone graft should be easily mouldable, resorbable, and should not evoke inflammatory reactions; it should be traceable *in vivo*, thermally non-inductive and sterilizable. Finally, the ideal bone graft should be readily available, in unlimited quantities and at reasonable costs (8).

In this context, varieties of bone graft substitutes are currently available on the market, which can be used for different spinal applications. These can be mainly categorized into bone grafts (autograft, allograft), growth factors (demineralised bone matrix, bone marrow concentrate, bone morphogenetic proteins, platelet-rich plasma) and synthetic bone graft substitutes (ceramics, cements, bioglasses, calcium phosphates, etc.), each of these have pros and cons (1, 2, 8-10). The rationale for the increasing number of bone grafts available on the market lies in many factors such as the need for an augmented volume of graft available during surgery (i.e., when vertebrae resection occurs extensively, due to the presence of tumour), the need to avoid autograft harvesting and donor site-related morbidity, or the potential improvement of fusion rates in revision and complex reconstructive surgery.

All this results in the need to find new biological

strategies and therapeutic solutions to get a solid bony fusion. For these reasons, in the last decades many efforts have been made for the development of new bone grafts, meeting the three biological requirements of osteogenesis, osteoconductivity and osteoinductivity, with easy-to-use and costless features and with evaluable rapid outcomes.

Autograft

Iliac crest bone graft (ICBG) remains the "gold standard" of graft options, as it is both osteogenic, osteoconductive and osteoinductive properties (11). Autologous laminectomy bone (ALB) is often used as a bone graft instead of ICBG and also has excellent fusion rates as it contains three critical elements to increase osteogenesis: the trabeculae of the bone, which provide an osteoconductive scaffold; the bone morphogenetic proteins (BMPs) with osteoinductive potential; the osteoblasts which are a source of osteogenic cells (12).

Harvesting of autologous bone graft has limitations and significant morbidity, including superficial infection, wound complications, sensory abnormalities, persistent pain, hematomas, re-operation requirements, scarring and graft site fracture with reported rates between 10% and 39%. Despite these associated donor site morbidities, increased blood loss, operating time and hospitalization time, ICBG is still the graft of choice for spine surgery because of the excellent fusion rates (13-16).

Allograft

Allograft is bone derived from cadavers and is often considered the second option for surgeons (17).. Allograft must be stored and processed by cryoconservation and lyophilisation in entities called "bone tissue banks" before implanting into the patient, in order to avoid immune responses and the risk of viral or disease transmissions. Because of the processing, it shows more limitations in the essential bone graft characteristics described for autologous bone. It is highly osteoconductive, variably osteoinductive and devoid of osteogenic properties due to the loss of cellular elements during the processing performed to reduce immunogenicity. Common processing techniques include freezing and lyophilization. Lyophilized allografts are processed by dehydration and vacuum packed, so they can be stored at room temperature. The process of lyophilization reduces immunogenicity more than freezing, but it causes a greater reduction of mechanical strength on rehydration (18, 19).

Bone tissue banks grew as of the 80's, but doubts and concerns arose for the costs-and storing-related processes, which can also affect local health care systems (20).

Since both autograft and allograft have drawbacks, scientists have long searched for materials that could be used in place of the transplanted bone. Some graft alternatives include Bone Marrow Concentrate (BMC), Demineralized Bone Matrix (DBM), Bone Morphogenetic Proteins (BMP) and synthetic bone graft substitutes.

Bone marrow concentrate

Bone Marrow Concentrate (BMC): Mesenchymal stem cells (MSCs), identified in a variety of tissues including bone marrow, muscle, periosteum and adipose tissue, have been a topic of research for many years, attracting interest because of their self-renewing potential and multi-potential for possible clinical applications (3).. Among all, bone marrow is well established as a source of MSCs. Autologous Bone Marrow Aspirate (BMA) can be harvested through minimally invasive procedure, providing a population of osteoprogenitor cells and critical growth factors for stem cells differentiation and therefore, showing osteoinductive and osteogenic properties. However, because of the lack of structural support, it is often used with an appropriate carrier (such as ceramic) to support stem cells colonization and differentiation.

Demineralised bone matrix

Demineralised Bone Matrix (DBM) is the result of allograft decalcification, which is an acid extraction procedure in order to lose most mineral components and retain the organic phase of allograft bone. Due to the presence of bone-forming growth factors (such as bone morphogenetic proteins (BMPs), DBM has osteoinductive properties, which allow progenitor cell growth and differentiation and the induction of

vascularisation. Compared to autograft or allograft bone, DBM lacks donor-site related morbidity and shows excellent handling properties; however, due to the absence of mineral component it lacks any mechanical strength.

Bone morphogenetic proteins

Bone Morphogenetic Proteins (BMPs): BMPs comprise a family of at least 20 structurally related growth factors. The original members (BMP-2 through BMP-8) are able to resemble endochondral ossification and new bone formation, by stimulating a cascade of cellular events which allow mesenchymal stem cells to differentiate into chondrocytes, creating a matrix which then mineralizes and is replaced by bone.

Bone Graft Substitutes

In order to overcome the limitations due to human-derived bone grafts (autograft, autologous local bone, DBM, etc.) previously reported, ongoing research has led to the development of new "osteobiologic" materials either as adjuncts or as alternatives to the "traditional" grafting materials for the management of any clinical condition requiring enhancement of bone regeneration. All of these biomaterials are indicated as "bone graft substitutes" (3, 9, 21, 22).

Synthetic bone graft substitutes have been proposed on the market as bioactive and safe alternatives for bone tissue engineering and regeneration (23-25). The main features of these synthetic materials are immediate unlimited availability, sterility, low costs, no patient-related drawbacks, no immunoreactions or risks of disease transmissions.

Synthetic bone graft substitutes are mainly represented by ceramic-derivative scaffolds like calcium phosphates (CaP) and hydroxyapatite (HA). Introduced in the 80's for clinical use in orthopaedic, craniofacial and orthognathic surgery (1, 3, 8, 10), CaP ceramics are derived from naturally occurring ceramics and considered the most promising biomaterials for biomedical applications. Preformed granules and blocks of CaP are manufactured using a high-temperature sintering process to produce a material with a high crystalline structure and interconnecting porosity similar to bone, which is extremely important for the penetration of ingrowing bone with its associated vasculature (22, 26, 27). They are used as implants in orthopedics, oral-maxillofacial surgery, neurosurgery and for dental applications, and they actively participate in the metabolic processes of an organism with predictable results (21, 22, 28-30).

The most widely used CaP-based bioceramics in spinal fusion are represented by HA, β-tricalcium phosphate (β-TCP) and blends of different calcium- and phosphorus-based phases (22, 30, 31), used as bone graft extenders to expand an existing quantity of available local autograft bone or iliac crest bone graft. With the support of rigid spinal fixation systems, ceramic scaffolds have been employed as efficient bone graft extenders in posterolateral spinal fusion applications (3, 29).

From 2011 until now, we proposed to study and analyze hydroxyapatite-based bone graft extenders. Hydroxyapatite (HA), which is a naturally occurring mineral form of calcium apatite with the formula $Ca5(PO4)3(OH)$, is a crystalline calcium phosphate that is also manufactured as a ceramic through a sintering process. Its close chemical similarity with the mineralized phase of bone (biomimetism) accounts for the osteoconductive potential and excellent biocompatibility of HA.

Extensive research efforts have been dedicated to the use of synthetic HA as a bone substitute and/or replacement in several biomedical applications, such as orthopaedic, dental, maxillofacial and spinal (27, 30, 32). The porous architecture of the HA substratum, with its macropore network and its micropore interconnections, induces rapid vascular and mesenchymal invasion and provides a specific cell flow. These cells can attach, proliferate and finally differentiate into functional osteoblasts. The osteoconductive property of HA has made this material of relevant interest during the decades as it can sustain new bone formation independently from the implantation site (22). As the new bone tissue incorporates the scaffold material, the scaffold itself should be biodegradable either through cellular events or as a result of the surrounding environment (33, 34).

Three types of synthetic bioceramic bone-graft substitutes, produced by Finceramica SpA (Faenza,

Italy) and currently in use, can be applied successfully in spinal surgery (35). The first one is the porous HA bone substitute in block form, ENGIpore®, which is characterized by high porosity (80-90%) and a trabecular structure similar to that of natural bone, allowing a good osteointegration and significant new bone regeneration. In spite of the high porosity, this biomaterial is capable of withstanding compression loads to a similar extent as spongy bone.

The second available bone substitute, SINTlife®, is composed by nanocrystals of Mg-substituted HA in putty, paste or granule form. In these formulations, the Mg ions are placed in the crystalline HA cell in the same position and percentage found in the mineral phase of human bone.

The presence of Mg ions deforms the crystalline structure of HA and makes it unstable and biologically active, aiding bone formation, remodelling and rapid resorption of the material. In addition, Mg ions change the chemico-physical surface properties of the biomaterial, which actively interacts with water molecules to capture the key proteins involved in osteogenesis.

Thus, SINTlife® is able to interact with the cells that form bone and foster the deposition of new bone tissue. Due to its specific chemical and biomimetic composition, it is remodelled and resorbed by the cellular action in a physiologically adequate amount of time (6-18 months), remaining at the application site during growth and maturation of the new bone. During the remodelling phase, osteoclasts are active around the particles of biomaterial, until complete bone regeneration.

The third type of bone substitute is the composite RegenOss®.. It also exploits the useful properties of Mg-substituted HA, which is nucleated onto equine type I collagen fibres. This material is engineered at macro-, micro- and nano- structural level in order to foster bone regeneration. During surgery, this biomimetic and biodegradable scaffold can be easily adapted to the size of the defect, saving time and facilitating positioning. RegenOss® is a completely biomimetic scaffold, as its structural and chemical composition give the product characteristics entirely similar to human bone. The patented process of nucleation of Mg-HA nanocrystals in the type I collagen fibres mimics the process occurring in nature during neo-ossification. Thanks to its high hydrophilicity, this biomaterial is also able to rapidly absorb biological fluids, molecules and cells that foster bone regeneration, thus promoting cell attachment and proliferation.

During the last years, we performed studies aimed to evaluate the potential of "bioceramics" as bone substitutes for orthopaedic procedures, in particular spine surgery, drawing a path which started from *in vitro* experiments (26, 36, 37), developed through preclinical (38) and post-market surveillance (39) studies and led to the use of a ceramic product in an ongoing clinical study. The results of these studies are reported and reviewed here.

MATERIALS AND METHODS

Manfrini et al (36), Barbanti Brodano et al (37) and Manfrini et al (26) analysed 2 different bioceramics, ENGIpore and SINTlife (Finceramica Faenza SpA) in *in vitro* experiments. ENGIpore samples were cut into 5x5 mm high-porosity blocks or into polygonal-shaped chips; SINTlife samples were used in nanostructured paste form, shaped into 5x5 mm cubes or microgranules. Iliac crest bone marrow aspirates were collected from patients who signed a study-specific informed consent document and human mesenchymal stem cells (hMSCs) were isolated from the samples by Ficoll-mediated density gradient centrifugation. After flow cytometric positive characterization of surface markers, hMSCs were cultured onto ENGIpore and SINTlife scaffolds and analyzed by using different *in vitro* assays.

Following *in vitro* results, Barbanti Brodano et al (38) performed an *in vivo* study to compare the efficacy of biomimetic Mg-HA (SINTlife) and of human demineralized bone matrix (HDBM) with that of an autologous bone graft both dispersed in biomimetic Mg-HA nanoparticles.

The experiment was performed using 18 adult female sheep exposed to a spine surgical procedure. The animals were divided in two experimental groups: in group 1, one fusion level was treated with Mg-HA and the other level received cortico-cancellous bone autograft; in group 2, one fusion level was treated with HDBM-MgHA and the other received cortico-cancellous bone autograft..

In both groups the treatment alternated between the cephalad and the caudal levels. After 6 months all the animals were sacrificed using Tanax intravenously under general anaesthesia and spine segments were retrieved for radiographical, histological and microtomografic analysis.

Recently, we reported the results of a post-market surveillance analysis performed on 4 independent cohorts of patients (total of 115 patients) to evaluate the safety of 3 different formulations of hydroxyapatite-derived products used as bone graft extenders/substitutes for lumbar arthrodesis (39). The bioceramics analysed were three different HA synthetic bone substitutes (Finceramica SpA, Faenza, Italy): HA chips with high porosity (ENGIpore), Mg-HA in putty, paste and granule form (SINTlife) and Mg-HA nucleated on equine collagen fibres type I (RegenOss). The occurrence of complications was analysed during a medium and long follow-up period (minimum 12 months-maximum 5 years).

From February 2017, we started a pilot study in our Spine Surgery Department approved by the local Ethics Committee aiming to evaluate the efficacy of Mg-HA as bone graft substitute in lumbar spine surgical procedures for degenerative diseases. We recruited 7 patients and the study is ongoing. Inclusion criteria was the presence of a degenerative disease requiring a spine fusion at levels L1-S1. Exclusion criteria was the presence of oncological and infectious diseases and previous spinal surgery. We propose to collect radiographic data of spine fusion at 6, 12 and 18 months follow-up, through CT scan analysis performed by an independent observer he clinical outcomes results obtained through auto-administered patient questionnaires and adverse events.

RESULTS

In vitro experiments

When hMSCs were seeded on ENGIpore and SINTlife scaffolds they showed a significant increase of their metabolic activity during the 9 days of culture, as evaluated by AlamarBlue assay (26, 36, 37). Concerning SINTlife scaffold, this effect was observed only with the granular form, while in the presence of SINTlife paste form, cells maintained the same metabolic activity during the 9 days of the assay.

In the morphological analysis of hMSCs seeded on the biomaterials and performed by scanned electron microscopy (SEM), the cells appeared to be well attached to the scaffolds. Cells grown on SINTlife granules and on high-porosity ENGIpore scaffolds showed an unaltered morphology and appeared well attached to the scaffold with a high number of long pseudopodia in contact with the extracellular matrix. The amount of debris on the cell surface was low, due to the low release of these types of biomaterials. A different behaviour was observed when cells were grown on SINTlife in paste form: cells attached to the scaffold showed a low number of shorter pseudopodia and a greater amount of debris on their surface due to the high release of debris by this type of biomaterial when placed in the culture medium.

The cytoskeleton architecture was not influenced by the cultivation of hMSCs on the different bioceramics and it was similar to that observed when cells were grown on tissue culture polystyrene (control).

We also studied hMSCs derived from vertebrae bone marrow for their *in vitro* kinetics in comparison to that observed for hMSCs derived from iliac crest bone marrow, colon mucosa and dental pulp. We observed that MSCs derived from vertebrae can be maintained in culture for a greater number of steps and also generate mature cells of all mesenchymal lineages with greater efficiency, when induced into osteogenic, adipogenic and chondrogenic differentiation. This ability of vertebrae-derived MSCs in terms of expansion and differentiation is very interesting in a clinical application for bone fusion in spine surgery perspective (40, 41).

Preclinical study

In the animal model regarding posterolateral fusion, radiographical, histological and microtomographic results indicated good osteointegration between the spinous process and the vertebrae foramen for both materials analysed (HDBM and Mg-HA). Histomorphometry revealed no significant differences between MgHA and autologous bone for all the parameters examined, whereas significantly lower values of bone volume were observed between HDBM-MgHA and autologous bone. Moreover, the normalization

of the histomorphometric data with autologous bone revealed that MgHA showed a significantly higher value of bone volume and a lower value of trabecular number, more similar to autologous bone than HDBM. We concluded that Mg-HA stimulated the deposition of newly formed bone tissue similar to autologous bone, whereas HDBM produced reduced deposition of newly-formed bone tissue with larger intertrabecular spaces. Thus, MgHA biomaterial could represent a valid alternative for achieving spinal fusion, avoiding problems related to the collection of autografts or to the use of allografts (38).

Post-market surveillance analysis and clinical study

In the cohorts examined for the post-market surveillance analysis, 85.4% of patients were surgically treated for spine diseases of degenerative origin and 14.6% of patients were treated for spine diseases of traumatic origin. Most of patients were treated by posterolateral lumbar and lumbo-sacral arthrodesis (89.6%).

HA in chips form with high porosity was used in 37 patients, alone or combined with autologous bone; Mg-HA in putty, paste and granule form was used in 54 patients, alone or combined with autologous bone; Mg-HA nucleated on equine collagen was used in 24 patients, alone or combined with autologous bone.

We observed the absence of adverse events related to the use of ceramic bone graft substitutes in the cohorts of patients examined. Thus, this post-market surveillance analysis evidenced the safety of ceramic products as bone graft extenders or substitutes for spine surgery (39).

Following these results, some clinical studies have been designed and conducted during the last years in order to evaluate the efficacy of HA-derived products in terms of fusion rates and clinical outcomes.

In particular, we are conducting a clinical trial using SintLife (Mg-HA) putty in patients who undergo lumbar arthodesis for degenerative diseases. In the 7 patients enrolled we registered no adverse events during or after the operative phase and the first patient we examined at 6 months follow-up showed good fusion at CT scan analysis and improvement of clinical parameters (pain and functionality).

DISCUSSION

The recent advancement concerning the comprehension of bone repair process and of factors involved has led to a significant progress for the generation of bone substitutes (34, 43).

The cascade of biological events leading to bone regeneration is complex: it involves stimulation of osteoblast response and development of an environment able to support this response. In addition, an adequate vascularization and stability of the system during the repair process is necessary, requiring osteoblasts migration, proliferation, differentiation and remodelling. In order to obtain excellent results, a combination of strategies is required to manage this process, depending on the clinical situation. Modern spinal surgery has benefited from the use of effective and readily available prosthetic substitutes and synthetic systems based on screws and rods for a rapid spinal stabilization; however, the need to integrate and replace bone components is still very important today.

Even if autologous bone graft is still the gold standard for spine fusion and allograft when available, several bone graft substitutes have been proposed and studied as valid alternatives.

Bone marrow-derived MSCs have demonstrated an efficacy in spinal fusion in a variety of animal models. Minamide et al. (44) cultured MSCs derived from bone marrow and implanted these cells into the posterolateral lumbar transverse process with a hydroxyapatite-granule carrier on a rabbit model, showing evidences of fusion achievement. Using a rhesus monkey model of anterior interbody fusion, Wang et al. (45) expanded autologous MSCs derived from bone marrow in culture, stimulated them with osteogenic supplements and used them in association with calcium phosphate ceramic composites, showing an enhancement of bone regeneration and achievement of osseous spinal fusion. Curylo, et al. used a rabbit posterolateral fusion model to show improved fusion rates with the concomitant use of BMA and ICBG, reporting 61% fusion rates with BMA and ICBG versus 25% fusion with ICBG only (46).

Few clinical studies are currently available evaluating the performance of BMA in human

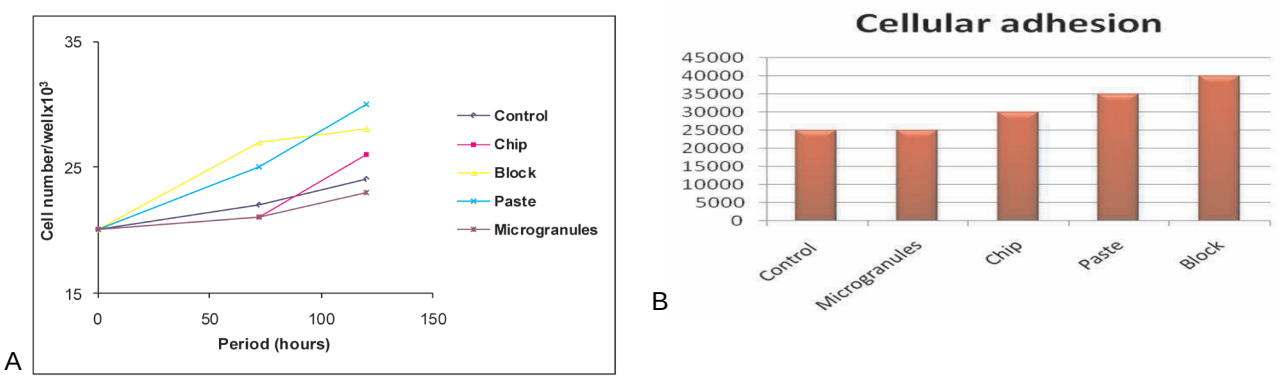

Fig. 1.. *In Panel **A**, the AlamarBlue assay was used to compare cell proliferation on different biomaterials: SINTlife in paste and microgranules configuration, ENGIpore in chips and blocks configuration. Control is created with polystyrene tissue culture flasks. SINTlife, in paste configuration, showed the best performance in terms of biocompatibility regarding the cellular proliferation. In panel **B**, the adhesion of hMSCs on biomaterials was evaluated. Comparative analyses showed a higher number of cells attached to ENGIpore block.*

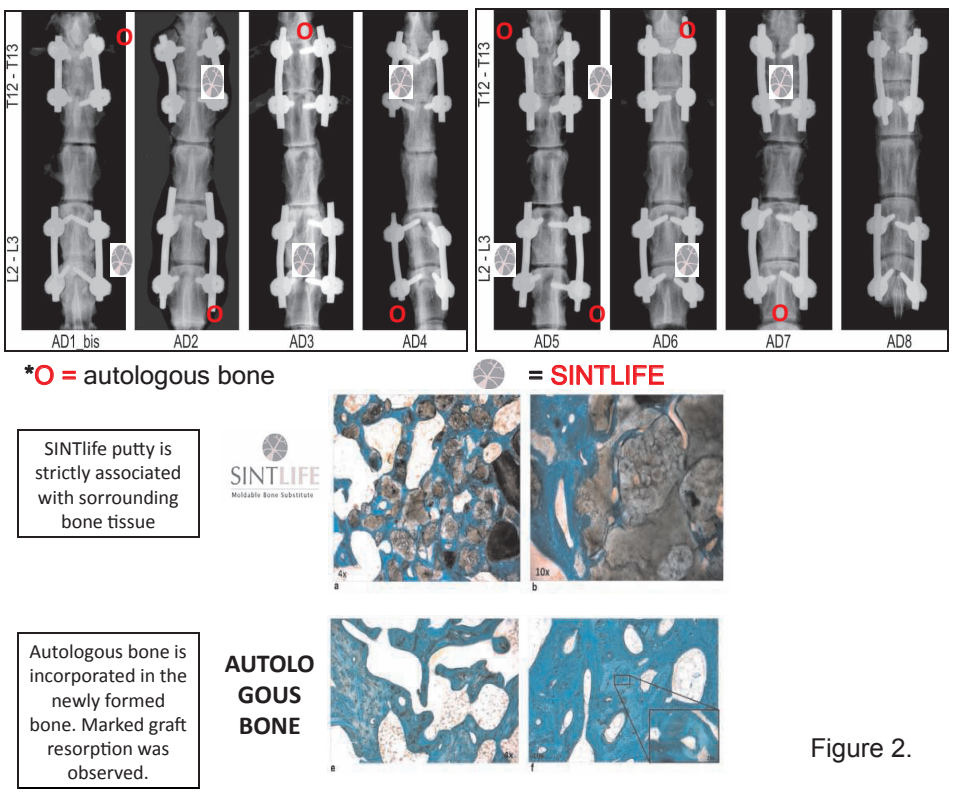

Figure 2.

Fig. 2.. *Upper panel shows the radiographic results obtained following postero-lateral instrumented fusion performed in 8 sheep at 2 non-consecutive levels, using autograft in one level and SINTlife in the other one. Images, collected 6 months after surgery, show clear signs of new bone deposition between intervertebral bodies. Lower panel shows the results of histological analysis performed at 6 months, in the presence of SINTlife (**a, b**) or autologous bone (**e, f**). SINTlife is completely osteointegrated, with structure morphology similar to the pre-existing bone. No signs of inflammation, no signs of cytotoxicity, no presence of connective tissue at the bone/biomaterial interface are detected.*

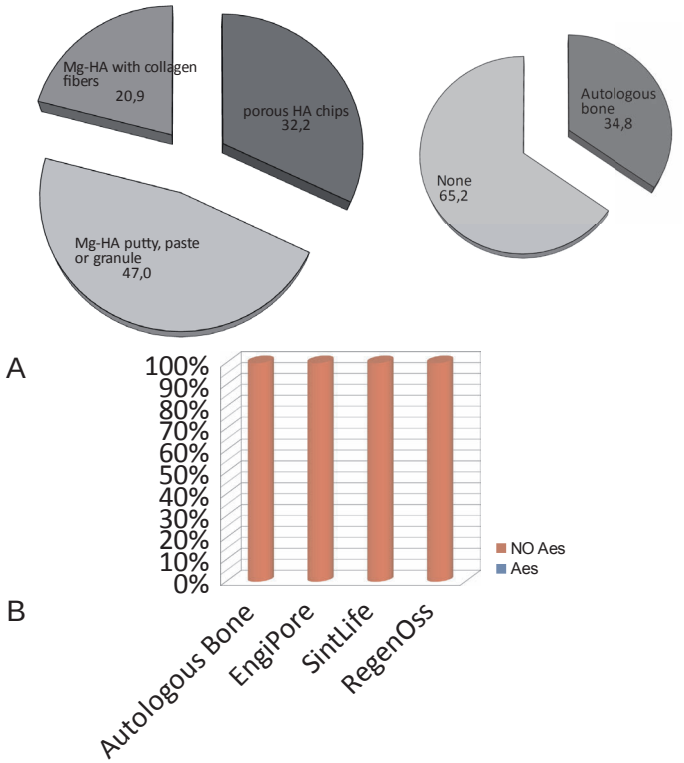

Fig. 3. *Results of a post-market surveillance analysis performed on 4 independent cohorts of 115 patients to evaluate safety and tollerance of bioceramics bone graft substitutes/extenders. In Panel **A,** the distribution of different biomaterials used is reported on the left and the use of autologous bone graft in association to biomaterials is showed on the right. Panel **B** reports post-operative adverse events collected using different biomaterials. No adverse events were registered and biomaterials resulted to be equivalent to autologous bone.*

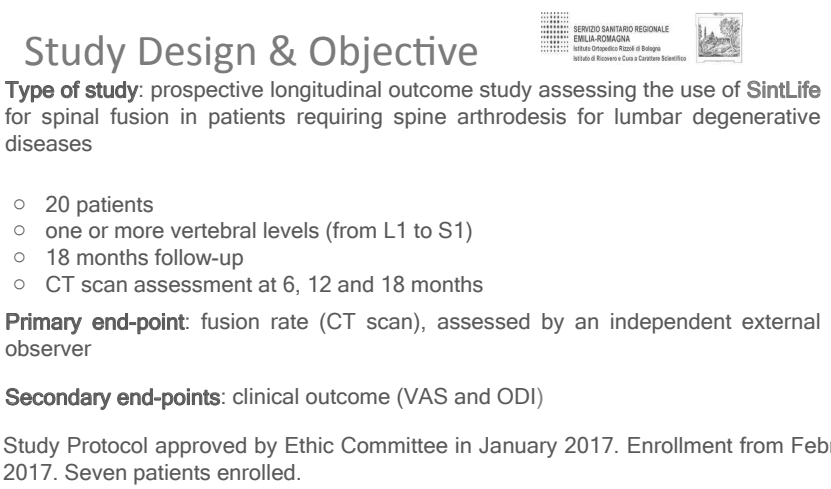

Fig. 4. *Description of a clinical trial designed to evaluate the efficacy of SINTlife for spine fusion in patients treated for lumbar degenerative diseases.*

subjects undergoing spinal fusion. Niu et al. prospectively evaluated 43 patients who underwent posterolateral fusion, showing equivalent fusion rates for BMA and local autograft versus ICBG alone at 12-month follow-up (86% versus 91%) (12). Gan et al. used bone-marrow-derived MSCs combined with porous beta-TCP for posterior spinal fusion, reporting 95.1% cases having positive spinal fusion results (47). Hart et al. (48) showed an improvement of posterolateral fusion when using BMA in conjunction with allograft, compared to the use of allograft alone. All this evidence underlines the efficacy of bone marrow aspirate in enhancing spinal fusion, together with the use of scaffolds to support stem cells colonization and differentiation. MSC therapy would be particularly beneficial for elderly patients and other subjects with reduced cellular stores.

We recently used human mesenchymal stem cells derived from iliac crest bone marrow aspirates as a cellular model for understanding the interaction between engineered matrices and osteoblast precursors, as well as their involvement in the modulation of developmental processes. In particular, we tested the new class of biomaterials named "ceramics", derived from hydroxyapatite, for their biocompatibility with MSCs and their ability to constitute a favourable microenvironment for cell adhesion, proliferation and differentiation, showing that "bioceramics" and MSCs can create a promising synergy in improving spine fusion (26, 36, 37).

We also characterized human MSCs derived from vertebrae for their ability to expand in culture for a greater number of steps with respect to MSCs derived from different body sites and to generate mature cells of all mesenchymal lineages with greater efficiency (40-42).

Concerning DBM, several *in vivo* preclinical studies have demonstrated the success of posterolateral spinal fusion using DBMs alone or in conjunction with autograft in a rabbit and non-human primate model (49-52); however, variability of potential bone regeneration among different commercially available DBMs has been demonstrated in several rat spinal fusion models (53-55).

In vivo clinical studies performed on humans have also supported the efficacy of DBM as bone graft substitute for posterolateral spinal fusion, although with variable results (56). Cammisa et al. (57) conducted a multicentre prospective study, comparing the effectiveness of a Grafton DBM gel composite with an iliac crest autograft in posterolateral spinal fusion.. The authors reported that Grafton DBM would only be used as bone graft extender together with autograft, when autologous bone quantity is inferior than normally required to achieve a solid spinal fusion. A prospective study performed, reported that a mixture of DBM and aspirated bone marrow offered similar performances as autologous bone in posterolateral spinal fusion.

Concerning BMPs, in 1965 Urist (58) demonstrated that demineralised matrix of bone graft was capable of inducing *de novo* bone formation. Purification, isolation and characterization of the organic component from demineralised bone matrix (DBM) have led to the identification of osteoinductive proteins, among which bone morphogenetic proteins (BMPs). The first studies on the efficacy of a bovine-derived osteoinductive growth factor in a rabbit and in a nonhuman primate model (adult rhesus macaques) for posterolateral applications, were performed by Boden during the 1990's. He found a dose-dependent response to the osteoinductive growth factor in the rabbit model, which indicated that a threshold must be overcome prior to bone formation. This methodology was successfully transferred over to the rhesus monkey, where the use of the osteoinductive growth factor resulted in spinal fusion in 18 weeks. Other primate experiments were performed by Boden, which were necessary to gain a better understanding of the higher doses of osteoinductive agents and longer healing time periods (18-24 weeks) required for spine fusions in primates (59, 60).

With the cloning and sequencing of the genes for specific BMPs, large quantities of recombinant proteins were made available. Several preclinical and clinical studies have been performed to investigate the ability of BMPs to achieve spinal fusion. In particular, recombinant human BMP-2 (rhBMP-2) and recombinant BMP-7 are the two most commonly studied and the only osteoinductive factors currently

being administered in human clinical studies. Recombinant human BMPs (rhBMPs) are soluble, so they can diffuse easily and any way from the fusion site: as they become inactivated if used alone, they are usually combined with a carrier matrix, the purpose of which is to retain rhBMPs concentration and release them consistently over time. These carrier matrices may also possess osteoinductive properties or they can allow mechanical strength. Common carriers include: type I collagen sponge, ceramics (hydroxyapatite, tricalcium phosphate), synthetic polymers (polylactic acid, polyglicolic acid) and allograft.

Data of all evidence levels and all areas of application in cervical and lumbar spine fusion support the use of rhBMP-2 for obtaining a predictable fusion outcome and comparable efficacy to the gold standard autologous ICBG. Concerning rhBMP-7, it has been studied only for posterolateral lumbar fusions and data are conflicting when it is compared to autologous bone graft in terms of fusion rates and clinical outcomes (61).

Finally, several synthetic bone graft substitutes or extenders have been studied to overcome problems related to human-derived bone grafts. Synthetic bone graft substitutes are mainly represented by ceramic-derivative scaffolds like calcium phosphates (CaP) and hydroxyapatite (HA). These biomaterials have been tested in some clinical trials, even if until now there is a paucity of data and many investigations have been carried out without the use of standardized protocols, therefore using or considering to use products with different chemical compositions and different applicable doses. This has generated an overlap of results and confusion on their clinical use, thus rendering meta-analysis or systematic reviews difficult to study in depth (9, 28, 29, 62, 63).

Focusing on lumbar spine fusion, ceramics were almost exclusively used as bone graft extenders with a variety of adjuncts. Considering the number of studies and of patients involved, interesting results in terms of fusion rate have been achieved using Beta tricalcium phosphate (Vitoss, Stryker), Calcium sulphate (Osteoset, Wright Medical Technology), Tricalcium phosphate/hydroxyapatite (Medtronic Sofamor Danek), Coralline hydroxyapatite (Pro-Osteon, Bomet), Type 1 collagen/hydroxyapatite (Healos, DePuy Synthes). These products showed a range of fusion rate between 83% and 93% (64).

A few years ago we proposed to increase our knowledge of bioceramics for spine fusion and investigate the use of these products, in particular a Mg-hydroxyapatite biomaterial (Sintlife, Finceramica, Italy), starting from *in vitro* experiments, through preclinical and post-market surveillance studies, concluding with a clinical trial which is ongoing in our Spine Surgery Department.

In vitro experiments revealed an active interaction between HA-based biomaterials used as scaffold and human mesenchymal stem cells grown on their surface. Cells showed an increase of their metabolic activity and they were well attached to the scaffold, with large pseudopodia.

These findings indicate that the physical and chemical features of HA materials may influence *in vitro* hMSCs behaviour. It is possible to suggest that the porous matrices, in the form of chips, blocks or granules, may constitute a favourable microenvironment for cell adhesion and growth. When bone precursor cells grow in a similar microenvironment they can found extracellular stimuli that influence their development and differentiation leading to an efficient bone tissue regeneration.

The osteogenic ability of products tested *in vitro* was evaluated and compared with a cortico-cancellous bone autograft in an ovine model of lumbar spine instrumented fusion to reproduce as close as possible the surgical procedure conducted on humans. The histological and histomorphometric results of the study showed that Mg-HA (Sintlife) stimulated the deposition of a large amount of newly formed bone tissue similar to the autologous bone. Human demineralized bone matrix (HDBM), which was evaluated in the same study for spine fusion, produced reduced deposition of newly-formed bone tissue with larger intertrabecular spaces.

The results of this *in vivo* study stimulated us to use of Mg-HA (Sintlife) in humans for spine surgery. First of all, the safety of this product and of other HA-based compounds was confirmed through a post-market surveillance analysis performed on

four independent cohorts of patients undergoing spinal fusion procedures, using ceramics alone or associated to autologous bone. The clinical studies were then designed..

A HA bone graft substitute (EngiPore, Finceramica SpA, Faenza, Italy) in form of chips mixed to autologous bone was used for posterolateral arthrodesis (Group A, 19 patients) or transforaminal interbody fusion (Group B, 17 patients) (65). Patients were treated for symptomatic degenerative spine diseases. Radiographic images showed instrumented stability with no signs of flexion-extension, hypermobility and breakage in 35 out 36 patients (one case of screw mobilization was recorded in group A and treated with surgical revision). The analysis performed evidenced the incorporation of EngiPore chips into the fusion mass with formation of mature bony trabeculae and no sign of pseudoarthrosis in 17 out of 19 patients in group A. Only 2 cases of non-fusion were recorded. In group B, successful fusion was outlined by the absence of interspaces between the cage and the vertebral bodies, no signs of pseudoarthrosis and new tissue formation in the interspaces between the vertebral bodies. Only 1 case of non-union was recorded in group B. No major complications related to the surgical procedures were recorded in both the treatment groups. According to the classification systems used, the fusion rate was 89.4% in group A and 94.1% in group B at a 4-year follow-up. Fusion resulted to be time-dependent within each group until the 4-year follow-up, however no differences were found between the two groups. No statistically significant differences were recorded for ODI and VAS scores between group A and group B.

Following a pre-clinical study on ovine model, a fully biomimetic HA-collagen bone graft substitute (RegenOss, Finceramica SpA, Faenza, Italy) is under evaluation in a single-centre prospective comparative clinical trial performed on patients exposed to single level Posterior Interbody Fusion (PLIF) for lumbar degenerative diseases. Because of a revision surgery due to a bar breakage, arthrodesis performed with RegenOss showed a good outcome in all the vertebral positions. A biopsy fragment was harvested for histological and immunohistochemical investigations (66). The analysis evidenced the presence of a lamellar bony-like tissue morphology with osteocyte component and presence of bone marrow at the site of bone substitute application. These results underline bone ingrowth and tissue remodelling. Immunohistochemical evaluation confirmed the good quality of the bone tissue, showing in particular a strong positivity for type I collagen at both cellular and extracellular levels in mature and new bone areas.

We are conducting a clinical study where Mg-HA bone graft substitute SintLife (Finceramica SpA, Faenza, Italy) is evaluated for spine fusion procedures in lumbar degenerative diseases.

Positive results from these studies are validating the use of HA-based products as bone graft substitutes or extenders for spine surgical procedures. This would potentially avoid or reduce the need of autologous bone harvesting and therefore, the risk of drawback-related side effects.

ACKOWLEDGEMENTS

The Authors thank Finceramica SpA, Faenza (Italy) for financial support to the studies.

REFERENCES

1. Gupta A, Kukkar N, Sharif K, Main BJ, Albers CE, El-Amin III SF. Bone graft substitutes for spine fusion: A brief review. World J Orthop 2015; 6:449-56.
2. Fischer CR, Cassilly R, Cantor W, Edusei E, Hammouri Q, Errico T. A systematic review of comparative studies on bone graft alternatives for common spine fusion procedures. Eur Spine J 2013; 22:1423-35.
3. Miyazaki M, Tsumura H, Wang JC, Alanay A. An update on bone substitutes for spinal fusion. Eur Spine J 2009; 18:783-99.
4. Boden SD. Overview of the biology of lumbar spine fusion and principles for selecting a bone graft substitute. Spine 2002; 27:S26-S31.
5. Ludwig SC, Kowalski JM, Boden SD. Osteoinductive bone graft substitutes. Eur Spine J 2000; 9:S119-S25.
6. McAfee PC, Farey ID, Sutterlin CE, Gurr KR,

Warden KE, Cunningham BW. 1989 Volvo Award in basic science. Device-related osteoporosis with spinal instrumentation. Spine 1989; 14:919-26.
7. McGuire RA, Amundson GM. The use of primary internal fixation in spondylolisthesis. Spine 1993; 18:1662-72.
8. Campana V, Milano G, Pagano E, Barba M, Cicione C, Salonna G, Lattanzi W, Logroscino G. Bone substitutes in orthopaedic surgery: from basic science to clinical practice. J Mater Sci Mater Med 2014; 25:2445-61.
9. Hsu W, Nickoli M, Wang J, Lieberman J, An H, Yoon S, Youssef J, Brodke D, McCullough C. Improving the clinical evidence of bone graft substitute technology in lumbar spine surgery. Global Spine J 2012; 2:239-48.
10. Park JJ, Hershman SH, Kim YH. Updates in the use of bone grafts in the lumbar spine. Bull Hosp Jt Dis 2013; 71:39-48.
11. Dimar JR, Glassman SD, Burkus JK, Pryor PW, Hardacker JW, Carreon LY. Two-year fusion and clinical outcomes in 224 patients treated with a single-level instrumented posterolateral fusion with iliac crest bone graft. Spine J 2009; 9:880-5.
12. Niu C-C, Tsai T-T, Fu T-S, Lai P-L, Chen L-H, Chen W-J. A comparison of posterolateral lumbar fusion comparing autograft, autogenous laminectomy bone with bone marrow aspirate, and calcium sulphate with bone marrow aspirate: a prospective randomized study. Spine 2009; 34:2715-9.
13. Ahlmann E, Patzakis M, Roidis N, Shepherd L, Holtom P. Comparison of anterior and posterior iliac crest bone grafts in terms of harvest-site morbidity and functional outcomes. J Bone Joint Surg Am 2002; 84-A(5):716-20.
14. Arrington ED, Smith WJ, Chambers HG, Bucknell AL, Davino NA. Complications of iliac crest bone graft harvesting. Clin Orthop Relat Res 1996; 329:300-9.
15. Younger EM, Chapman MW. Morbidity at bone graft donor sites. J Orthop Trauma 1989; 3:192-5.
16. Babbi L, Barbanti-Brodano G, Gasbarrini A, Boriani S. Iliac crest bone graft: a 23-years hystory of infection at donor site in vertebral arthrodesis and a review of current bone substitutes. Eur Rev Med Pharmacol Sci 2016; 20:4670-6.
17. Giannoudis PV, Dinopoulos H, Tsiridis E. Bone substitutes:an update. Injury 2005; 36(S3):S20-S7.
18. Stevenson S, Emery SE, Goldberg VM. Factors affecting bone graft incorporation. Clin Orthop Relat Res 1996; 324:66-74.
19. Hamer AJ, Strachan JR, Black MM, Ibbotson CJ, Stockley I, Elson RA. Biochemical properties of cortical allograft bone using a new method of bone strength measurement. A comparison of fresh, fresh-frozen and irradiated bone. J Bone Joint Surg Br 1996; 78:363-8.
20. Calvo R, Figueroa D, Díaz-Ledezma C, Vaisman A, Figueroa F. [Bone allografts and the functions of bone banks]. Rev. Médica Chile 2011; 139:660-6.
21. De Long WGJ, Einhorn TA, Koval K, McKee M, Smith W, Sanders R, Watson T. Bone grafts and bone graft substitutes in orthopaedic trauma surgery. A critical analysis. J Bone Joint Surg Am 2007; 89:649-58.
22. Kurien T, Pearson RG, Scammell BE. Bone graft substitutes currently available in orthopaedic practice:the evidence for their use. Bone Joint J 2013; 95-B:583-97.
23. Anselme K, Noël B, Flautre B, Blary MC, Delecourt C, Descamps M, Hardouin P. Association of porous hydroxyapatite and bone marrow cells for bone regeneration. Bone 1999; 25(2S):S51-4.
24. Hench LL, Polak JM. Third-generation biomedical materials. Science 2002; 295:1014-1017.
25. Cancedda R, Dozin B, Giannoni P, Quarto R. Tissue engineering and cell therapy of cartilage and bone. Matrix Biol 2003; 22:81-91.
26. Manfrini M, Di Bona C, Canella A, Lucarelli E, Pellati A, D'Agostino A, Barbanti-Bròdano G, Tognon M. Mesenchymal stem cells from patients to assay bone graft substitutes. J Cell Physiol 2013; 228:1229-37.
27. Nandi SK, Roy S, Mukherjee P, Kundu B, De DK, Basu D. Orthopaedic applications of bone graft & graft substitutes:a review. Indian J Med Res 2010; 132:15-30.
28. Abdullah KG, Steinmetz MP, Benzel EC, Mroz TE. The state of lumbar fusion extenders. Spine 2011; 36:E1328-34.
29. Alsaleh KAM, Tougas CA, Roffey DM, Wai EK. Osteoconductive bone graft extenders in

posterolateral thoracolumbar spinal fusion:a systematic review. Spine 2012; 37:E993-E1000.
30. Alves Cardoso D, Jansen JA, Leeuwenburgh SCG. Synthesis and application of nanostructured calcium phosphate ceramics for bone regeneration. J Biomed Mater Res B Appl Biomater 2012; 100:2316-26.
31. Paderni S, Terzi S, Amendola L. Major bone defect treatment with an osteoconductive bone substitute. Chir Organi Mov 2009; 93:89-96.
32. Dinopoulos H, Dimitriou R, Giannoudis PV. Bone graft substitutes: What are the options? Surgeon 2012; 10:230-9.
33. Mastrogiacomo M, Papadimitropoulos A, Cedola A, et al. Engineering of bone using bone marrow stromal cells and a silicon-stabilized tricalcium phosphate bioceramic:evidence for a coupling between bone formation and scaffold resorption. Biomaterials 2007; 28:1376-84.
34. Tampieri A, Celotti G, Landi E. From biomimetic apatites to biologically inspired composites. Anal Bioanal Chem 2005; 381:568-76.
35. Barbanera A, Longo GP, Vitali M, Sprio S, Tampieri A. Potential applications of synthetic bioceramic bone graft substitute in spinal surgery. Prog Neurosci 2012; 97-104.
36. Manfrini M, Fiorni M, Barbanti Brodano G, Pressato D, Tognon M. New generation of orthopedic mimetic bioceramics assayed with human mesenchymal stem cells. European Musculoskeletal Review 2011; 6:3-6.
37. Barbanti Brodano G, Mazzoni E, Tognon M, Griffoni C, Manfrini M. Human mesenchymal stem cells and biomaterials interaction:a promising synergy to improve spine fusion. Eur Spine J 2012; 21(Sl)1:S3-9.
38. Barbanti Bròdano G, Giavaresi G, Lolli F, et al. Hydroxyapatite-Based Biomaterials vs Autologous Bone Graft in Spinal Fusion:An in Vivo Animal Study. Spine (Phila Pa 1976) 2014; [Epub ahead of print].
39. Barbanti Brodano G, Griffoni C, Zanotti B, Gasbarrini A, Bandiera S, Ghermandi R, Boriani S. A post-market surveillance analysis of the safety of hydroxyapatite-derived products as bone graft extenders or substitutes for spine fusion. Eur Rev Med Pharmacol Sci 2105; 19:3548-55.
40. Barbanti Brodano G, Terzi S, Trombi L, Griffoni C, Valtieri M, Boriani S, Magli MC. Mesenchymal stem cells derived from vertebrae (vMSCs) show best biological properties. Eur Spine J 2013; 22(S6):S979-S84.
41. Salamanna F, Sartori M, Brodano GB, Griffoni C, Martini L, Boriani S, Fini M. Mesenchymal Stem Cells for the Treatment of Spinal Arthrodesis: From Preclinical Research to Clinical Scenario. Stem Cells Int 2017; 2017:3537094.
42. Salamanna F, Contartese D, Nicoli Aldini N, Barbanti Brodano G, Griffoni C, Gasbarrini A, Fini M. Bone marrow aspirate clot: A technical complication or a smart approach for musculoskeletal tissue regeneration? J Cell Physiol 2017; [Epub ahead of print].
43. Wang H, Li Y, Zuo Y, Li J, Ma S, Cheng L. Biocompatibility and osteogenesis of biomimetic nano-hydroxyapatite/polyamide composite scaffolds for bone tissue engineering. Biomaterials 2007; 28:3338-48.
44. Minamide A, Yoshida M, Kawakami M, Yamasaki S, Kojima H, Hashizume H, Boden SD. The use of cultured bone marrow cells in type I collagen gel and porous hydroxyapatite for posterolateral lumbar spine fusion. Spine 2005; 30:1134-8.
45. Wang T, Dang G, Guo Z, Yang M. Evaluation of autologous bone marrow mesenchymal stem cell-calcium phosphate ceramic composite for lumbar fusion in rhesus monkey interbody fusion model. Tissue Eng 2005; 11:1159-67.
46. Curylo LJ, Johnstone B, Petersilg CA, Janicki JA, Yoo JU. Augmentation of spinal arthrodesis with autologous bone marrow in a rabbit posterolateral spine fusion model. Spine 1999; 24:434-8; discussion 438-9.
47. Gan Y, Dai K, Zhang P, Tang T, Zhu Z, Lu J. The clinical use of enriched bone marrow stem cells combined with porous beta-tricalcium phosphate in posterior spinal fusion. Biomaterials 2008; 29:3973-82.
48. Hart R, Komzák M, Okál F, Náhlík D, Jajtner P, Puskeiler M. Allograft alone versus allograft with bone marrow concentrate for the healing of the instrumented posterolateral lumbar fusion. Spine J 2014; 14:1318-24.
49. Choi Y, Oldenburg FP, Sage L, Johnstone B, Yoo JU. A bridging demineralized bone implant facilitates posterolateral lumbar fusion in New Zealand white

rabbits. Spine 2007; 32:36-41.
50. Louis-Ugbo J, Murakami H, Kim H-S, Minamide A, Boden SD. Evidence of osteoinduction by Grafton demineralized bone matrix in nonhuman primate spinal fusion. Spine 2009; 29:360-366.
51. Martin GJ, Boden SD, Titus L, Scarborough NL New formulations of demineralized bone matrix as a more effective graft alternative in experimental posterolateral lumbar spine arthrodesis. Spine 1999; 24:637-45.
52. Yee AJM, Bae HW, Friess D, Robbin M, Johnstone B, Yoo JU. Augmentation of rabbit posterolateral spondylodesis using a novel demineralized bone matrix-hyaluronan putty. Spine 2003; 28:2435-40.
53. Lee Y-P, Jo M, Luna M, Chien B, Lieberman JR, Wang JC. The efficacy of different commercially available demineralized bone matrix substances in an athymic rat model. J Spinal Disord Tech 2005; 18:439-44.
54. Peterson B, Whang PG, Iglesias R, Wang JC, Lieberman JR. Osteoinductivity of commercially available demineralized bone matrix. Preparations in a spine fusion model. J Bone Joint Surg Am 2004; 86-A:2243-50.
55. Wang JC, Alanay A, Mark D, Kanim LEA, Campbell PA, Dawson EG, Lieberman JR. A comparison of commercially available demineralized bone matrix for spinal fusion. Eur Spine J 2007; 16:1233-40.
56. Sassard WR, Eidman DK, Gray PM, Block JE, Russo R, Russell JL, Taboada EM. Augmenting local bone with Grafton demineralized bone matrix for posterolateral lumbar spine fusion: avoiding second site autologous bone harvest. Orthopedics 2000; 23:1059-1064; discussion 1064-5.
57. Girardi FP, Cammisa FP. The effect of bone graft extenders to enhance the performance of iliac crest bone grafts in instrumented lumbar spine fusion. Orthopedics 2003; 26:s545-8.
58. Urist MR. Bone: formation by autoinduction. Science 1965; 150:893-9.
59. Boden SD, Schimandle JH, Hutton WC. 1995 Volvo Award in basic sciences. The use of an osteoinductive growth factor for lumbar spinal fusion. Part II: Study of dose, carrier, and species. Spine 1995; 20:2633-44.
60. Boden SD, Moskovitz PA, Morone MA, Toribitake Y. Video-assisted lateral intertransverse process arthrodesis. Validation of a new minimally invasive lumbar spinal fusion technique in the rabbit and nonhuman primate (rhesus) models. Spine 1996; 21:2689-97.
61. Kadam A, Millhouse PW, Kepler CK, et al.. Bone substitutes and expanders in Spine Surgery:A review of their fusion efficacies. Int J Spine Surg 2016; 10:33. eCollection 2016.
62. Kinaci A, Neuhaus V, Ring DC. Trends in bone graft use in the United States. Orthopedics 2014; 37:e783-8.
63. Mobbs RJ, Chung M, Rao PJ. Bone graft substitutes for anterior lumbar interbody fusion. Orthop Surg 2103; 5:77-85.
64. Nickoli MS, Hsu WK. Ceramic-based bone grafts as a bone grafts extender for lumbar spine arthrodesis: a systematic review. Global Spine J 2014; 4:211-6.
65. Giorgi P, Capitani D, Schirò GR. Use of a novel porous hydroxyapatite bone graft substitute in postero-lateral and interbody spinal fusion: clinical and radiographic analysis at 4 years follow up. Progress in Neuroscience 2015; 3:1-4.
66. Grigolo B, Dolzani P, Giannetti C, Tenucci M, Calvosa G. Use of a fully-resorbable, biomimetic composite hydroxyapatite as bone graft substitute for posterolateral spine fusion: a case report. Int J Clin Exp Med 2016; 9:22458-62.

TARGETED MUSCLE REINNERVATION FOR IMPROVED CONTROL OF MYOELECTRIC UPPER LIMB PROSTHESES

G. VADALÀ[1], G. DI PINO[2], L. AMBROSIO[1], L. DIAZ BALZANI[1] and V. DENARO[1]

[1]Department of Orthopaedic and Trauma Surgery, Università Campus Bio- Medico di Roma;
[2]NeXT: Neurophysiology and Neuroengineering of Human-Technology Interaction Research Unit, Università Campus Bio-Medico, Rome, Italy

Targeted muscle reinnervation (TMR) is a novel surgical technique developed to improve the control of myoelectric upper limb prostheses. Nerves transected by the amputation, which retain their original motor pathways even after being severed, are redirected to residual denervated muscles that serve as target for consequent reinnervation. Once the process is complete, reinnervated muscles will contract upon voluntary activation of transferred nerves while attempting to move missing regions of the amputated limb, generating EMG signals that can be recorded and used to control a prosthetic device. This allows creating new control sites that can overcome major drawbacks of conventional myoelectric prostheses by offering a more natural and intuitive control of prosthetic arms. TMR has been widely performed in individuals who underwent shoulder disarticulation amputation and transhumeral amputation since proximal amputations do not leave enough functional muscles exploitable to control independent degree of freedoms of multi-articulated prostheses. TMR application is currently under investigation in patients suffering further distal amputations, as well as for treating and preventing painful post-amputation neuromas. The purpose of this paper is to describe the physiologic basis and the surgical technique of TMR, reporting current knowledge on the clinical results.

Upper limb amputation is a dramatic event leading to enormous disability due to physical, psychological and social burdens (1).. The main cause of upper limb amputation is trauma due to motor vehicle collisions, industrial accidents and blunt injuries; less frequent causes include dysvascular disease or therapeutic amputation for cancer removal (2)..

The primary treatment for upper limb amputation is based on preparing or readapting the stump in order to wear a prosthetic device designed to substitute limb function. Myoelectric prostheses represent the current state of the art commercially available for patients. They are mechatronic devices controlled through the activity of residual muscles picked up as electric signals by surface electromyographic (EMG) electrodes.

It is reported that 68% of non-prosthetic-users would be eager to reconsider the use of a prosthetic device if improvements in dexterity, sensory feedback, range of movement, intuitiveness of control and coordination of multiple joints were made at an acceptable cost (4).. Those arguments raise the need for developing more advanced prosthetic devices. A possibility today to face prosthesis control issues is through the development of neural interfaces able to decode motor intentions formulated by the nervous system and novel computational algorithms to translate them into the corresponding movement

Key words: targeted muscle reinnervation, TMR, myoelectric prostheses, upper limb amputation, nerve transfers

Mailing address:
Gianluca Vadalà, MD, PhD
Department of Orthopedic and Trauma Surgery,
Università Campus Bio-Medico di Roma,
Via Alvaro del Portillo 200, 00128 Rome, Italy
Tel.: +39 06 22 54 11613
Fax: +39 06 22 54 11638

0393-974X (2017)

of the prosthesis. Those improvements may allow an intuitive and natural use of the robotic limb. In this regard, innovative systems involving implantable intraneural electrodes have recently showed great potential for implementing sensory feedback (5) and bidirectional interfacing with the cybernetic prosthesis (6, 7).

Another viable option is through targeted muscle reinnervation (TMR). TMR is a novel surgical procedure that allows the nerves to interface easier by exploiting the original biological amplifier of their efferent activity: the muscle. This is achieved by transferring residual arm nerves to surgically denervated redundant muscles in the residual limb (8). The technique is indicated in patients who complain of poor function with a standard prosthesis after following an appropriate rehabilitation protocol.

Anatomic and physiologic basis of TMR

Despite the peripheral damage due to amputation, motor fibers have shown to still carry the information needed to control muscles and once re-attached to both native and non-native muscles, are able to create new connections, possibly leading to reinnervation. When this happens, the target muscle eventually becomes controlled by a different spinal segment and a different area of the primary motor cortex (M1), whose activation elicits a measurable EMG (9). In light of prosthesis control, this process leads to several advantages.

In order to obtain successful reinnervation after TMR, each target muscle must be surgically denervated of its original motor nerves. The trophic factors released by the targeted orphan muscle attract the transferred nerve, leading to an enhanced sprouting of donor fibers (namely hyper-reinnervation), which have shown to improve muscle mass and strength, as well as reorganization of the original structure of the motor unit, with the target muscle motor units progressively resembling the muscle originally innervated by the donor nerve. Moreover, the denervation of the targeted muscle avoids development of a mixed innervation from both original and transferred nerves, which would result in a weaker reinnervation, due to fiber competition and in EMG signal overlapping (10)..

For a successful procedure, it is fundamental that each donor nerve reinnervates a distinct and independent component of the targeted muscle. Especially when large nerve fibers are transferred to small muscle targets, excessive reinnervation may spread towards contiguous muscle segments, thus causing a cross-reinnervation, which would result in mixed EMG signals and prevent their separate decoding. This drawback can be overcome by surgically separating muscle segments, so as to produce a scar tissue barrier or, alternatively, by opportunely positioning an adipofascial flap.

Additional key factors needed for a strong EMG signal are muscle size and overlying subcutaneous fat thickness. Indeed, muscle mass is directly proportional to EMG signal amplitude, while subcutaneous fat acts as a spatial filler that attenuates the signal magnitude and decreases the focus of the recording area (10).

Although the loss of the peripheral effector induced by the amputation favors the invasion of hand cortical motor representation by the motor representation of face and stump, hand area somehow persists in M1, but shifts away from its original location (3). By reestablishing a functional target to the motor fibers that once innervated forearm muscles, TMR has shown the ability to restore central motor representations of the amputated limb. Using high-density electroencephalography it has been shown that TMR remapped the motor representations for the missing limb closer to its original location (11).

Shoulder Disarticulation

TMR was developed and applied for the first time in a woman with shoulder disarticulation (12). The rationale of the technique is to restore 4 basic functions of the upper limb: elbow flexion/extension and hand open/close. However, shoulder disarticulation is often a result of a devastating trauma, leading to a dramatic distortion of the anatomy and the donor muscles available are few and often disrupted. Therefore, it is not possible to standardize transfers in a single pattern. Potential muscles target are *pectoralis major*, *pectoralis minor*, *latissimus dorsi* and *serratus anterior*. In

a case series involving 10 patients with shoulder disarticulation, 7 different patterns of transfers were used (13)..

The *pectoralis major* muscle offers the greatest possibilities of use. It can be separated into three distinct portions due to the peculiar innervations: the superior, middle and inferior pectoral nerve innervate, respectively the clavicular, sternal and sternoabdominal head of the *pectoralis major,* providing 3 possible targets for reinnervation (14).. The pectoralis minor muscle can be further used after being mobilized laterally and superficially, to part from the pectoralis major to prevent EMG signal cross-talking. Indeed, nerve transfers are commonly performed as follows: the musculocutaneous nerve is transferred to the clavicular head of *pectoralis major* to restore the elbow flexion; the median nerve is transferred to the largest segment of the sternal head of *pectoralis major*; the radial nerve is generally transferred to *latissimus dorsi* through coaptation to the thoracodorsal nerve or to the inferior segment of the sternal head of *pectoralis major*.. The ulnar nerve is then transferred deeply and laterally to *pectoralis minor* or to the serratus anterior via coaptation with the long thoracic nerve (15) (Fig. 1).

Transhumeral Amputation

TMR for transhumeral ampution is less challenging, in fact both biceps and triceps muscle are present and can provide a signal for two of the four fundamental functions: flexion and extension of the elbow. Therefore, the musculocutaneous nerve is left intact in its innervation of the long head of the biceps as it yields a natural elbow flexion signal, while the median nerve is transferred to the short head of the biceps in order to provide a hand close signal; similarly, native innervation of the long head of the *triceps* by the proximal radial nerve is preserved to provide an elbow extension input, whereas the distal radial nerve is transferred to the lateral head of the *triceps* in order to yield a hand open input (16, 17) (Fig. 1).

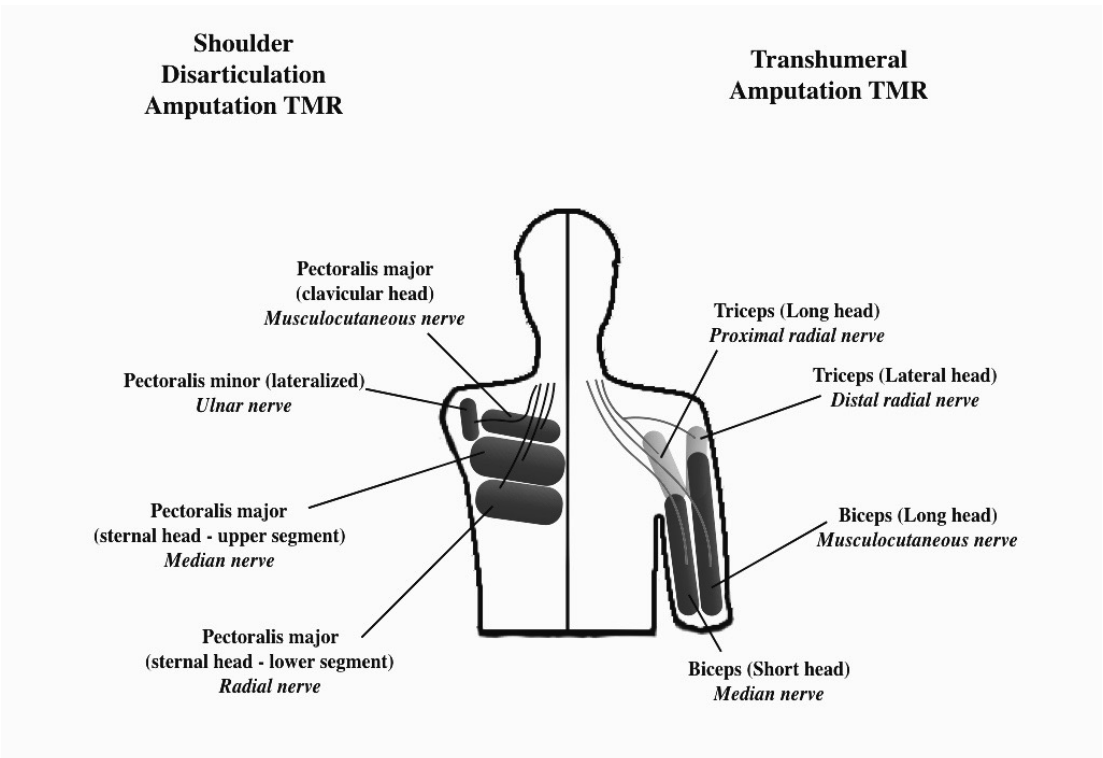

Fig. 1. *TMR transfer patterns: on the left side a possible scheme for shoulder disarticulation, on the right side the fixed pattern for transhumeral amputation.*

Transradial Amputation

Although transradial represents the most common level of upper limb amputation, TMR at this level is currently under clinical investigation (17). Transradial amputees can easily control wrist movement (flexion/extension and prono/supination) while lacking a good control of the hand function. TMR improves movement of the hand, transferring nerves that originally innervate the thumb, fingers and intrinsic hand musculature, carrying information for multiple hand-grasp patterns (18) TMR for transradial amputees is performed by transferring the median nerve to the flexor *digitorum superficialis* and the ulnar nerve to the *flexor carpi ulnaris*; both muscles are superficial and thus provide a strong and easily measurable EMG signals (19).

EMG signal decoding for prosthetic control in TMR

Compared to conventional myoelectric prosthesis control, TMR essentially relies on EMG signals produced within reinnervated muscles, which offer an increased number of independent control signals that directly correlate with original function of the missing limb (20).

Following TMR surgery, muscle generating myoelectric sites are controlled by appropriate transferred nerves; this allows intuitive and simultaneous control of multiples degrees of freedom (DOFs) at the same time, in striking contrast to conventional myoelectric prostheses (15).

Even providing a more natural and immediate control, this setting does not access the complex neural information contained in transferred nerves, which inherently carry motion control for every single muscle of the hand and the forearm.

High-density EMG recordings of reinnervated muscles have demonstrated the presence of complex specific activation patterns that can be depicted upon different attempts of moving either the thumb, a finger or the wrist (21). Pattern recognition algorithms, based on a machine learning approach, may help in predicting the patient's intended movement in real time by decoding complex EMG signal patterns (18).

In contrast to conventional myoelectric control methods, pattern recognition control may also be able to decode signals from electrodes not perfectly located upon high amplitude control sites and it is less impaired by EMG cross-talk. In addition, pattern recognition techniques have been shown to be equally or even more effective when adopting a grid arrangement of electrodes on the residual limb skin surface (22).

In virtual environments, which have been proved to be of great value for training pattern recognition control, after TMR subjects showed performance similar to age-matched non-amputated individuals, thus demonstrating that this approach results in excellent control after TMR (8). Wearing physical prostheses, pattern recognition allowed TMR patients to perform better during standardized test than when wearing classical myoelectric prostheses (23).

New devices are currently under development to optimize EMG recording. While surface electrode recording is noninvasive and easy to perform, it can be impaired by repetitive prosthesis wearing and removal as well as by alterations in skin impedance from sweating and signal amplitude reduction due to the presence of subcutaneous tissues.. This has led to the design of wireless intramuscular implantable devices, which can yield stable recording of enriched high-quality EMG signals from deep muscles while being free of cross-talk (24).

Optimizing intramuscular electrodes with high-density EMG spatial sampling systems may allow, in the near future to identify the electrical activity of each single motor unit, thus accessing even more complex information. However, available multichannel EMG system prototypes have been tested only in acute settings and hence require investigation for longer periods considering a future chronic application (25).

Rehabilitation and occupational therapy after TMR

Immediately after TMR surgery, main issues include post-surgical edema, pain and phantom limb sensation (26).. Reinnervation occurs gradually and becomes noticeable between 8 and 12 weeks after surgery. It is crucial to strengthen reinnervating muscles to produce recordable EMG signals that can be detected by surface electrodes.

Occupational therapy should start approximately

3 weeks after surgery: first exercises consist in inviting the patient to imagine "moving" every segment of the missing limb repetitively, several times every day. These mental attempts may favor activation of central and peripheral pathways in order to promote reinnervation.

At 6-15 weeks after surgery, when reinnervation is identified in the process of muscle twitching under voluntary control, the patient is advised to mentally visualize gross motor patterns corresponding to the distribution of nerve transfers. This process, called motion imagery, has shown to activate cortical areas that are equally operating during actual movement and thus is able to reinforce peripheral reinnervation.

At 3 to 5 months after surgery, the amputee is invited to discontinue gross movement patterns in favor of discrete muscle actions. The underlying rationale is to develop strong, isolated and independent motion controls so that the patient would be able to activate each single prosthetic function independently after fitting the new TMR-controlled device.

Approximately 6 months after surgery, target muscles are fully reinnervated and ready to allow TMR prosthesis fitting and EMG testing of attempted movements. Starting with a single DOF (e.g. elbow flexion/extension), an adequate EMG activity is sought by adjusting electrode settings in order to optimize signal balance and strength.
Concurrently, the patient is asked to accurately describe very attempted movement by reproducing it with his intact limb. The aim of this process is to isolate functional movements and to identify corresponding, independent and strong EMG signals.. When each prosthetic function has been isolated and linked with a distinct EMG signal, the prosthetist may proceed with diagnostic socket fabrication.

Once the latter is fitted, initial TMR training consists in repetitive activation of each separate function with relaxation between contractions; this is to reinforce distinct EMG signals, to encourage their separation and to optimize socket fitting and electrode configuration.

When independent control of each single DOF is mastered, the therapist instructs the patient to achieve simultaneous control of two DOFs or to complete more complex tasks, such as moving faster while maintaining signal separation, combine different actions and switching among diverse functions.

When the amputee becomes proficient with all prosthetic functions, training progresses towards one-handed activities, e.g. grasping and releasing objects, holding them while moving proximal joints of the prosthesis and bimanual activities that include everyday tasks such as zipping a jacket, folding clothes etc.

Once the entire rehabilitative team agrees on the individual's ability to control the TMR prosthesis, the patient is eventually discharged (26, 27).

TMR to treat or prevent post-amputation neuroma

In amputees, TMR may have effective applications that go beyond prosthesis control. Painful neuroma is a daunting complication that affects functional outcomes negatively. It depends on a disorganized proliferation of transected axons developing abnormal connections with nociceptive fibers, together with an inflammatory milieu that triggers ectopic discharges, eventually establishing a hyperalgesic state causing a focal neuropathic pain that is commonly disabling and difficult to treat.

Surgical, pharmacological strategies have currently been developed, however none of the proposed techniques has shown optimal efficacy, and pain recurrence rates are still significant (17).

By redirecting transected nerves onto a denervated muscle, TMR inhibits neuroma formation, as it allows axon regeneration within a physiological target therefore restoring original continuity of the peripheral nerve.. The first clinical evidence of TMR efficacy for treating painful neuromas was a retrospective review of 28 patients treated with TMR from 2002 to 2012. Of the 15 patients suffering from post-amputation neuroma pain, 14 reported total resolution of pain after TMR and the remaining patient improved to such a degree that he was able to fit a prosthesis (13). Rather than a solely elective and delayed approach, these results may provide a solid basis for the routine application of TMR to prevent neuroma formation by performing nerve transfer surgery in the acute traumatic amputation setting (28).

CONCLUSION

TMR allows building neuro-muscle interfaces for the control of upper limb myoelectric prostheses. Together with ongoing advances in implantable EMG recorders, pattern recognition technologies, robotic prosthesis design, as well as reducing the incidence of amputation neuroma, TMR will likely further enhance functional performance, physical activity and quality of life in individuals struggling with limb amputation.

ACKNOWLEDGEMENTS

The Italian Institute for Labor Accidents (INAIL) supported this work in the framework of the PCR1/2 project (E57B16000160005).

REFERENCES

1. Ziegler-Graham K, MacKenzie EJ, Ephraim PL, Travison TG, Brookmeyer R. Estimating the prevalence of limb loss in the United States: 2005 to 2050. Arch Phys Med Rehabil 2008; 89(3):422-9.
2. Kuiken T.. Introduction. In: Todd Kuiken ASF, Ann Barlow, editor. Targeted Muscle Reinnervation: A Neural Interface for Artificial Limbs. Boca Raton FL: Taylor & Francis 2014; 1-8.
3. Di Pino G, Guglielmelli E, Rossini PM. Neuroplasticity in amputees: main implications on bidirectional interfacing of cybernetic hand prostheses. Prog Neurobiol 2009; 88(2):114-26.
4. Engdahl SM, Chestek CA, Kelly B, Davis A, Gates DH. Factors associated with interest in novel interfaces for upper limb prosthesis control. PLoS One 2017; 12(8):e0182482.
5. Oddo CM, Raspopovic S, Artoni F, et al. Intraneural stimulation elicits discrimination of textural features by artificial fingertip in intact and amputee humans. eLife 2016; 5:e09148.
6. Lotti F, Ranieri F, Vadala G, Zollo L, Di Pino G. Invasive Intraneural Interfaces: Foreign Body Reaction Issues. Front Neurosci 2017; 11:497.
7. Di Pino G, Denaro L, Vadala G, et al. Invasive neural interfaces: the perspective of the surgeon. J Surg Res 2014; 188:77-87.
8. Kuiken TA, Li G, Lock BA, Lipschutz RD, Miller LA, Stubblefield KA, Englehart KB. Targeted muscle reinnervation for real-time myoelectric control of multifunction artificial arms. Jama 2009; 301:619-28.
9. Farina D, Castronovo AM, Vujaklija I, Sturma A, Salminger S, Hofer C, Aszmann OC. Common synaptic input to motor neurons and neural drive to targeted reinnervated muscles. J Neurosci 2017.
10. Kuiken T The Scientific Basis of Targeted Muscle Reinnervation. In: Todd Kuiken ASF, Ann Barlow, editor. Targeted Muscle Reinnervation: A Neural Interface for Artificial Limbs. Boca Raton FL: Taylor & Francis 2014; 9-18.
11. Chen A, Yao J, Kuiken T, Dewald JP. Cortical motor activity and reorganization following upper-limb amputation and subsequent targeted reinnervation. Neuroimage Clin 2013; 3:498-506.
12. Kuiken TA, Dumanian GA, Lipschutz RD, Miller LA, Stubblefield KA. The use of targeted muscle reinnervation for improved myoelectric prosthesis control in a bilateral shoulder disarticulation amputee. Prosthet Orthot Int 2004; 28:245-53.
13. Souza JM, Cheesborough JE, Ko JH, Cho MS, Kuiken TA, Dumanian GA. Targeted muscle reinnervation: a novel approach to postamputation neuroma pain. Clin Orthop Relat Res 2014; 472:2984-90.
14. Aszmann OC, Rab M, Kamolz L, Frey M. The anatomy of the pectoral nerves and their significance in brachial plexus reconstruction. J Hand Surg Am 2000; 25:942-7.
15. Cheesborough JE, Smith LH, Kuiken TA, Dumanian GA. Targeted muscle reinnervation and advanced prosthetic arms. Semin Plast Surg 2015; 29:62-72.
16. Gregory A. Dumanian JMS Surgical Techniques for Targeted Muscle Reinnervation. In: Todd Kuiken ASF, Ann Barlow, editor. Targeted Muscle Reinnervation: A Neural Interface for Artificial Limbs. Boca Raton FL: Taylor & Francis 2014; 22-43.
17. Kuiken TA, Barlow AK, Hargrove L, Dumanian GA. Targeted muscle reinnervation for the upper and lower extremity. Tech Orthop 2017; 32: 109-16.
18. Levi J. Hargrove BAL Future Research Directions. In: Todd Kuiken ASF, Ann Barlow, editor. Targeted muscle reinnervation: a neural interface for artificial limbs.

Boca Raton FL: Taylor & Francis 2014; 165-80.
19. Morgan EN, Kyle Potter B, Souza JM, Tintle SM, Nanos GP, 3rd. Targeted muscle reinnervation for transradial amputation: description of operative technique. Tech Hand Up Extrem Surg 2016; 20:166-71.
20. Kuiken T. Targeted reinnervation for improved prosthetic function. Phys Med Rehabil Clin N Am 2006; 17:1-13.
21. Zhou P, Lowery MM, Englehart KB, Huang H, Li G, Hargrove L, Dewald JP, Kuiken TA. Decoding a new neural machine interface for control of artificial limbs. J Neurophysiol 2007; 98:2974-82.
22. Tkach DC, Young AJ, Smith LH, Rouse EJ, Hargrove LJ. Real-time and offline performance of pattern recognition myoelectric control using a generic electrode grid with targeted muscle reinnervation patients. IEEE Trans Neural Syst Rehabil Eng 2014; 22:727-34.
23. Hargrove LJ, Lock BA, Simon AM. Pattern recognition control outperforms conventional myoelectric control in upper limb patients with targeted muscle reinnervation. Conf Proc IEEE Eng Med Biol Soc 2013; 2013:1599-602.
24. Weir RF, Troyk PR, DeMichele GA, Kerns DA, Schorsch JF, Maas H. Implantable myoelectric sensors (IMESs) for intramuscular electromyogram recording. IEEE Trans Biomed Eng 2009; 56(1):159-71.
25. Bergmeister KD, Vujaklija I, Muceli S, et al.. Broadband Prosthetic Interfaces: Combining Nerve Transfers and Implantable Multichannel EMG Technology to Decode Spinal Motor Neuron Activity. Front Neurosci 2017; 11:421.
26. Stubblefield KA, Miller LA, Lipschutz RD, Kuiken TA. Occupational therapy protocol for amputees with targeted muscle reinnervation. J Rehabil Res Dev 2009; 46:481-8.
27. Kuiken TA. Occupational Therapy for the Targeted Muscle Reinnervation Patient. In: Todd Kuiken ASF, Ann Barlow, editor. Targeted Muscle Reinnervation: A Neural Interface for Artificial Limbs. Boca Raton FL: Taylor & Francis 2014; 99-117.
28. Cheesborough JE, Souza JM, Dumanian GA, Bueno RA, Jr. Targeted muscle reinnervation in the initial management of traumatic upper extremity amputation injury. Hand (NY) 2014; 9:253-7.